Assessment of shear stress limits in New Zealand design standards for high-strength concrete bridge beams

November 2012

M Al-Ani, R Rogers and J Ingham
University of Auckland

NZ Transport Agency research report 501

ISBN 978-0-478-39494-8 (electronic)
ISSN 1173-3764 (electronic)

NZ Transport Agency
Private Bag 6995, Wellington 6141, New Zealand
Telephone 64 4 894 5400; facsimile 64 4 894 6100
research@nzta.govt.nz
www.nzta.govt.nz

Al-Ani, M, R Rogers and J Ingham (2012) Assessment of shear stress limits for high-strength concrete bridge beams. *NZ Transport Agency research report 501.* 163pp.

Keywords: beams, bridges, capacity, concrete, design, experimental, high-strength, limits, New Zealand, NZS 3101, shear

An important note for the reader

The NZ Transport Agency is a Crown entity established under the Land Transport Management Act 2003. The objective of the Agency is to undertake its functions in a way that contributes to an affordable, integrated, safe, responsive and sustainable land transport system. Each year, the NZ Transport Agency funds innovative and relevant research that contributes to this objective.

The views expressed in research reports are the outcomes of the independent research, and should not be regarded as being the opinion or responsibility of the NZ Transport Agency. The material contained in the reports should not be construed in any way as policy adopted by the NZ Transport Agency or indeed any agency of the NZ Government. The reports may, however, be used by NZ Government agencies as a reference in the development of policy.

While research reports are believed to be correct at the time of their preparation, the NZ Transport Agency and agents involved in their preparation and publication do not accept any liability for use of the research. People using the research, whether directly or indirectly, should apply and rely on their own skill and judgement. They should not rely on the contents of the research reports in isolation from other sources of advice and information. If necessary, they should seek appropriate legal or other expert advice.

.

Acknowledgements

The authors would like to thank Peter Libscombe of URS and Len McSaveney of Golden Bay Cement, who were members of the project steering group chaired by Associate Professor Jason Ingham, and provided important input and support during the formative phase of the project. The contribution of the peer reviewers, Dr. Alessandro Palermo (University of Canterbury) and Peter Wiles (OPUS) was also critical during the final phase of the project, and their participation is greatly appreciated.

The staff at Stresscrete Papakura, and particularly Paul Cane, were instrumental in the completion of the experimental investigation, and their generosity of both time and resources was greatly appreciated. The help of Luke Storie, from the University of Auckland, was also crucial throughout the experimental investigation.

Abbreviations and acronyms

ACI	American Concrete Institute
a/d	span-to-unit depth ratio
AASHTO	American Association of State Highway and Transportation Officials
CFT	Compression Field Theory
CHBDC	Canadian Highway Bridge Design Code
EC2	Eurocode 2
ECS	surface concrete strain
FA-STM	Fixed-Angle Softened-Truss Model
(f_c')	compressive strength
ICS	internal concrete strain
ISS	stirrup strain
kN	kilonewton
MCFT	Modified Compression Field Theory
kNm	kilonewton-metre
(ρ_l)	longitudinal reinforcement ratio
PC	prestressed concrete
PG	displacement portal gauge
RA-STM	Rotating-Angle Softened-Truss Model
RC	reinforced concrete
RHS	rectangular hollow section
UoA	University of Auckland

Contents

Executive summary **7**
Abstract **9**
1 Introduction **11**
1.1 Overview 11
1.2 Web shear in New Zealand concrete bridge beams 11
1.3 Outline of this report 12
2 Models for the behaviour of concrete in shear **14**
2.1 Shear transfer mechanisms 14
2.1.1 Shear in compression zone 15
2.1.2 Dowel action 15
2.1.3 Aggregate interlock/interface shear transfer 15
2.1.4 Residual tensile stresses 16
2.1.5 Transverse reinforcement 16
2.1.6 Vertical prestressing force 16
2.2 Parameters influencing shear behaviour 16
2.3 Models for concrete shear behaviour 17
2.3.1 Parallel chord truss models 17
2.3.2 Compression field theories 20
2.3.3 Softened truss models 25
2.4 Conclusions 28
3 Design standards **29**
3.1 ACI 318-11 29
3.1.1 Reinforced concrete (RC) beams 29
3.1.2 Prestressed concrete (PC) beams 30
3.2 NZS 3101:2006 32
3.2.1 RC beams 32
3.2.2 PC beams 32
3.3 CSA A23.3-04 and AASHTO LRFD 6th edition 33
3.4 Eurocode 2 (EC2) 34
3.5 fib model code 2010 35
3.6 Comparison of design standards 36
3.7 Conclusions 38
4 Shear test database **39**
4.1 Objectives 39
4.2 Database composition 39
4.2.1 RC beam database 40
4.2.2 PC beam database 43
4.3 Influence of design parameters 46
4.3.1 RC database 46
4.3.2 PC database 52
4.4 Evaluation of shear design standards 57
4.4.1 ACI 318-11 57
4.4.2 NZS 3101:2006 67
4.4.3 CSA A23.3-04 and AASHTO LRFD 6th edition 77
4.4.4 Eurocode 2 (EC2) 86

4.4.5 fib model code 2010 95
4.5 Conclusions 105
5 Experimental investigation 107
5.1 Objectives and scope 107
5.2 Test rig 107
5.3 Design of test beams and setup 110
5.4 Construction of test beams 113
5.5 Testing 114
5.6 Test results 115
5.6.1 Unit 40-8-A 115
5.6.2 Unit 40-8-B 118
5.6.3 Unit 40-10-A 120
5.6.4 Unit 40-10-B 121
5.6.5 Unit 60-8-A 122
5.6.6 Unit 60-8-B 124
5.6.7 Unit 60-10-A 125
5.6.8 Unit 60-10-B 126
5.6.9 Unit 80-8-A 127
5.6.10 Unit 80-8-B 129
5.6.11 Unit 80-10-A 130
5.6.12 Unit 80-10-B 131
5.6.13 Summary 132
5.7 Conclusions 133
6 Analysis of investigation results 134
6.1 Capacity analysis 134
6.1.1 Summary of experimental investigation results 136
6.2 Design code based analysis 136
6.2.1 ACI 318 137
6.2.2 NZS 3101 138
6.2.3 CSA A23.3 and AASHTO LRFD 140
6.2.4 Eurocode 2 (EC2) 141
6.2.5 fib model code 2010 142
6.2.6 Comparison of limits in design standards 143
6.3 Alternative limits for NZS 3101 144
6.4 Conclusions 148
7 Conclusions and recommendations 150
7.1 Recommendations 152
8 References 153
Appendix A Shear test databases 155
Appendix B Calculation of prestress losses 161
B.1 Elastic shortening losses 161
B.2 Creep losses 161
B.3 Shrinkage losses 162
B.4 Relaxation losses 162
B.5 Prestress after all losses 162
Appendix C Concrete cylinder tests 163

Executive summary

Concrete is one of the most frequently used construction materials in the world, and the material is widely used in the construction of bridges due to its strength in compression and the ability to account for tension through the embedment of steel reinforcing bars. The increasing prevalence of concrete construction during the twentieth century resulted in a number of significant developments in concrete technology, two of which were the introduction of prestressed concrete and vast improvements in concrete compressive strength. The combination of these two developments provided significant improvements in the efficiency of design of concrete beams for flexure, allowing for thinner beams and leading to increased applied shear stresses.

The design of concrete beams for shear is governed in New Zealand by provisions in NZS 3101:2006, which are based on an outdated model of concrete shear behaviour and are augmented using empirical data. The provisions impose a limit of 'the smaller of $0.2f_c'$ and 8MPa' to avoid brittle failure of the diagonal concrete compression struts. The absolute limit of 8MPa means that all beams with concrete compressive strengths greater than 40MPa are limited to the same allowable design shear capacity as beams that have a concrete compressive strength of 40MPa.

The main objective of the research detailed in this report was to assess the validity of the 8MPa limit imposed in NZS 3101 on allowable design shear capacity through an examination of concrete shear theory, investigation of shear design provisions in international design standards, analysis of previous experimental research, and the undertaking of a series of experimental testing. Theoretical models for the behaviour of concrete beams subjected to shear were found to considerably differ from one another in their formulation, and it was found that no existing model was able to accurately account for all the factors influencing concrete shear behaviour and the interactions between these factors.

Six international design standards, comprising four different approaches to concrete shear design, were detailed and analysed. The design standards were found to provide significantly varied approaches to concrete shear design, and to be based on different theoretical shear behaviour models. The six design standards were also found to impose different limits on the allowable design shear capacity of a concrete beam, with NZS 3101 imposing markedly lower limits than permitted in CSA A23.3, AAHSTO LRFD and Eurocode 2, particularly for high-strength concrete beams.

Two databases consisting of all previously tested RC and PC beams (from all accessible global research) that had failed in shear were compiled and initially contained almost 2500 beams. The databases were then refined by excluding all beams containing less than minimum quantities of transverse reinforcement, as prescribed in NZS 3101. The refined databases were analysed to assess the influence of various design parameters on the ultimate shear capacity of concrete beams, and to assess the performance of the six design standards when predicting the ultimate shear capacity of RC and PC beams. For beams in the RC database, measured ultimate shear capacity was observed to increase with increasing concrete compressive strength, longitudinal reinforcement ratio and transverse reinforcement ratio, while decreasing for increasing beam effective depths and shear span-to-depth ratios. Measured ultimate shear capacities of beams in the PC database were observed to increase for increasing values of concrete compressive strength, beam effective depth, longitudinal reinforcement ratio and transverse reinforcement ratio, while decreasing for increasing ratios of shear span-to-depth. Eurocode 2 was found to be the most conservative of the six design standards considered, while CSA A23.3 and AASHTO LRFD were found to be the most accurate for predicting the shear capacity of RC beams, and NZS 3101 was found to be the most accurate for predicting the shear capacity of PC beams. However, the standards found to be most accurate were also observed to be unconservative for significant proportions of the

respective database. There was an absence of any discernible influence of ultimate shear capacity on the accuracy of the design provisions for ultimate shear capacities greater than 8MPa, despite the omission of the 8MPa limit on allowable shear capacity during this evaluation. This observation indicated that the removal of the 8MPa absolute limit on the allowable shear capacity of concrete beams would not unduly affect the integrity of the design provisions in NZS 3101.

An experimental investigation was conducted to augment the findings from the analysis of the RC and PC databases. The investigation consisted of testing 12 single-tee prestressed concrete beams that were designed to fail at applied shear stresses greater than or equal to the 8MPa absolute in NZS 3101. The 12 test units were designed and constructed with concrete compressive strengths ranging from 40–80MPa, and varying quantities of transverse reinforcement. Two of the four test units that were designed to have a concrete compressive strength of 40MPa failed in flexure at shear stresses lower than the predicted shear capacity, while another test unit with 40MPa concrete failed due to strand slip. The remainder of the test units all failed at shear stresses greater than the design shear capacities, with strong evidence of predominantly shear failure modes. A comparative analysis of the performance of the nine experimental test units known to fail in shear supported the need for a limit on the nominal design shear capacity, but the performance of the high-strength concrete test units indicated that an absolute limit of 8MPa is overly conservative.

An analysis of the nine test units using the shear design provisions of the six international design standards assessed throughout this report, with and without absolute limits, was conducted. It was observed that the provisions of ACI 318 and NZS 3101, with their existing limits, provided conservative predictions of shear capacity for the test units, while omission of the absolute limits in these two standards resulted in non-conservative predictions of shear capacity. The shear design provisions of CSA A23.3, AASHTO LRFD and Eurocode 2 all provided overly conservative predictions of shear capacity for the high-strength concrete test units.

Finally, a statistical analysis of the effect of four alternatives to the existing NZS 3101 limits imposed on shear capacity was conducted using the results of the experimental investigation, the beams in the RC database, and the beams in the PC database. It was concluded that the existing limits on design shear capacity in the provisions of NZS 3101 could be modified to 'the minimum of $0.2f_c'$ and 10MPa' to improve the accuracy of the design provisions for beams that have large quantities of transverse reinforcement, without compromising the conservatism inherent in any design standard for safety. This conclusion was guided by the non-conservative predictions of ultimate shear capacity that arose when considering the other proposed alternative limits for the experimental test units. The proposed increase of the absolute limit on design shear capacity to 10MPa would both improve the accuracy of the shear design provisions of NZS 3101 and allow for more efficient design of concrete bridge beams than allowed by the 8MPa limit currently imposed by the design standard. In particular, the revised 10MPa limit on shear capacity would result in the threshold concrete compressive strength for which an elevated shear capacity could be accounted for to increase from f_c' = 40MPa to f_c' = 50MPa.

Abstract

The design of concrete beams for shear loading is governed in New Zealand by the provisions of NZS 3101. The shear design provisions of NZS 3101 impose two limits on the permissible design shear capacity, including a maximum shear capacity of 8MPa. This 8MPa limit influences the efficiency of concrete beam design, and in particular the design of concrete bridge beams that have concrete compressive strengths greater than 40MPa. The validity of this limit was assessed through an examination of a number of other international design standards, statistical analyses using databases composed of all previous experimental testing of reinforced concrete (RC) and prestressed concrete (PC) beams, and results from an experimental investigation aimed at addressing deficiencies in the compiled databases.

The research found that the limits in NZS 3101 are excessively conservative compared with the limits imposed in most other design standards. This observation was reinforced by analysis of the databases and results of the experimental investigation, which supported the need for a limit on the nominal design shear capacity but found that an absolute limit of 8MPa was overly restrictive. Alternative limits were proposed, and the absolute limit of 10MPa was found to provide improved design accuracy without compromising safety.

1 Introduction

1.1 Overview

The role of cementitious materials in construction dates back several millennia and includes a wide variety of material forms and structural functions. Over the course of the 20th century, concrete material technology developed significantly and the resulting improvement in material performance, along with improved understanding of the behaviour of concrete, led to increased efficiency in the design and construction of concrete structures. Today, concrete is the most widely used construction materials in New Zealand and in the majority of the developed world (Mehta and Monteiro 2006).

Bridges are an integral part of New Zealand's transportation network. Due to the country's geography, bridges will be required for the foreseeable future regardless of which form of land transport is dominant. Concrete is the most commonly used material in bridge construction in New Zealand, and is the primary material used in a large proportion of New Zealand's bridge stock (Gray et al 2003).

1.2 Web shear in New Zealand concrete bridge beams

Concrete as a material is inherently strong in compression but weak in tension, and is commonly categorised and referred to based on its compressive strength (f_c'). To overcome the deficiencies in tension, concrete beams are reinforced using materials that are known to be stronger in tension than concrete. The most common form of reinforcement is through the use of steel bars placed into the regions of the beam that are expected to experience the greatest tensile stresses. The resulting composite members are commonly referred to as reinforced concrete (RC) beams.

One of the most important developments in concrete construction form is prestressed concrete (PC). PC beams differ from RC beams in that the reinforcement, usually the longitudinal reinforcement provided to resist applied flexural actions, is put into tension during fabrication, independently from the concrete, and then released once the concrete has hardened. Due to strain compatibility requirements, the resulting configuration results in the development of compressive stresses in the concrete. When the PC beam is in service, these built-in compressive stresses must be overcome before any applied loads are able to cause cracking in the concrete. Therefore, application of prestressing partially overcomes the inherent low tensile strength of concrete and allows for the design and construction of beam sections with high flexural efficiency when compared with RC beams. This high flexural efficiency of PC bridge beams has two effects on the shear design of these beams: the development of large shear forces at and near supports; and the utilisation of thinner webs than is typical for RC bridge beams. As a consequence of these two effects, much higher shear stresses are usually developed in PC bridge beam sections near a support than are usually encountered in RC beams.

Historically, the majority of structural concrete has been of relatively low compressive strength (f_c' = 20-40MPa). However, significant development in concrete material technology over the past five decades now provides engineers the option of concrete with much greater compressive strengths. New Zealand bridge designers often specify concrete with compressive strengths up to f_c' = 70MPa, and even higher strengths are used internationally. For significant bridge projects in New Zealand, the use of 70MPa concrete has become common.

The reasons for the use of higher-strength concrete in bridges are two-fold.

- The primary cause of deterioration in concrete bridges is corrosion of the steel reinforcement caused by water-borne salts (dominantly chlorides). An increase in concrete strength leads to higher concrete density and therefore lower permeability, and the decreased permeability helps to alleviate reinforcement corrosion by inhibiting the migration of salts through the concrete and towards the surface of the reinforcement.
- Increased concrete strength is correlated with an increased modulus of elasticity, leading to reduced deformations – therefore an increased concrete compressive strength results in an improvement in the serviceability limit state performance of the bridge.

The shear resistance of concrete structures, whether reinforced or prestressed, is a complex phenomenon due to the influence of several mechanisms and the intricate interactions between these mechanisms. Generally it is assumed that shear is distributed through a beam via a network of diagonal compression struts and transverse tension ties, and a variety of sophisticated models have been developed using this assumption. The inadequacy of concrete to resist the transverse tensile stresses is counteracted by the placement of steel reinforcement in the form of stirrups to resist these stresses. Meanwhile, the concrete is designed to provide sufficient compressive strength to resist the diagonal compressive struts. However, crushing of the diagonal struts is known to result in an undesirable brittle mode of failure. All current design standards, in New Zealand and internationally, impose a limit on the maximum shear stress that a section can resist in order to avoid this form of failure.

New Zealand bridge designers follow the provisions of the *Transit bridge manual* (Transit NZ[1] 2003), which refers to *NZS 3101 Concrete structures standard* (NZS 2006), for the design of concrete beams. The NZS 3101:2006 shear design method is based on procedures developed in the US during the 1960s, which in turn were based on the truss model mentioned above and discussed in further detail in section 2.3.1. The provisions of NZS 3101 impose a limit on the maximum applied shear stress of '$\leq 0.2 f_c'$ or 8MPa', which prevents designers from taking advantage of concrete with compressive strengths greater than 40MPa. However, there is no theoretical or experimental support for imposing an absolute limit on allowable shear stresses. Both NZS 3101 and ACI 318 (ACI 2011) are strongly reliant on experimental data for empirically determined shear capacity provisions, and the experimental datasets that these standards rely on primarily consist of normal-strength concrete units (<40MPa). While there has been an increase in the number of high-strength concrete units tested for shear behaviour in recent years, there is still a relative shortage of tests addressing this issue. It is for this reason that these standards still impose an absolute limit on allowable shear stresses.

1.3 Outline of this report

The main objective of this project was to investigate the validity of the 8MPa shear stress limit found in NZS 3101:2006, through both an experimental investigation and the analysis of other international design standards and previous experimental research. This project was undertaken between June 2008 and July 2012, with all research carried out in Auckland, New Zealand. The project aimed to provide design benefits for New Zealand bridge designers.

- Chapter 2 of this report presents an overview of the behaviour of concrete in shear, and the theoretical models most commonly used to characterise the shear behaviour.

1 Now NZTA.

- Chapter 3 outlines the concrete shear design provisions specified in six major international design standards, including the New Zealand *Concrete structures standard* (NZA 2006).
- Chapter 4 introduces the shear test database, which comprises experimental results of previous research on the shear capacity of concrete beams from all published literature. It also presents details of how this database was used to evaluate the influence of various design parameters on both the shear capacity of the beams in the database and the accuracy of the six design standards in predicting the experimentally observed shear capacity.
- Chapter 5 outlines an experimental investigation conducted during this project on the shear capacity of high-strength prestressed concrete beams and offers preliminary experimental results.
- Chapter 6 presents an analysis of results of the experimental investigation detailed in chapter 5.
- Finally, chapters 7 and 8 present the conclusions and recommendations of the project arising from the research.

2 Models for the behaviour of concrete in shear

A typical concrete beam will be subjected to a combination of three possible actions – bending, shear, and axial tension and compression. The behaviour of a concrete beam when subjected to bending moments or axial forces, both pre- and post-cracking, can be predicted with reasonable accuracy using classical beam theory. However, when subjected to shear forces, including torsion, the behaviour of a concrete beam is much more difficult to predict to a similar level of accuracy. This lack of accuracy is because the mechanisms by which concrete beams resist applied shear forces are numerous, and the interaction between these mechanisms is poorly understood. Section 2.1 presents a summary of these mechanisms.

Due to the generally poor understanding of some concrete shear transfer mechanisms and of the interaction between these mechanisms, a number of theoretical models have been developed by previous researchers in an attempt to explain the behaviour of concrete beams when subjected to shear loading. The most highly used and accepted of these models are detailed in section 2.3.

In attempting to understand the concrete shear design methodology provided by the various international design standards, it is important to thoroughly appreciate the background of these standards. The concrete shear design provisions of all existing design standards are based on empirical interpretations of the shear behaviour models presented in this chapter, while accounting for the limitations imposed by some of the shear transfer mechanisms. Therefore, a critique of the shear behavioural models reported in this chapter was important in determining the primary parameters that needed to be considered when evaluating the shear design standards, as reported in chapters 3 and 4, and when analysing the performance of units that were tested in the experimental investigation, as reported in chapter 6.

2.1 Shear transfer mechanisms

The transfer of shear stresses along a concrete beam is a complex phenomenon that is reliant on numerous mechanisms, and is further complicated by the stress redistributions that occur after concrete cracking. Previous research has identified five shear transfer mechanisms that have significant influence on the shear resistance of reinforced concrete, consisting of:

- shear in the uncracked compression zone of the beam
- dowel action of the longitudinal reinforcement; interface shear due to aggregate interlock
- residual tensile stresses across the cracked concrete
- shear transfer along the transverse reinforcement.

In the case of prestressed concrete, a sixth mechanism can result from the presence of a component of the prestressing force aligned with the applied shear stresses. These mechanisms are assigned differing levels of relative importance by different researchers. Figure 2.1 shows the six possible mechanisms, and each mechanism is discussed in further detail below.

Figure 2.1 Shear transfer mechanisms (Vecchio and Collins 1981)

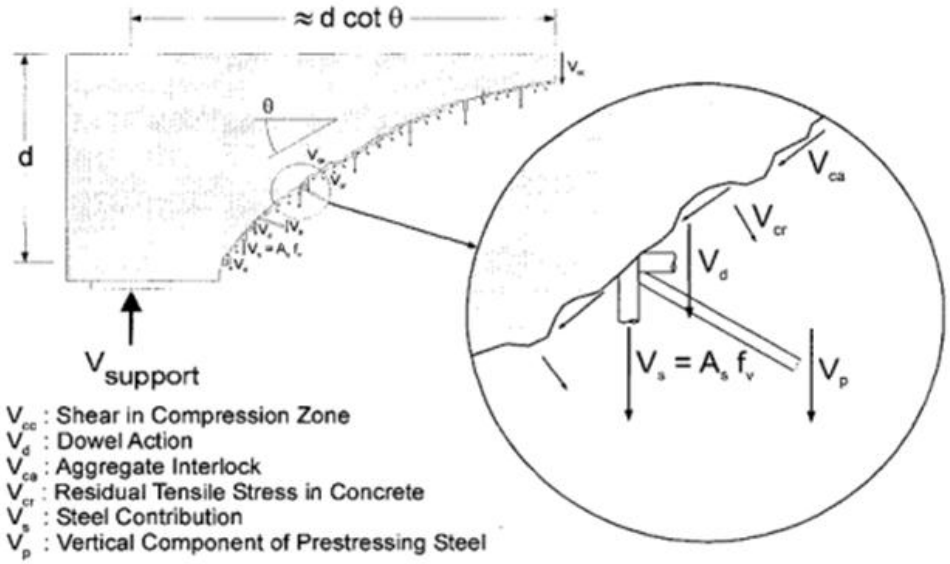

2.1.1 Shear in compression zone

The compression zone in a concrete beam provides some shear resistance before and after cracking of the concrete, and the magnitude of this resistance is based on the depth of the uncracked compression zone (Pang and Hsu 1995). Therefore, as cracking is initiated in the concrete in the form of either flexural or shear cracking, the contribution of the compression zone to the shear capacity of the beam decreases.

For both RC and PC beams, the mechanism of shear transfer through the concrete compression zone is accounted for in all major design standards. This mechanism is predominantly characterised by the concrete contribution component, often termed 'V_c'. As the location and nature of concrete cracking is difficult to predict in design practice, only the contribution of uncracked concrete is usually considered.

2.1.2 Dowel action

Dowel action represents the contribution of the longitudinal reinforcement to resist shear forces once cracking has commenced in the surrounding concrete. The contribution of dowel action to shear resistance is a function of the depth of concrete cover beneath the longitudinal reinforcing bars and the degree to which vertical displacements of those bars at crack locations are restrained by transverse reinforcement (So and Karihaloo 1993). The significance of dowel action is diminished for longitudinal reinforcement with little concrete cover depth, or for beams with no transverse reinforcement (Jelić et al 1999).

2.1.3 Aggregate interlock/interface shear transfer

The mechanism of aggregate interlock is dependent on the compressive strength of the concrete. In normal-strength concrete, the strength of the aggregate exceeds the strength of the cement matrix and inclined shear cracks propagate through the cement matrix. However, in high-strength concrete the strength of the cement matrix exceeds that of the aggregate and therefore inclined shear cracking occurs through the aggregate (Kim 2004). As such, the mechanism of aggregate interlock is more prominent in normal-strength concrete than in high-strength concrete – the mechanism consists of both the interlocking action of exposed aggregate and the shear resistance provided by local roughness of the inclined shear crack plane, whereas only local crack plane roughness can be relied upon to resist shear

stresses in high-strength concrete. The contribution of interface shear transfer to total shear resistance is a function of crack width and, in normal-strength concrete units, of maximum aggregate size (Bazant and Gambarova 1980).

2.1.4 Residual tensile stresses

The ability of concrete to resist tensile stresses is severely compromised following the commencement of cracking, but previous research has shown that cracked concrete is still able to transmit tensile stresses across cracks widths of 0.06–0.16mm (Pang and Hsu 1995). Prior to cracking, and when the crack width is small, the resistance provided by residual tensile stresses is considerable. However, as the crack increases in width its ability to transmit tensile stress is reduced considerably. Therefore, the contribution of residual tensile stresses to shear resistance in large beams is less significant than in small beams, as large cracks are often evident in large beams prior to failure.

2.1.5 Transverse reinforcement

The influence of transverse reinforcement on the shear behaviour of concrete beams is critical, as not only does transverse reinforcement provide a large proportion of the shear resistance where included, but transverse reinforcement also significantly changes the relative contributions of the other mechanisms. Once concrete cracking commences, stirrups crossing these cracks are able to transmit a large proportion of the applied shear force. The magnitude of this proportion is dependent on the angle of shear cracking, which is predicted by different methods in various concrete shear models, and is typically considerably lower for PC beams than for RC beams (Kim 2004). The ability of stirrups to transmit shear stresses across cracks is also significant, as stirrups provide restraint against continuing crack growth following initial crack formation, allowing for a far more ductile failure than that exhibited by beams with no transverse reinforcement (Hsu 1994). Finally, the presence of stirrups provides some resistance to shear displacements along the inclined crack through the mechanism of dowel action. The contribution of transverse reinforcement to the shear capacity of a beam is addressed directly in all major design standards.

2.1.6 Vertical prestressing force

In prestressed beams with draped tendons, such as frequently occur in large-span concrete bridge beams, the vertical component of the prestressing force provides direct resistance to the applied vertical shear forces (Elzanaty et al 1986). This mechanism is addressed directly in all major design standards.

Another mechanism, referred to as ‘arch action’, is also evident in ‘deep’ beams. Deep beams are defined as having a low shear span-to-unit depth ratio (a/d), where the shear span is defined as the shortest distance between an applied load and a support. The limits for this ratio vary between design standards. While research has shown that arch action may be present in beams with an a/d ratio as high as 6–7 (ASCE-ACI 1998), only beams with an a/d ratio lower than 2.5 have been shown to reliably exhibit full deep-beam effects (Tan et al 1995). Arch action is the direct transfer of applied shear to the support through an inclined strut, with a lower a/d ratio resulting in a higher proportion of applied shear being transferred along the inclined strut. However, the significance of this mechanism is minimal for typical concrete bridge beams, as the vast majority of bridge beams are of much longer spans.

2.2 Parameters influencing shear behaviour

The parameters that influence the behaviour of concrete beams with applied shear are markedly different for beams that have transverse reinforcement than for beams with no transverse reinforcement (Bazant

and Kazemi 1991). As virtually all bridge beams contain some transverse reinforcement, the topic of beams without transverse reinforcement was deemed to be outside the scope of this research.

The parameters prescribed in major design standards to influence the capacity of concrete beams are based on the mechanisms discussed above. The mechanisms of shear in compression zone, interface shear transfer and residual tensile stresses are all accounted for through empirical provisions relating to the concrete compressive strength (f_c'). This relationship is based on the observation that all three mechanisms are to some degree dependent on f_c', as discussed above, and the complex nature of these mechanisms necessitates the reliance on empirical relationships. Similarly, the mechanism of dowel action is accounted for in most major design standards through the term 'longitudinal reinforcement ratio' (ρ_l), which is a ratio of the total area of longitudinal reinforcement to the cross-sectional concrete area of the beam.

The major parameter that influences the shear behaviour of concrete beams is the amount of provided transverse reinforcement (ASCE-ACI 1998). As discussed earlier, transverse reinforcement is influential in not only providing shear resistance but also restricting the opening of shear cracks, which in turn increases the influence of interface shear transfer and residual tensile stresses. Unlike the previous mechanisms, the influence of transverse reinforcement is well understood. However, the proportion of applied shear that transverse reinforcement transmits across a crack opening is dependent on the angle of cracking (Collins et al 1996). Prediction of crack angle is addressed differently in various design standards, with prestressing acknowledged to substantially reduce this angle (Kim 2004). The other major factor known to affect the cracking angle, and therefore the contribution of transverse reinforcement to shear resistance, is the ratio of quantity of transverse reinforcement to quantity of longitudinal reinforcement (Elias and Robert 2009).

The contribution of prestressing to shear resistance is addressed directly in design standards, with the vertical component of the prestressing force added to the calculated concrete and transverse reinforcement contributions. And while most design standards account for deep-beam effects in beams with a shear span-to-unit depth ratio of 2.5 or lower, the influence of deep-beam effects is deemed to be minimal for narrower beams (Yang and Ashour 2008), which includes the vast majority of bridge beams.

2.3 Models for concrete shear behaviour

2.3.1 Parallel chord truss models

The concept of a parallel chord truss being used to model the post-cracking behaviour of reinforced concrete when subjected to shear and torsion was originally developed by Ritter in 1899 (Ritter 1899), and modified three years later by Mörsch (Mörsch 1902). In this model, shown in figure 2.2, diagonal concrete struts were considered to be the diagonal members of the truss; horizontal concrete struts in the flexural compression zone were the top chords of the truss; and the transverse and longitudinal reinforcement served as the vertical ties and the chords of the truss respectively.

2.3.1.1 45° truss model

Ritter's original model assumed that diagonal compression was resisted by discrete concrete struts (Vecchio and Collins 1981), as can be seen in figure 2.2(a). Morsch later modified this model by suggesting that the diagonal compression component is composed of a continuous field rather than discrete struts (ibid), as shown in figure 2.2(b).

Figure 2.2 Parallel chord truss model (Collins et al 1996)

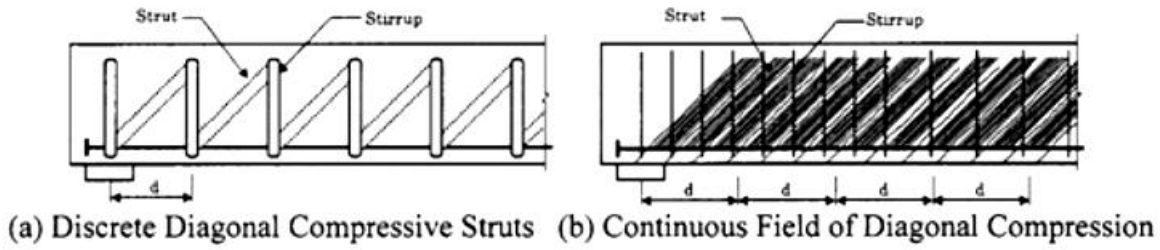

The 45˚ truss model was the original proposed parallel chord truss model, in which the angle of the diagonal concrete struts, and therefore the angle of concrete cracking, is assumed to be 45˚. There are three assumptions associated with this model: first, there are negligible tensile stresses perpendicular to the diagonal compression; second, cracking occurs along the same angle as the diagonal compressive stresses, which is 45˚, and remains so following initial cracking and further load application; and finally, there is a uniform distribution of applied shear stresses over an area defined by the product of b_w (web width) and j_d (flexural lever arm), and no shear is carried by the top and bottom chords (Kim 2004).

The equilibrium conditions at a sectional cut of a concrete beam subjected to bending and shear forces are shown in figure 2.3. Based on these conditions, the design equations for the 45˚ truss model are developed as follows:

$$f_2 = \frac{2V}{b_w j_d} \quad \text{(Equation 2.1)}$$

$$N_v = A_l f_l = V \quad \text{(Equation 2.2)}$$

$$f_v = \frac{Vs}{A_v j_d} \quad \text{(Equation 2.3)}$$

where:

f_2 is the principal compressive stress

f_l and N_v are the tensile stress and force, respectively, in the longitudinal reinforcement

A_l is the area of the longitudinal reinforcement

f_v is the tensile stress in the stirrups, and A_v is the area of stirrups within a spacing of s.

Figure 2.3 Equilibrium conditions for the 45˚ truss model (Sun 2007)

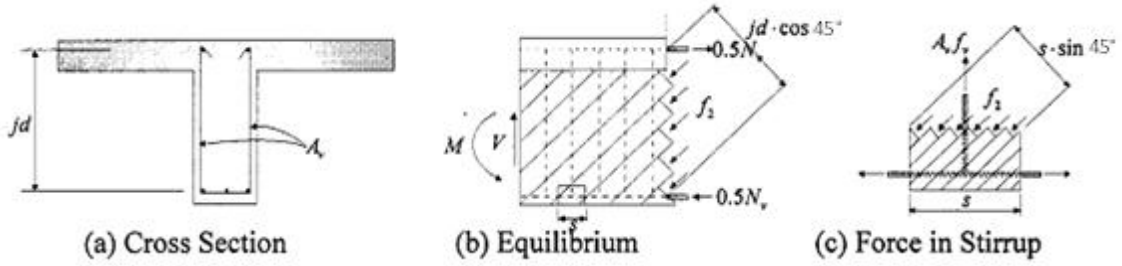

Equation 2.1 was used by engineers to check the diagonal compressive stresses in the concrete and indicate the maximum allowable shear stresses to avoid brittle failure, while equation 2.3 was used to design the amount of transverse reinforcement required for effective shear resistance. However, it was consistently observed by researchers that there was significant discrepancy between experimental results and expected capacities calculated using these equations (ASCE-ACI 1998). Research conducted over the course of the 20th century attributed this discrepancy to the following two major factors:

- The contribution of concrete to shear capacity, V_c: Researchers in the first decade of the 20th century found that measured stirrup stresses in experimental investigations were lower than calculated by equation 2.3 by a relatively constant amount (Collins et al 1996). This observation led to the introduction of V_c into most applications of the 45˚ truss model to account for the concrete shear transfer mechanisms discussed in section 2.1. This concrete contribution was, and for the most part still is, primarily an empirical factor.
- The assumption of a 45˚ compressive strut angle for the derivation of stirrup contribution to shear capacity: In the mid-1960s the 45˚ truss model was again re-examined (Kupfer 1964), as it produced overly conservative shear capacities for beams containing transverse reinforcement. Researchers concluded that this conservatism was due to the reduced effectiveness of stirrups caused by the assumption of a 45˚ compressive strut angle (Kim 2004). Subsequently, considerable effort was directed towards predicting the actual angle of the compressive strut, which led to the variable-angle truss model.

2.3.1.2 Variable-angle truss model

The variable-angle truss model is a variation of the 45˚ truss model in which the angle of diagonal compression, and therefore the angle of crack inclination, is not assumed to be 45˚ but rather is calculated by a variety of methods. This angle has been found to range between approximately 25˚ and 65˚, with different design methods specifying different limits. The equilibrium conditions for this model are similar to those for the 45˚ truss model, and are shown in figure 2.4 and equations 2.4–2.6.

$$f_2 = \frac{V}{b_w j_d}\frac{1}{\sin\theta\cos\theta} = \frac{V}{b_w j_d}(\tan\theta + \cot\theta) \qquad \text{(Equation 2.4)}$$

$$N_v = V\cot\theta \qquad \text{(Equation 2.5)}$$

$$f_v = \frac{Vs}{A_v j_d}\tan\theta \qquad \text{(Equation 2.6)}$$

Figure 2.4 Equilibrium conditions for the variable-angle truss model (Sun 2007)

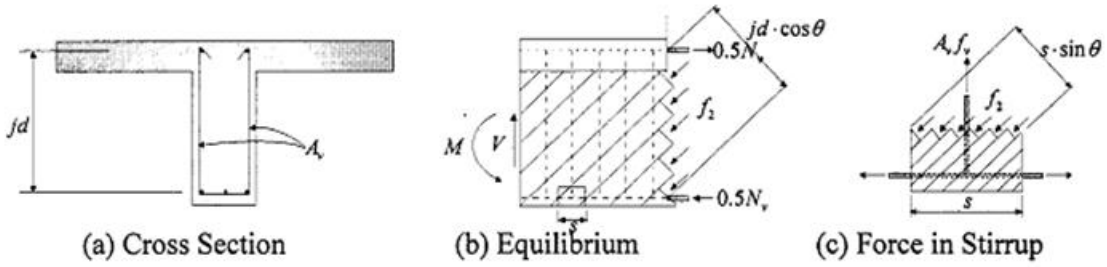

With the introduction of a variable strut angle, ϑ, a fourth variable was introduced into the system of three equilibrium equations, meaning that this system of equations is not solvable for member forces without a prediction or assumption of one of the variables. There have been different approaches used to calculate

ϑ, with the most notable method being proposed by Kupfer in 1964 (Kupfer 1964), involving the use of the principles of minimum energy to determine ϑ while assuming linear elastic behaviour of both concrete and reinforcement. This method was further developed in 1972 by Baumann (Baumann 1972) and most significantly, was adopted by Collins and Vecchio in their Compression Field Theory.

2.3.2 Compression field theories

Compression Field Theory (CFT) and the subsequent Modified Compression Field Theory (MCFT) are the products of extensive research carried out over several decades at the University of Toronto by Professor Michael Collins and several of his colleagues.

2.3.2.1 Compression Field Theory

In 1929, Wagner proposed a 'tension field theory' for the shear design of thin 'stressed-skin' aircraft. By considering shear to be carried by a diagonal tension field after buckling of the thin metal web (Wagner 1929), and by assuming the inclination angle of diagonal tensile stresses to coincide with the inclination angle of the principal tensile strain, Wagner was able to predict the deformations of the system.

Inspired by a combination of Wagner's theory and the work of Kupfer (Kupfer 1964) and Baumann (Baumann 1972), Collins and Mitchell proposed the Compression Field Theory (CFT). CFT used equilibrium conditions (figure 2.5(a) and (b)), compatibility conditions (figure 2.5(c) and (d)) and constitutive material relationships (figure 2.5(e) and (f)), along with the assumption that the angles of diagonal compression and concrete shear cracking coincide. These equilibrium conditions were considered in a similar manner as in the variable angle truss model, leading to equations 2.7–2.9, which when expressed in terms of stresses, are:

$$f_2 = v(tan\,\theta + cot\,\theta) \qquad \text{(Equation 2.7)}$$

$$f_{sx} = \frac{v}{\rho_x} cot\,\theta \qquad \text{(Equation 2.8)}$$

$$f_{sy} = \frac{v}{\rho_v} tan\,\theta \qquad \text{(Equation 2.9)}$$

Manipulation of the compatibility relationships and basic equations found in figure 2.5(c) and (d) results in the following expression:

$$tan^2\,\theta = \frac{\varepsilon_x - \varepsilon_2}{\varepsilon_y - \varepsilon_2} \qquad \text{(Equation 2.10)}$$

Equation 2.10, developed previously by Wagner and Baumann, can be applied to cracked concrete using average (sometimes referred to as 'smeared') strains to determine ϑ. From inspection of equation 2.10 it can be observed that larger (ie steeper) crack angles produce higher longitudinal concrete strains, while smaller (flatter) angles result in higher transverse concrete strains.

Figure 2.5(e) and (f) shows the material stress-strain relationships assumed in the development of CFT. It can be seen that a bilinear stress-strain relationship was assumed for both the longitudinal and the transverse steel reinforcement, while a 'softened' concrete compressive stress-strain relationship for cracked concrete was proposed.

The original 'softened concrete' (Vecchio 1993) model was refined by extensive experimental research, resulting in the following equations, in which concrete softening is expressed as a function of the principal tensile strain, ε_1:

$$\frac{f_{2max}}{f_c'} = \frac{1}{0.8 + 170\varepsilon_1} \leq 1.0 \qquad \text{(Equation 2.11)}$$

$$f_2 = f_{2max}\left[2\left(\frac{\varepsilon_2}{\varepsilon_2'}\right) - \left(\frac{\varepsilon_2}{\varepsilon_2'}\right)^2\right] \qquad \text{(Equation 2.12)}$$

By satisfying equilibrium conditions, compatibility conditions and constitutive material relationships, CFT was able to predict the stress-strain behaviour of concrete when subjected to shear loading for any load up to the point of failure. However, as CFT neglects to account for the tensile stresses in cracked concrete, the model resulted in conservative predictions of shear behaviour, underestimating both shear stiffness and shear capacity (Vecchio and Collins 1986). To correct for this conservatism, the Modified Compression Field Theory (MCFT) was developed.

Figure 2.5 Basic relationships used in compression field theories (Vecchio and Collins 1981)

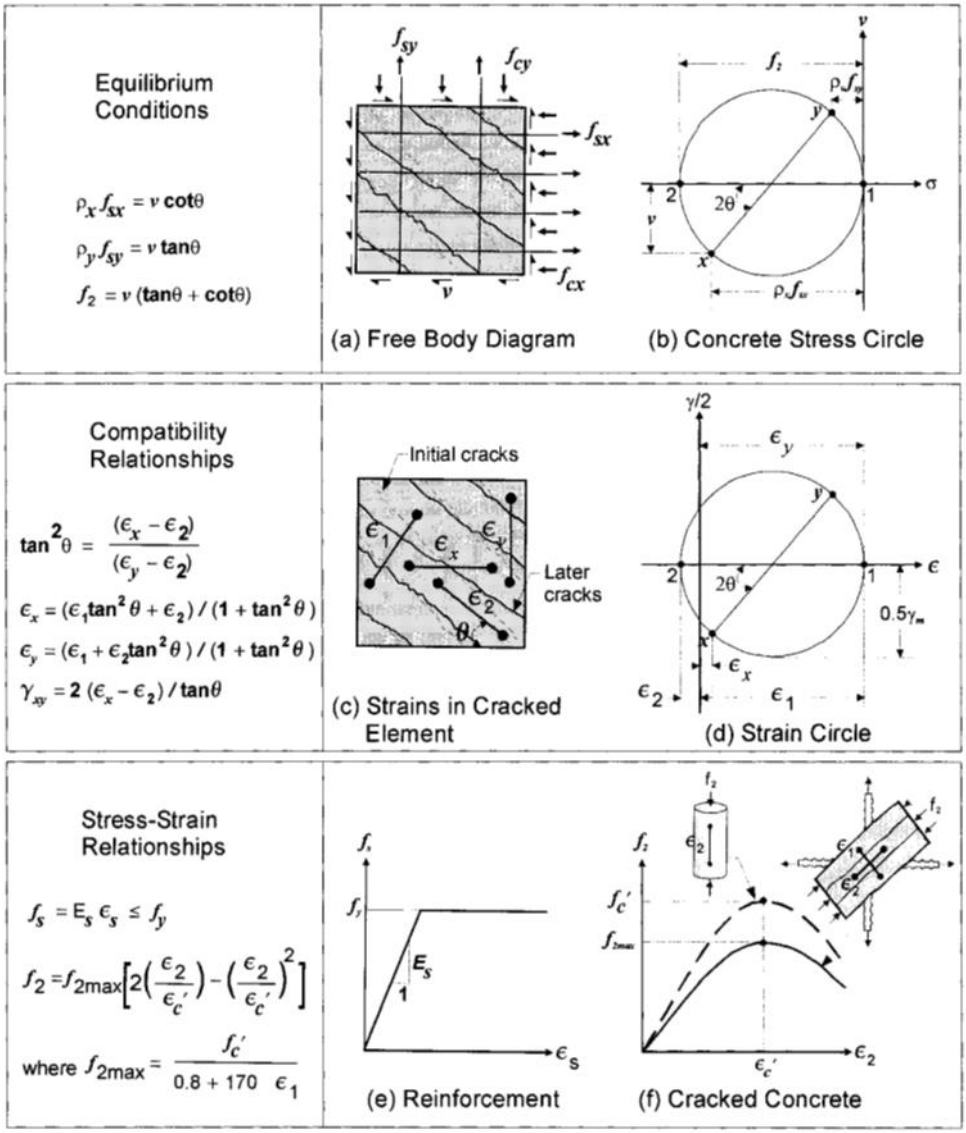

2.3.2.2 Modified Compression Field Theory

To remedy the deficiencies encountered in the CFT, Collins and Vecchio proposed the MCFT in 1986. There were two main improvements in MCFT over CFT: the principal tensile stress was considered and related to the stress transfer across the crack surface; and there was a stronger emphasis on local stress conditions at crack locations as these conditions could be more critical to failure than the average stresses experienced by the beam (Vecchio and Collins 1986). MCFT relies on the same equilibrium conditions, compatibility conditions and constitutive relationships as CFT, with the added complexity of tensile stresses at concrete cracks, resulting in the following equations:

$$f_2 = v(\tan\theta + \cot\theta) - f_1 \quad \text{(Equation 2.13)}$$

$$f_{sx} = \frac{v\cot\theta - f_1}{\rho_x} \quad \text{(Equation 2.14)}$$

$$f_{sy} = \frac{v\tan\theta - f_1}{\rho_y} \quad \text{(Equation 2.15)}$$

where f_1 is the tensile stress in the principal direction after cracking, and all stress terms are average stresses. Collins and Mitchell suggested that f_1 be taken as:

$$f_1 = \frac{f_{cr}}{1 + \sqrt{200\varepsilon_1}} \quad \text{(Equation 2.16)}$$

where f_{cr} is the cracking strength of the concrete. Equations 2.13–2.16 define the response of concrete for average stress-average strain conditions. However, the ultimate capacity of a beam may be governed by the local stress-strain conditions at crack locations (Vecchio and Collins 1986). Therefore, the conditions at a crack also need to be checked.

Concrete is not able to transfer tensile forces across cracks, and therefore the concrete tensile stresses oriented parallel to the longitudinal axis of the beam at a crack will be zero, leading to higher than average tensile stresses in the reinforcement. Meanwhile, the concrete tensile stresses midway between cracks will be higher than the average concrete tensile stress throughout the beam, leading to reduced reinforcement tensile stresses. This phenomenon is referred to as 'tension stiffening'. Assuming cracks to be parallel and using equilibrium conditions at a crack as shown in figure 2.6(c) and (d) results in:

$$\rho_x f_{sxcr} = v\cot\theta + v_{ci}\cot\theta \quad \text{(Equation 2.17)}$$

$$\rho_y f_{sycr} = v\tan\theta - v_{ci}\tan\theta \quad \text{(Equation 2.18)}$$

where v_{ci} is the interface shear stress at a crack. Equations 2.17 and 2.18 show that as v_{ci} increases, the longitudinal reinforcement stress at that crack, $\rho_x f_{sxcr}$, increases while the transverse reinforcement stress at the same crack, $\rho_y f_{sycr}$, decreases. Based on earlier research by Walraven (Walraven 1981), Vecchio and Collins suggested that v_{ci} be expressed as:

$$v_{ci} = 0.18v_{cimax} + 1.64f_{ci} - 0.82\frac{f_{ci}^2}{v_{cimax}} \quad \text{(Equation 2.19)}$$

$$v_{cimax} = \frac{\sqrt{f'_c}}{0.31 + \frac{24w}{a+16}} \quad \text{(Equation 2.20)}$$

where w and a are, respectively, crack width and maximum aggregate size. The expression for v_{ci} was later simplified to:

$$v_{ci} \leq \frac{0.18\sqrt{f'_c}}{0.31 + \frac{24w}{a+16}} \quad \text{(Equation 2.21)}$$

where w is taken as the product of the principal tensile strain, ε_1, and the crack spacing, s_θ,:

$$w = \varepsilon_1 s_\theta \quad \text{(Equation 2.22)}$$

and

$$s_\theta = \frac{1}{\frac{\sin\theta}{s_{mx}} + \frac{\cos\theta}{s_{my}}} \quad \text{(Equation 2.23)}$$

with s_{mx} and s_{my} being the predicted crack spacings in the longitudinal and transverse direction of the beam, respectively.

When a beam is subjected to gravity loads greater than the loads for which that beam was designed, the average stirrup strain exceeds the yield strain. In this case, equations 2.15 and 2.18 become equivalent, leading to:

$$f_1 \leq v_{ci} \tan\theta = \frac{0.18\sqrt{f'_c}}{0.31 + \frac{24w}{a+16}} \tan\theta \quad \text{(Equation 2.24)}$$

The limit imposed on f_1 in equation 2.24 allows the MCFT to account for failure of the aggregate interlock mechanism (Collins et al 1996).

While both the CFT and the MCFT are able to predict the behaviour of concrete beams subjected to shear for all shear loads up to failure, only MCFT considers the contribution of tensile stresses in cracked concrete. It is for this reason that only MCFT is able to predict the shear capacity of beams that have no transverse reinforcement, with CFT predicting a shear capacity of zero for such beams (Collins et al 1996). Using the relationships discussed in this section, a design method for reinforced and PC beams subjected to shear loading was developed and adopted into a number of design standards, including CSA A23.3 2004 and the *AASHTO*[2] *LRFD Bridge design specifications* (AASHTO 2012).

2 American Association of State Highway and Transportation Officials

Figure 2.6 Conditions and relationships used for the Modified Compression Field Theory (Vecchio and Collins 1986)

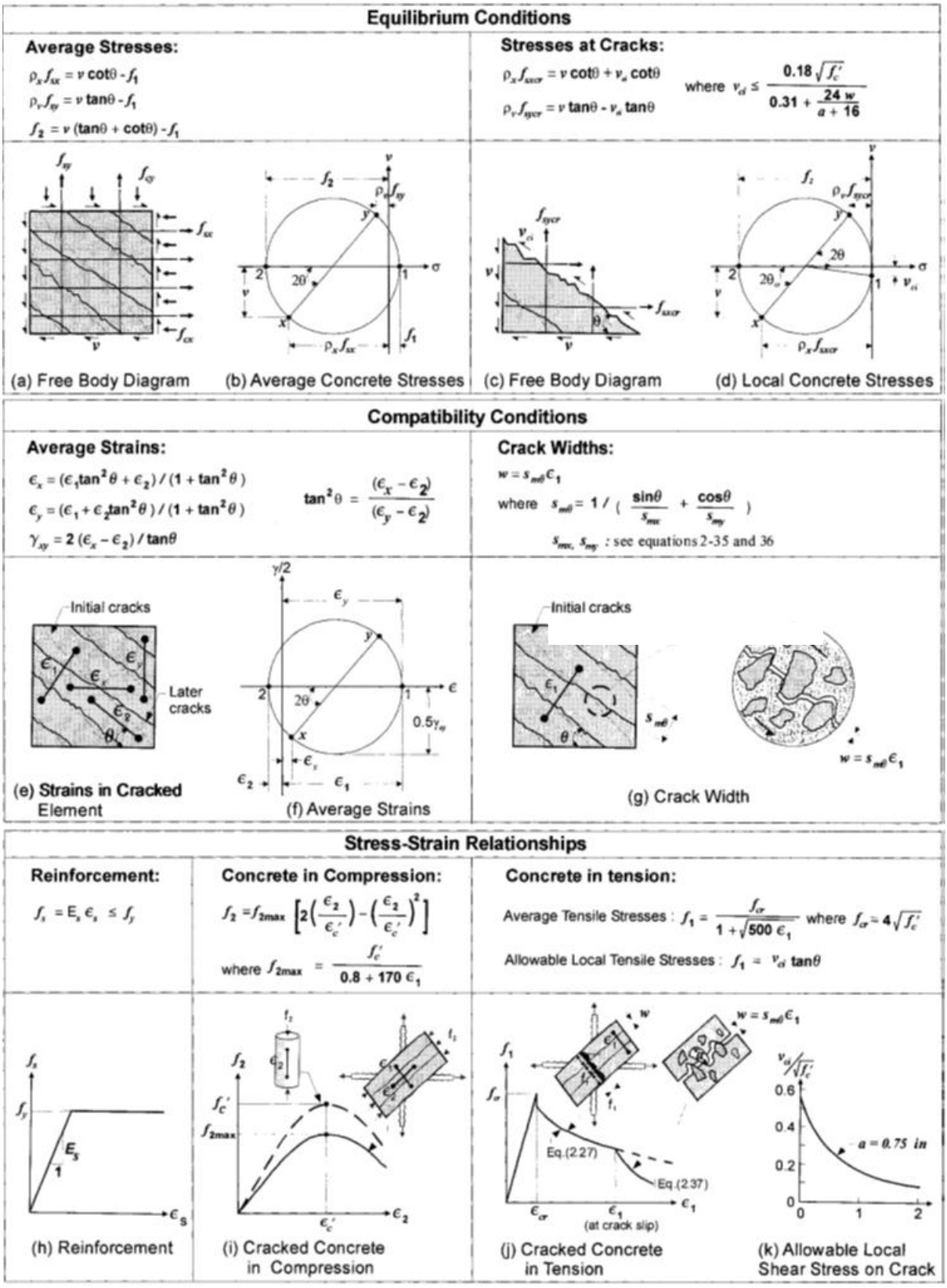

2.3.3 Softened truss models

The softened truss models – the Rotating-Angle Softened-Truss Model (RA-STM) and the Fixed-Angle Softened-Truss Model (FA-STM) – were both developed by Hsu and colleagues over the course of the 1990s. The models were named the 'softened truss models' as they account for the reduced strength and stiffness of cracked concrete in compression when compared with uncracked concrete loaded in uniaxial compression (such as in concrete cylinder testing), which is a phenomenon termed 'concrete softening' (Vecchio 1993). Only the RA-STM is described in this chapter, as this model is the most relevant for design purposes (Kim 2004).

2.3.3.1 Rotating-angle softened truss model

Hsu's original theory of a softened truss model, presented in (Hsu 1988), was later renamed the 'Rotating-Angle Softened Truss Model' (RA-STM) due to the assumption within the model that the angle of cracks in the post-cracking concrete coincides with a 'rotating angle', α, as shown in figure 2.7(a). α is termed the rotating angle because the d-r axes are rotated with respect to the longitudinal-transverse (*l*-t) axes, as shown in figure 2.7(a), to represent the expected angle of cracking.

Figure 2.7 Stress conditions for RA-STM (Hsu 1988)

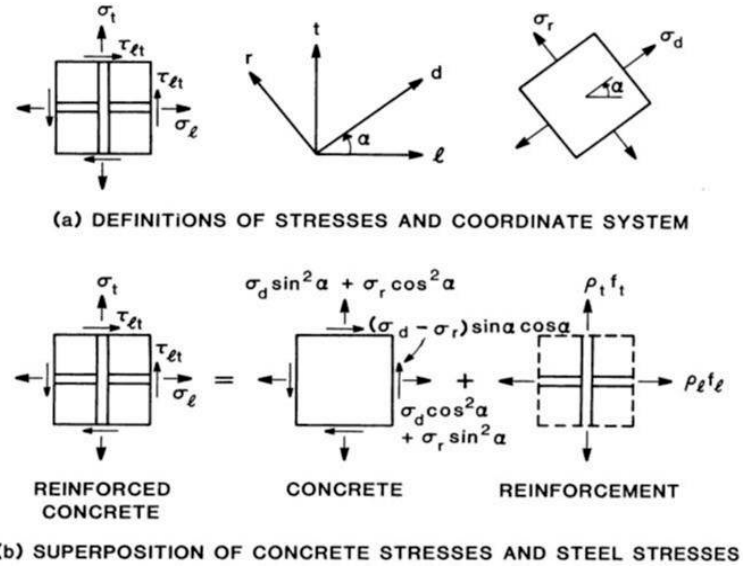

As with compression field theories, the RA-STM employs equilibrium and compatibility conditions, and constitutive material relationships, as well as the definitions presented in figure 2.7, to develop a system of governing stress and strain relationships for a concrete element subject to shear. These relationships can be used to ascertain the stress-strain behaviour of a beam subjected to shear stresses, for any stress or strain not exceeding failure.

The equilibrium relationships used throughout the RA-STM can be established from figure 2.7(b), with terms defined in figure 2.7(a), and by assuming that any longitudinal and transverse steel reinforcement can only resist axial stresses:

$$\sigma_\ell = \sigma_d \cos^2 \alpha + \sigma_r \sin^2 \alpha + \rho_\ell f_\ell \qquad \text{(Equation 2.25)}$$

$$\sigma_t = \sigma_d \sin^2 \alpha + \sigma_r \cos^2 \alpha + \rho_t f_t \qquad \text{(Equation 2.26)}$$

$$\tau_{\ell t} = (\sigma_d - \sigma_r) \sin\alpha \cos\alpha \quad \text{(Equation 2.27)}$$

The assumption that the longitudinal reinforcement in a concrete beam is only able to resist axial stresses indicates that the RA-STM is unable to account for the contribution of dowel action to the shear resistance of a concrete beam.

The compatibility equations derived for use in the RA-STM are established in a similar manner to those of the truss model, with the average strains satisfying Mohr's strain circle, resulting in:

$$\epsilon_\ell = \epsilon_d \cos^2\alpha + \epsilon_r \sin^2\alpha \quad \text{(Equation 2.28)}$$

$$\epsilon_t = \epsilon_d \sin^2\alpha + \epsilon_r \cos^2\alpha \quad \text{(Equation 2.29)}$$

$$\gamma_{\ell t} = 2(\epsilon_d - \epsilon_r) \sin\alpha \cos\alpha \quad \text{(Equation 2.30)}$$

where ϵ_ℓ, ϵ_t, ϵ_d and ϵ_r are average strains in the *l*, t, d and r directions, respectively, and $\gamma_{\ell t}$ is the average shear strain in the *l*-t orientation.

To bind the equilibrium and compatibility conditions of the RA-STM together, a set of constitutive material relationships were proposed by Hsu (1988). For the stress-stress response of concrete in the d-direction, the following equations, proposed by Vecchio and Collins (1981), are used:

$$\sigma_d = \zeta f_c' \left[2\left(\frac{\epsilon_d}{\zeta\epsilon_o}\right) - \left(\frac{\epsilon_d}{\zeta\epsilon_o}\right)^2\right] \qquad |\epsilon_d| \le |\zeta\epsilon_o| \quad \text{(Equation 2.31)}$$

$$\sigma_d = \zeta f_c' \left[1 - \left(\frac{\epsilon_d/\epsilon_o - \zeta}{2 - \zeta}\right)^2\right] \qquad |\epsilon_d| > |\zeta\epsilon_o| \quad \text{(Equation 2.32)}$$

where ϵ_o is the strain at the maximum compressive stress of concrete loaded in uniaxial compression, typically taken to be -0.002 (Vecchio 1993), and ζ is a softening coefficient suggested as:

$$\zeta = \sqrt{\frac{\epsilon_d}{(1-\mu)\epsilon_d - \epsilon_r}} \quad \text{(Equation 2.33)}$$

The strains in equations 2.31–2.33 are defined as negative in compression, positive in tension, and μ in equation 2.33 is Poisson's ratio, with a widely accepted value of 0.3 (Vecchio 1993).

The stress-strain relationship of concrete in the r-direction (ie concrete in tension) is expressed by Hsu as:

$$\sigma_r = E_c\epsilon_r \qquad \epsilon_r \le \epsilon_{cr} \quad \text{(Equation 2.34)}$$

$$\sigma_r = \frac{f_{cr}}{1 + \sqrt{\frac{\epsilon_r - \epsilon_{cr}}{0.005}}} \qquad \epsilon_r > \epsilon_{cr} \quad \text{(Equation 2.35)}$$

where E_c is the initial modulus of elasticity of concrete (taken as $-2f_c'/\epsilon_o$); f_{cr} is the cracking stress of concrete ($0.332\sqrt{f_c'}$, when f_c' is in MPa); and ϵ_{cr} is the concrete strain at cracking (f_{cr}/E_c). Figure 2.8 presents a graphical depiction of the stress-strain relationships detailed in equations 2.31–2.35.

Figure 2.8 Softened concrete stress-strain relationships for RA-STM (Hsu 1994)

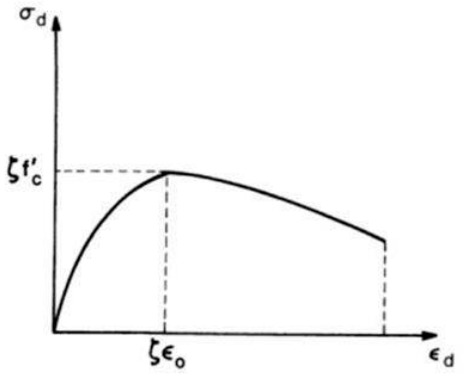

(a) Compression Stress-Strain Relationship

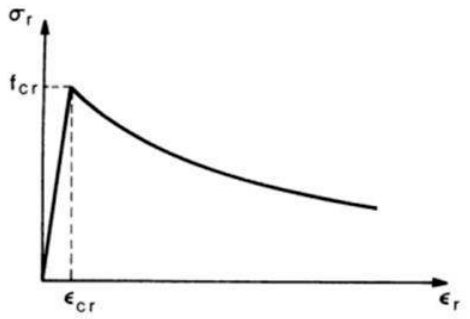

(b) Tension Stress-Strain Relationship

The final set of relationships in the RA-STM is the stress-strain response of longitudinal and transverse reinforcement, assumed to be elastic-perfectly plastic:

$$f = E_s\epsilon \qquad \epsilon < \epsilon_y \qquad \text{(Equation 2.36)}$$

$$f = f_y \qquad \epsilon \geq \epsilon_y \qquad \text{(Equation 2.37)}$$

where E_s, f_y, and ϵ_y are, respectively, the modulus of elasticity, yield stress, and yield strain of the steel reinforcement. Equations 2.36 and 2.37 are applicable to both longitudinal, *l*-direction, and transverse, t-direction, reinforcement.

The relationships detailed above result in a system of 11 governing equations with 14 unknowns, consisting of seven stresses (σ_ℓ, σ_t, σ_d, σ_r, $\tau_{\ell t}$, f_ℓ, and f_t), five strains (ϵ_ℓ, ϵ_t, ϵ_d, ϵ_r, and $\gamma_{\ell t}$), an angle (α) and a material coefficient (ζ). If 3 of the variables are known or reasonably estimated then the system of 11 equations can be used to solve for the remaining 11 variables. For the case of pure shear, σ_ℓ and σ_t are both known to equal zero, meaning that a convenient variable can be chosen to track the loading behaviour of the beam with respect to changes in the chosen variable.

It has been established that the contribution of concrete to shear capacity can be accounted for by the shear stresses developed along the shear cracks in the concrete. The assumption used in the RA-STM that the orientation of the concrete struts coincides with the orientation of the post-cracking principal compressive stress means that in this model shear stresses cannot exist along the assumed shear cracks. Therefore, RA-STM is unable to predict the concrete contribution to shear capacity, producing conservative

predictions for beams with transverse reinforcement and a prediction of zero shear capacity for beams having no transverse reinforcement.

2.4 Conclusions

Presented in this chapter were the various mechanisms by which shear stresses are transferred along a concrete beam; the parameters that are known to influence the performance of concrete beams to transfer those shear stresses; and some of the widely used theoretical models that aim to predict the shear behaviour of concrete beams subjected to shear stresses by accounting for the mechanisms of shear transfer and the influence of various design parameters. It was observed that there are a large number of mechanisms and parameters influencing the shear behaviour and shear capacity of concrete beams, and that the interaction between these mechanisms and parameters continues to be poorly understood. This deficiency is demonstrated by the variety of models for concrete shear behaviour presented in this chapter, and the variety of approaches to concrete shear design provided by the design standards detailed in the following chapter. Based on the shear transfer mechanisms detailed in section 2.1 and the prominent terms found in the shear behaviour models presented in section 2.3, the following parameters were acknowledged as significant for the analyses conducted in subsequent sections:

- concrete compressive strength; beam size, and in particular beam depth
- shear span-to-depth ratio
- quantities of transverse reinforcement and longitudinal reinforcement.

A number of behavioural models were detailed in section 2.3. The main conclusion drawn from the study of behavioural models was that while there has been considerable development in the ability of these models to account for the influence of various shear transfer mechanisms and design parameters, no existing model is able to accurately account for all the relevant factors and the interactions between these factors. Because of the recognised deficiencies of existing models, all current design standards rely, to various extents, on empirical relationships. Reliance on empirical data is only adequate for the range of values of each parameter over which the empirical relationships were developed, and it is for this reason that a number of limits, including the 8MPa limit on allowable shear capacity found in NZS 3101, are imposed on concrete shear design provisions. However, it is the aim of subsequent chapters in this report to examine previous experimental testing and to provide additional experimental data to assess the validity of this 8MPa limit.

3 Design standards

The shear design provisions found in six of the most frequently used design standards globally are presented in this chapter. The provisions detailed are: ACI 318-11; NZS 3101:2006; CSA A23.3-04; *AAHSTO LRFD Bridge design specifications*; Eurocode EC2 (CEN 2005); and the fib Model Code 2010.

All current concrete structural design standards commonly used by designers globally are based on a combination of theoretical models, as detailed in chapter 2, and empirically determined parameters. Of the models discussed in chapter 2, current major international design standards rely primarily on two models: the parallel-chord truss model; and the Modified Compression Field Theory.

Due to the reliance on empirically developed relationships by existing design standards and the often considerable difference in shear response of RC and PC sections, some standards offer a set of shear design provisions for PC beams that are separate from the shear provisions for RC beams. Where applicable, both sets of shear provisions are discussed in the subsequent sections. All equations presented in the subsequent sections of this chapter were based on SI units, and equations from standards utilising different unit systems were converted for use with SI units.

3.1 ACI 318-11

ACI 318-11: Building code requirements for structural concrete (ACI 2011) is the most recent version of the code developed by the American Concrete Institute (ACI). ACI 318 is regularly used by structural engineers in the US, although bridge designers are known to more frequently use the shear provisions in AASHTO LRFD (discussed in section 3.3) (Kim 2004). The ACI code is of particular relevance to New Zealand engineers as it is the basis for NZS 3101, which is the concrete structures standard governing shear design for New Zealand engineers. The concrete shear design provisions of the Australian design standard *AS 5100.5 – Bridge design – Concrete* are also based on ACI 318, but contain a maximum limit on allowable design shear capacity of $0.2f_c'$ and a maximum design concrete compressive strength of 65MPa. Therefore, the maximum allowable design shear capacity in AS 5100.5 is 13MPa. ACI 318-11 contains separate shear provisions for RC and PC beams.

3.1.1 Reinforced concrete (RC) beams

The provisions in ACI 318 for RC beams are based on the 45° truss model discussed in section 2.3.1.1. However, when this model was originally introduced into the ACI code, it was observed to be overly conservative when compared with experimental results (Kim 2004, ASCE-ACI 1998). This excessive conservatism was due to the assumption inherent in the truss model of zero shear capacity for beams with no transverse reinforcement, and the resulting implication of zero contribution to a section's shear capacity from the concrete. This assumption was known to be inaccurate (Vecchio and Collins 1986), and so to account for the contribution of concrete to shear resistance a concrete contribution term, V_c, was subsequently added to the steel contribution, V_s, from the 45° truss model.

The equation arrived at by ACI-ASCE Committee 326 in 1962 to account for the concrete contribution to shear capacity was based on the shear at inclined cracking, because beams without transverse reinforcement often failed simultaneously with the initiation of inclined cracking.

Unless designed by strut-and-tie methods, the nominal shear capacity of a RC beam is taken as the sum of the concrete contribution, V_c, and the transverse reinforcement contribution, V_s:

$$V_n = V_c + V_s \quad \text{(Equation 3.1)}$$

where V_c can be calculated by either of the following two equations:

$$V_c = \left(\frac{\sqrt{f_c'}}{6}\right) b_w d \quad \text{(Equation 3.2)}$$

$$V_c = \left(\sqrt{f_c'} + 120\rho_w \frac{V_u d}{M_u}\right) \frac{b_w d}{7} \leq 0.3\sqrt{f_c'} b_w d, \qquad \frac{V_u d}{M_u} \leq 1.0 \quad \text{(Equation 3.3)}$$

and V_s is calculated as:

$$V_s = \frac{A_v f_{vy} d}{s} \leq 0.66\sqrt{f_c'} b_w d \quad \text{(Equation 3.4)}$$

where M_u is the maximum factored bending moment in the beam during the application of external loading, and V_u is the corresponding shear force.

Equation 3.3 is rarely used by engineers because it is the more complex of the two equations provided for calculating the concrete contribution to shear capacity, but seldom provides a significant increase in predicted shear capacity (Elias 2009). The transverse reinforcement contribution calculated using equation 3.4 is based on the 45° truss model, with a maximum limit placed in order to avoid crushing of the concrete compression struts and to guard against excessive crack widths. A further limit is placed on the maximum design shear capacity by limiting the concrete compressive strength value used in shear capacity calculations to 69MPa for beams with less than the prescribed minimum level of transverse reinforcement. ACI 318-11 prescribes the minimum allowable transverse reinforcement required for beams with a design shear force exceeding half of the calculated concrete contribution as:

$$A_{v,min} = 0.062\sqrt{f_c'} \frac{b_w s}{f_{vy}} \quad \text{(Equation 3.5)}$$

3.1.2 Prestressed concrete (PC) beams

ACI 318-11 provides two independent methods for calculating the shear capacity of a PC beam: a simplified method; and a detailed method. The simplified method provides the following equation for calculating the concrete contribution to shear capacity:

$$0.17\sqrt{f_c'} b_w d \leq V_c = \left(0.05\sqrt{f_c'} + 4.8\frac{V_u d_p}{M_u}\right) b_w d \leq 0.42\sqrt{f_c'} b_w d \quad \text{(Equation 3.6)}$$

where $\frac{V_u d_p}{M_u} \leq 1.0$. The concrete contribution calculated using equation 3.6 also should not exceed the web-shear cracking strength, V_{cw}, which is given in the detailed method.

As well as the concrete contribution and transverse reinforcement contribution, the detailed method also accounts for the contribution of vertical components of prestressing, V_p, which impose vertical compressive stresses on the concrete. During loading, the vertical compressive stresses must be overcome before the concrete surrounding the prestressing can be subjected to the tensile stresses necessary for

cracking to commence. V_p accounts for the resulting enhancement in shear capacity due to prestressing, taken as the vertical component of the prestressing force in the tendons.

The two possible mechanisms of cracking in a PC beam are web-shear cracking and flexure-shear cracking. The detailed method in ACI 318 accounts for these two distinct modes of cracking by introducing two separate equations. Web-shear cracking occurs in regions of high shear stress when the tensile strength of the concrete is exceeded by the principal tensile stress in that region. The web-shear cracking force, V_{cw}, specified in ACI 318 is:

$$V_{cw} = \left(0.29\sqrt{f_c'} + 0.3f_{pc}\right) b_w d_p + V_p \qquad \text{(Equation 3.7)}$$

in which f_{pc} is the compressive stress in the concrete (after allowance for all prestress losses) at the centroid of the section that is resisting the externally applied loads.

In beam regions where high bending moments and moderate-to-high shear forces are applied simultaneously, flexure-shear cracking is known to initiate before the section reaches its web-shear cracking capacity (Lyngberg 1976). The first phase of flexure-shear cracking is the formation of vertical flexural cracks caused by the application of high flexural stresses. As the flexural cracks spread further into the section, the effective concrete area available to resist the applied shear force decreases. The decreased effective shear area results in a higher applied shear stress that leads to the commencement of shear cracking, propagating from the ends of the flexural cracks. Therefore, the flexure-shear cracking capacity of a section is dependent on both the cracking-moment capacity, M_{cr}, and some tensile capacity of the concrete (typically considered to be a function of $\sqrt{f_c'}$). ACI 318 defines the cracking moment as:

$$M_{cr} = \left(\frac{I}{y_t}\right)\left(0.5\sqrt{f_c'} + f_{pe} - f_d\right) \qquad \text{(Equation 3.8)}$$

and the resulting flexure-shear capacity as:

$$V_{ci} = 0.05\sqrt{f_c'} b_w d_p + V_d + \frac{V_u M_{cr}}{M_u} \geq 0.14\sqrt{f_c'} b_w d \qquad \text{(Equation 3.9)}$$

In equations 3.8 and 3.9:

- f_{pe} is the compressive stress in concrete due to effective prestress forces only (after allowance for all prestress losses) at the extreme tensile fibre of the section when external loads are applied
- f_d is the stress due to factored dead load at the extreme tensile fibre of the section when external loads are applied
- V_d is the shear force due to dead load.

It is important to note that while vertical prestressing components increase the web-shear cracking capacity, they have no equivalent effect on flexure-shear capacity. Therefore, while the use of draped strands may result in an increased web-shear capacity of the section, these strands may lead to a decreased flexure-shear capacity due to the reduced effective depth, d.

As for RC beams, the contribution of transverse reinforcement to the shear capacity of a PC section is accounted for using the 45° truss model. Thus, V_s for PC beams is calculated using equation 3.4.

3.2 NZS 3101:2006

New Zealand bridge designers follow the provisions of section 4.2 of the *Transit bridge manual* (TNZ 2003), which addresses the design of RC and PC beams by referring directly to *NZS 3101 Concrete structures standard* (NZS 2006). The shear design provisions found in NZS 3101 are based on those found in ACI 318, as detailed above, using the 45° truss model as the core basis.

The transverse reinforcement contribution for both RC and PC beams is calculated in NZS 3101, using an identical equation to that specified in ACI 318, found above as equation 3.4. Clause 7.5.2 of NZS 3101 limits the maximum allowable nominal shear stress to be the smaller of $0.2f_c'$ or 8MPa. Therefore, all beams with a concrete compressive strength greater than 40MPa are limited to the same maximum nominal shear stress as beams with 40MPa concrete strength.

3.2.1 RC beams

As with ACI 318, NZS 3101 predicts the shear capacity of RC beams by combining the contributions attributed to concrete, V_c, and transverse reinforcement, V_s. The concrete contribution is given as:

$$V_c = k_a k_d v_b b_w d \qquad \text{(Equation 3.10)}$$

in which:

$$0.08\sqrt{f_c'} \le v_b = (0.07 + 10\rho_w)\sqrt{f_c'} \le 0.2\sqrt{f_c'} \qquad \text{(Equation 3.11)}$$

k_a in equation 3.10 is a factor to account for the influence of maximum aggregate size, taken as 0.85 and 1.0 for maximum aggregate sizes lower than 10mm and greater than 20mm respectively, and interpolated for intermediate values of maximum aggregate size. k_d is a factor allowing for the influence of beam depth, taken as 1.0 for beams with transverse reinforcement equal to or greater than the minimum transverse reinforcement. The value of unity for k_d is consistent with findings from previous research indicating that size effects are relatively insignificant for beams containing transverse reinforcement (ASCE-ACI 1998, Bazant and Kazemi 1991, So and Karihaloo 1993). The minimum area of transverse reinforcement required by NZS 3101 is the same as that required by ACI 318, as specified in equation 3.5. The value of f_c' to be used in calculating v_b in equation 3.11 is limited to a maximum of 50MPa.

The transverse reinforcement contribution specified in NZS 3101 is identical to the provision in ACI 318, set out in equation 3.4.

3.2.2 PC beams

Similarly to the provisions of ACI 318, a choice of two methods is presented in NZS 3101 for designers to calculate the concrete contribution to the shear capacity of PC beams. The simplified method provides the following equation:

$$0.14\sqrt{f_c'}b_w d \le V_c = \left(\frac{\sqrt{f_c'}}{20} + 5\frac{V_u d_c}{M_u}\right) b_w d \le 0.4\sqrt{f_c'}b_w d \qquad \text{(Equation 3.12)}$$

It is clear that equation 3.12 is almost identical to equation 3.6, used in ACI 318, except for a slight difference in the constants used.

The general method provided in ACI 318 accounts for the two possible cracking mechanisms: web-shear cracking and flexure-shear cracking. The concrete contribution is taken as the lower of the two components, calculated using the following sets of equations:

$$V_{cw} = 0.3\left(\sqrt{f_c'} + f_{pc} + f_{sw}\right) b_w d + V_p \quad \text{(Equation 3.13)}$$

$$V_{ci} = V_b + \frac{V_u M_o}{M_u} \geq 0.14\sqrt{f_c'} b_w d \quad \text{(Equation 3.14)}$$

$$M_o = \left(\frac{I}{y_t}\right)\left(f_{pe} + f_{ss}\right) \quad \text{(Equation 3.15)}$$

f_{sw} in equation 3.13 is the longitudinal prestress and f_{sw} is the corresponding stress at the neutral axis due to this prestress and the self-weight of the beam. The V_b term referred to in equation 3.14 is equal to the concrete contribution, V_c, of an equivalent RC beam. f_{ss}, referred to in equation 3.15, is the stress due to prestress and self-weight at the extreme tension fibre during loading.

3.3 CSA A23.3-04 and AASHTO LRFD 6th edition

The method set out in the Canadian Standards Association (CSA) document *A23.3-04: Design of concrete structures* (CSA 2004) is based on the Modified Compression Field Theory (MCFT) discussed in section 2.3.2.2. The Canadian standard was the first international design standard to incorporate MCFT into a formal design process (ASCE-ACI 1998). The departure from using truss models as a basis for the design process was significant, as MCFT allows for a holistic design approach that incorporates the influence of all actions, including prestressing, on a section. Therefore CSA A23.3, as with other MCFT-based design standards, provides a single procedure for both RC and PC beams.

The procedure first introduced into CSA A23.3 has been gradually introduced into the *AASHTO LRFD Load and resistance factor design* (AASHTO 2012). Previous revisions of the AASHTO LRFD specifications varied in their implementations of MCFT into the design procedure, and sometimes required iteration. However, the shear design methodology provided in the most recent revision (6th edition, 2012) of AASHTO LRFD is identical to the methodology found in CSA A23.3. The concrete shear design provisions of the Canadian Highway Bridge Design Code (CHBDC) were also noted to directly mirror those found in CSA A23.3.

The nominal shear resistance of a beam, according to CSA A23.3, is composed of:

$$V_n = V_c + V_s + V_p \leq 0.25 f_c' b_w \mathrm{d} + V_p \quad \text{(Equation 3.16)}$$

for which:

$$V_c = \beta\sqrt{f_c'} b_w \mathrm{d} \leq 8\beta b_w \mathrm{d} \quad \text{(Equation 3.17)}$$

$$V_s = \frac{A_v f_{vy} d \cot\theta}{s} \quad \text{(Equation 3.18)}$$

β, found in equation 3.17, is a factor accounting for the shear resistance of cracked concrete, while θ in equation 3.18 is the angle of inclination of the diagonal compressive stresses to the longitudinal axis of the beam. Both of these terms are determined based on the calculated longitudinal strain, which is the principal term in this procedure used to define the predicted shear performance of concrete beams. Of particular significance is the limit in equation 3.16, which is noted to be applied to avoid crushing failure

of the diagonal concrete compressive struts. This $0.25f_c'$ limit therefore serves the same purpose as the '$0.2f_c'$ *or 8MPa'* limit in NZS 3101, but is set at a higher value and has no direct absolute upper maximum. However, both CSA A23.3 and AASHTO LRFD specify maximum design concrete compressive strengths to be used when using each standard. CSA A23.3 limits design concrete compressive strengths to 80MPa, which result in a maximum design shear capacity of 20MPa, while AASHTO LRFD specifies a maximum design concrete compressive strength of 69MPa (10ksi), which equates to a maximum design shear capacity of 17.25MPa.

The longitudinal strain at mid-depth of the beam, ε_x, is calculated in CSA A23.3 using:

$$0 \leq \varepsilon_x = \frac{M_u/_d + 0.5N_u + V_u - V_p - A_p f_{po}}{2\left(E_s A_s + E_p A_p\right)} \leq 3.00 \times 10^{-3} \quad \text{(Equation 3.19)}$$

and the resulting equations of most relevance to bridge designers are:

$$\beta = \frac{0.40}{(1 + 1500\varepsilon_x)} \quad \text{(Equation 3.20)}$$

$$\theta = 29 + 7000\varepsilon_x \quad \text{(Equation 3.21)}$$

where M_u, N_u and V_u are the maximum bending moment, axial force and shear force applied, respectively. f_{po} is the stress in the prestressing strands when strain in the surrounding concrete is zero, and is usually taken as $0.7f_{pu}$ for bonded reinforcement outside the transfer length. Equation 3.21 shows that this design procedure allows for significantly lower angles of diagonal compressive struts, and therefore lower angles of shear crack inclination, than is assumed in ACI 318 or NZS 3101, resulting in significantly larger transverse reinforcement contributions to shear capacity.

3.4 Eurocode 2 (EC2)

The most recent revision of the European Standards Eurocode 2 *Design of concrete structures* (EC2) (CEN 2005) was published in 2005, with the section of most relevance to bridge engineers being 'Part 2: Concrete bridges – design and detailing rules'. The format of EC2 is such that, in many instances, only recommended values or specifications are given and the values used in different countries are varied as deemed fit via a National Annex. Where applicable, recommended values have been presented in the following outline.

It is important to note that EC2 uses the term f_{ck} when referring to 28-day compressive cylinder strength, although the standard cylinders used in Europe differ considerably from the cylinders used in New Zealand. However, previous research (Day 1994) has shown that results from testing cylinders constructed of the different sizes differ by less than 5% and can be considered equivalent. Therefore, in the following equations f_{ck} has been replaced with f_c', for consistency with the notation used in previous sections of this report.

The design value for the uniaxial concrete compressive strength, based on f_c', is:

$$f_{cd} = \frac{\alpha_{cc} f_c'}{\gamma_c} \quad \text{(Equation 3.22)}$$

where γ_c is the partial safety factor for concrete (normally taken as 1.5), and α_{cc} is the coefficient used to take account of long-term effects on the compressive strength, with a recommended value of 1.

EC2 offers separate equations for beams with and without transverse reinforcement, with the latter deemed largely irrelevant for bridge design, as the vast majority of concrete bridge beams contain transverse reinforcement. Only one design method is provided for beams with transverse reinforcement, based on the variable-angle truss model described in section 2.3.1.2.

The nominal shear resistance, V_{Rd}, is the smaller of:

$$V_{Rd,s} = \frac{A_v}{s} d f_{vy} \cot\theta \quad \text{(Equation 3.23)}$$

and

$$V_{Rd,max} = \left[\frac{\alpha_{cw} v_1 f_{cd}}{\cot\theta + \tan\theta}\right] b_w d \quad \text{(Equation 3.24)}$$

in which α_{cw} is a coefficient used to account for the interaction between stress in the compression chord and any applied axial compressive stress, and v_1 is a strength reduction factor for concrete that has cracked due to shear loads. The recommended values of these two terms are:

$$\alpha_{cw} = \begin{cases} 1, \text{for RC beams} \\ 1 + {}^{\sigma_{cp}}/_{f_{cd}}, \text{for } 0 < \sigma_{cp} \leq 0.25 f_{cd} \\ 1.25, \text{for } 0.25 f_{cd} < \sigma_{cp} \leq 0.5 f_{cd} \\ 2.5\left(1 - {}^{\sigma_{cp}}/_{f_{cd}}\right), \text{for } 0.5 f_{cd} < \sigma_{cp} \leq 1.0 f_{cd} \end{cases} \quad \text{(Equation 3.25)}$$

$$v_1 = 0.6(1 - {}^{f_c'}/_{250}) \quad \text{(Equation 3.26)}$$

σ_{cp} is the mean compressive stress in the concrete due to the design axial force. This stress is obtained by averaging the compression applied to the section, including prestressing effects, over the cross-sectional area of the beam taking account of all longitudinal reinforcement.

The limits placed in EC2 on the shear capacity calculations are threefold. First, EC2 is applicable to beams with concrete compressive strengths up to, and including, 90MPa. Second, the angle of compressive strut inclination is limited to $1 \leq \cot\theta \leq 2.5$, allowing for inclination angles as low as 21.8°. Finally, the maximum effective cross-sectional area of the transverse reinforcement, $A_{v,max}$, for $\cot\theta = 1$ is given by:

$$\frac{A_{v,max} f_{vy}}{b_w s} \leq \frac{1}{2} \alpha_{cw} v_1 f_c' \quad \text{(Equation 3.27)}$$

3.5 fib model code 2010

The latest revision of the Model Code released by fib as *fib Bulletin 66: model code 2010* (fib 2010) allows for four levels of approximation for the shear capacity of a concrete beam. The first of the three levels utilise different models of concrete shear behaviour to provide increasingly sophisticated estimates of ultimate shear capacity, while the fourth level of approximation allows the engineer to determine the ultimate shear capacity based on applicable conditions of strain equilibrium and compatibility. The 'Level I Approximation' is based on a variable angle truss model, with no allowance for the contribution of the concrete to ultimate shear capacity, and minimum angles of inclination of the compressive stress field of 25° for PC beams and 30° for RC beams. The 'Level II Approximation' is based on a generalised stress field approach, with an ultimate shear capacity consisting solely of the contribution of transverse reinforcement

and an angle of compressive stress field inclination based on the longitudinal strain at mid-depth of the beam.

The 'Level III Approximation' is based on the Modified Compression Field Theory. The nominal design shear capacity, V_{Rd}, of RC and PC beams is given by:

$$V_{Rd} = \begin{cases} V_s + V_c, \text{for } V_s + V_c \leq V_{Rd,max}(\theta_{min}) \\ V_s, \text{for } V_s + V_c > V_{Rd,max}(\theta_{min}) \end{cases} \quad \text{(Equation 3.28)}$$

where

$$V_{Rd,max}(\theta_{min}) = \frac{k_c f_c'}{\gamma_c} b_w z \sin\theta_{min} \cos\theta_{min} \quad \text{(Equation 3.29)}$$

The minimum allowable angle of compressive strut inclination, θ_{min}, is given by:

$$\theta_{min} = 20 + 10000\varepsilon_x \quad \text{(Equation 3.30)}$$

where the longitudinal strain at mid-depth of the beam, ε_x, is defined as:

$$0 \leq \varepsilon_x = \frac{M_u/_z + V_u + N_u \frac{(z_p - e_p)}{z}}{2\left(\frac{z_s}{z} E_s A_s + \frac{z_p}{z} E_p A_p\right)} \leq 3.00 \times 10^{-3} \quad \text{(Equation 3.31)}$$

z, z_s, and z_p in equation 3.31 are the overall flexural lever arm, the flexural lever arm to the non-prestressed longitudinal reinforcement, and the flexural lever arm to the prestressed longitudinal reinforcement, respectively. e_p is the distance between the neutral axis and the centre of the prestressed longitudinal reinforcement.

The transverse reinforcement contribution, V_s, and concrete contribution, V_c, to ultimate shear capacity are given by:

$$\boldsymbol{V_s = \frac{A_v}{s} f_{vy} z \cot\theta} \quad \text{(Equation 3.32)}$$

$$\boldsymbol{V_c = k_v \frac{\sqrt{f_c'}}{\gamma_c} b_w z \leq k_v \frac{8}{\gamma_c} b_w z} \quad \text{(Equation 3.33)}$$

where the k factors used in equations 3.29–3.33 are defined as:

$$\boldsymbol{k_\varepsilon = \frac{1}{1.2 + 55\varepsilon_1} \leq 0.65} \quad \text{(Equation 3.34)}$$

$$\boldsymbol{k_v = \frac{0.4}{1 + 1500\varepsilon_x}\left(1 - \frac{V_u}{V_{Rd,max}(\theta_{min})}\right) \geq 0} \quad \text{(Equation 3.35)}$$

$$\boldsymbol{k_c = k_\varepsilon \eta_{fc}} \quad \text{(Equation 3.36)}$$

$$\boldsymbol{\eta_{fc} = \left(\frac{30}{f_c'}\right)^{1/3} \leq 1.0} \quad \text{(Equation 3.37)}$$

The concrete compressive strength, f_c', is limited in the fib model code to 120MPa.

3.6 Comparison of design standards

It is clear from inspection of the shear design provisions of the six design standards discussed in this chapter that no consensus exists for the best approach to shear design of a concrete beam. While there is some similarity in the method used by each design standard to predict the transverse reinforcement contribution, the predicted contributions can differ significantly due to the angle of cracking assumed in each standard. ACI 318 and NZS 3101 assume a 45° cracking angle, CSA A23.3 and AASHTO LRFD predict

this angle using a method based on the MCFT, and EC2 allows for the use of a cracking angle other than 45° but provides no explicit guidance as to how this angle may be predicted. The fib model code was not included in this comparison, due to the lack of a limit on ultimate shear capacity in the shear design provisions of this design standard.

The design standards presented in this chapter differ more in their approach to accounting for the contribution of concrete to shear capacity than they do for the prediction of the contribution of transverse reinforcement. ACI 318 and NZS 3101 both use strongly empirical relationships, while CSA A23.3 and AASH LRFD augment the MCFT with some empirical relationships. EC2 differs from the other four design standards in that the relationships it specifies for transverse reinforcement contribution and concrete contribution are not combined, but rather the shear capacity is taken as the lower of the two calculated contributions.

As well as differing in the approaches used to predict the shear capacity of concrete beams, the six design standards also impose varying limits on the maximum design shear capacity. Five of the six standards express this limit as a function of f_c'. While NZS 3101 is the only standard of the six standards detailed in this chapter to also impose an absolute limit on design shear capacity, the other four standards achieve this limit indirectly by instead limiting the maximum value of design concrete compressive strength. Figure 3.1 presents a comparison of these maximum limits for concrete compressive strengths up to 120MPa. In the case of EC2 there are two limits shown to account for the different values of α_{cw} specified for RC and PC beams. EC2 specifies α_{cw} = 1 for RC beams, while the maximum possible value of α_{cw} for a PC beam of 1.25 was used for this comparison. It was observed during this comparison that for all concrete strengths greater than 18MPa, NZS 3101 imposed the second-lowest limit on shear capacity, with ACI 318 specifying the lowest limit. While the difference in these limits between the standards is significant for normal strength concrete ($f_c' \leq$ 40MPa), this difference is much greater for higher concrete compressive strengths. In the case of a beam constructed with a concrete compressive strength of 70MPa, CSA A23.3 (17.5MPa) and AASHTO LRFD (17.25MPa) specifications allow for a maximum design shear capacity more than twice that allowable in NZS 3101 (8MPa). EC2 limits the shear capacity of RC and PC beams with concrete compressive strengths of 70MPa to 15.1MPa and 18.9MPa, respectively.

Two additional design standards, CHBDC and AS 5100.5, were briefly investigated and found to be closely aligned in their approaches to concrete shear design to CSA A23.3 and ACI 318, respectively. The maximum allowable design shear capacity in CHBDC was identical to that specified in CSA A23.3, while AS 5100.5 allowed for a maximum design shear capacity of $0.2f_c'$ with a maximum design concrete compressive strength of 65MPa.

Figure 3.1 Maximum design shear capacity specified by design standards

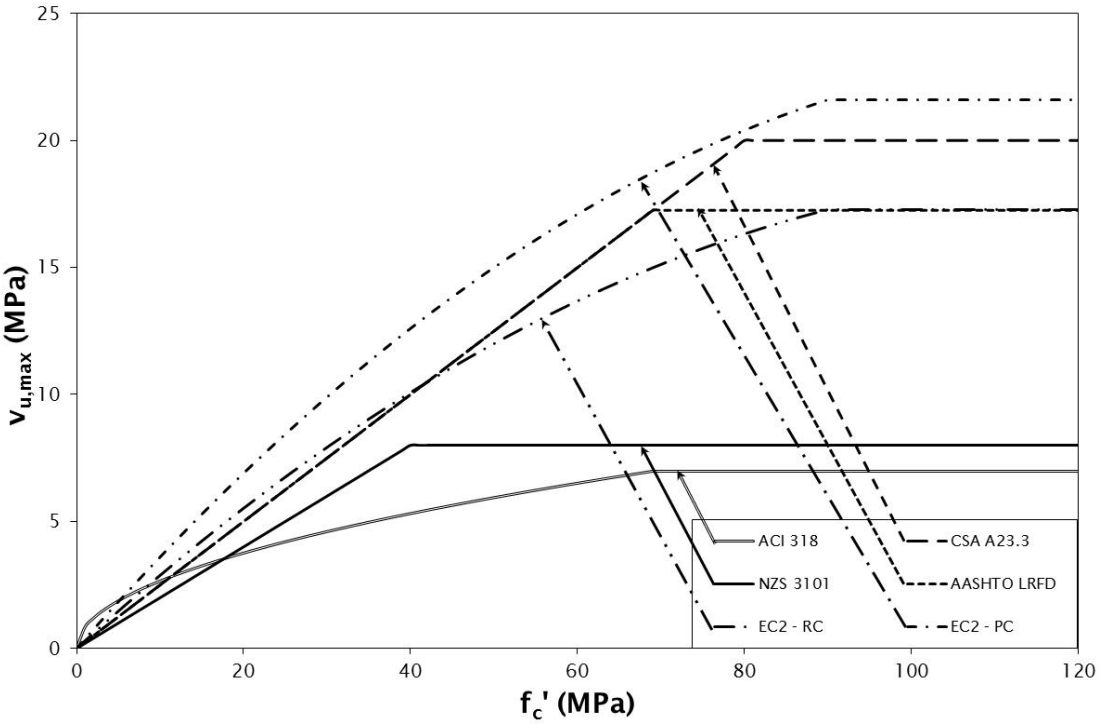

3.7 Conclusions

Presented in this chapter were four different concrete shear design provisions specified in six different international design standards, and it was shown that each of the four sets of design provisions used a different approach for shear design. Two of the provisions presented unified approaches for reinforced and PC beam shear design, while the other two provisions provided separate specifications for RC and PC beams. The considerable level of uncertainty associated with concrete shear design was demonstrated through the considerable difference between the shear design provisions within the design standards considered in this report.

It was observed during examination that the six design standards detailed in this chapter differ not only in the approaches they employ for shear design, but also in the limits imposed by each standard on the allowable shear capacities. ACI 318 and EC2 both eschew specifying a direct limit on predicted shear capacity, although EC2 does specify limits on concrete compressive strength, inclination angle of compression struts and effective area of transverse reinforcement, which indirectly limit the predicted ultimate shear capacity. Meanwhile, CSA A23.3, AASHTO LRFD and NZS 3101 all limit the maximum allowable shear capacity to a proportion of the concrete compressive strength, which is 0.25 for the first two standards and 0.2 for NZS 3101. The fib model code was the only design standard of the six considered to not include any limits on shear capacity, only limiting the effective concrete compressive strength to 120MPa. However, NZS 3101 also specifies an absolute limit of 8MPa for the maximum allowable shear capacity for all concrete beams. It was shown in section 3.5 that this 8MPa limit restricts the maximum shear capacity of concrete beams designed using the provisions in NZS 3101 to extremely low values compared with the shear capacities allowable by the provisions in CSA A23.3, AASHTO LRFD, EC2, CHBDC and AS 5100.5.

4 Shear test database

To allow a number of analyses to be conducted, a database was compiled of previous experimental testing, conducted locally and internationally, relating to the shear behaviour of concrete beams. The database consisted of almost 2000 RC beams and 500 PC beams from all accessible published research. This chapter details the constitution of the RC and PC databases, a variety of analyses conducted on the databases, and the conclusions resulting from the analyses.

A database was compiled of previous experimental testing relating to the shear behaviour of concrete beams, to allow for a number of analyses to be conducted. The database consisted of almost 2000 RC beams and 500 PC beams from all accessible published research. This chapter details the composition of the RC and PC databases, a variety of analyses conducted on the databases, and the conclusions resulting from the analyses.

4.1 Objectives

The main objective of the composition and analysis of the RC and PC databases mentioned above was to investigate the influence of various design parameters on the shear behaviour and ultimate shear capacity of concrete beams using available experimental data. By examining the trends in several failure criteria across a variety of parameters, it was possible to identify the parameters most influential in the shear performance of concrete beams over varying ranges of design parameters. Of most interest to the overall objective of the project, which was to assess the validity of absolute limits being placed on allowable shear stresses in high-strength concrete beams, were those parameters that were most influential on the total applied shear stress experienced by each tested beam.

A second objective of the analysis of previous experimental testing was to evaluate the ability of existing design standards to accurately predict the ultimate shear capacity of concrete beams. The accuracy of each of a number of international design standards was examined with varying input design parameters, allowing for identification of any ranges of the input parameters over which the design standard was either significantly conservative or significantly non-conservative. The use of experimental data in this analysis was particularly advantageous, as all current design standards rely, to varying degrees, on empirical data.

Finally, the composition of the RC and PC databases was used to inform the design of the experimental investigation detailed in chapter 5.

4.2 Database composition

The database compiled for this investigation was divided into two sections: a RC database, and a PC database. This separation was instituted for a number of reasons. First, the procedure used in all major design standards to design a RC beam varies significantly from that for a PC beam. Also, inherent efficiencies in PC beams can result in considerable differences between RC beams and PC beams in section and span geometry. Finally, it is well established that the angle of inclination of compression struts, and resulting cracking, in PC beams is generally substantially lower than that found in RC beams. This dissimilarity of crack angles was considered important, as the inclination of shear cracks affects not only the concrete contribution to shear resistance, but also the contribution of any transverse reinforcement in the beam.

Together, the RC and PC databases contained details of all accessible experimental testing that was focused on determining the shear capacity of concrete beams, the earliest of which dated back to 1948. A total of almost 2500 beams were included in the databases, with a large variety of concrete compressive strengths (between 6–128MPa) and beam geometries.

In order for a beam to be added to the assembled database, the available information needed to include details of the geometry and reinforcement of each beam, as well as sufficient details to allow for both the calculation of applied flexural stresses and for calculation of predicted shear capacities based on the various design standards utilised in subsequent sections of this chapter. Therefore, compilation of the RC and PC databases required the following information to be gathered for each beam:

- General test information: name of researcher, date of research, and beam name
- Section geometry: section shape (rectangular, tee, or I-girder), beam height, effective depth, and web and flange thicknesses
- Loading geometry: load span, support configuration (simply supported or continuous), load configuration (single point load, double point load or distributed loading), shear span-to-depth ratio (a/d)
- Concrete material properties: compressive cylinder strength (or equivalent where cube tests or non-standard cylinders were used), maximum aggregate size
- Longitudinal reinforcement properties: cross-sectional area, yield strength
- Transverse reinforcement properties: cross-sectional area, yield strength, spacing
- Prestressing properties (for PC database only): cross-sectional area, yield strength, ultimate strength, angle (if draped strands were used), effective prestress at time of testing (if not explicitly provided, this parameter was calculated based on NZS 3101:2006 provisions)
- Failure details: maximum shear force at failure, observed crack angles (where provided).

Complete reproductions of both databases can be found in appendix A.

4.2.1 RC beam database

The RC beam database contained a total of 2009 beams that were deemed relevant for inclusion. Only beams that could be confirmed to have failed in shear were included, as this investigation focused on shear performance and shear capacity.

Contained within the RC database were beams with a large variety of material properties, section sizes and reinforcement details – 1493 (74%) were fabricated with concrete compressive strengths of 40MPa or lower; 226 (11%) were fabricated with concrete strengths between 40 and 60MPa, and the remaining 290 (14%) were fabricated with concrete strengths greater than 60MPa. The low number of experimental tests conducted on high-strength concrete beams can be seen in figure 4.1(a).

Figure 4.1(b) shows that the vast majority (93%) of previous testing on RC beams has been on rectangular beams. Meanwhile, figures 4.2 and 4.3 show the over-representation in the database of test beams with effective depths below 400mm. This over-representation is of particular significance for the shear capacity of beams with no transverse reinforcement, as previous research has shown that such beams exhibit markedly different shear capacities with varying section sizes. This size effect, however, is not considered significant for bridge beams as most, if not all, bridge beams contain at least minimum levels of transverse reinforcement, and it has been shown (Bazant and Kazemi 1991, Bazant and Kim 1984, So and Karihaloo 1993) that for such designs there is no significant size effect. Also, to achieve the large applied

shear stresses that were of interest for this project, it was found that much higher levels of transverse reinforcement were provided than the minimum quantity specified in NZS 3101:2006, further diminishing the importance of the size effect for this research.

As mentioned in the previous section, the shear span-to-depth ratio (a/d) of the loading configuration of a test beam can greatly impact the observed shear performance of the beam. A total of 718 beams in the RC database were tested with a/d ratios lower than 2.5. The majority of the beams (1086) were tested with an a/d ratio between 2.5 and 5, and only 10% of tested beams had an a/d ratio greater than 5.

Figure 4.1 Distribution of basic parameters for beams in the RC database

(a) f'_c distribution **(b) Shape distribution**

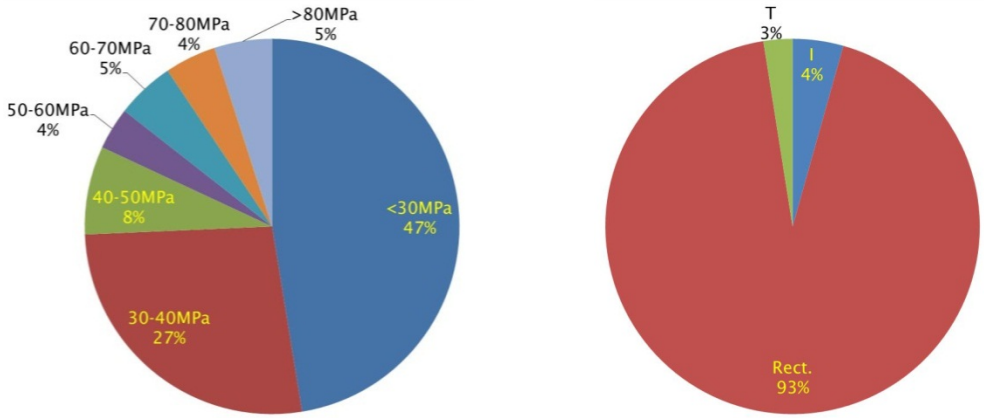

Figure 4.2 Distribution of beam effective depth in the RC database

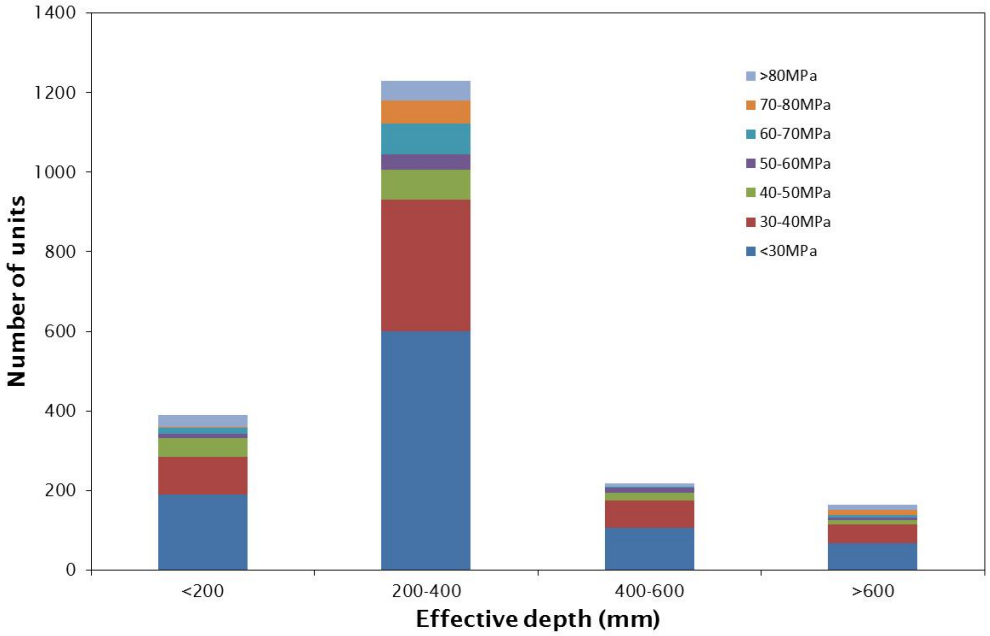

Figure 4.3 Distribution of beam effective depth and beam shape in the PC database

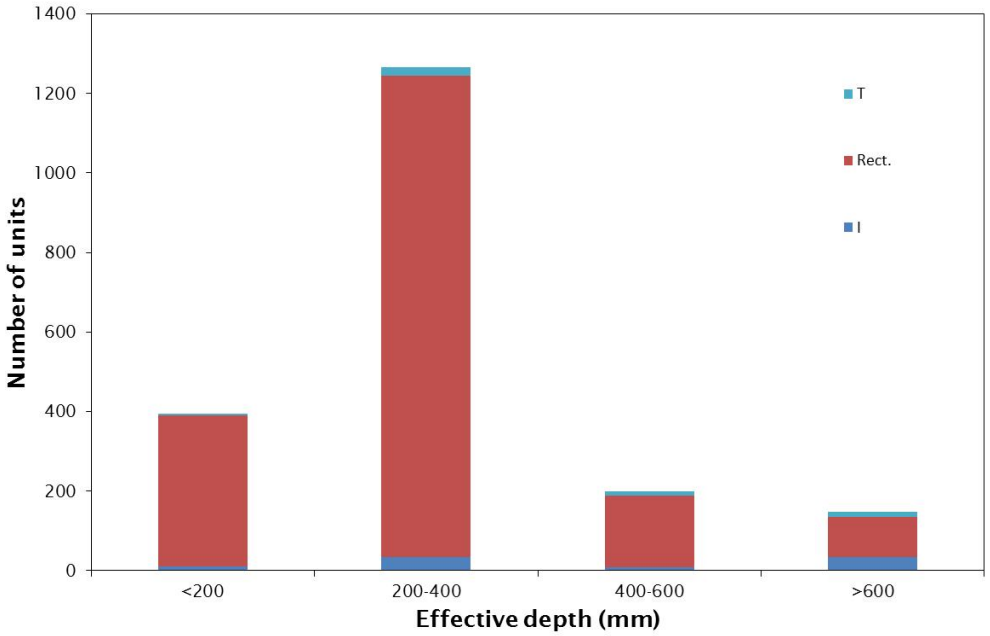

Figure 4.4 shows the distribution of concrete strength of the beams in the RC database relative to the applied shear stress at failure. It can be seen in this figure that there were few tests (1%) conducted previously on high-strength (f_c' > 40MPa) RC beams that developed high applied shear stresses (v_u ≥ 8MPa).

Figure 4.4 Distribution of measured shear capacities and concrete strengths for beams in the RC database

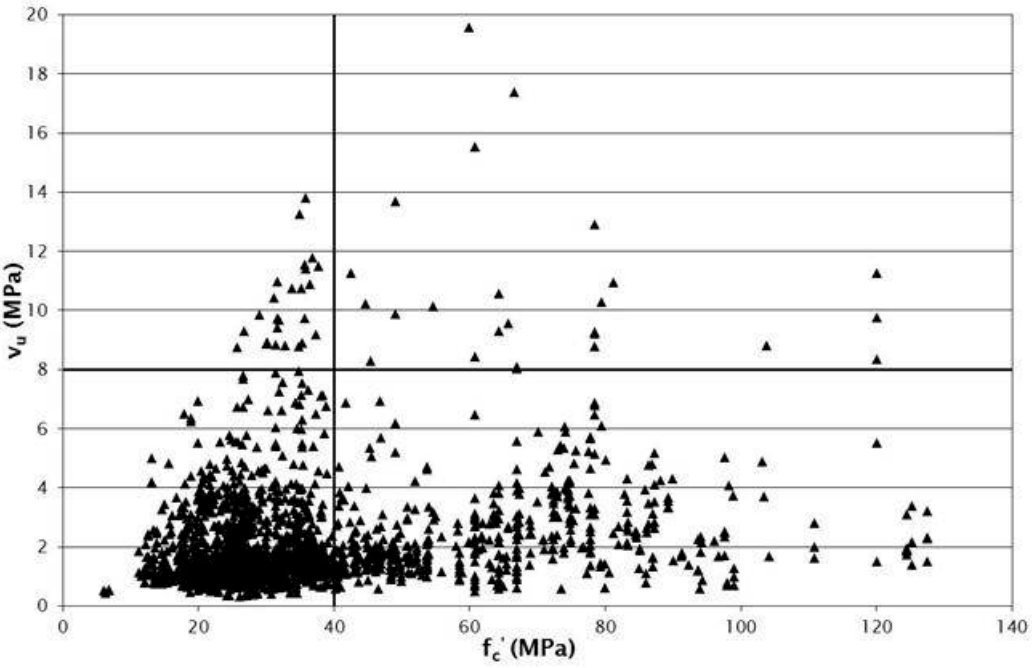

4.2.2 PC beam database

The PC beam database contained a total of 485 beams that were deemed relevant for inclusion. It was important to omit any beams that could not be confirmed to have failed in shear, as this investigation focused on shear performance and capacity.

Contained within the PC database were beams with a large variety of material properties, section sizes and reinforcement details. Concrete compressive strengths ranged from 12MPa to 123MPa, with over 60% of beams having a concrete compressive strength of less than 40MPa, and only 10% greater than 60MPa. This concrete compressive strength distribution can be seen in figure 4.5(a). The low number of experimental tests that have been conducted on high-strength concrete beams provides some explanation for the absolute 8MPa limit imposed in NZS 3101:2006 on allowable shear capacity – a large proportion of shear design provisions are based on empirical data, and without the data to confirm the adequate shear performance of high-strength concrete beams it is more prudent for the authors of the design standard to limit the allowable shear stresses to known achievable levels.

Figure 4.5(b) shows that the majority of previous testing has been performed on I-beams. Meanwhile, figures 4.6 and 4.7 show the vast under-representation of large test beams (d > 400mm) in the database. This disparity in the size of experimental beams can be explained by the increase in both beam and test rig construction costs inherent in testing large beams to failure.

Of the 485 beams in the PC database, 321 beams contained no transverse reinforcement, with the remaining 164 beams containing at least the minimum transverse reinforcement required by NZS 3101:2006. It is well documented that beams tested with a loading configuration resulting in shear a/d ratios below 2.5 exhibit increased shear capacity due to deep-beam effects. This phenomenon explains the tendency of researchers to avoid such low a/d ratios, with only 12 beams tested having an a/d ratio below 2.5, 423 between 2.5 and 5, and the remaining 50 above 5. The vast majority of tests were conducted with a/d ratios below 5 because higher a/d ratios would result in greater applied bending moments, relative to the shear capacity of the beam, and would increase the likelihood of flexural failure.

Figure 4.5 Distribution of basic parameters for beams in the PC database

(a) f'_c distribution

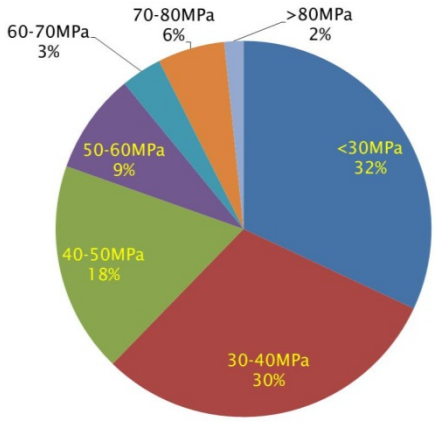

(b) Shape distribution

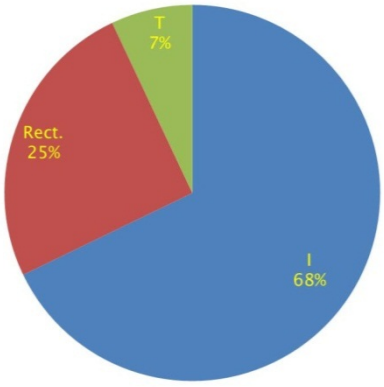

Figure 4.6 Distribution of beam effective depth and concrete compressive strength in the PC database

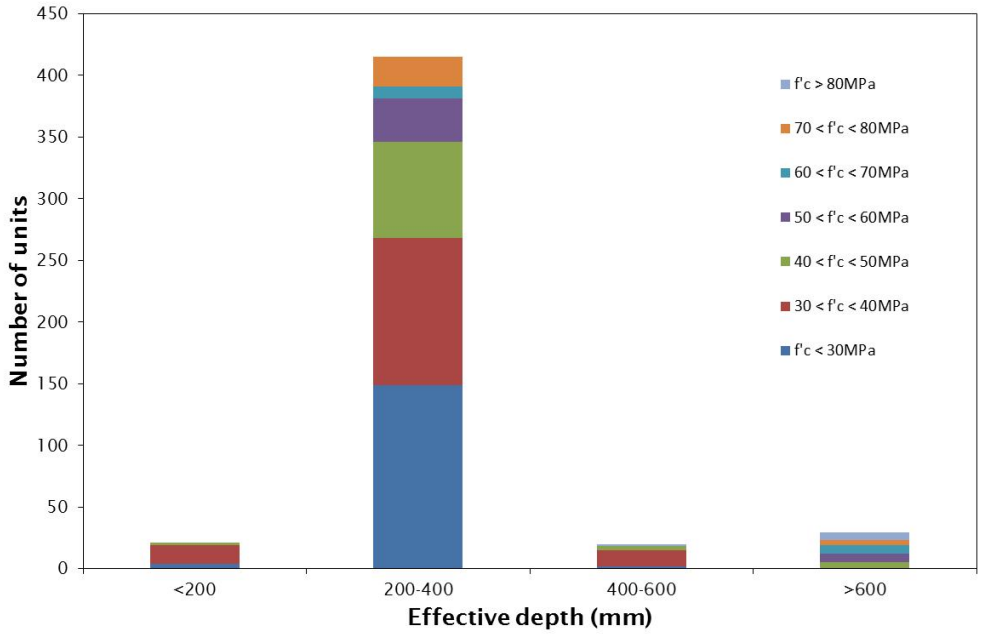

Figure 4.7 Distribution of beam effective depth and beam shape in the PC database

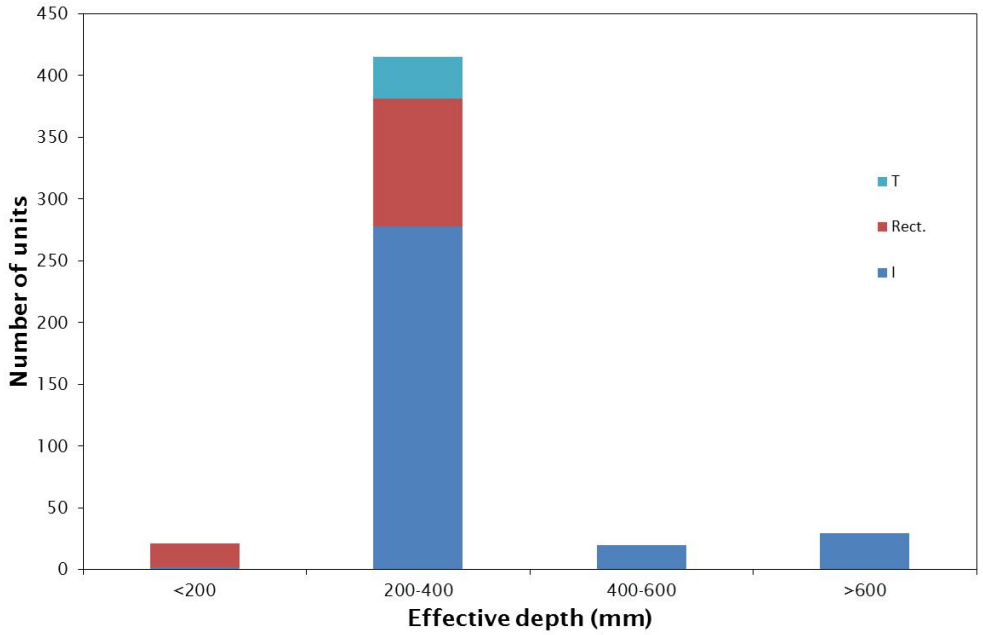

Over 90% of the beams in the PC database failed at an applied shear stress below 8MPa, and almost two-thirds of those beams failed at a shear stress of less than 4MPa. This tendency towards lower levels of shear stress capacities, most likely due to the cost implications of increased cement quantities required for higher-strength concrete, coupled with the under-representation of high-strength concrete beams in the database, can be seen in figure 4.8. The main observation to be made from this figure is the presence

of few beams that were suitable for addressing the primary objective of this project, which was to investigate the maximum applied shear stresses that can be relied upon in high-strength concrete beams.

Figure 4.8 Distribution of measured shear capacities and concrete strengths for beams in the PC database

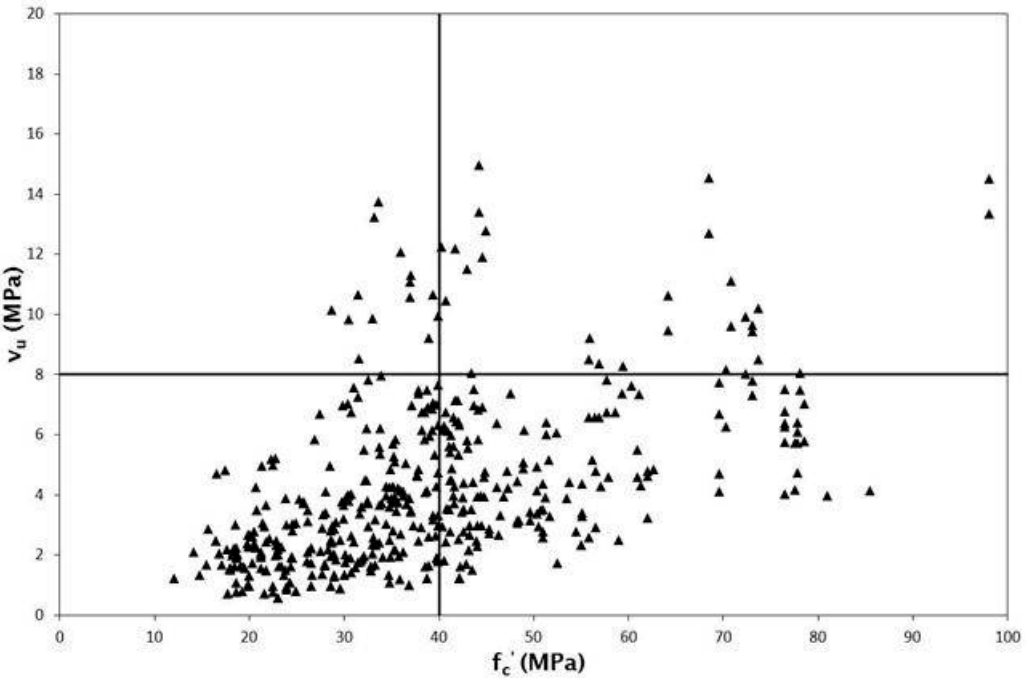

4.3 Influence of design parameters

The influence of a variety of design parameters on the shear capacity measured during previous experimental testing of concrete beams is discussed in this section. Both the RC and PC databases were analysed for these influences by observing any discernible trends in the performance of beams as each parameter was varied.

After initial analyses of the two compiled databases, it became clear that more stringent criteria needed to be applied to the selection of beams included in the comprehensive analysis of the databases. There were two main factors leading to this decision. First, the inclusion of both PC and reinforced beams with no transverse reinforcement introduced an additional level of unnecessary complexity. The shear behaviour of concrete beams with no transverse reinforcement can differ markedly from the behaviour of beams that incorporate transverse reinforcement, as the presence of transverse reinforcement in a concrete beam not only allows for better crack control but also increases the influence of dowel action on the shear performance of the beam. The shear performance of concrete beams with no transverse reinforcement has also been shown (Bazant and Kazemi 1991, Bazant and Kim 1984) to be significantly influenced by the beam effective depth, which is a phenomenon commonly referred to as the 'size effect'. It has also been shown (Bazant and Kazemi 1991, Bazant and Kim 1984) that the size effect is not influential in the behaviour of beams containing some transverse reinforcement. Additionally, the shear performance of concrete beams with no transverse reinforcement was deemed to be a topic with little relevance to this project, and to concrete bridge beams in general, as the overwhelming majority of concrete bridge beams are designed to contain at least minimum levels of transverse reinforcement.

The second factor that led to the decision to refine the databases for the analysis procedure was the inclusion of beams tested with shear a/d ratios lower than 2.5. Beams with an a/d ratio lower than 2.5 are known (Yang 2008, Tan et al 1995, Smith and Vantsiotis 1982) to exhibit increased shear capacities that are deemed to be artificially enhanced, as such capacities are not replicable when the beam is subjected to different loading conditions. These artificially enhanced capacities would skew the databases. Therefore, the decision was taken to omit all beams that were tested with an a/d ratio below 2.5. This decision was validated by the awareness that bridge beams generally have a long span, and support moving loads, and therefore a reliance on restricting loading conditions to a/d ratios would be completely unrealistic.

Introduced in this section is the term $\rho_v f_{vy}$, which refers to the transverse reinforcement ratio, ρ_v, multiplied by the yield stress of the transverse reinforcement, f_{vy}. The term $\rho_v f_{vy}$ was used in the following analyses to normalise the quantity of transverse reinforcement when assessing the effect of varying levels of transverse reinforcement. Also included in this section is a line of best fit for each plot, which was generally chosen to be linear unless a different line type was observed to be more representative of the trend of the data.

4.3.1 RC database

The original RC database, detailed in section 4.2.1, was refined by eliminating all beams that either contained no transverse reinforcement or had an a/d ratio lower than 2.5 during testing. The final RC database contained 160 beams – 38 had a concrete compressive strength lower than 40MPa, 95 ranged between 40 and 80MPa, and the remaining 27 exceeded 80MPa. The majority of the 160 beams failed at relatively low applied shear stresses, with 129 failing at a shear stress below 4MPa, 23 between 4MPa and 8MPa, and only 8 at greater than 8MPa.

4.3.1.1 Concrete compressive strength

Figure 4.9 shows the ultimate shear capacity of RC test beams with varying concrete compressive strengths and varying transverse reinforcement quantities. For beams with low to moderate levels of transverse reinforcement ($\rho_v f_{vy}$ < 4MPa), there is a relatively well-defined correlation between increasing concrete compressive strength and ultimate shear capacity. While the number of beams with high levels of transverse reinforcement was insufficient to reasonably detect any trends, it was notable that all such beams failed at a shear stress greater than 8MPa.

Figure 4.9 Shear capacity versus concrete strength of beams in the RC database

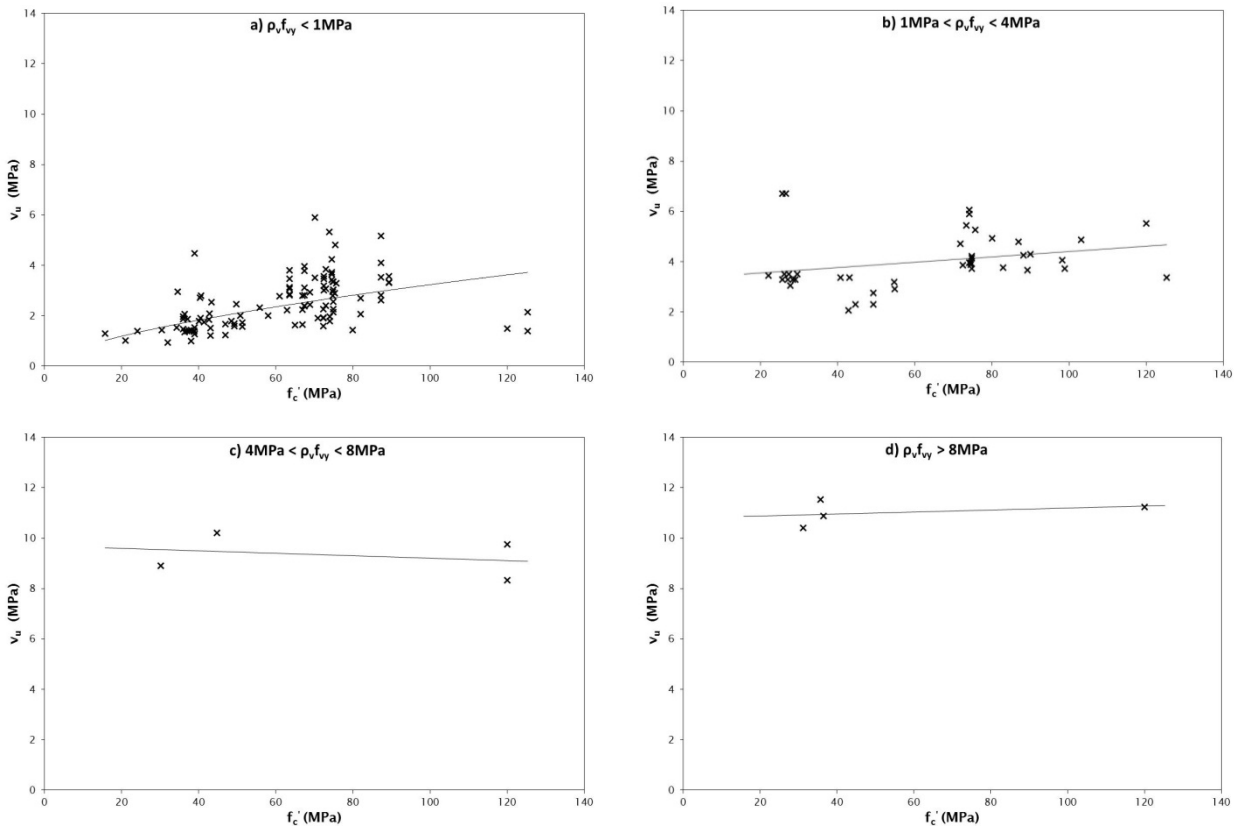

4.3.1.2 Effective depth

In figure 4.10, the ultimate shear capacity of beams in the refined RC database is plotted against the effective depth of the beams. For beams with very low levels of transverse reinforcement ($\rho_v f_{vy}$ < 1MPa), there is evidence of a general decrease in ultimate shear capacity as the effective depth increases from 200mm to 400mm. This capacity decrease is an indication of some influence of size effects, and can be explained by the quantity of transverse reinforcement provided being close to the minimum quantity specified in design standards, above which size effects are considered to be negligible. As the transverse reinforcement in a beam decreases, some characteristics of the beam will tend towards the characteristics of a beam with no transverse reinforcement, and this phenomenon is demonstrated by the presence of a size effect for beams with lower quantities of transverse reinforcement. In figure 4.10 there is no evidence of this size effect for beams with moderate and high levels of transverse reinforcement ($\rho_v f_{vy}$ > 1MPa).

Figure 4.10 Shear capacity versus effective depth of beams in the RC database

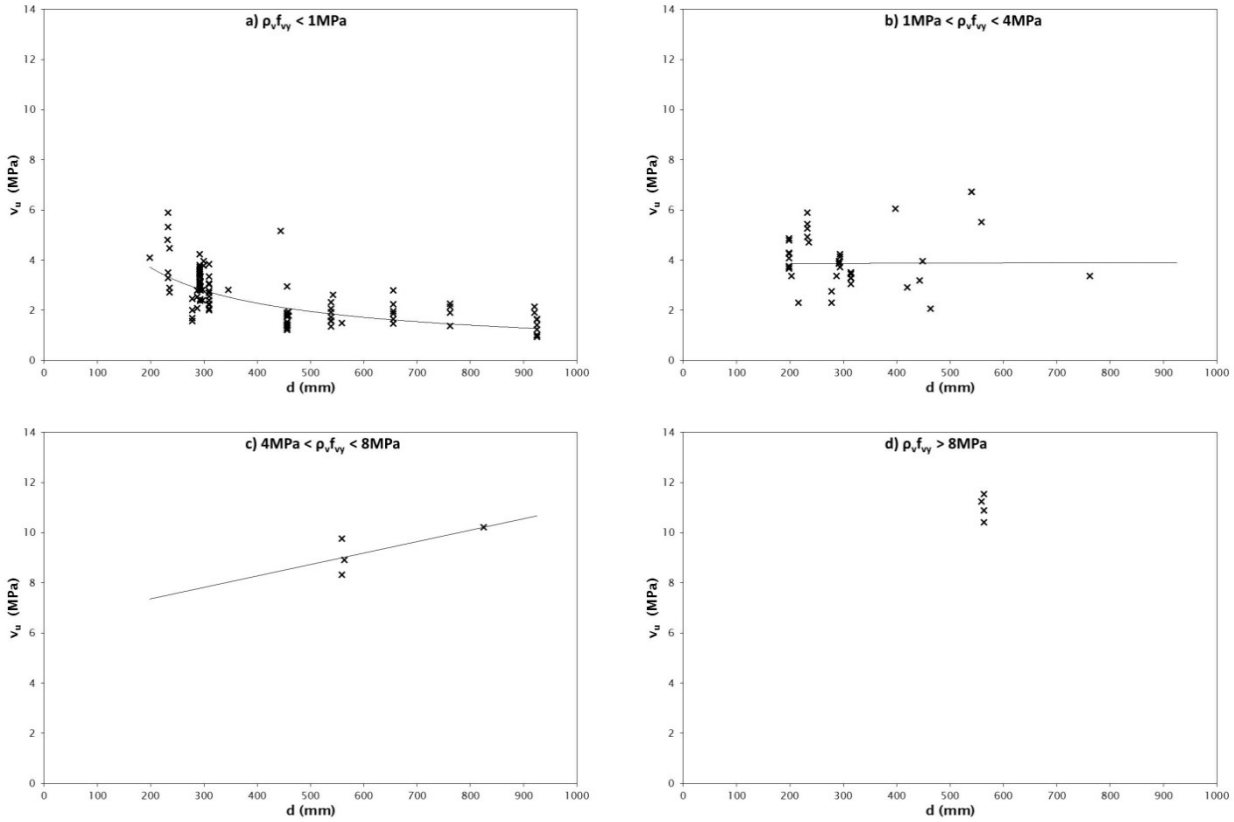

4.3.1.3 Shear span-to-depth (a/d) ratio

As all beams with a shear a/d ratio lower than 2.5 were omitted from the refined RC database used for this analysis, it was anticipated that the parameter a/d would not have a discernible influence on the shear capacity of the test beams. Figure 4.11 shows the shear capacity of RC test beams versus their a/d ratios, and despite the presence of significant scatter, the data confirms the hypothesis that changes in the a/d ratio for values greater than 2.5 does not significantly influence the shear capacity of RC beams. It was noted that the only beams to exhibit shear capacities greater than 8MPa were those with a large amount of transverse reinforcement ($\rho_v f_{vy}$ > 4MPa), and that to achieve those high shear stresses the test beams needed to have an a/d ratio close to 2.5. This observation was valuable in informing the researcher for the design of the experimental investigation, detailed in chapter 5, as this observation provided some warning of possible difficulties associated with achieving shear failure at high loads while avoiding flexural failure.

Figure 4.11 Shear capacity versus shear a/d ratio of beams in the RC database

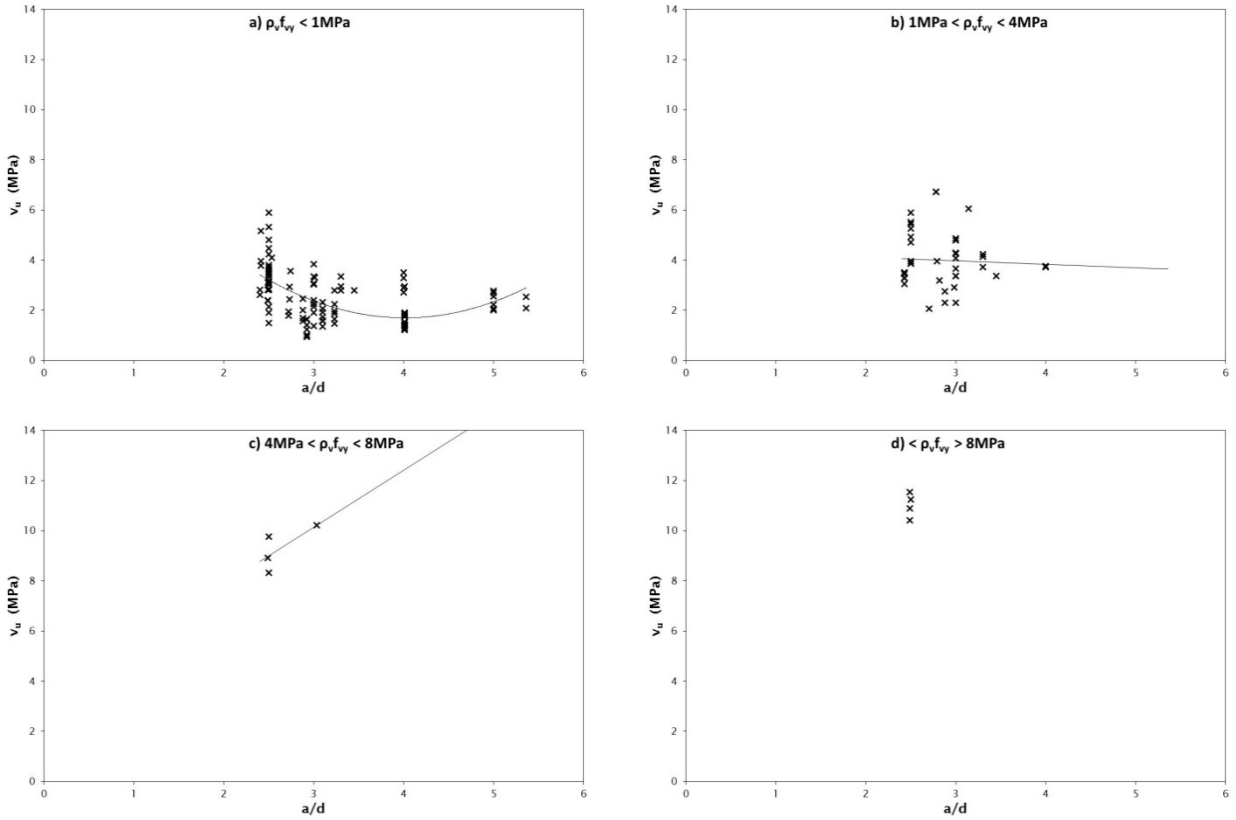

4.3.1.4 Longitudinal reinforcement

The longitudinal reinforcement ratios, ρ_l, used in this analysis were normalised against the average yield stress of the longitudinal reinforcement of all beams in the refined RC database. This normalisation was implemented in order to ensure that the ratios considered accurately represented the level of longitudinal reinforcement provided. The measured shear capacities of all beams in the refined RC database were plotted against the resulting normalised ρ_l, as shown in figure 4.12. The figure illustrates the abundance of heavily reinforced beams within the database, which was a direct effect of the need to ensure that shear was the principal failure mechanism.

As can be clearly seen in figure 4.12, for beams with very low ($\rho_v f_{vy}$ < 1MPa) and low (1 < $\rho_v f_{vy}$ < 4MPa) quantities of transverse reinforcement, the shear capacity increased with increasing longitudinal reinforcement ratios. This trend is characteristic of the influence of dowel action, as a greater number of longitudinal bars crossing a crack results in a greater shear capacity. There is also some influence shown in figure 4.12 of the level of transverse reinforcement on dowel action, as more closely spaced stirrups result in an increased transverse stiffness of the longitudinal reinforcement, which increases the shear capacity attributable to dowel action.

Figure 4.12 Shear capacity versus longitudinal reinforcement of beams in the RC database

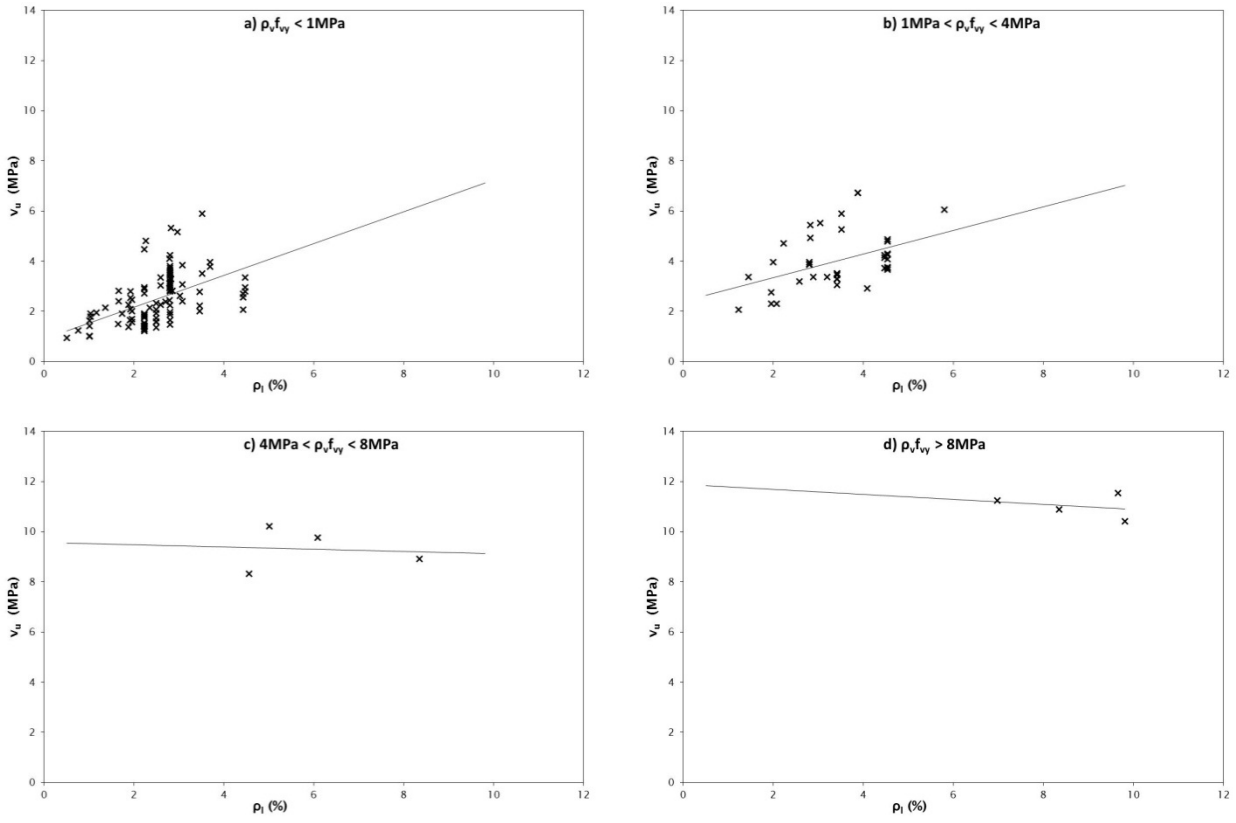

4.3.1.5 Transverse reinforcement

Figure 4.13 shows the influence of transverse reinforcement on the ultimate shear capacity of RC beams, by plotting the measured shear capacity against the level of transverse reinforcement provided in each beam. There is a clear positive relationship evident between ultimate shear capacity and the quantity of transverse reinforcement provided, as is expected due to the direct contribution of transverse reinforcement to the shear resistance of concrete beams following the commencement of inclined shear cracking. There is a discernible difference in shear capacity between the three subsets of concrete compressive strength at low quantities of transverse reinforcement ($\rho_v f_{vy}$ < 4MPa), as beams with a high concrete strength sustained greater shear stresses. However, there was an insufficient number of beams with large quantities of transverse reinforcement ($\rho_v f_{vy}$ > 8MPa) to be able to infer the same relationship between concrete compressive strength and beam shear capacity over all ranges of transverse reinforcement levels.

Figure 4.13 Shear capacity versus transverse reinforcement of beams in the RC database

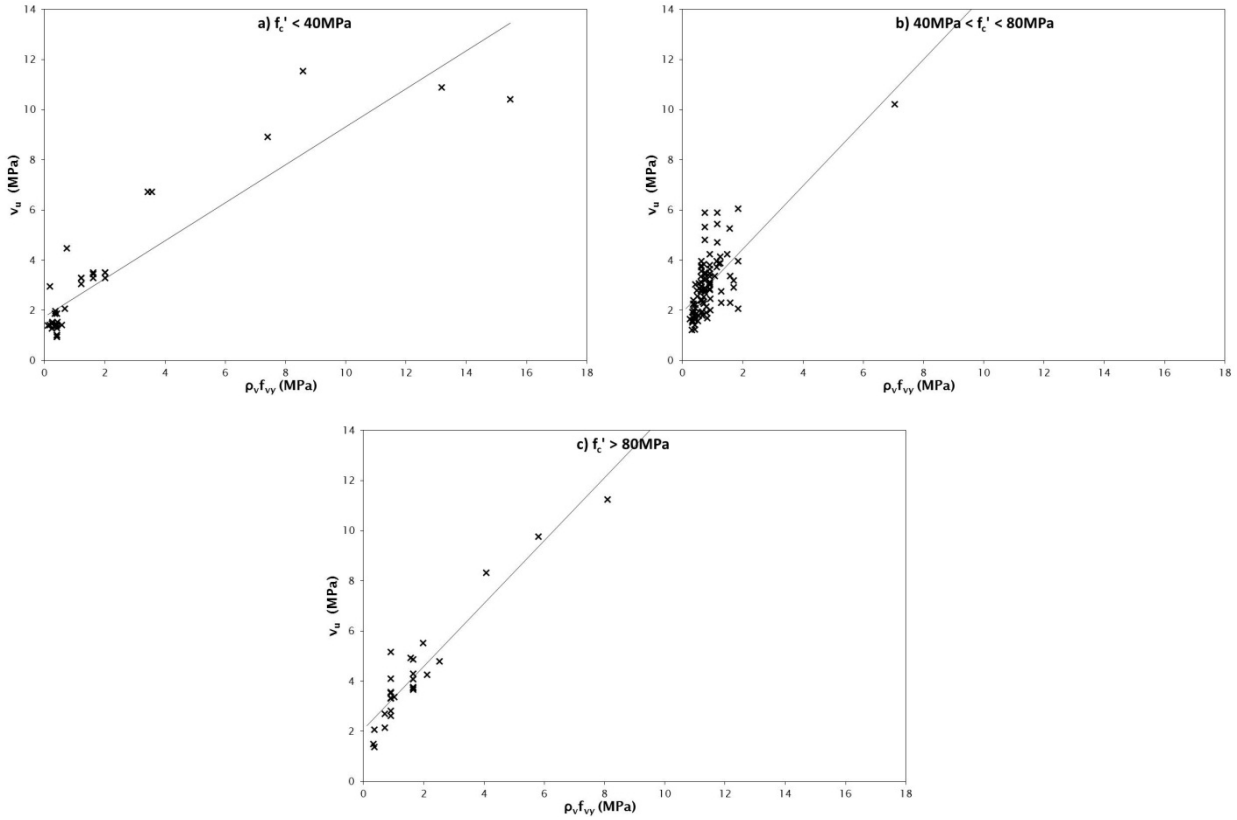

4.3.2 PC database

The complete PC database was refined by removing all beams that either contained no transverse reinforcement or that had an a/d ratio lower than 2.5 during testing. The final database contained 164 beams – 63 had a concrete compressive strength below 40MPa, 93 were between 40 and 80MPa, and the remaining 8 exceeded 80MPa. Of the 164 beams in the refined PC database, 32 failed at a shear stress below 4MPa, 88 failed at a shear stress between 4MPa and 8MPa, and the remaining 44 achieved an ultimate shear capacity greater than 8MPa.

4.3.2.1 Concrete compressive strength

Figure 4.14 shows the shear stress capacity plotted against the concrete cylinder strength of beams in the refined PC database. It can be seen that the shear capacities had a large scatter but were influenced by the level of transverse reinforcement (different levels of transverse reinforcement are represented in the figure by different markers). There was also a discernible general increase in observed shear capacity with increasing concrete compressive strength. This influence of concrete strength was true for all levels of transverse reinforcement. Significantly, there was no indication from this plot that the ultimate shear capacity was limited to 8MPa.

Figure 4.14 Shear capacity versus concrete compressive strength of beams in the PC database

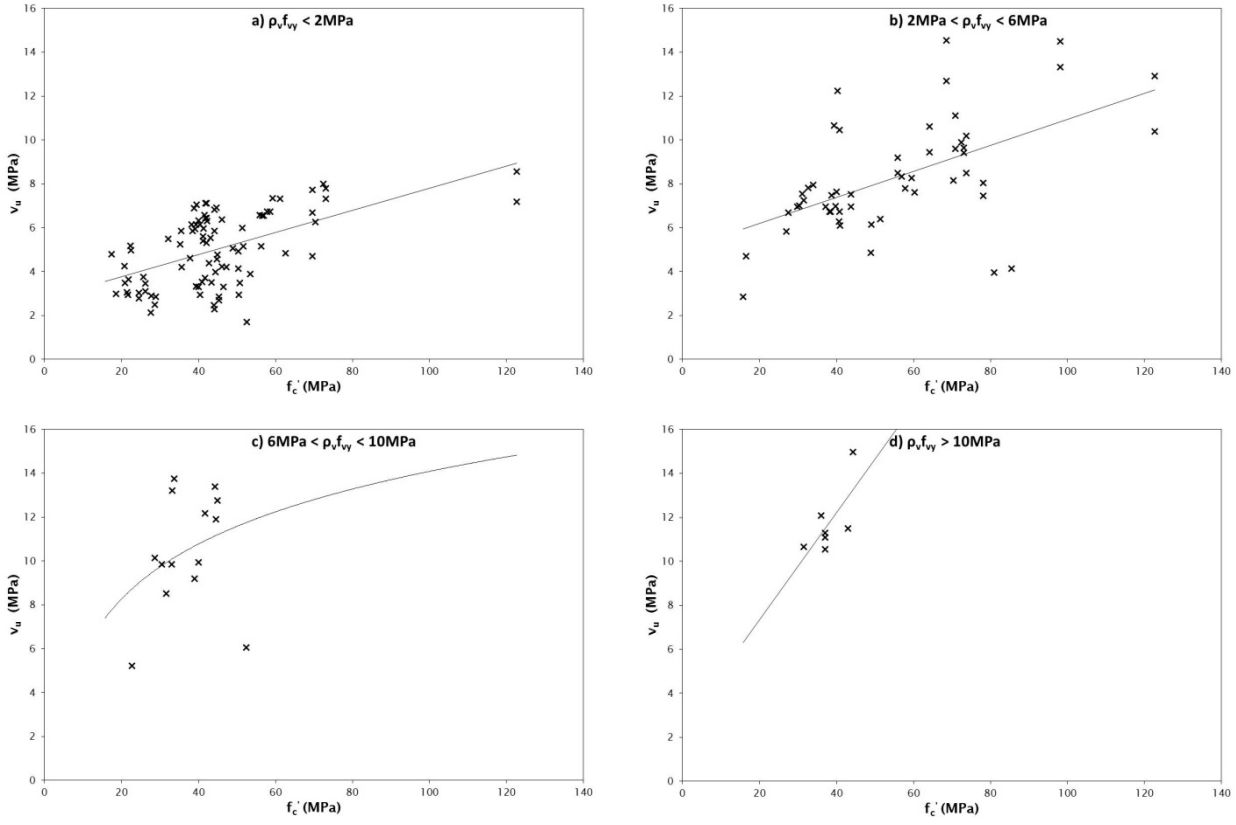

4.3.2.2 Effective depth

In figure 4.15, the shear capacity of each beam in the refined PC database is plotted against the beam effective depth. As observed above in section 4.2, there was a relative paucity of beams tested in previous research that had an effective depth greater than 1m, or even greater than 500mm. There was an observed slight increase in ultimate shear capacity with increased effective depths for beams that contained very low ($\rho_v f_{vy}$ < 1MPa) and low (1 < $\rho_v f_{vy}$ < 4MPa) quantities of transverse reinforcement. This observation is consistent with previous findings that the size effect is not applicable to beams with at least code-minimum levels of transverse reinforcement (Bazant and Kazemi 1991, Bazant and Kim 1984).

Figure 4.15 Shear capacity versus effective depth of beams in the PC database

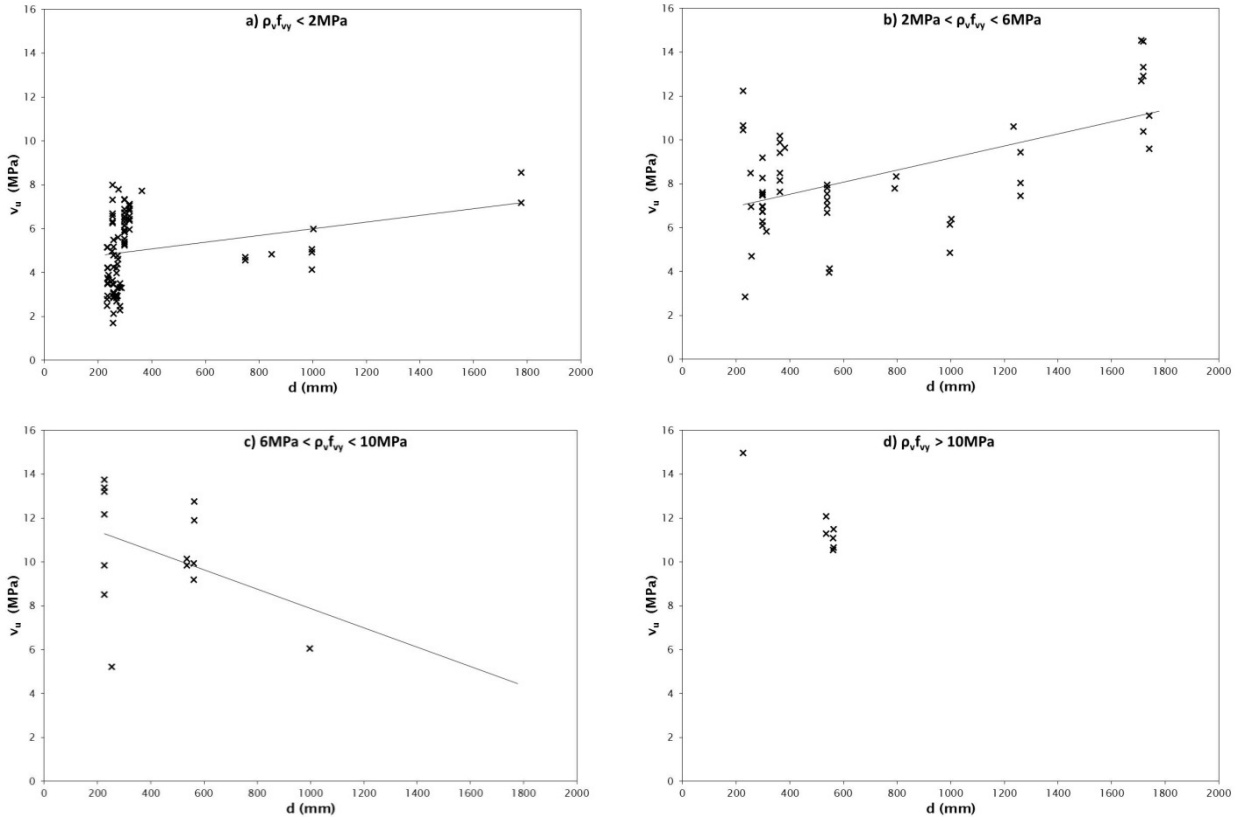

4.3.2.3 Shear span-to-depth (a/d) ratio

As discussed earlier in this chapter, all beams with a shear a/d ratio below 2.5 were omitted from this analysis to avoid deep-beam effects. In figure 4.16, the ultimate shear capacities of all beams in the refined PC database are plotted against a/d ratios. While there was the expected increase in shear capacity with increasing levels of transverse reinforcement, measured strengths were extremely scattered at constant values of a/d. There was no trend in the data with increasing a/d for all beams except those containing low quantities of transverse reinforcement (1 < $\rho_v f_{vy}$ < 4MPa), indicating the lack of correlation between a/d and ultimate shear capacity.

Figure 4.16 Shear capacity versus shear a/d ratio of beams in the PC database

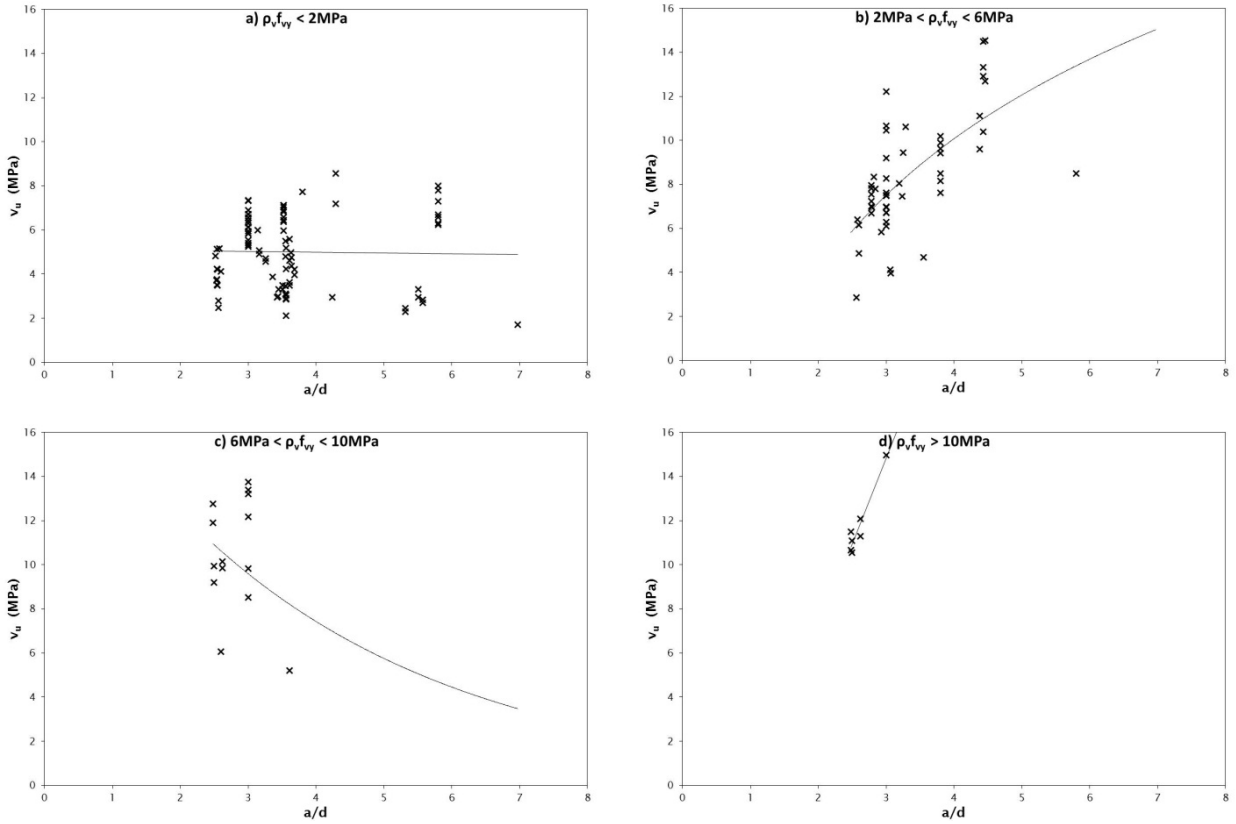

4.3.2.4 Longitudinal reinforcement

It is important to note that the longitudinal reinforcement ratios considered in this section are standardised ratios dependent on the yield strength of both prestressed and non-prestressed longitudinal reinforcement relative to the average yield strength of prestressed reinforcement. Standardisation was achieved using the following equation:

$$\rho_l^* = \frac{\rho_s f_{sy}}{f_{py,average}} + \frac{\rho_{ps} f_{py}}{f_{py,average}} \qquad \text{(Equation 4.1)}$$

where:

ρ_s and ρ_{ps} are the reinforcement ratios

f_{sy} and f_{py} are the yield strengths of the nonprestressed and prestressed reinforcement, respectively

$f_{py,average}$ = 1626MPa is the average yield strength of prestressed reinforcement of all beams considered in the analysis.

In figure 4.17, the standardised values of longitudinal reinforcement ratio are plotted against the experimental shear capacities of each beam in the refined PC database. For similar levels of transverse reinforcement, figure 4.17 shows a tendency for ultimate shear capacity to increase with an increasing quantity of longitudinal reinforcement.

There are two phenomena likely to cause this trend. First, larger amounts of longitudinal prestressing correlate to, in general, higher prestressing stresses. Higher prestressing compressive stresses are beneficial to the shear performance of a PC beam, as those compressive stresses lead to larger loads being required in order to initiate cracking. Also, increased longitudinal reinforcement results in a more pronounced impact of dowel action, increasing the shear resistance at an inclined crack.

Figure 4.17 Shear capacity versus longitudinal reinforcement ratio of beams in the PC database

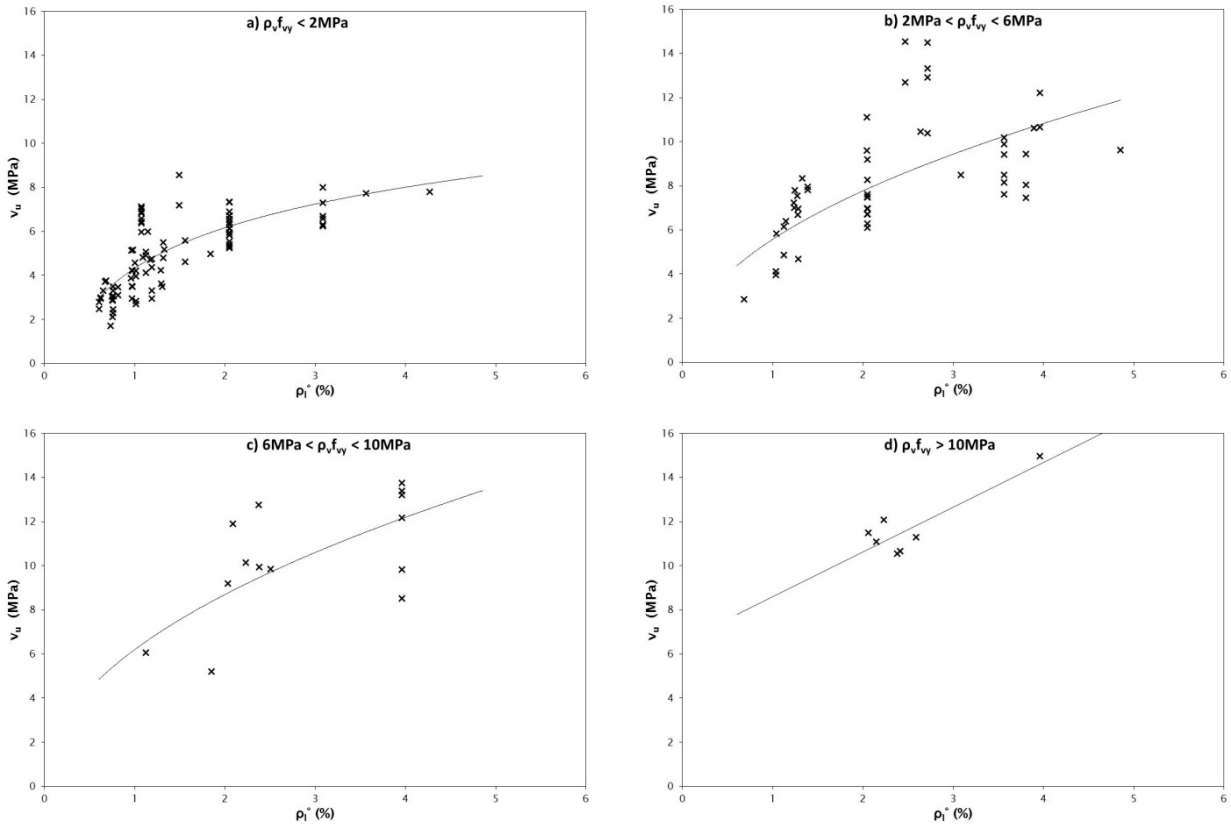

4.3.2.5 Transverse reinforcement

Figure 4.18 presents a plot of the measured shear capacity versus relative levels of transverse reinforcement. There was a clear positive linear relationship between the ultimate shear capacity of a beam and the amount of transverse reinforcement present within that beam. This positive correlation is consistent with the expected high contribution of transverse reinforcement to the shear capacity of a PC beam.

A second trend that is evident in figure 4.18 is the increase in shear capacity of beams with higher concrete compressive strengths, over the full range of levels of transverse reinforcement. In particular, it was observed that beams with a concrete compressive strength of 40–80MPa consistently reached higher ultimate shear capacities at similar levels of transverse reinforcement than did beams with a concrete compressive strength lower than 40MPa. Significantly, this trend was noted to continue beyond shear stresses of 8MPa for beams with a concrete strength above 40MPa, while the shear capacity of beams with

a concrete strength lower than 40MPa plateaued at approximately 8MPa. Therefore, the data in figure 4.18 supported the hypothesis that with the appropriate combination of concrete compressive strength and transverse reinforcement, it was possible to achieve a shear capacity higher than 8MPa, and undermined the validity of an absolute limit being imposed on maximum allowable shear stresses for concrete compressive strengths up to 80MPa. There were insufficient data points for beams with a concrete compressive strength greater than 80MPa to enable the hypothesis to be confirmed for concrete compressive strengths greater than 80MPa.

Figure 4.18 Shear capacity versus transverse reinforcement ratio of beams in the PC database

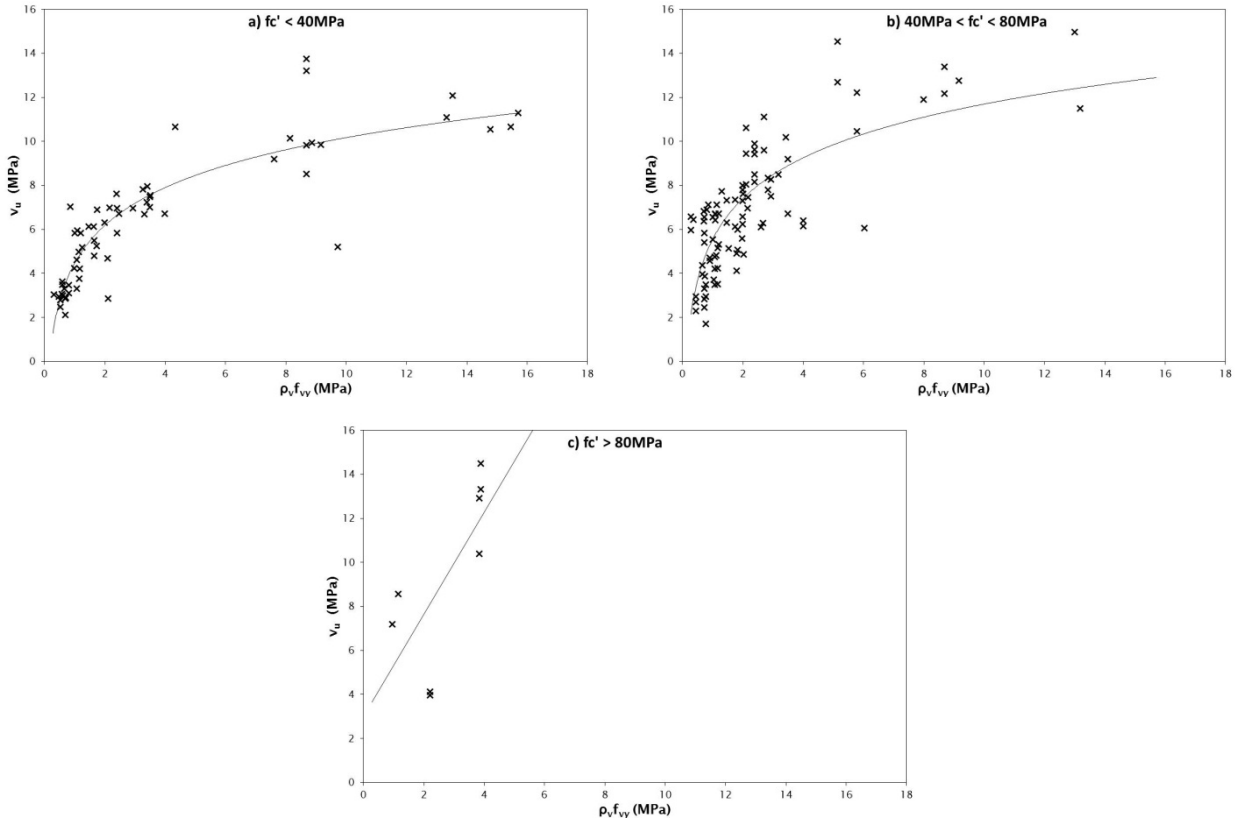

4.4 Evaluation of shear design standards

In this section the databases detailed in section 2 are used to evaluate the five design procedures, encompassing the six international design standards that were discussed in chapter 3. Evaluation of the design procedures involved not only assessment of each procedure's accuracy in predicting the shear capacity of concrete bridge beams, but also the ability of the procedure to account for variations in the main parameters influencing shear behaviour.

A total of 324 test results, composed of 160 RC beams and 164 PC beams from previous shear-focused research, were used in the evaluation process. Only data from beams containing transverse reinforcement that were known to fail in shear and that were tested with shear a/d ratios greater than 2.5 were included in the evaluation, as only such beams were considered relevant to the objectives of this project (see the reasons for these selection criteria earlier in this chapter).

In the evaluation of shear design standards, the beams from previous testing were divided into RC beams and PC beams, because these two beam types have distinct characteristics in shear behaviour and are treated separately in some design code provisions. It is important to note that load factors, strength-reduction factors, and all other known sources of conservatism inherent in design standards were assigned a value of 1.0 for the purposes of this analysis. This allowed for a more thorough evaluation of design standard approaches, based on the design philosophy inherent within the standard, than would otherwise be possible. The limits on concrete compressive strength in these standard provisions were applied in this evaluation, such that the applicability of the various standards for the design of high-strength concrete bridge beams could be examined.

For the comparisons of experimentally observed shear capacities with predicted shear capacities that are presented in this section, the data was divided into four series based on the relative quantity of transverse reinforcement in each beam. The exception to these classifications was for the plots that illustrated the influence of shear stress capacity and transverse reinforcement – for these, the data was divided into three series based on the concrete compressive strength of each beam.

Included in each plot in this section is a line to represent an accurate prediction, or a shear capacity ratio of 1.0. Also included in the plots is a line of best fit, which was generally chosen to be linear except in cases where a different line type was considered to be significantly more representative of the data.

4.4.1 ACI 318-11

As detailed in section 3.1, ACI 318-11 provides separate provisions for the shear design of RC and PC beams. For evaluating the accuracy of ACI 318 in predicting the shear performance of RC beams, both of the equations presented in section 3.1.1 were used and the lower predicted strength was adopted. Meanwhile, evaluation of the PC design provisions was based on the detailed method described in section 3.1.2, as the simplified method is much less frequently used by engineers (Kim 2004, ASCE-ACI 1998). The detailed method provides equations for the web-shear capacity and the flexure-shear capacity, with the lower of the two calculated capacities used to account for the contribution of concrete to beam shear capacity. For both RC and PC beams, ACI 318 specifies a transverse reinforcement contribution based on the 45° truss model. For the purposes of this evaluation, the limit on concrete contribution of $0.3\sqrt{f_c'}b_w d$ and the limit on transverse reinforcement contribution of $0.66\sqrt{f_c'}b_w d$ were both applied, as both limits are critical to preventing unwanted failure mechanisms.

4.4.1.1 RC database

Figures 4.19–4.24 show the influence of various design parameters on the ability of ACI 318 to predict the ultimate shear capacity of 160 RC beams. The average ratio of observed to predicted shear capacity was

1.30, with a standard deviation of 0.36 and a coefficient of variation of 0.27. These statistical values were reflected in the large scatter evident in figures 4.19–4.24, and the combination of this scatter and the average ratio of 1.30 resulted in 27 beams failing at shear capacities below those predicted by ACI 318.

Figure 4.19 shows the influence of concrete compressive strength on the accuracy of ACI 318 in predicting the ultimate shear capacity of 160 RC beams categorised based on the level of transverse reinforcement in each beam. There was no visible effect on accuracy of increasing concrete strength, and ACI 318 was found to be non-conservative for a number of beams over the full range of concrete strengths examined. There was no discernible change in the accuracy of ACI 318 for beams with a concrete strength greater than 40MPa, which is a significant observation as NZS 3101 places an absolute limit of 8MPa on the allowable shear stress capacity of beams with a concrete compressive strength greater than 40MPa.

Figure 4.19 Influence of concrete strength on the accuracy of ACI 318 for beams in the RC database

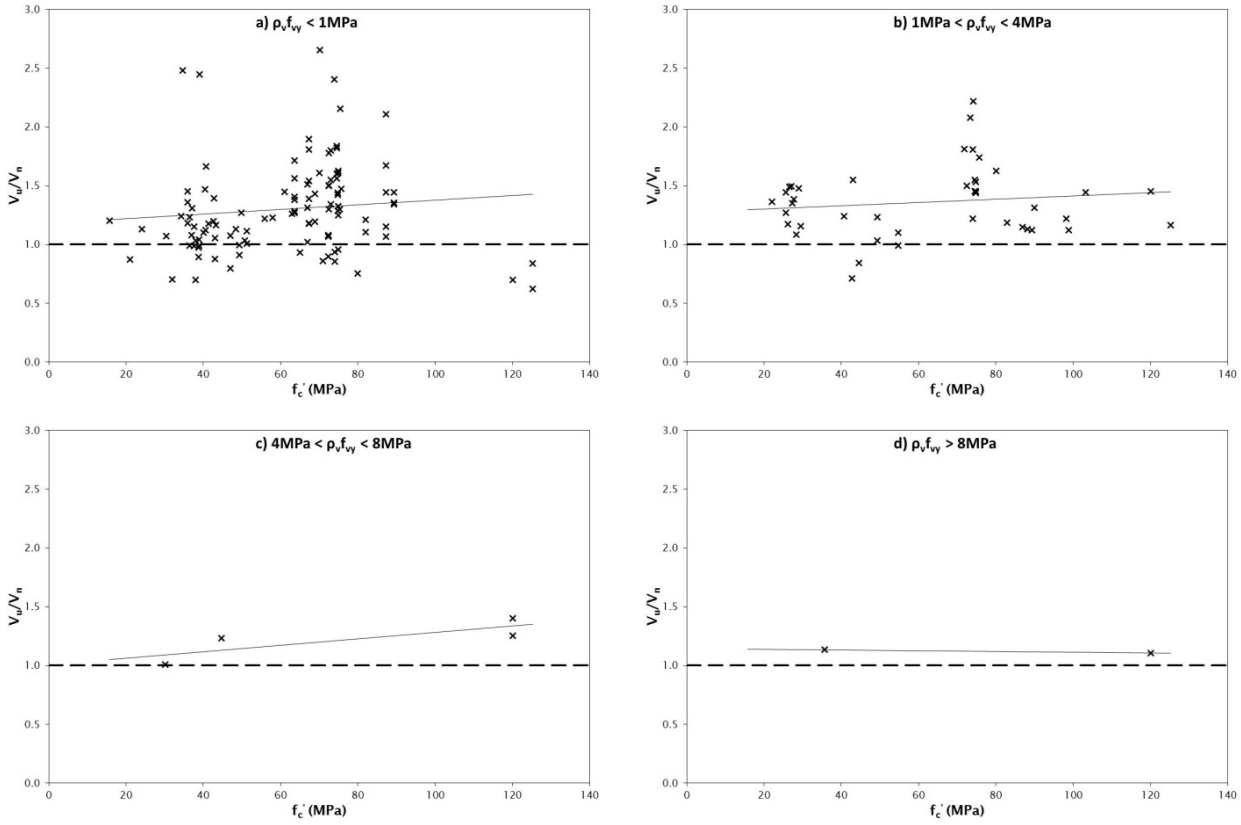

The effect of ultimate shear capacity on the accuracy of ACI 318 is shown in figure 4.20. ACI 318 was observed to overestimate the ultimate shear capacity of beams with either a low (approximately 2MPa) or high (greater than 8MPa) shear stress capacity, while greatly underestimating the ultimate shear capacity of beams with a shear stress capacity of 4–6MPa. Significantly, it was observed that at shear stress capacities greater than 8MPa, only the beams with normal-strength concrete (lower than 40MPa) failed at shear capacities below their predicted strengths.

Figure 4.20 Influence of ultimate shear capacity on the accuracy of ACI 318 for beams in the RC database

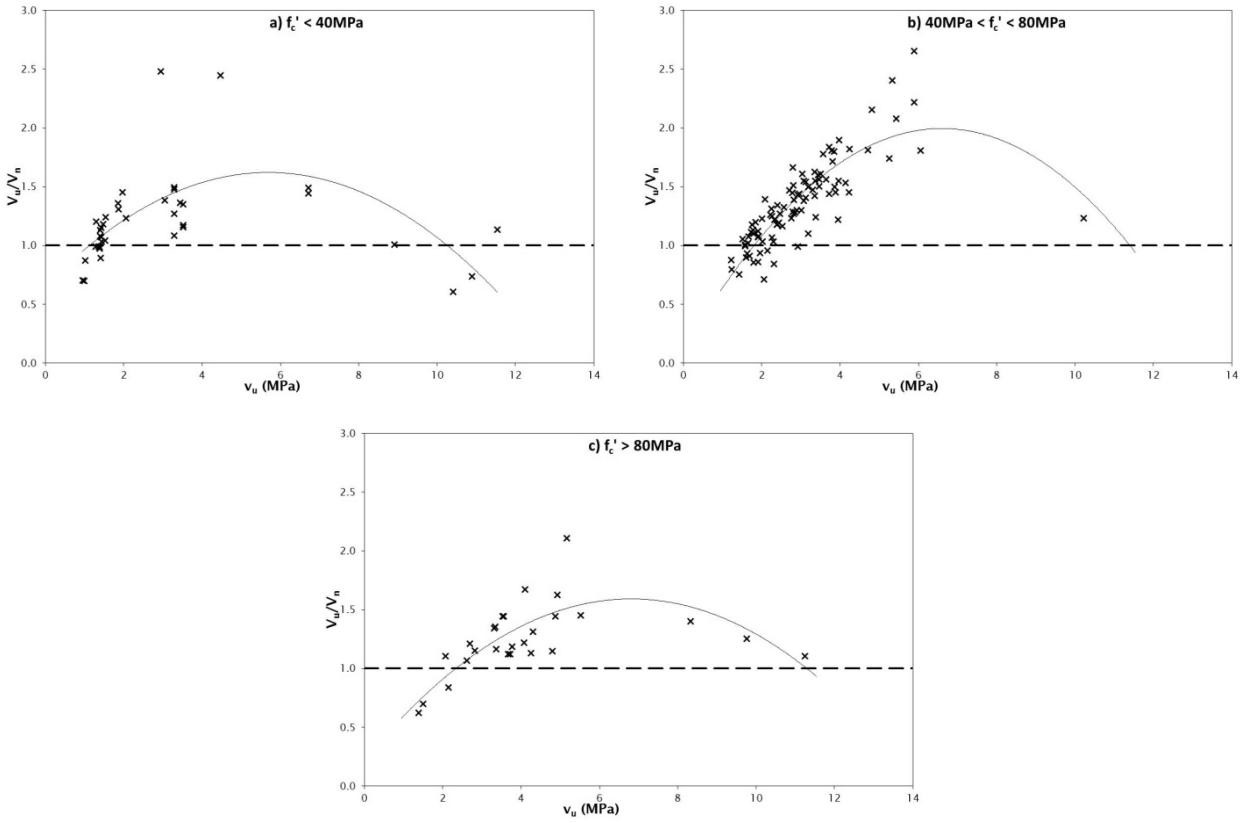

Figures 4.21 and 4.22 show the ratio of observed to predicted shear capacities plotted against beam effective depths and shear a/d ratios, respectively. For beams with increasing effective depths, the predicted ACI 318 shear capacities decreased in conservatism. In particular, ACI 318 was observed to overestimate the shear capacity of large beams (d > 700mm) with low levels of transverse reinforcement ($\rho_v f_{vy}$ < 1MPa). This trend, similar to the observed trend reported in section 4.3.1.2, was attributed to the influence of size effects on lightly reinforced beams, as ACI 318 does not account for size effects in the design of RC beams with transverse reinforcement. Despite the large scatter at shear a/d ratios of approximately 2.5, there was no significant effect of increasing a/d on the accuracy of predicted strengths. The large observed scatter in figure 4.22 was credited to the presence of some deep-beam effects in beams with a/d close to 2.5.

Figure 4.21 Influence of effective depth on the accuracy of ACI 318 for beams in the RC database

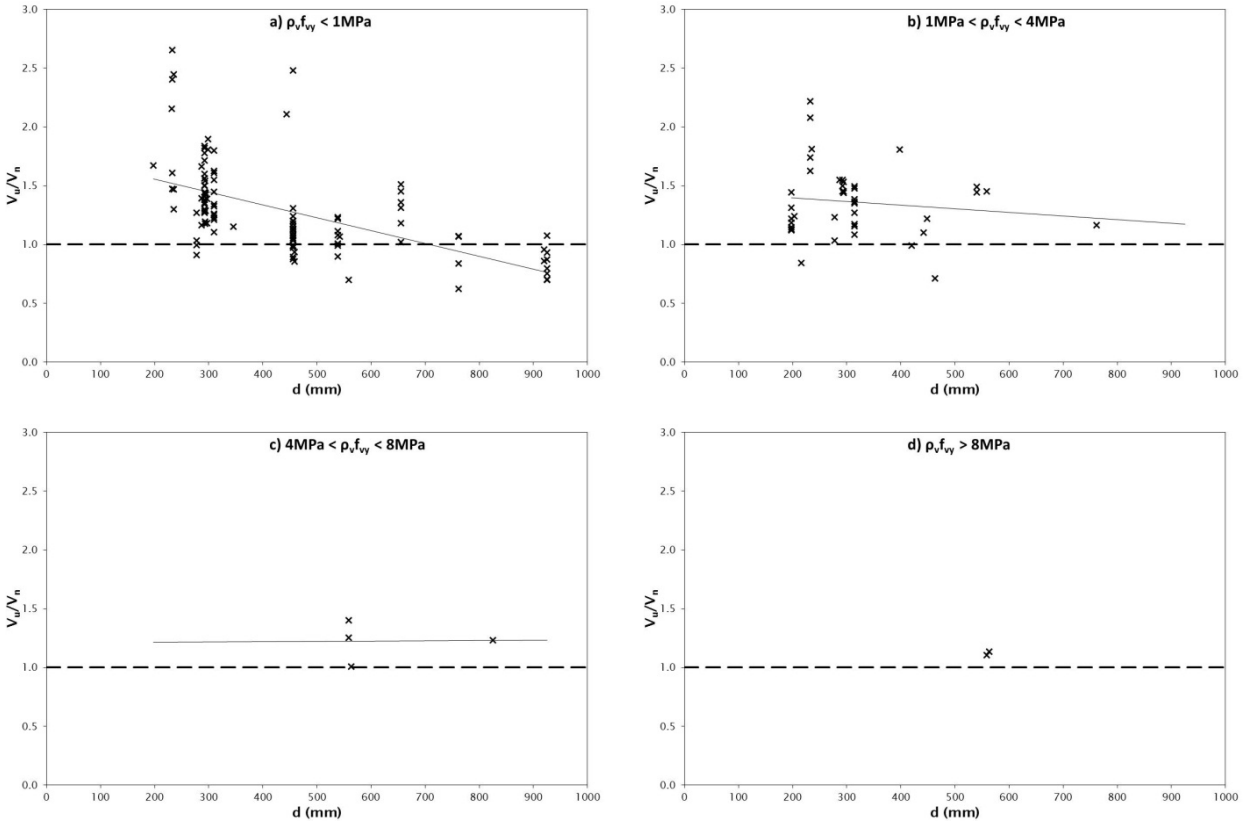

Figure 4.22 Influence of shear a/d ratio on the accuracy of ACI 318 for beams in the RC database

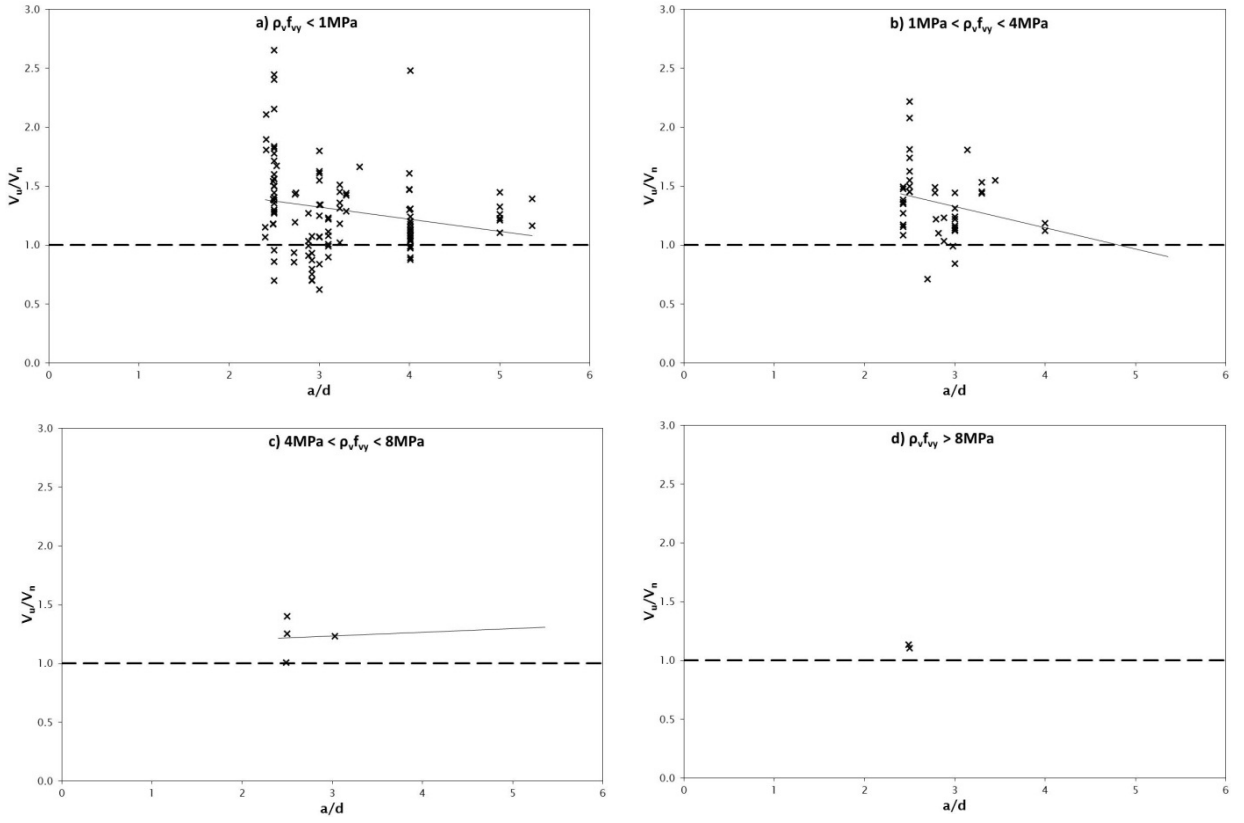

Figure 4.23 shows that ACI 318 provides consistently non-conservative predictions of shear capacity for beams containing very low quantities of transverse ($\rho_v f_{vy}$ < 1MPa) and low quantities of longitudinal reinforcement. Figure 4.24 indicate that the influence of transverse reinforcement is adequately accounted for in ACI 318, as evident by the relatively flat trendlines.

Figure 4.23 Influence of longitudinal reinforcement on the accuracy of ACI 318 for beams in the RC database

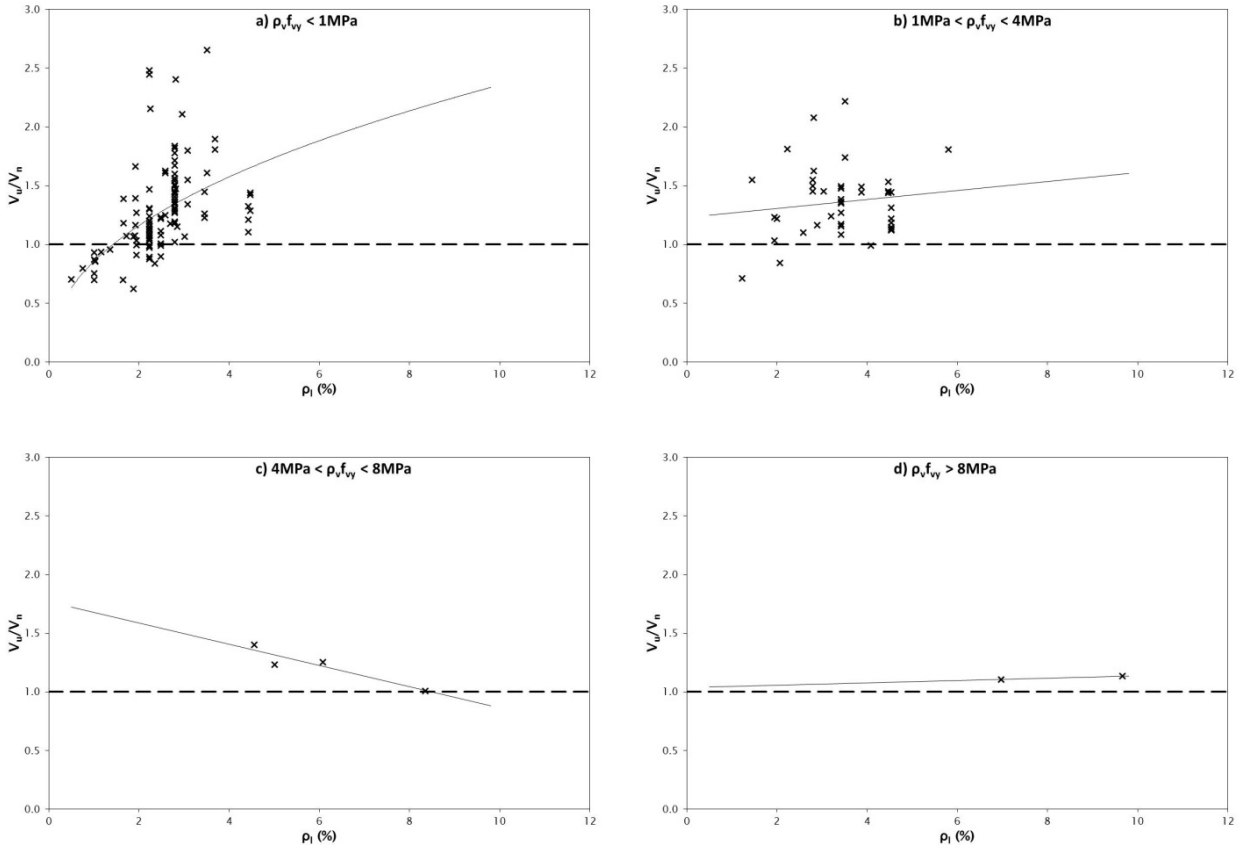

Figure 4.24 Influence of transverse reinforcement on the accuracy of ACI 318 for beams in the RC database

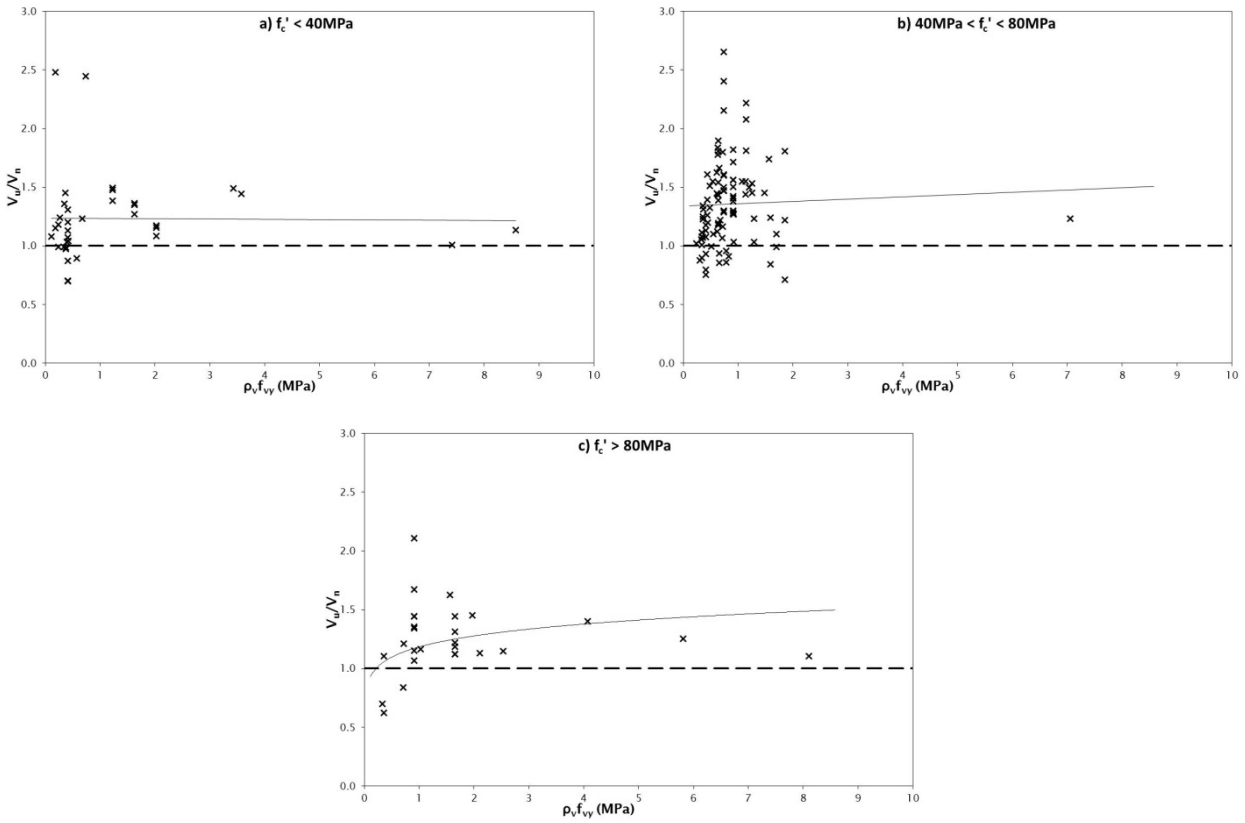

4.4.1.2 PC database

Figures 4.25–4.30 show the influence of various design parameters on the accuracy of ACI 318 in predicting the ultimate shear capacity of 164 PC beams. The average ratio of observed to predicted shear capacity was 1.18, with a standard deviation and coefficient of variation of 0.36 and 0.30, respectively. These statistical values were reflected in the large scatter that is evident in the figures. The combination of the average ratio of 1.18 and the large scatter resulted in 61 beams failing at ultimate shear capacities below those predicted by ACI 318, which is an alarming proportion (37%) of the refined PC database.

Figures 4.25 and 4.26 show the influence of concrete compressive strength and shear stress capacity on the accuracy of ACI 318 in predicting the shear capacity of 164 PC beams. The average ratio of measured to predicted strengths increased slightly as the concrete strength of the beams increased, with a lower proportion of overestimated capacities for beams with a concrete compressive strength greater than 50MPa. Significantly, the majority of beams containing high (6MPa < $\rho_v f_{vy}$ < 10MPa) and very high ($\rho_v f_{vy}$ > 10MPa) quantities of transverse reinforcement failed at ultimate shear capacities lower than those predicted by ACI 318. This trend indicates that ACI 318 does not adequately account for increased quantities of transverse reinforcement. While the data in figure 4.26 is scattered over the full range of shear stress capacities, there was a general trend of decreasing strength ratio with increasing shear stress capacity. It is noted that for the higher range of shear stress capacities (v_u > 6MPa), a greater proportion of the beams that failed at lower-than-predicted ultimate shear capacities contained normal-strength concrete ($f_c' \leq$ 40MPa).

Figure 4.25 Influence of concrete compressive strength on the accuracy of ACI 318 for beams in the PC database

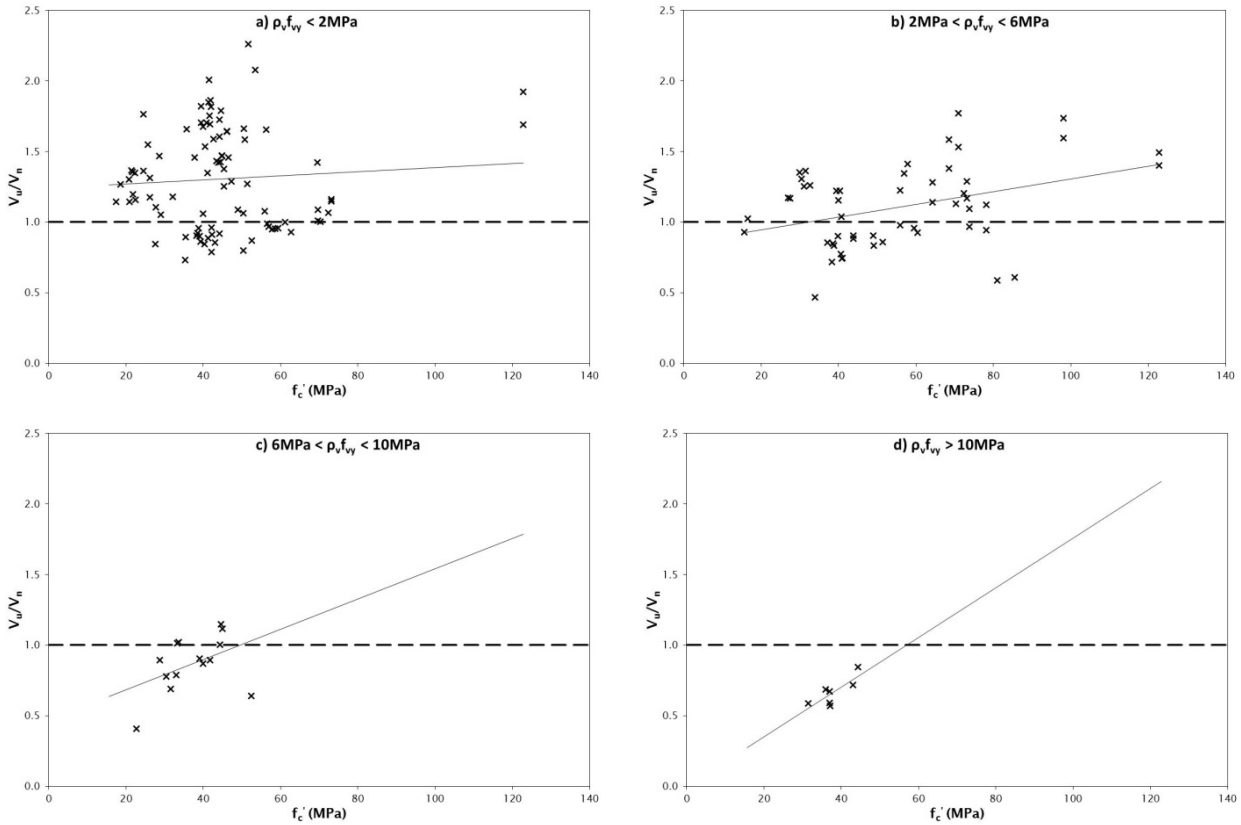

Figure 4.26 Influence of ultimate shear capacity on the accuracy of ACI 318 for beams in the PC database

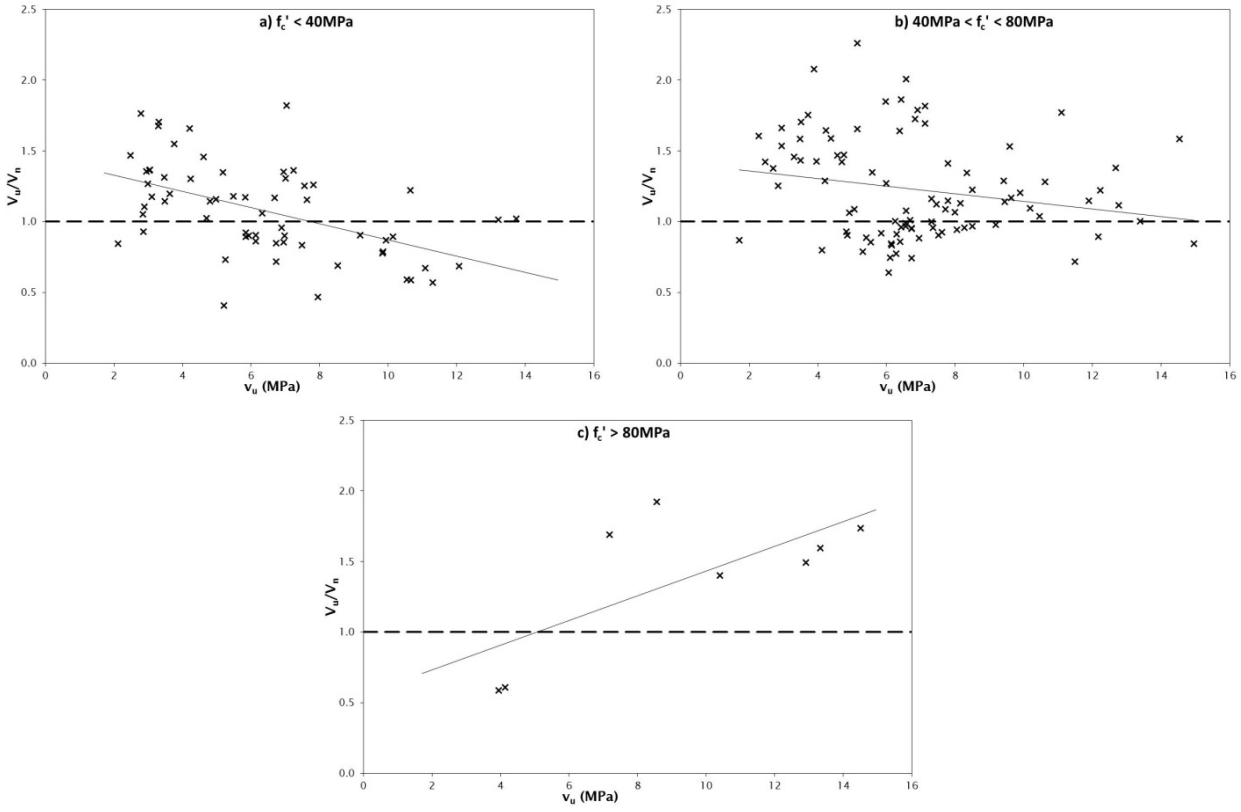

Figures 4.27 and 4.28 show observed to predicted shear capacities plotted against beam effective depths and shear a/d ratios, respectively. As opposed to the trend observed with RC beam ultimate shear capacities, ACI 318 was generally more conservative in predicting the ultimate shear capacity of larger PC beams (d > 1000mm). It was also noted that ACI 318 was regularly non-conservative for beams with a shear a/d ratio lower than 3.5.

Figure 4.27 Influence of effective depth on the accuracy of ACI 318 for beams in the PC database

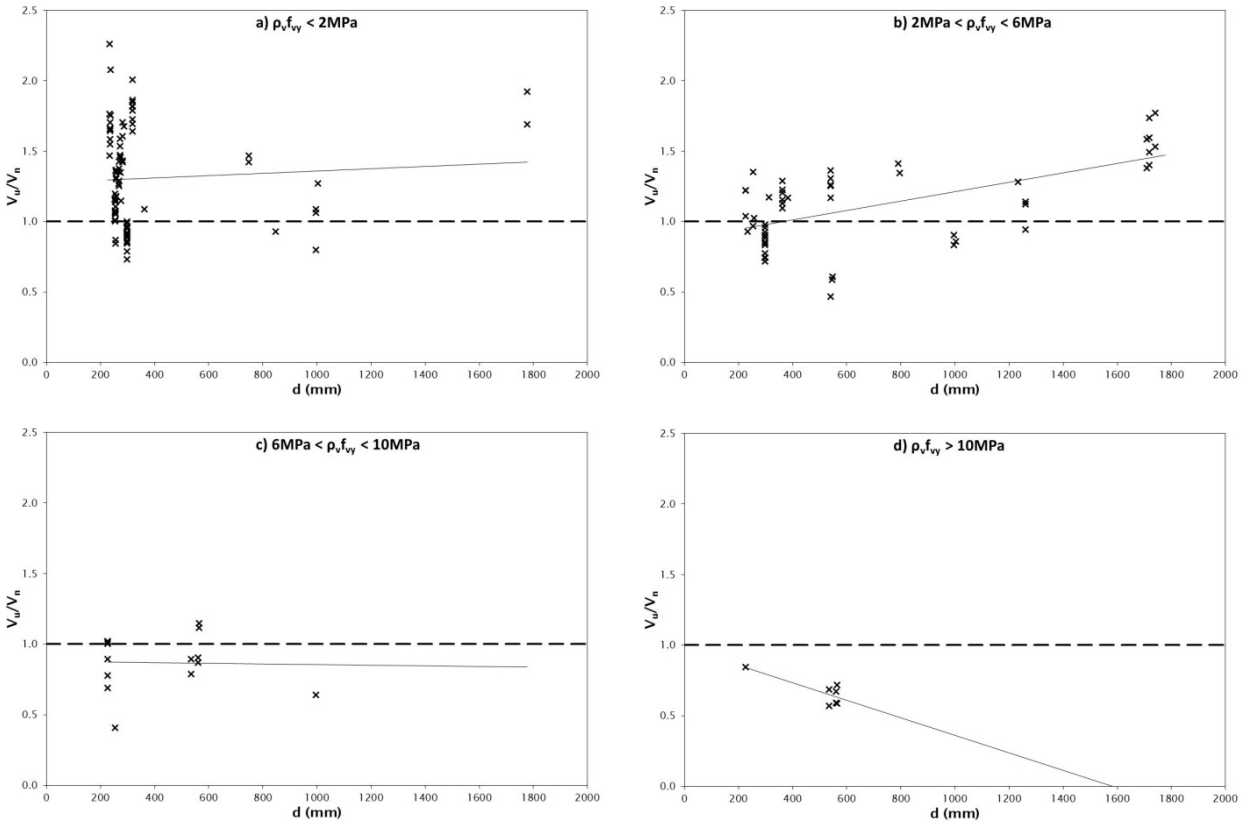

Figure 4.28 Influence of shear a/d ratio on the accuracy of ACI 318 for beams in the PC database

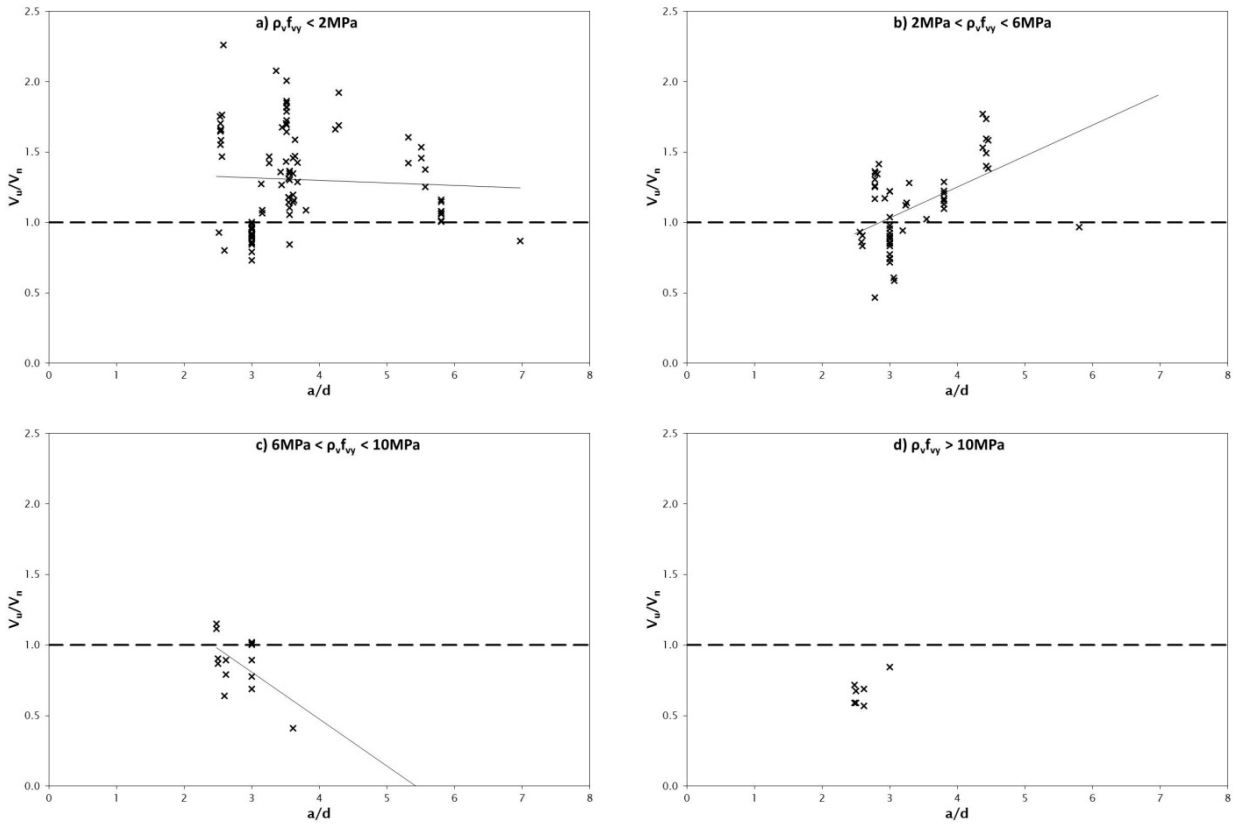

Figures 4.29 and 4.30 demonstrate that ACI 318 increasingly overestimated the ultimate shear capacity of PC beams with increasing levels of longitudinal and transverse reinforcement.

Figure 4.29 Influence of longitudinal reinforcement on the accuracy of ACI 318 for beams in the PC database

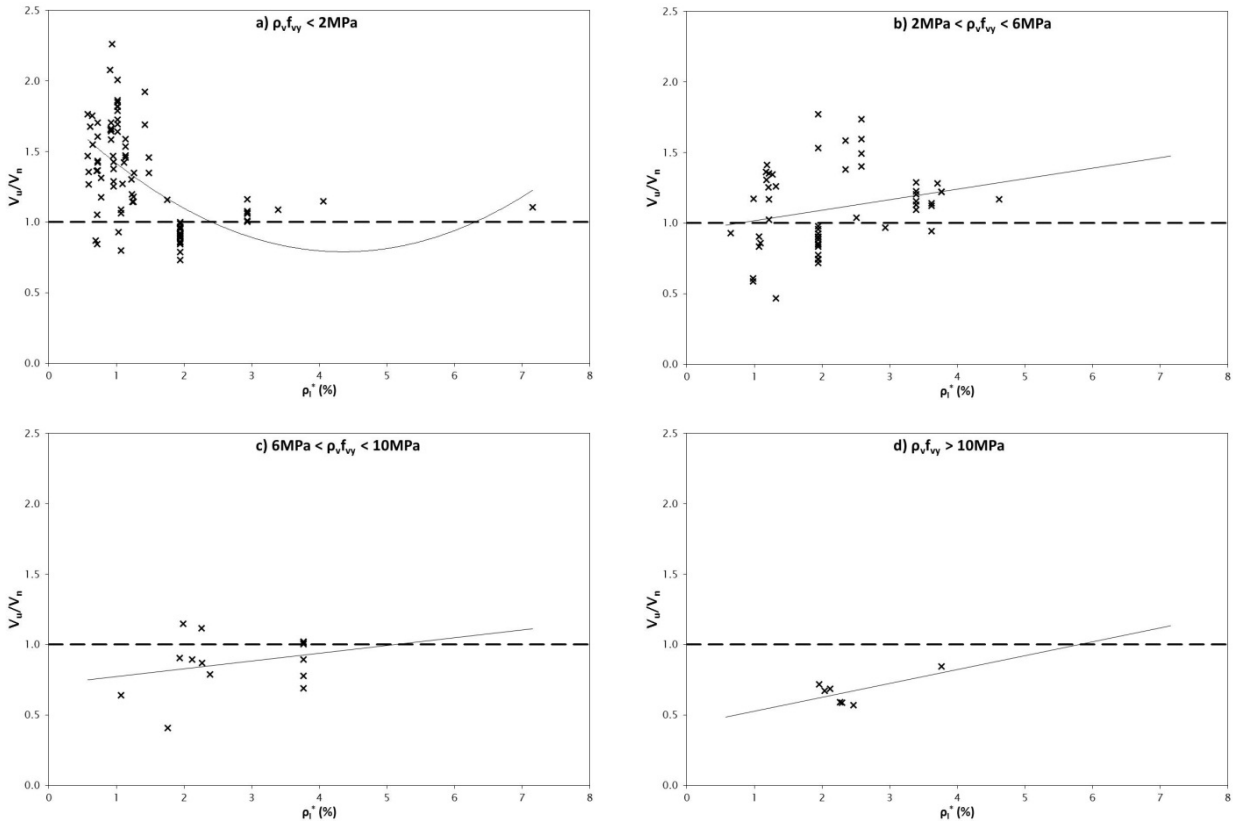

Figure 4.30 Influence of transverse reinforcement on the accuracy of ACI 318 for beams in the PC database

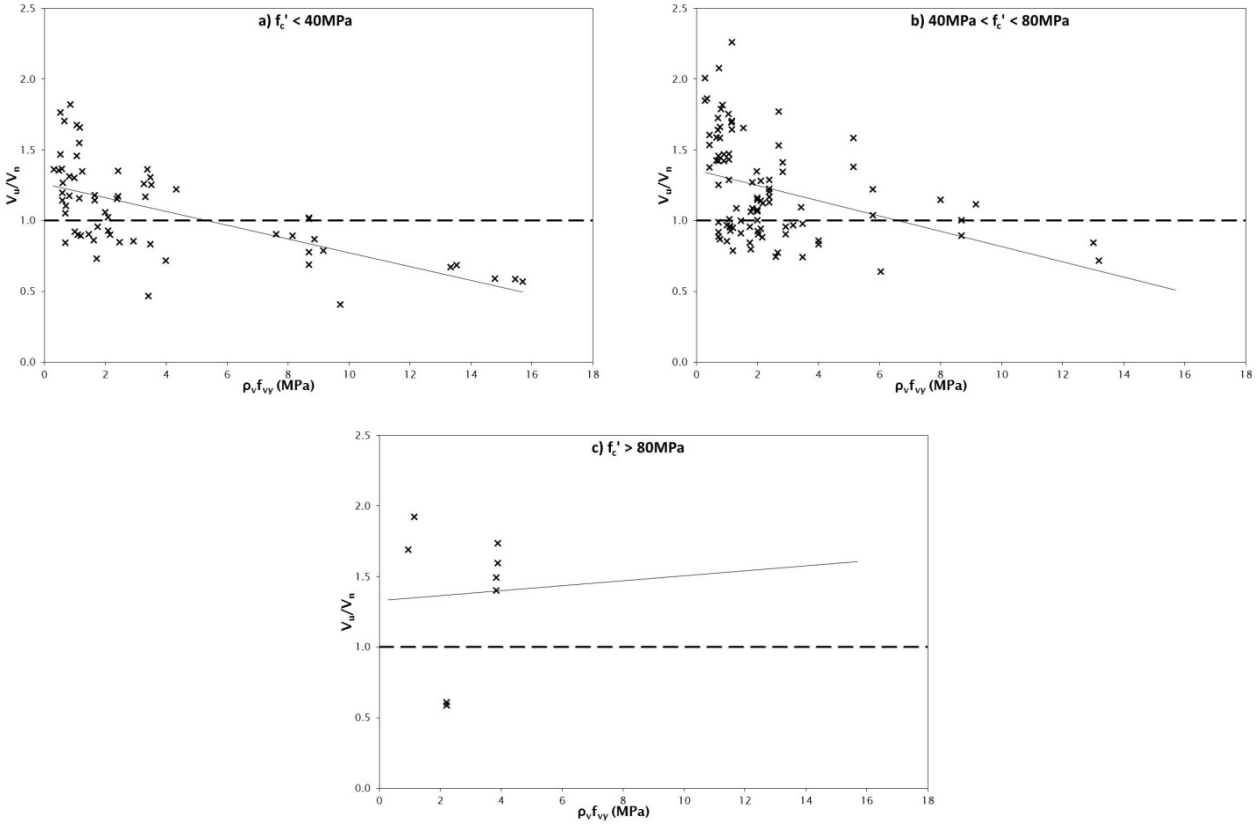

4.4.2 NZS 3101:2006

The provisions used to evaluate the performance of NZS 3101 were detailed in section 3.2. Equation 3.11 was used to calculate the predicted concrete contribution for each RC beam, with k_a taken as 1.0 because all beams considered contained at least the specified minimum transverse reinforcement. When using equation 3.11, the minimum and maximum limits specified for the concrete contribution were applied, while also limiting the value of f_c' to 50MPa.

As in ACI 318, NZS 3101 provides equations for web-shear and flexure-shear failure mechanisms, as reported in section 3.2.2. The contribution of transverse reinforcement for both RC and PC beams was calculated using equation 3.4, although the limit of $0.66\sqrt{f_c'}b_w d$ was not applied as it is not specified in NZS 3101. It is important to note that while the limit of $0.2f_c'$ was applied as the maximum allowable shear stress, the absolute limit of 8MPa was not applied, so that the validity of this limit could be specifically investigated.

4.4.2.1 RC database

The influence of various parameters on the accuracy of NZS 3101 in predicting the ultimate shear capacities of 160 RC beams is presented in figures 4.31–4.36. The average ratio of measured to predicted shear capacity was 1.39, while the standard deviation and coefficient of variation were 0.40 and 0.29 respectively. Twenty-one (13%) of the 160 RC beams exhibited ultimate shear capacities lower than predicted when using NZS 3101.

An examination of figure 4.31 reveals a general increase in the ratio of measured to predicted shear capacity with increasing beam concrete compressive strength, particularly for beams with a concrete strength between 50MPa and 90MPa. The average strength ratio for beams with a concrete strength less than 50MPa was 1.17, while for beams with a concrete strength greater than 50MPa, the average ratio was 1.53. The 50MPa concrete strength value is significant, as it is the maximum value allowed by NZS 3101 for calculation of v_b, and it was concluded that this maximum was overly limiting.

Figure 4.31 Influence of concrete compressive strength on the accuracy of NZS 3101 for beams in the RC database

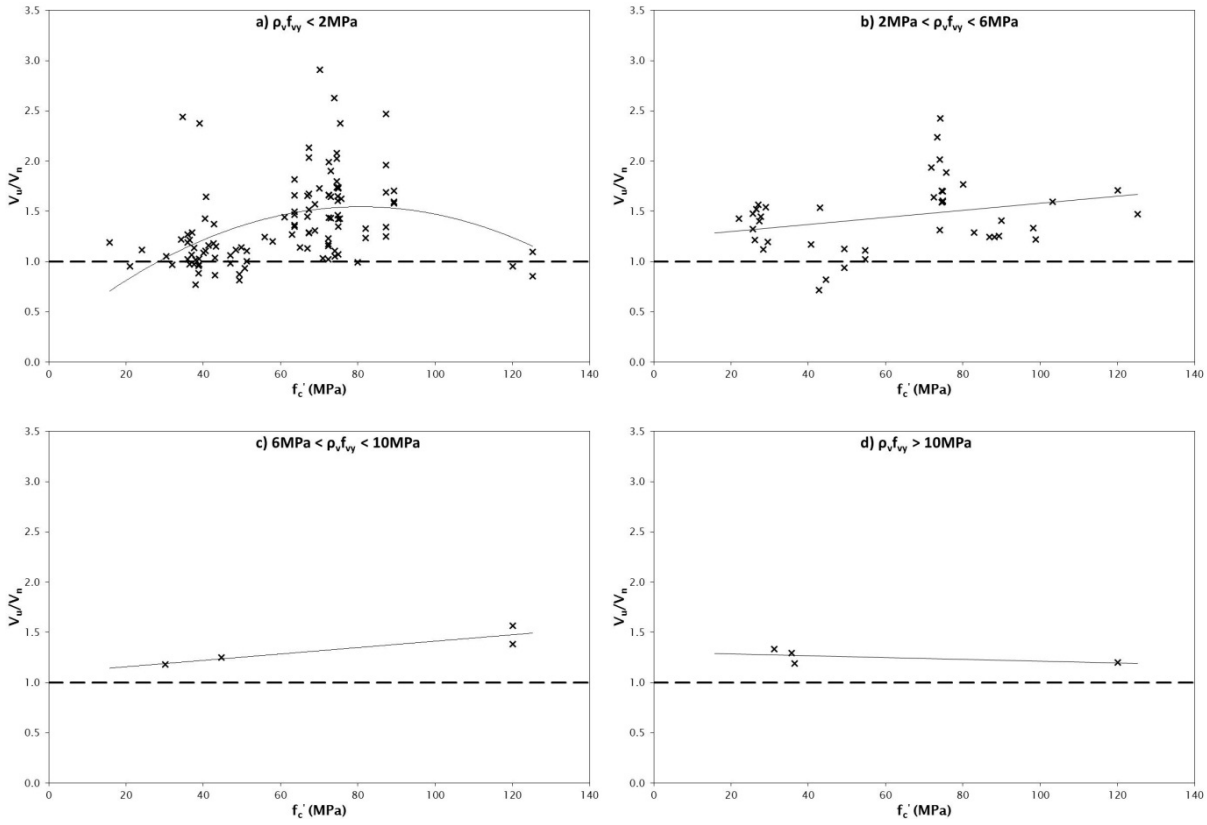

The effect of shear stress capacity on the accuracy of NZS 3101 in predicting beam shear capacity is shown in figure 4.32. NZS 3101 was found to increasingly underestimate the ultimate shear capacity of beams with increasing shear stress capacities, for shear stress capacities up to 6MPa. The few RC beams with shear stress capacities greater than 6MPa failed at applied shear forces much closer to the ultimate shear capacities predicted, using NZS 3101, than did beams with shear capacities less than 6MPa. Two such beams demonstrated ultimate shear capacities lower than those predicted by the design standard.

Figure 4.32 Influence of ultimate shear capacity on the accuracy of NZS 3101 for beams in the RC database

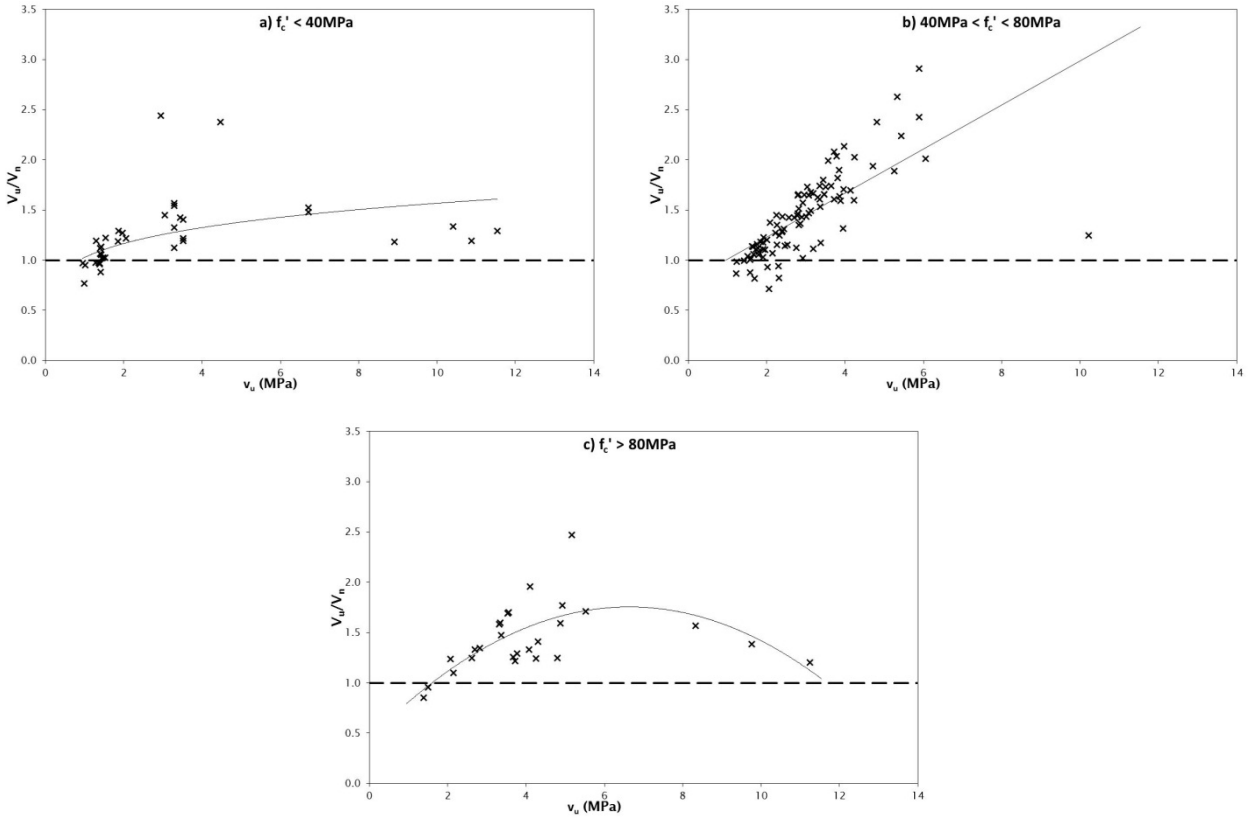

Figures 4.33 and 4.34 show the ratios of observed to predicted shear capacities plotted against beam effective depths and shear a/d ratios, respectively. NZS 3101 was found to improve in accuracy with increasing beam effective depth, and was particularly conservative for a number of the beams with a smaller depth (d < 350mm). As with ACI 318, it was observed that NZS 3101 overestimated the shear capacity of lightly reinforced, large RC beams ($\rho_v f_{vy}$ < 4MPa and d > 350mm). When excluding RC beams tested with a shear a/d ratio close to 2.5, there was no general trend observed in the effect of a/d on shear capacity ratio.

Figure 4.33 Influence of effective depth on the accuracy of NZS 3101 for beams in the RC database

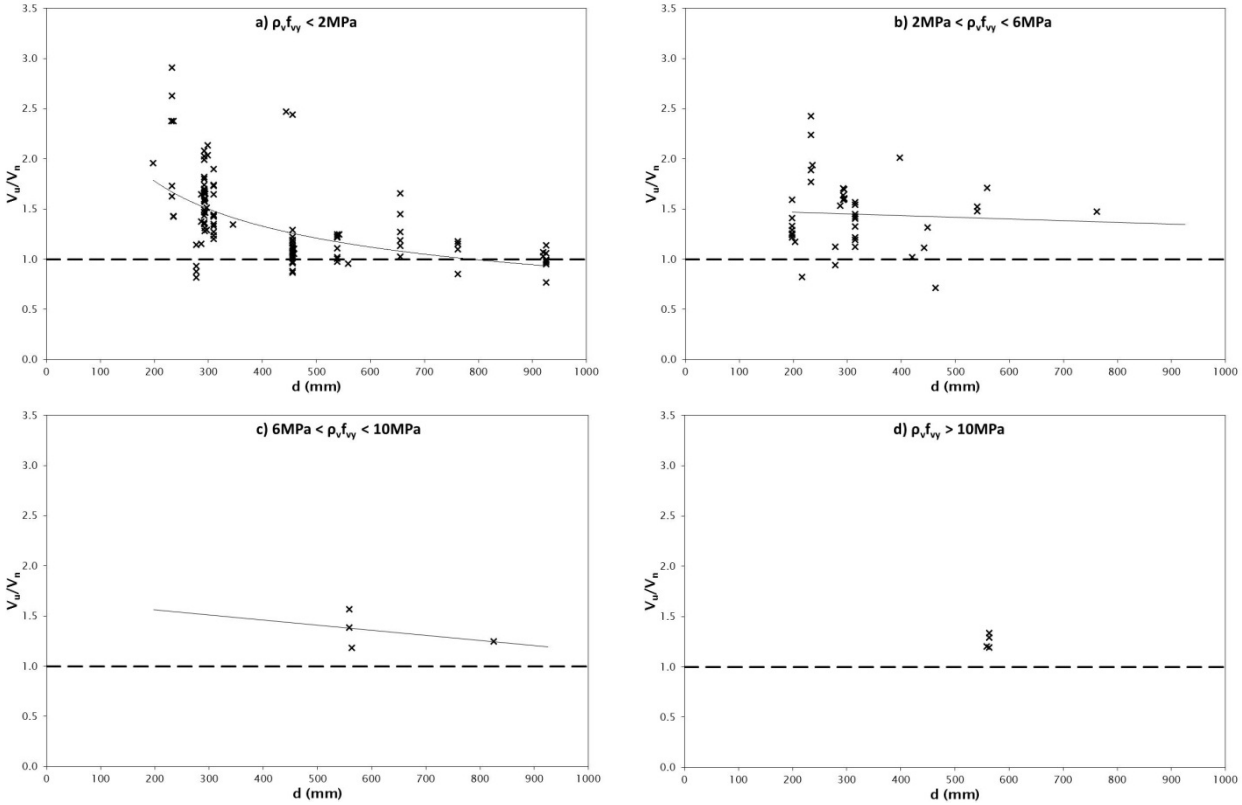

Figure 4.34 Influence of shear a/d ratio on the accuracy of NZS 3101 for beams in the RC database

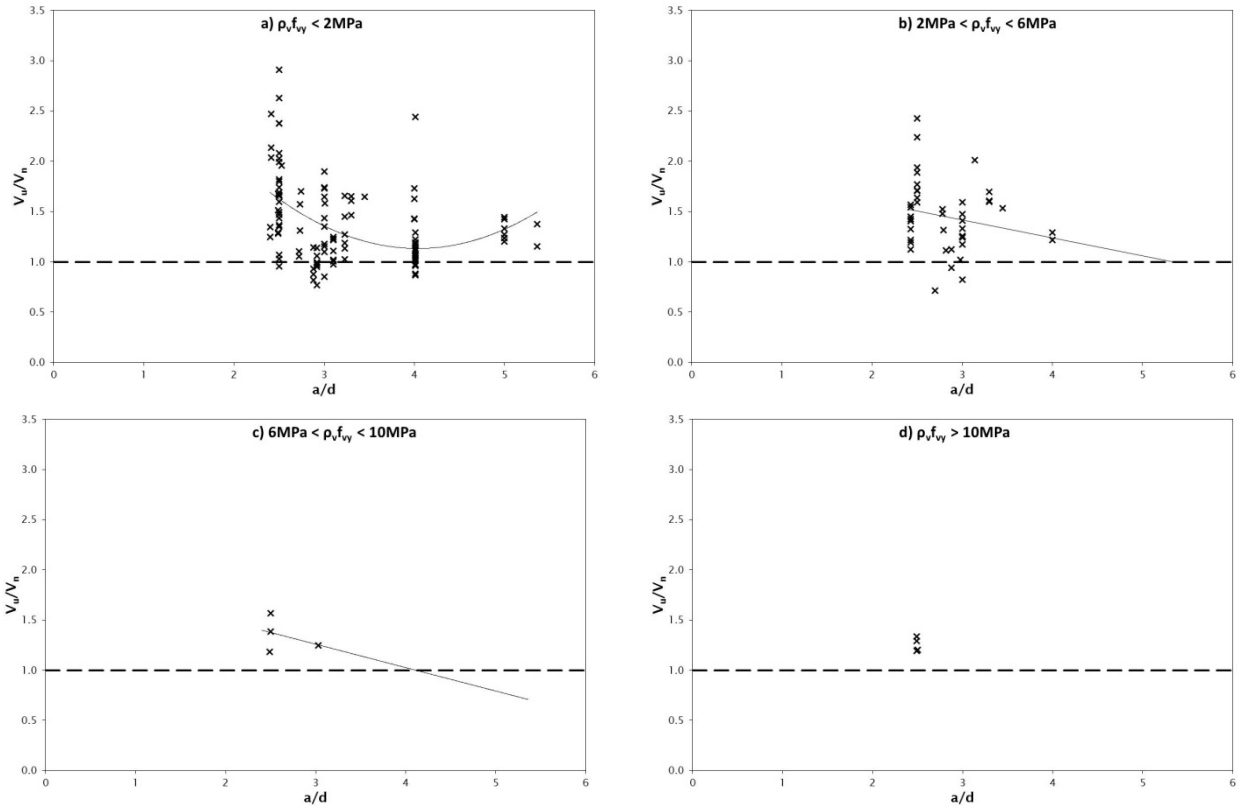

The influence of longitudinal and transverse reinforcement on the shear capacity ratio determined using NZS 3101 is shown in figures 4.35 and 4.36. NZS 3101 was observed to provide increasingly conservative predicted shear capacities as the longitudinal reinforcement in the beam increased. This trend indicates that the design method does not sufficiently account for the influence of dowel actions. Meanwhile, there was no evident trend in figure 4.36, and a great deal of scatter is observed at low levels of transverse reinforcement ($\rho_v f_{vy}$ < 2MPa).

Figure 4.35 Influence of longitudinal reinforcement on the accuracy of NZS 3101 for beams in the RC database

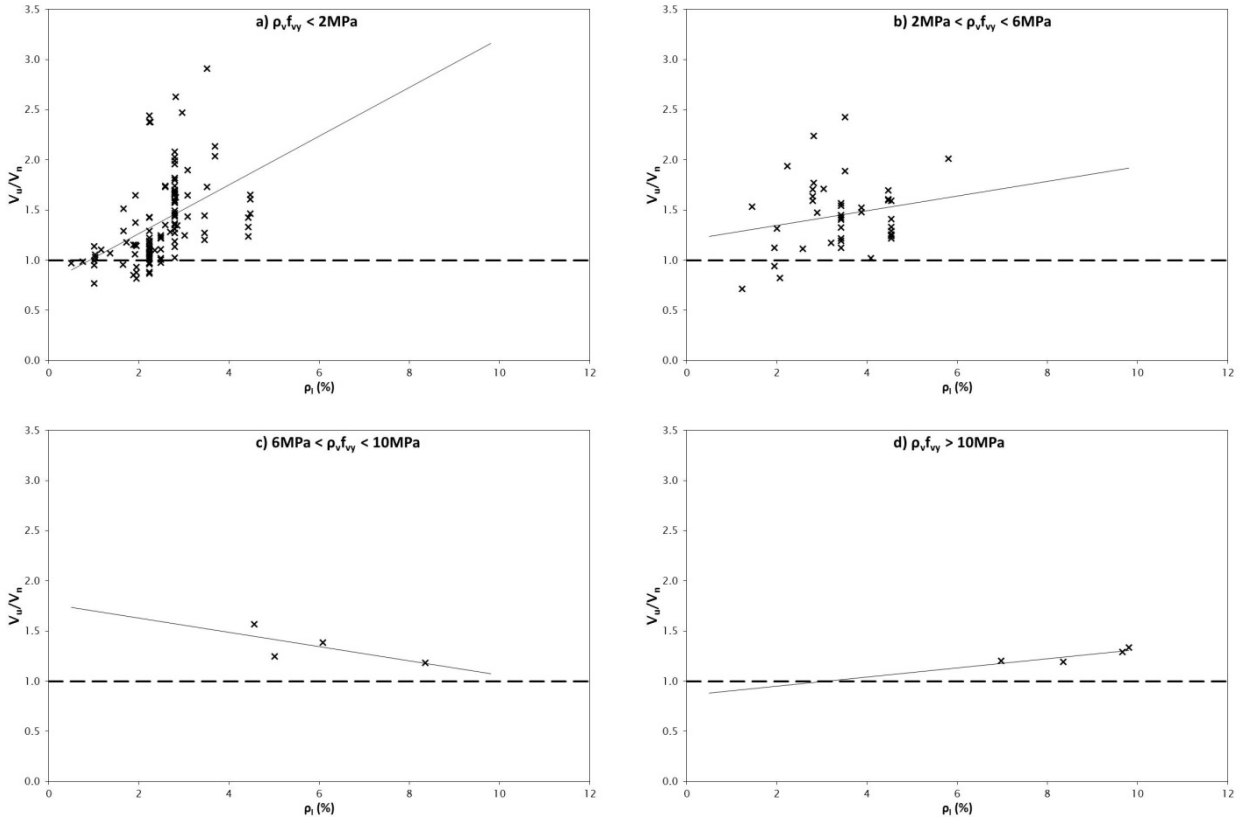

Figure 4.36 Influence of transverse reinforcement on the accuracy of NZS 3101 for beams in the RC database

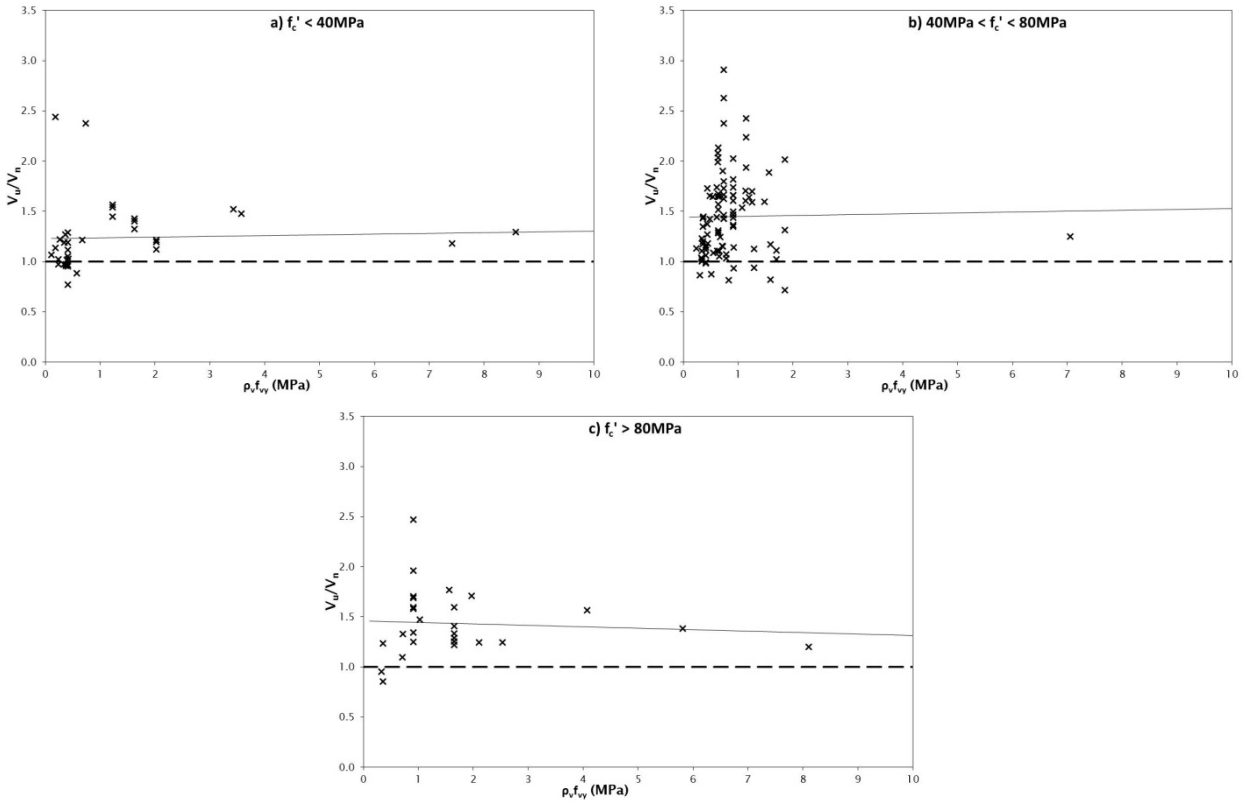

4.4.2.2 PC database

Figures 4.37–4.42 show the influence of various design parameters on the accuracy of NZS 3101 in predicting the ultimate shear capacity of 164 PC beams. The average ratio of observed to predicted shear capacity was 1.12, with a standard deviation and coefficient of variation of 0.31 and 0.28, respectively. Sixty-six (40%) of the 164 PC beams in this analysis failed at ultimate shear capacities that were lower than predicted using NZS 3101.

Figures 4.37 and 4.38 show the observed to predicted shear capacity ratios plotted against the concrete compressive strength and shear stress capacity, respectively, of 164 PC beams with varying levels of transverse reinforcement. No strong relationship was observed between the shear capacity ratios and concrete compressive strength, although the ultimate shear capacity of beams with a low level of transverse reinforcement and with a concrete compressive strength less than 50MPa was generally found to be underestimated by the design standard to a greater extent than for other beams. It was also observed that the shear capacity ratios for beams with an ultimate shear capacity greater than 8MPa increased with increasing ultimate shear capacity.

Figure 4.37 Influence of concrete compressive strength on the accuracy of NZS 3101 for beams in the PC database

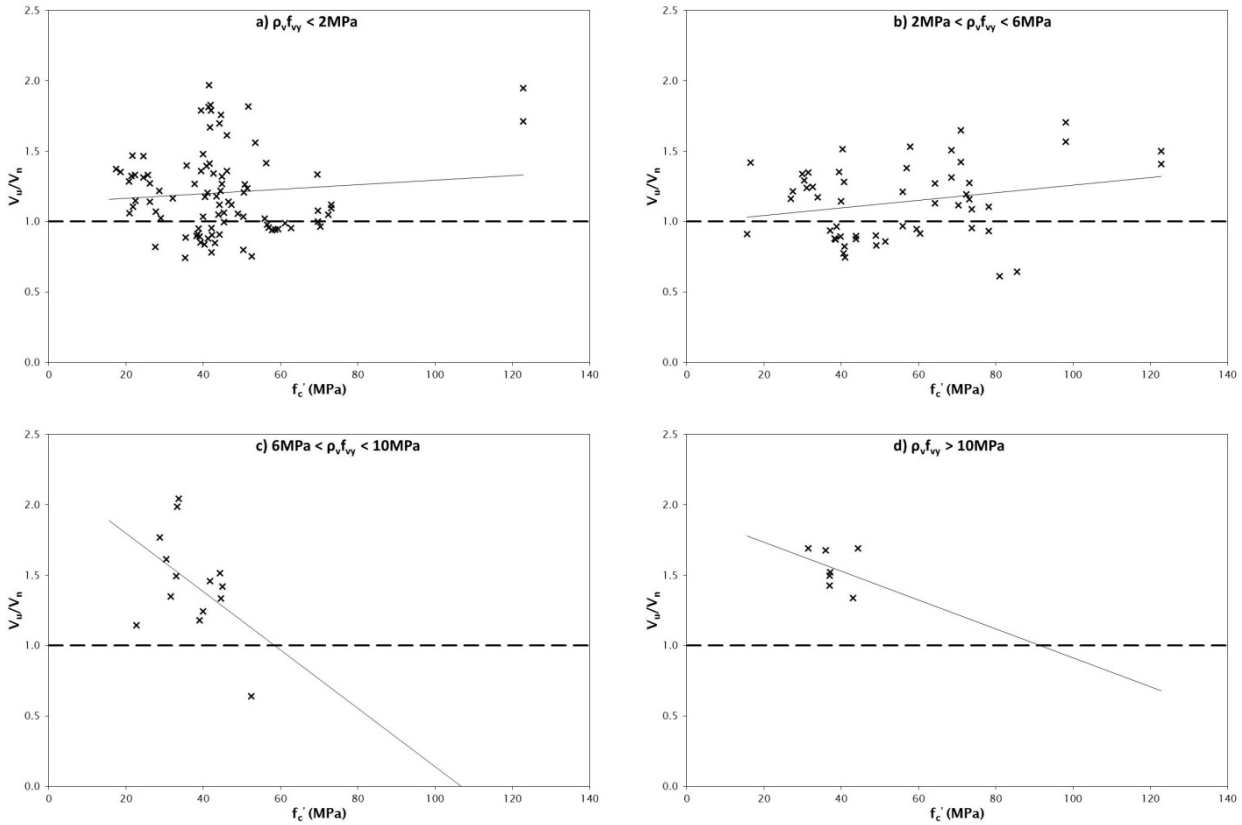

Figure 4.38 Influence of ultimate shear capacity on the accuracy of NZS 3101 for beams in the PC database

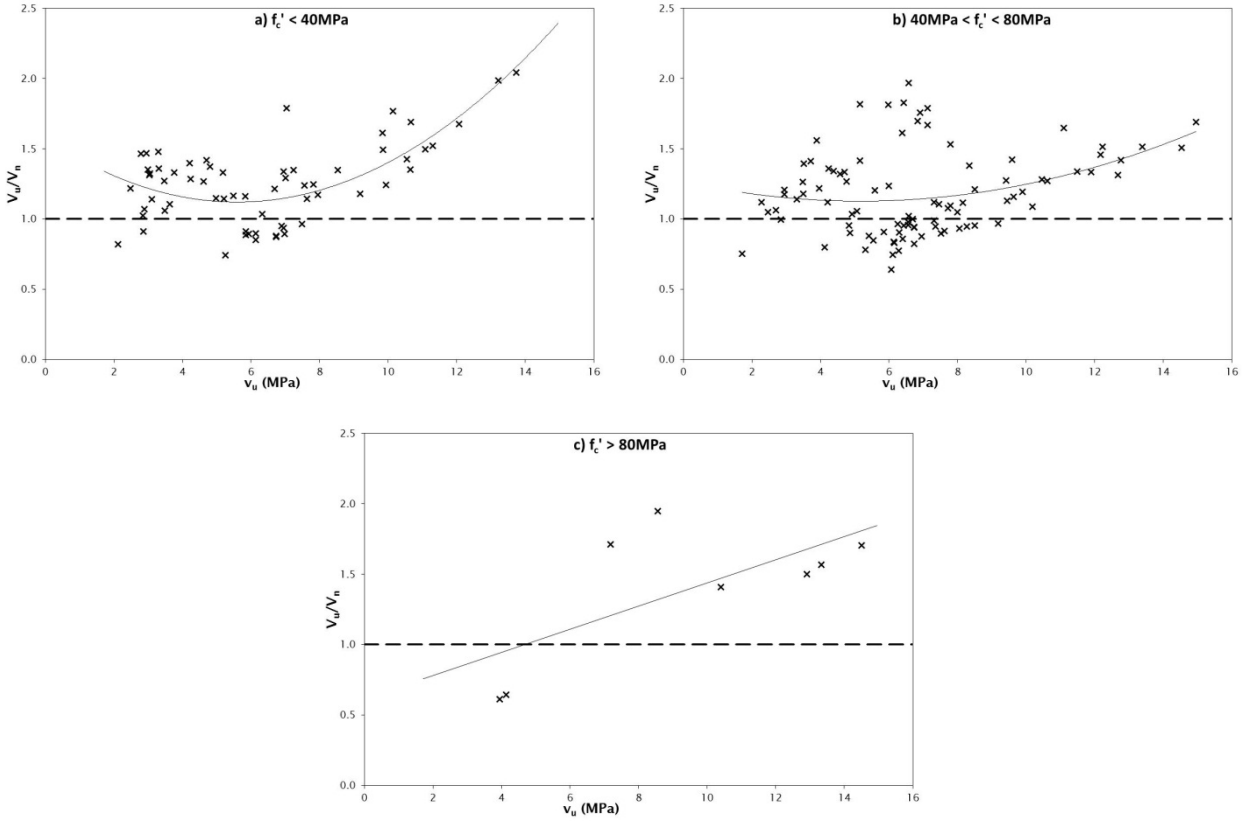

The influence of beam effective depth and shear a/d ratio on the accuracy of NZS 3101 in predicting the ultimate shear capacity of PC beams is shown in figures 4.39 and 4.40. Beam effective depth was found to not be of great significance to the accuracy of NZS 3101, although the 10 large beams (approximately 1800mm deep) all achieved shear capacities considerably greater than predicted by the design standard. In figure 4.40 the large amount of scatter at all values of a/d led to no trend being visible.

Figure 4.39 Influence of effective depth on the accuracy of NZS 3101 for beams in the PC database

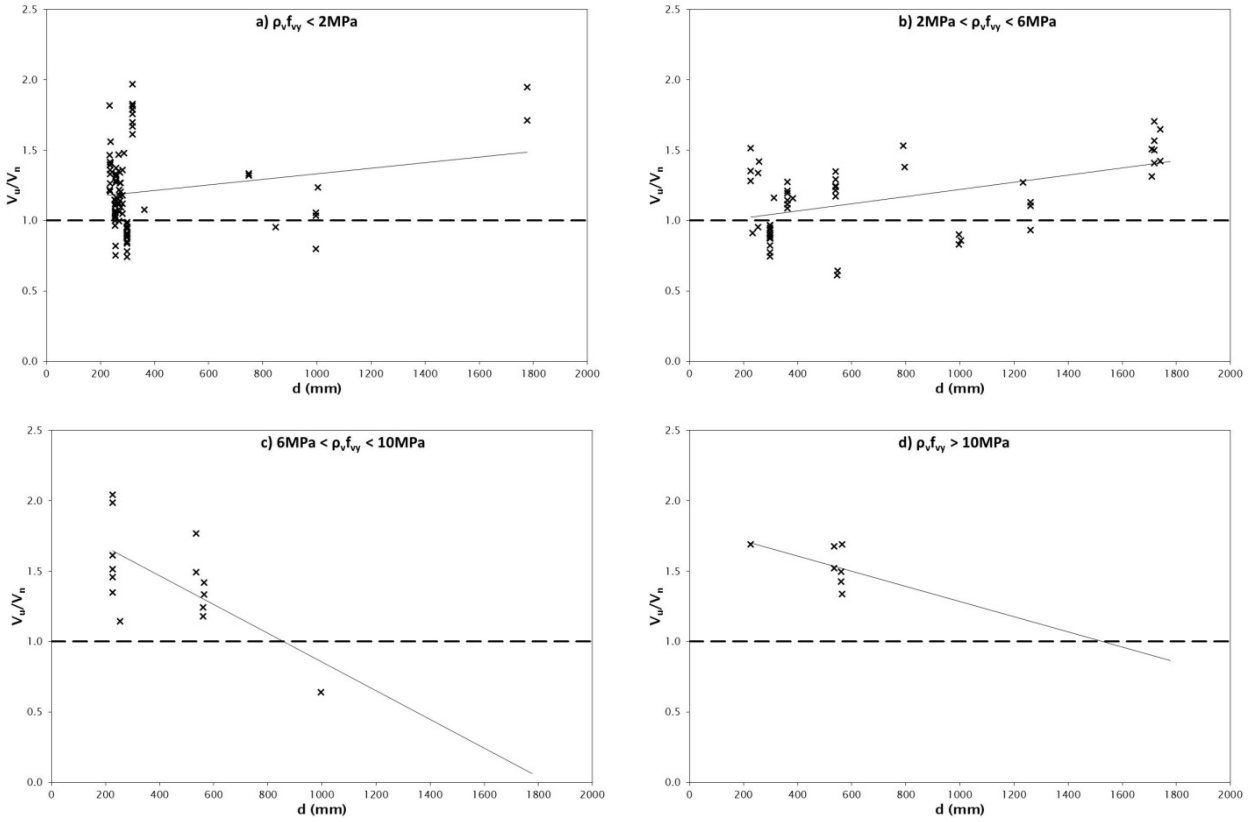

Figure 4.40 Influence of shear a/d ratio on the accuracy of NZS 3101 for beams in the PC database

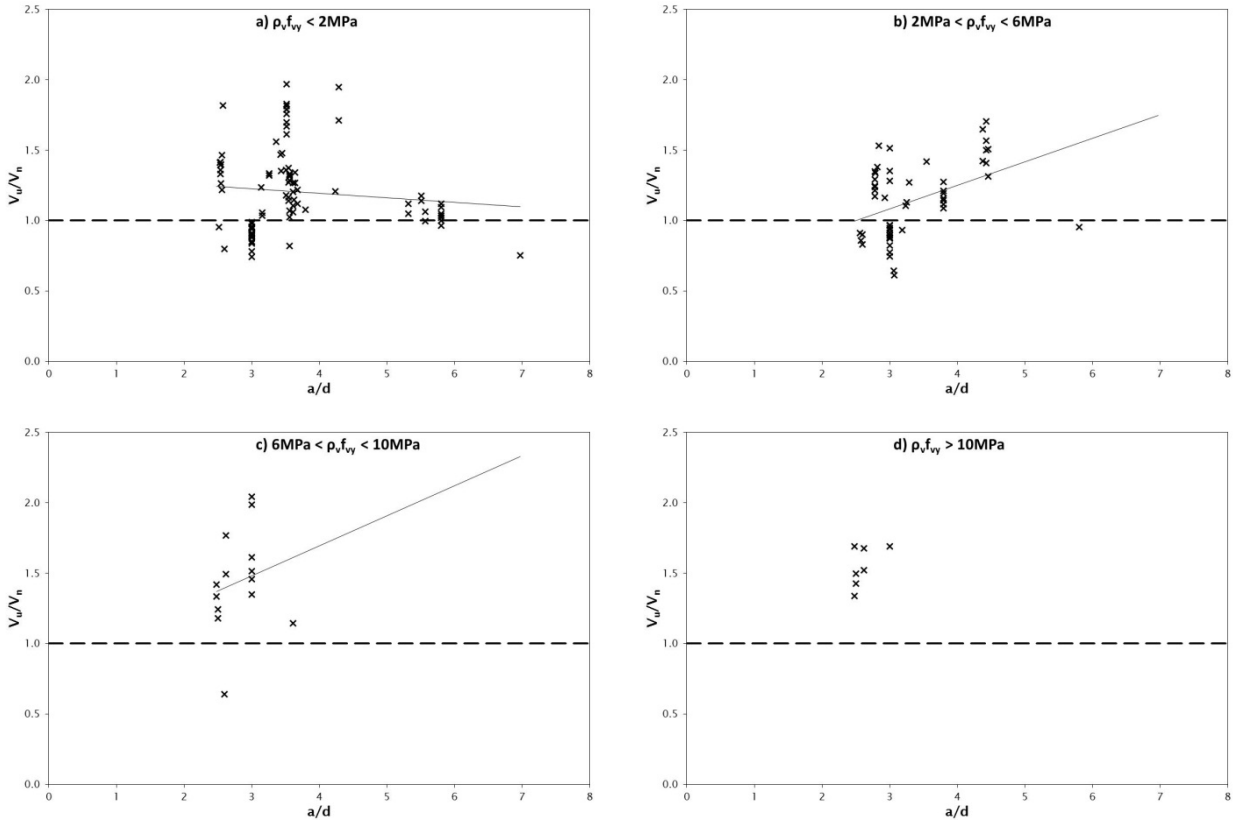

Figure 4.41 demonstrates that the ultimate shear capacity predictions of NZS 3101 increased in accuracy with increasing quantities of longitudinal reinforcement for all but the lowest quantities of transverse reinforcement ($\rho_v f_{vy}$ < 2MPa), while figure 4.42 shows that NZS 3101 increasingly overestimated the ultimate shear capacity of PC beams with increasing levels of transverse reinforcement.

Figure 4.41 Influence of longitudinal reinforcement on the accuracy of NZS 3101 for beams in the PC database

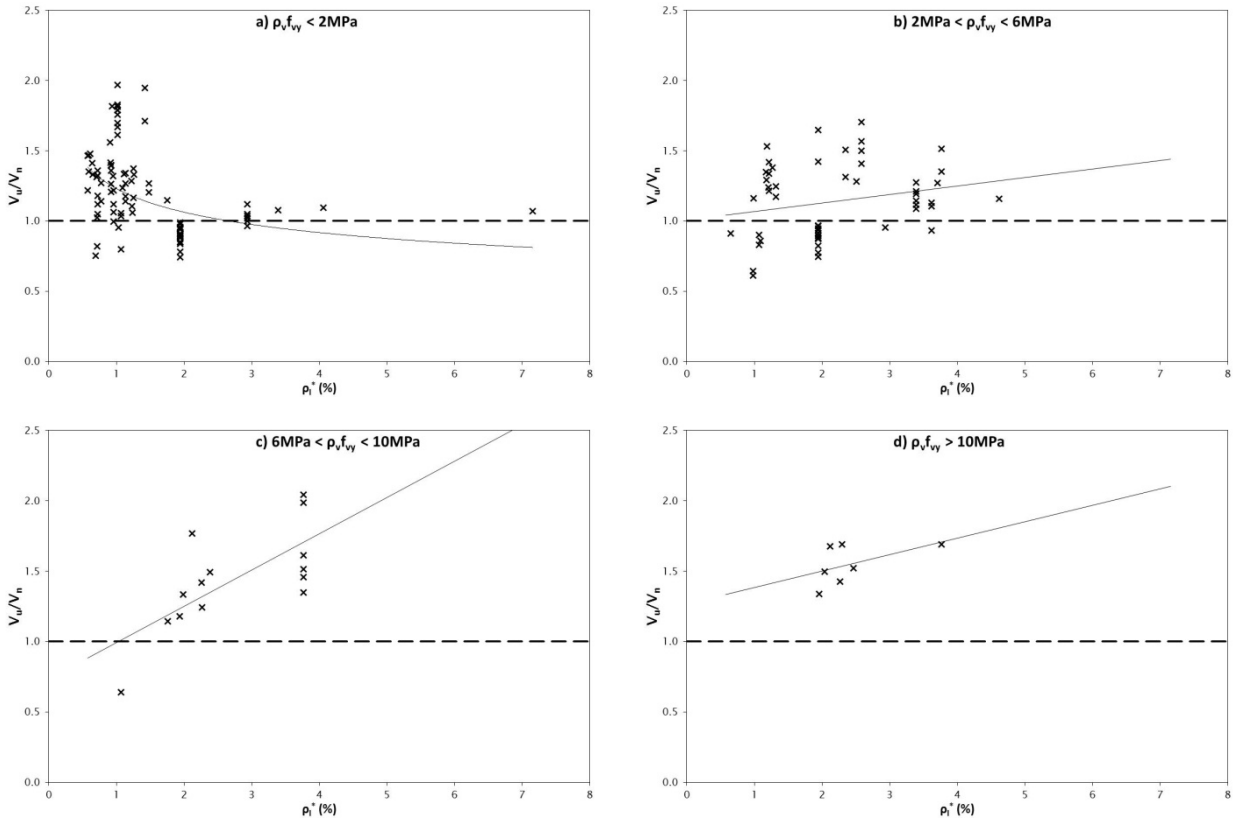

Figure 4.42 Influence of transverse reinforcement on the accuracy of NZS 3101 for beams in the PC database

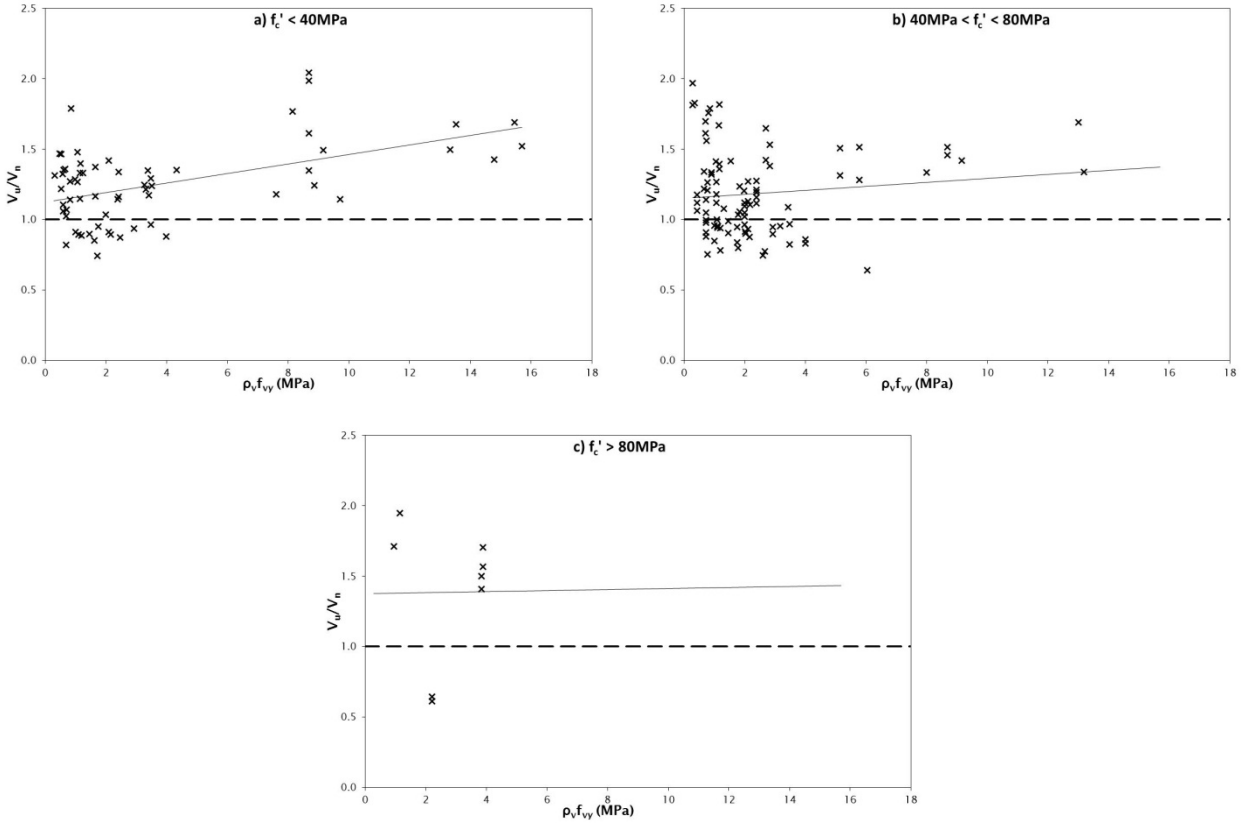

4.4.3 CSA A23.3-04 and AASHTO LRFD 6th edition

The method provided by CSA A23.3 and AASHTO LRFD for calculating the ultimate shear capacity of RC and PC beams was described earlier in section 3.3. As neither design standard imposes an absolute limit on the maximum allowable shear stress, all limits detailed in section 3.3 have been applied for this evaluation.

4.4.3.1 RC database

Figures 4.44–4.48 show the influence of concrete compressive strength, shear stress capacity, beam effective depth, shear a/d ratio, and levels of longitudinal and transverse reinforcement on the accuracy of CSA A23.3 and AASHTO LRFD in predicting the ultimate shear capacity of RC beams. When calculated using the CSA A23.3 and AASHTO LRFD provisions, the average ratio of measured to predicted shear capacity for RC beams was 1.23. The corresponding standard deviation and coefficient of variation were 0.46 and 0.38, respectively, and 53 (33%) of the total 160 RC beams exhibited ultimate shear capacities that were lower than predicted.

As shown in figure 4.44, the ultimate shear capacities predicted by CSA A23.3 and AASHTO LRFD were observed to slightly increase in conservatism with increasing concrete compressive strength. The design standards were also found to increasingly underestimate the ultimate shear capacity of beams with increasing shear stress capacities, for shear stress capacities up to 6MPa, as shown in figure 4.43. For the few beams that exhibited shear stress capacities greater than 6MPa, and in particular greater than 8MPa, the design provisions were found to provide generally non-conservative predictions of ultimate shear capacity.

Figure 4.43 Influence of concrete compressive strength on the accuracy of CSA A23.3 for beams in the RC database

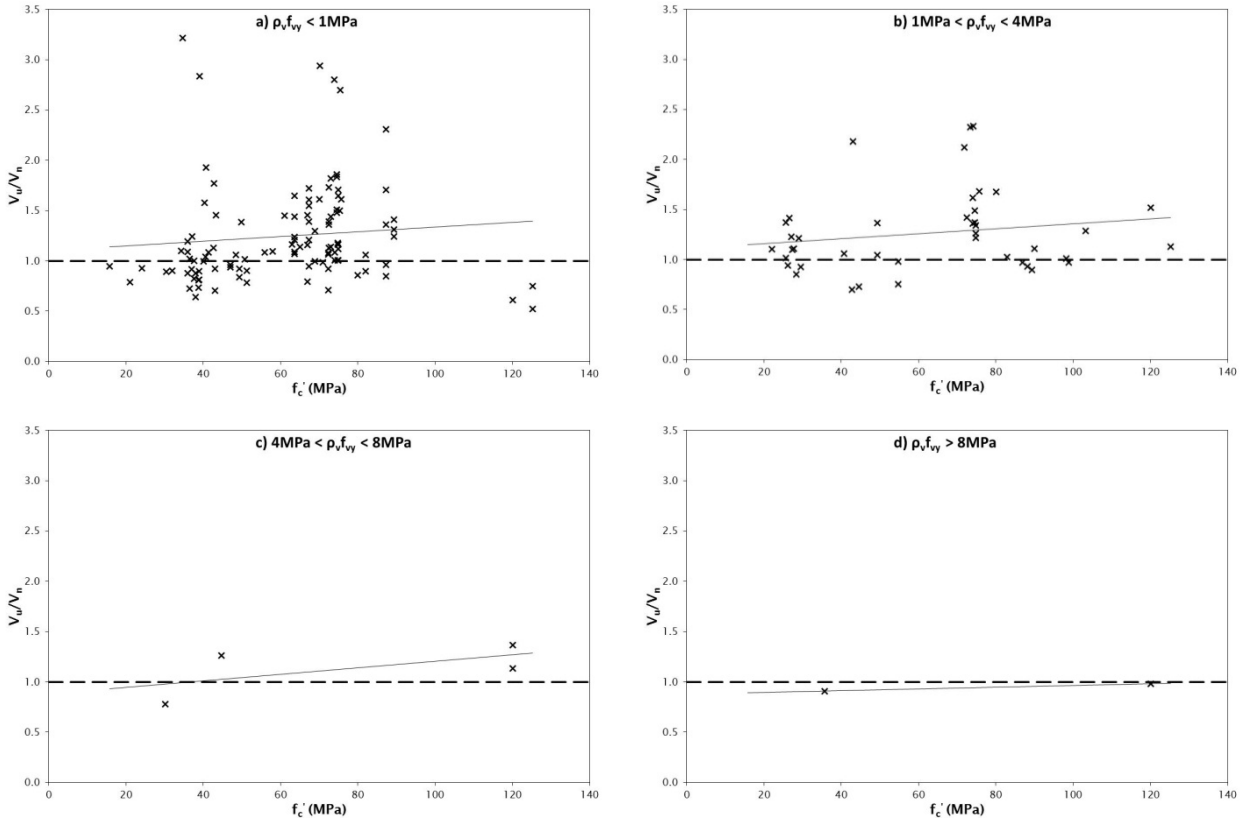

Figure 4.44 Influence of ultimate shear capacity on the accuracy of CSA A23.3 for beams in the RC database

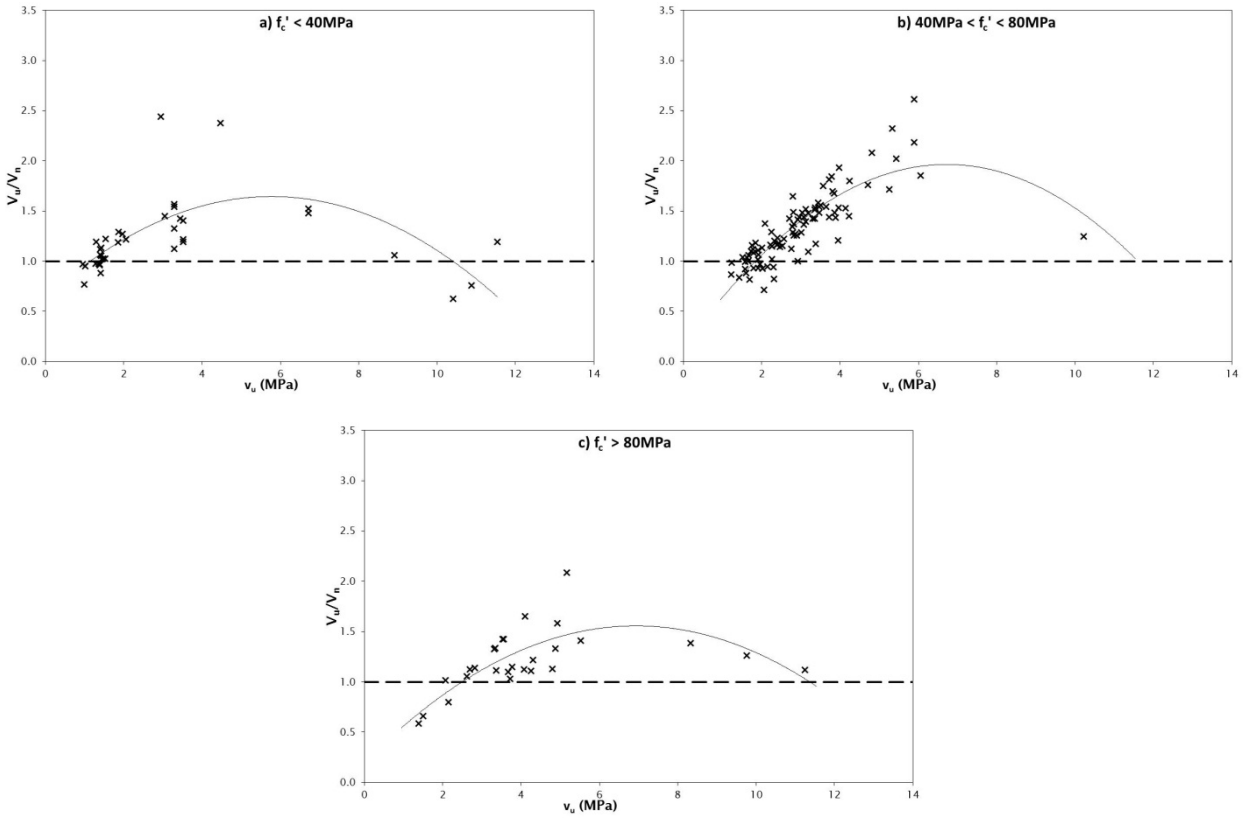

The ratios of measured to predicted shear capacity were observed to decrease with increasing beam effective depth for the vast majority of beams, changing from being generally conservative for smaller beams (effective depths below 400mm) to somewhat non-conservative for larger beams (depths greater than 400mm). This trend, as shown in figure 4.45, was observed for beams with all levels of transverse reinforcement. Except for beams tested with shear a/d ratios close to 2.5, figure 4.46 shows that there was no general trend in the effect of a/d on shear capacity ratio.

Figure 4.45 Influence of effective depth on the accuracy of CSA A23. 3 for beams in the RC database

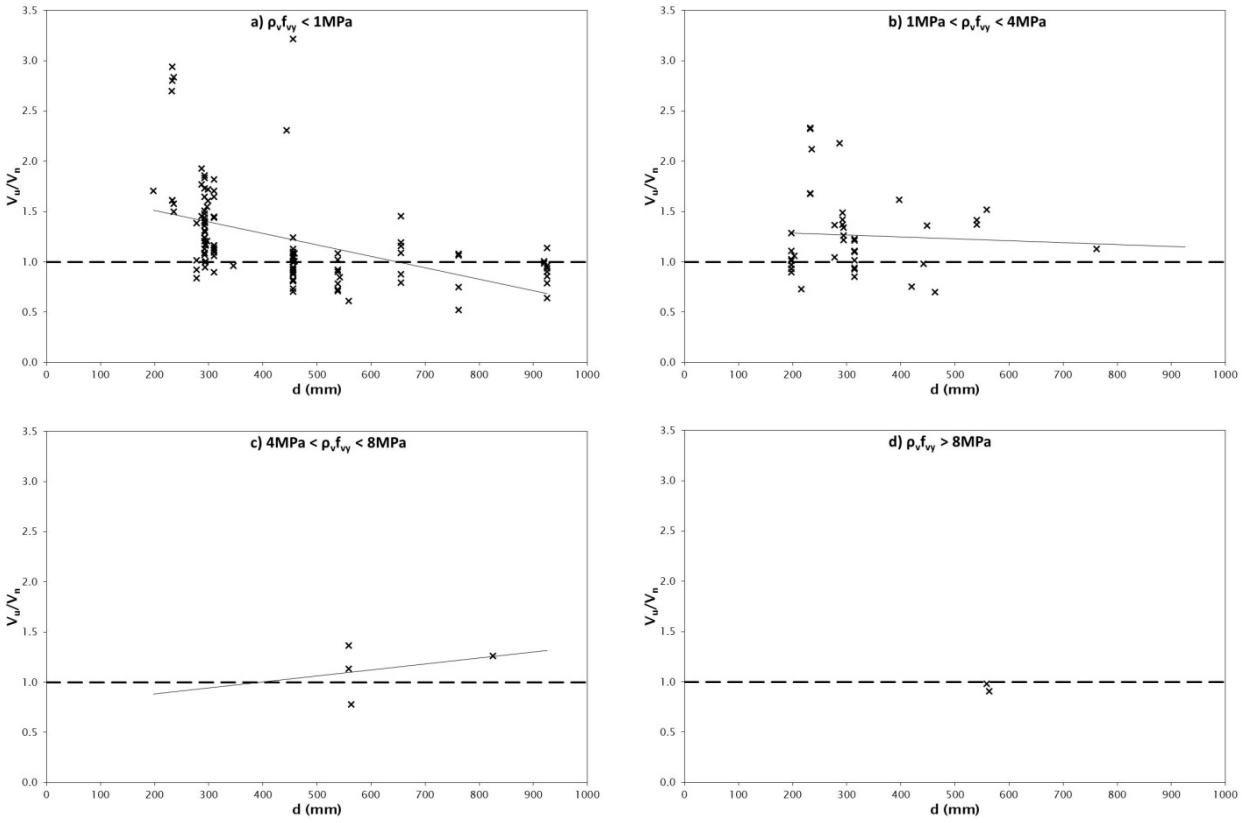

Figure 4.46 Influence of shear a/d ratio on the accuracy of CSA A23.3 for beams in the RC database

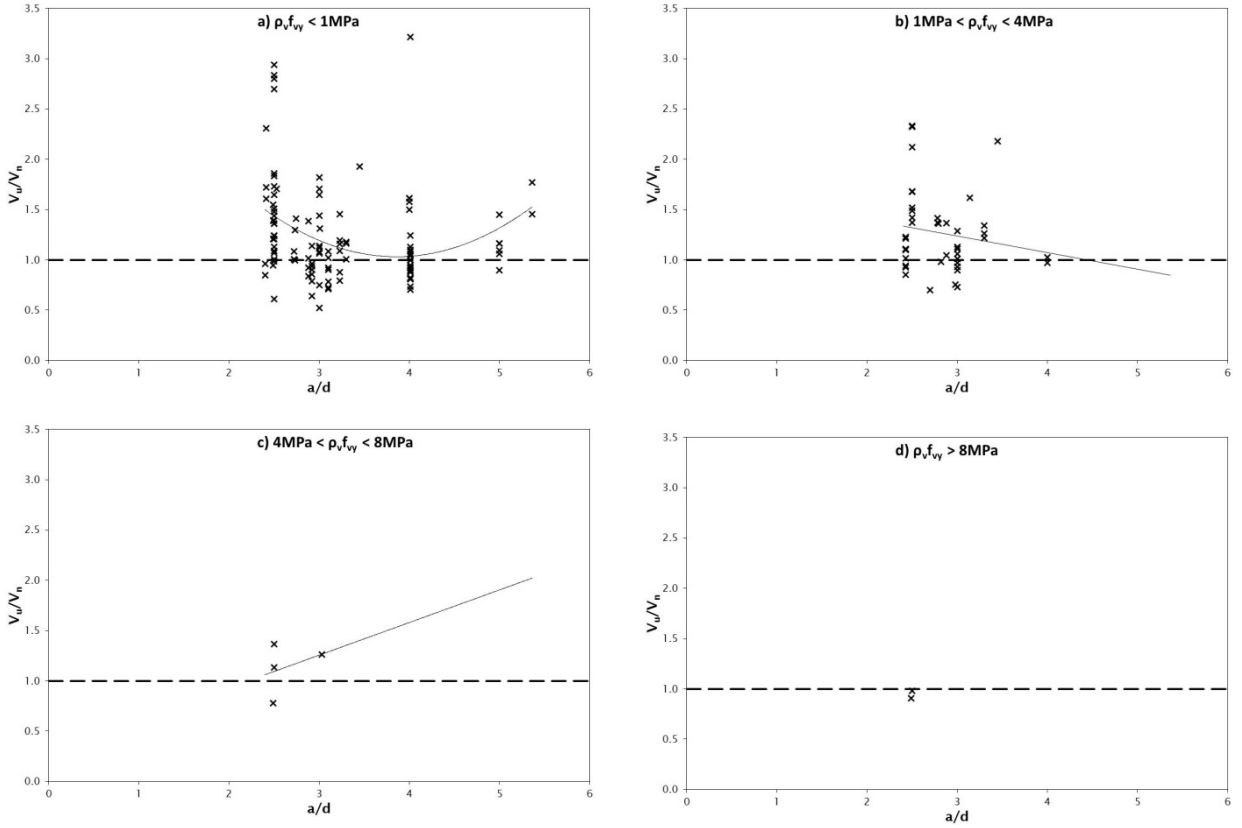

As shown in figure 4.47, when using CSA A23.3 the predicted shear capacities of a significant proportion of beams with a longitudinal reinforcement ratio lower than 4% were substantially more conservative than for other beams. The large amount of scatter visible in figure 4.48 illustrates the absence of a relationship between accuracy of predicted ultimate shear capacity and level of transverse reinforcement, indicating that the accuracy of the design provisions is more dependent on other parameters.

Figure 4.47 Influence of longitudinal reinforcement on the accuracy of CSA A23.3 for beams in the RC database

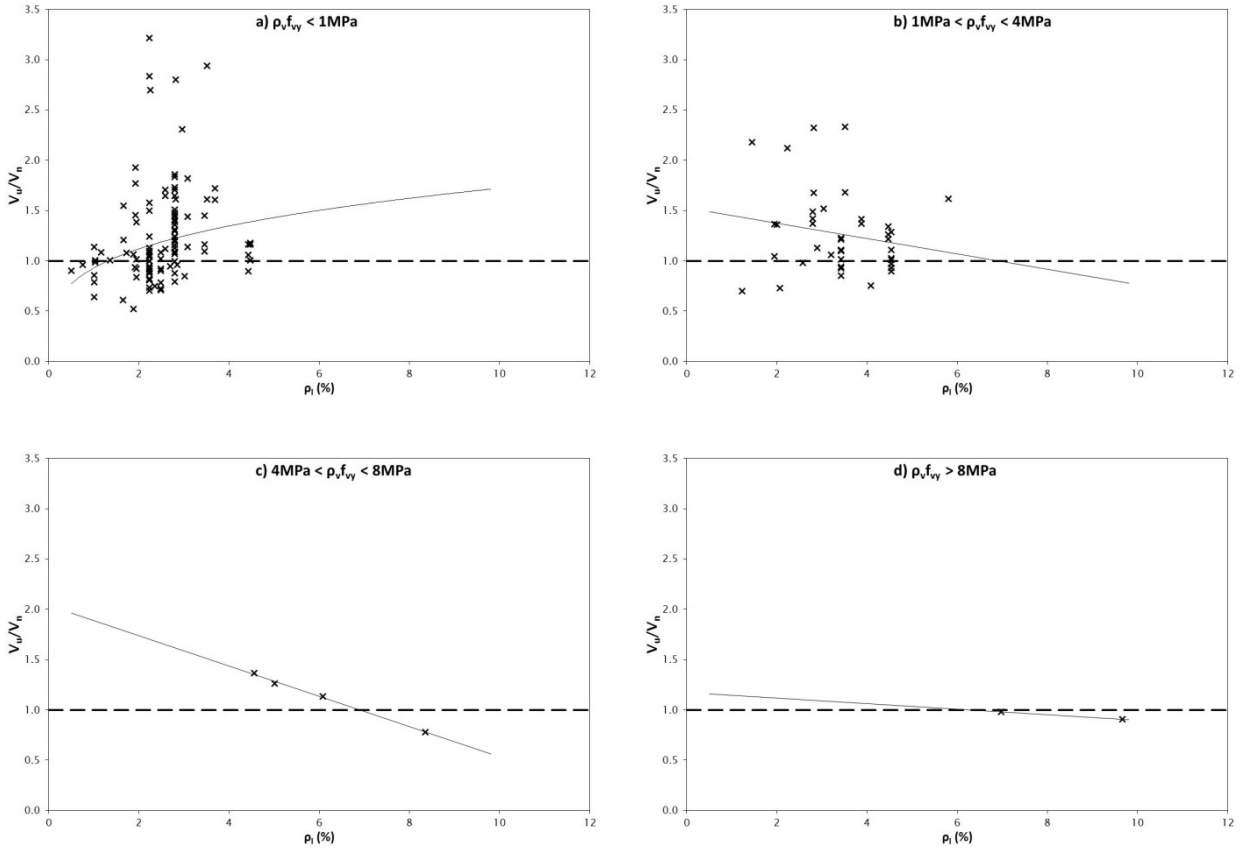

Figure 4.48 Influence of transverse reinforcement on the accuracy of CSA A23.3 for beams in the RC database

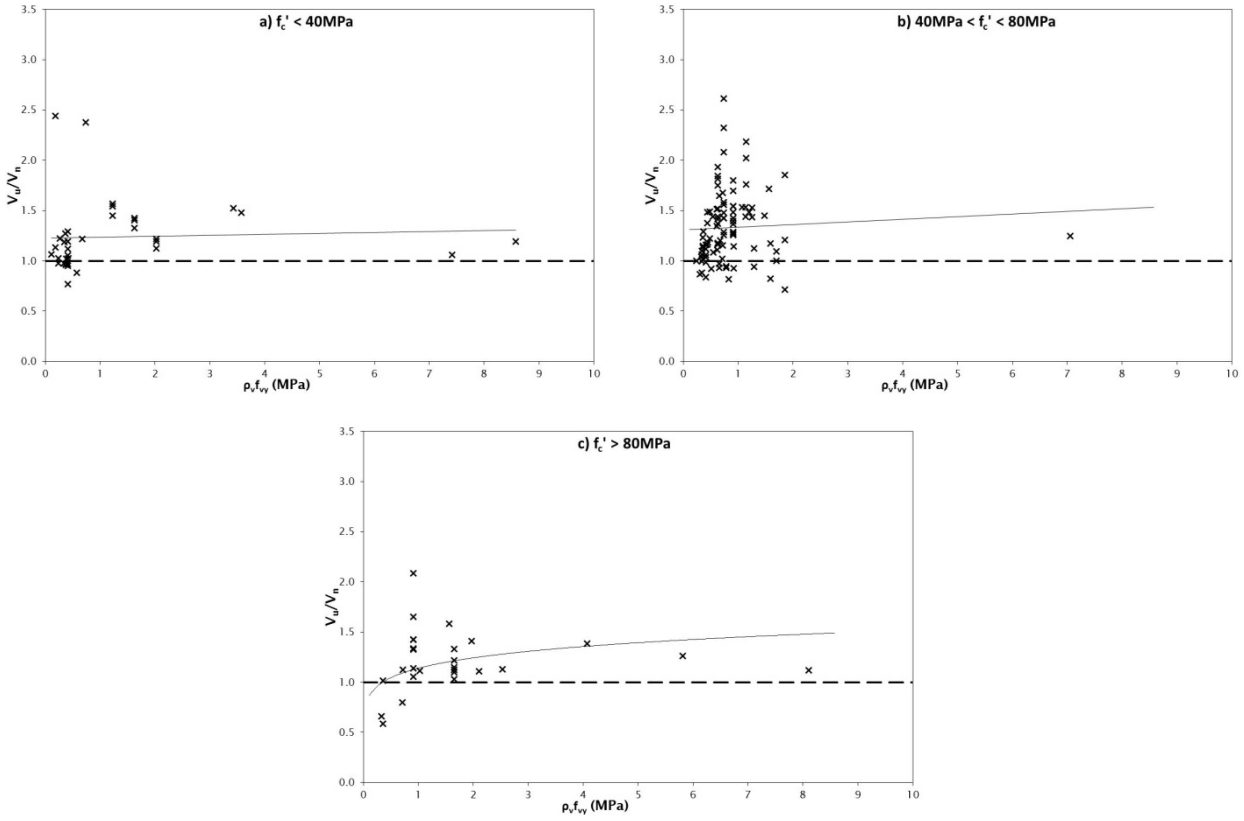

4.4.3.2 PC database

The provisions found in CSA A23.3 and AASHTO LRFD were substantially more conservative for PC beams than those found in ACI 318 and NZS 3101, with an average shear capacity ratio of 2.34. The standard deviation was 1.31, with a corresponding coefficient of variation of 0.56, indicating heavy scatter. Only six (4%) of the 164 PC beams included in this evaluation were found to have predicted ultimate shear capacities greater than the observed capacity.

Figures 4.49–4.53 show ratios of measured to predicted shear capacities plotted against concrete compressive strength, shear stress capacity, beam effective depth, shear a/d ratio, and longitudinal and transverse reinforcement ratios. In figure 4.49 the CSA A23.3 and AASHTO LRFD provisions were found to increase in conservatism with increasing concrete compressive strength for beams containing low ($\rho_v f_{vy}$ < 2MPa) and moderate (2MPa < $\rho_v f_{vy}$ < 6MPa) quantities of transverse reinforcement. For a constant concrete strength, the design provisions were consistently more conservative for beams with a low level of transverse reinforcement. Meanwhile, figure 4.50 shows that the accuracy of the design provisions was found to increase with increased measured ultimate shear capacity for beams with a concrete compressive strength of less than 80MPa.

Figure 4.49 Influence of concrete compressive strength on the accuracy of CSA A23.3 for beams in the PC database

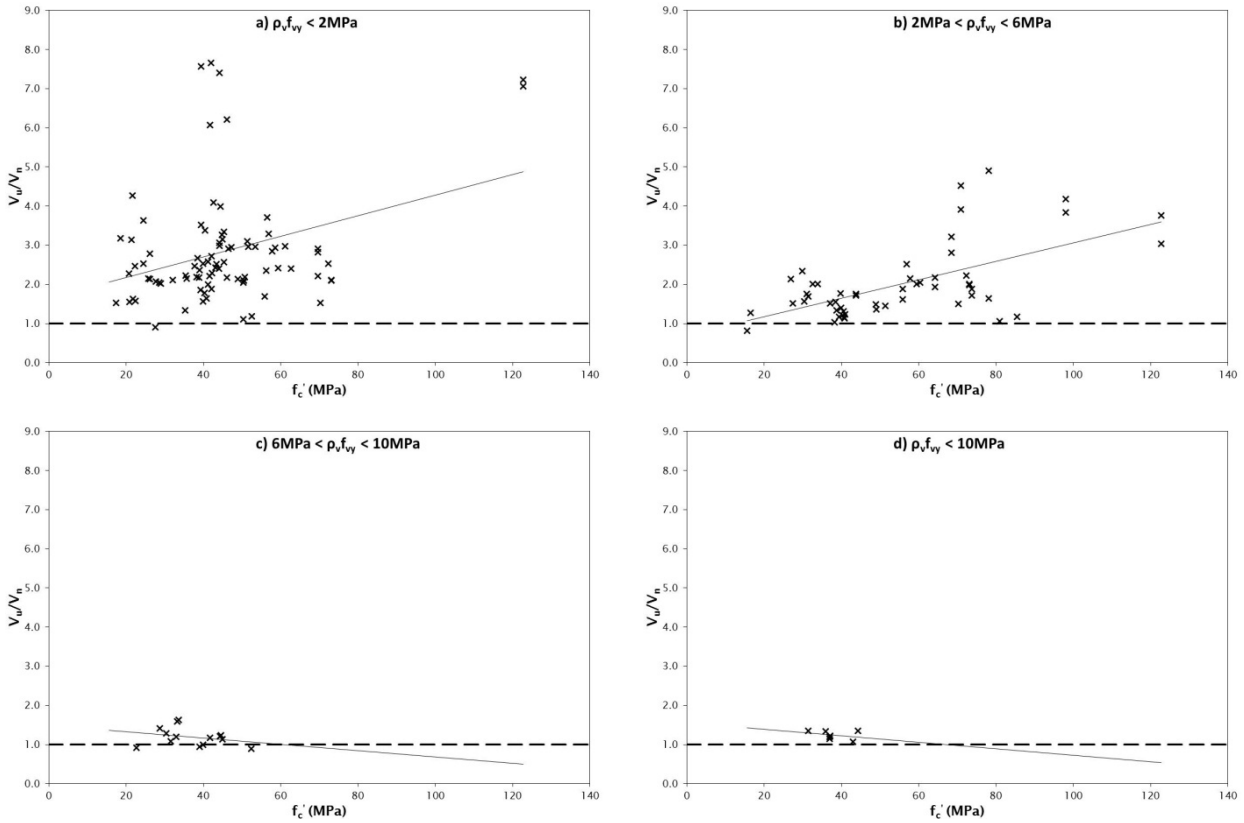

Figure 4.50 Influence of ultimate shear capacity on the accuracy of CSA A23.3 for beams in the PC database

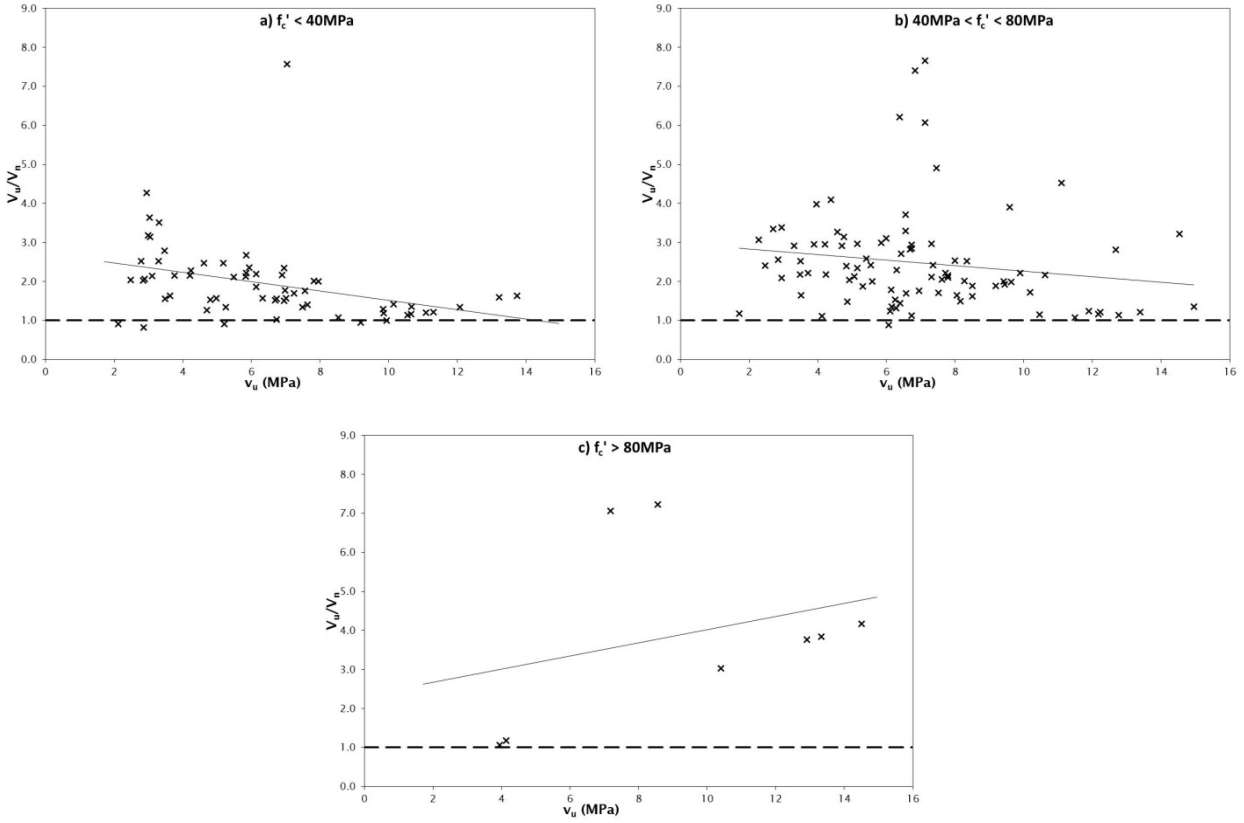

For increasing beam effective depths, the shear design provisions of CSA A23.3 and AASHTO LRFD were observed to increase in conservatism and inaccuracy of predicted ultimate shear capacities with increasing beam effective depths for beams containing low ($\rho_v f_{vy}$ < 2MPa) and moderate (2MPa < $\rho_v f_{vy}$ < 6MPa) quantities of transverse reinforcement. This trend is shown in figure 4.51. Figure 4.52 shows that smaller beams (effective depths no greater than 400mm) with a low level of transverse reinforcement ($\rho_v f_{vy}$ < 2MPa) were regularly noted to fail at applied shear stresses much greater than those predicted by the design standards.

Figure 4.51 Influence of effective depth on the accuracy of CSA A23.3 for beams in the PC database

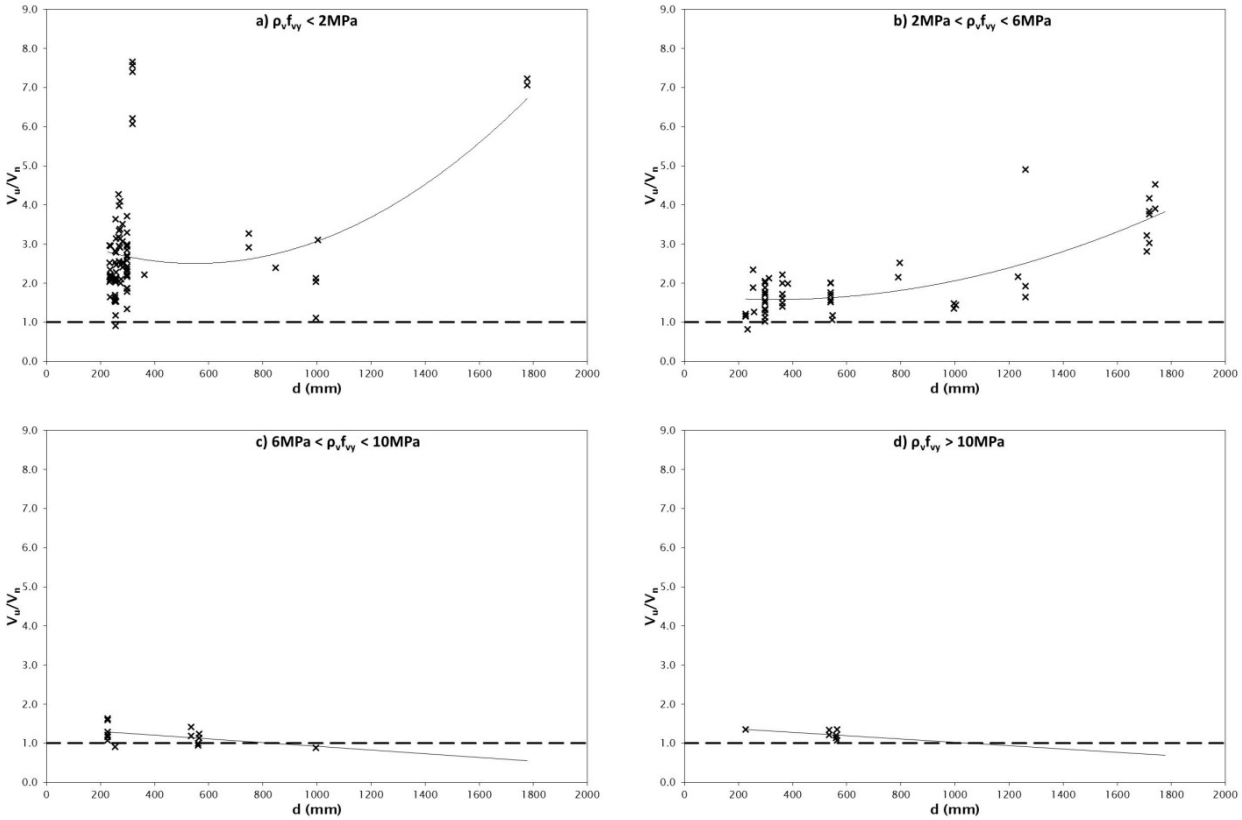

Figure 4.52 Influence of shear a/d ratio on the accuracy of CSA A23.3 for beams in the PC database

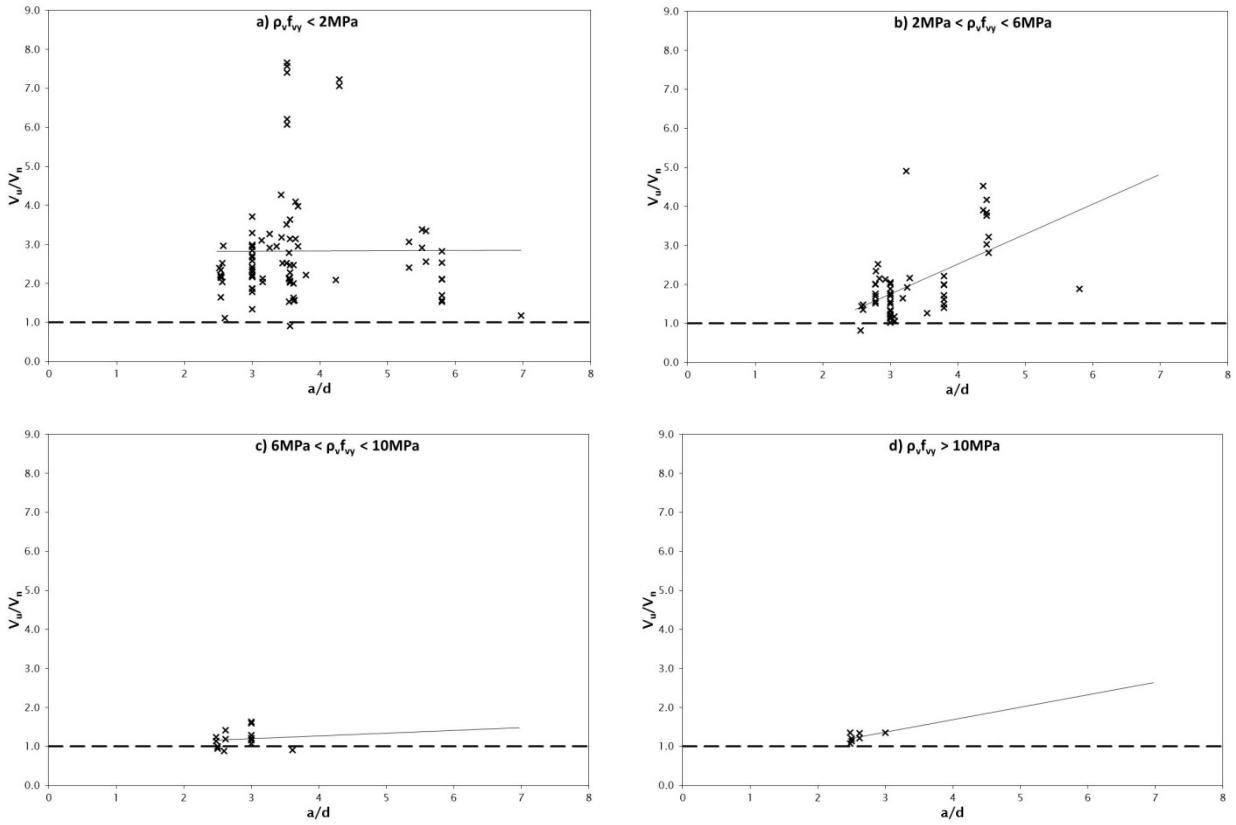

In figure 4.53, CSA A23.3 and AASHTO LRFD were noted to increasingly overestimate the ultimate shear capacity of PC beams with decreasing levels of longitudinal reinforcement for beams containing low quantities of transverse reinforcement ($\rho_v f_{vy}$ < 2MPa) and with increasing levels of longitudinal reinforcement for beams containing moderate quantities of transverse reinforcement (2MPa < $\rho_v f_{vy}$ < 6MPa). Figure 4.54 shows that the shear design provisions of CSA A23.3 and AASHTO LRFD provide very conservative predictions of shear capacity for beams containing low quantities of transverse reinforcement for all concrete compressive strengths, increasing in accuracy for increased quantities of transverse reinforcement.

Figure 4.53 Influence of longitudinal reinforcement on the accuracy of CSA A23.3 for beams in the PC database

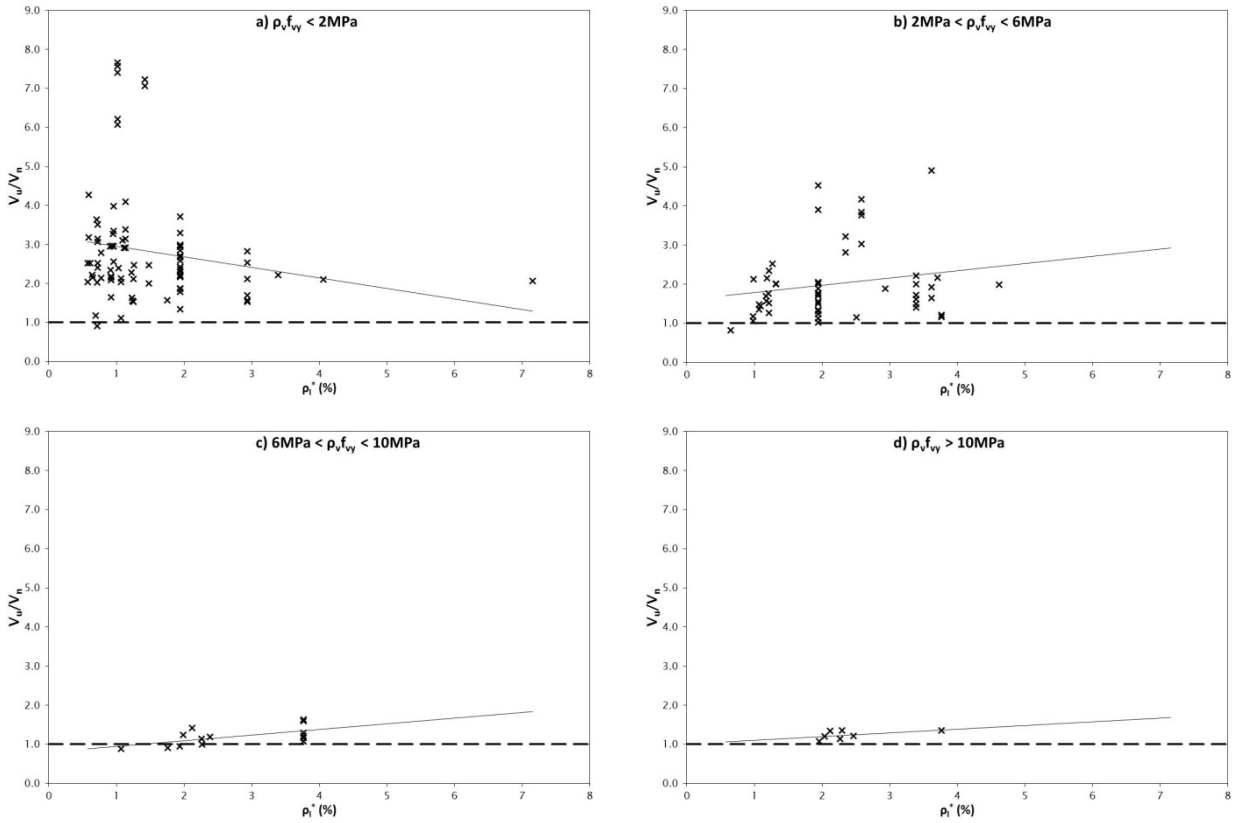

Figure 4.54 Influence of transverse reinforcement on the accuracy of CSA A23.3 for beams in the PC database

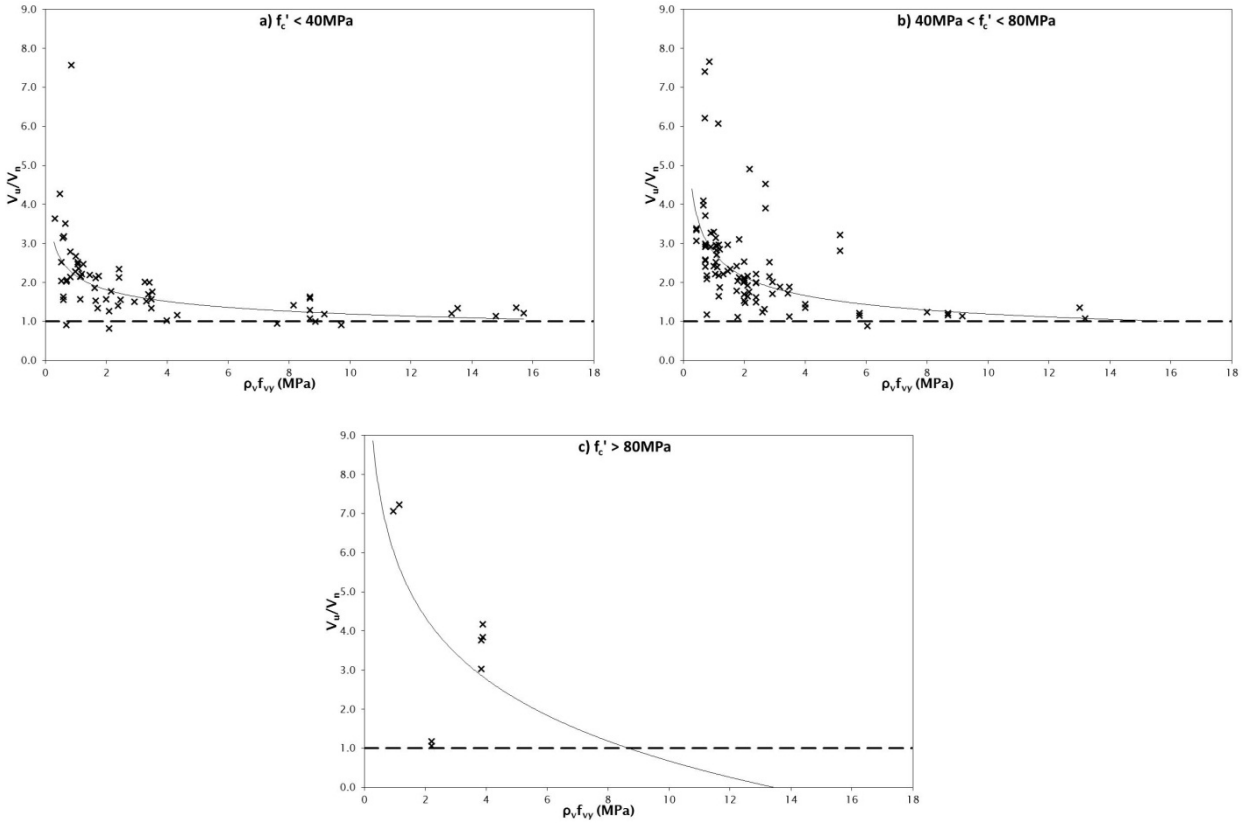

4.4.4 Eurocode 2 (EC2)

Eurocode 2 (EC2) provides a unified approach for shear design of RC and PC beams by accounting for the effect of axial stresses, including prestressing, on ultimate shear capacity. This approach was detailed earlier in section 3.4, with the results of an evaluation of the design standard presented in figures 4.55–4.66. For beams with transverse reinforcement, EC2 neglects the contribution of concrete to shear capacity. The predicted ultimate shear capacities calculated using EC2 design provisions are also strongly dependent on the angle of compressive strut inclination, but the design standard provides no rational method for calculating this angle. Therefore, throughout this evaluation the angle of inclination predicted by the CSA A23.3 and AASHTO LRFD provisions were used. It is important to note that the concrete partial safety factor, γ_c, found in equation 3.22, was assigned a value of 1.0 throughout this evaluation.

4.4.4.1 RC database

Figures 4.55–4.60 show the influence of concrete compressive strength, shear stress capacity, beam effective depth, shear a/d ratio, and levels of longitudinal and transverse reinforcement on the accuracy of EC2 in predicting the shear capacity of RC beams. EC2 was found to be excessively conservative for predicting the ultimate shear capacity of RC beams, with an average ratio of measured to predicted shear capacity of 2.84. The corresponding standard deviation and coefficient of variation were 1.29 and 0.45, respectively. EC2 provided conservative shear capacity predictions for all but one of the 160 RC beams used for this evaluation.

As shown in figure 4.55, the shear capacities predicted by EC2 were observed to slightly increase in conservatism with increasing concrete compressive strength. EC2 was observed to be markedly more conservative, and less accurate, for beams with lower levels of transverse reinforcement ($\rho_v f_{vy}$ < 1MPa), regardless of the concrete compressive strength of the beam, than for beams with higher levels of transverse reinforcement ($\rho_v f_{vy}$ > 1MPa). The design standard predictions were also found to increase in c with increasing shear stress capacities for beams that had a concrete compressive strength of less than 40MPa or greater than 80MPa, particularly for shear stress capacities greater than 6MPa, as shown in figure 4.56.

Figure 4.55 Influence of concrete compressive strength on the accuracy of EC2 for beams in the RC database

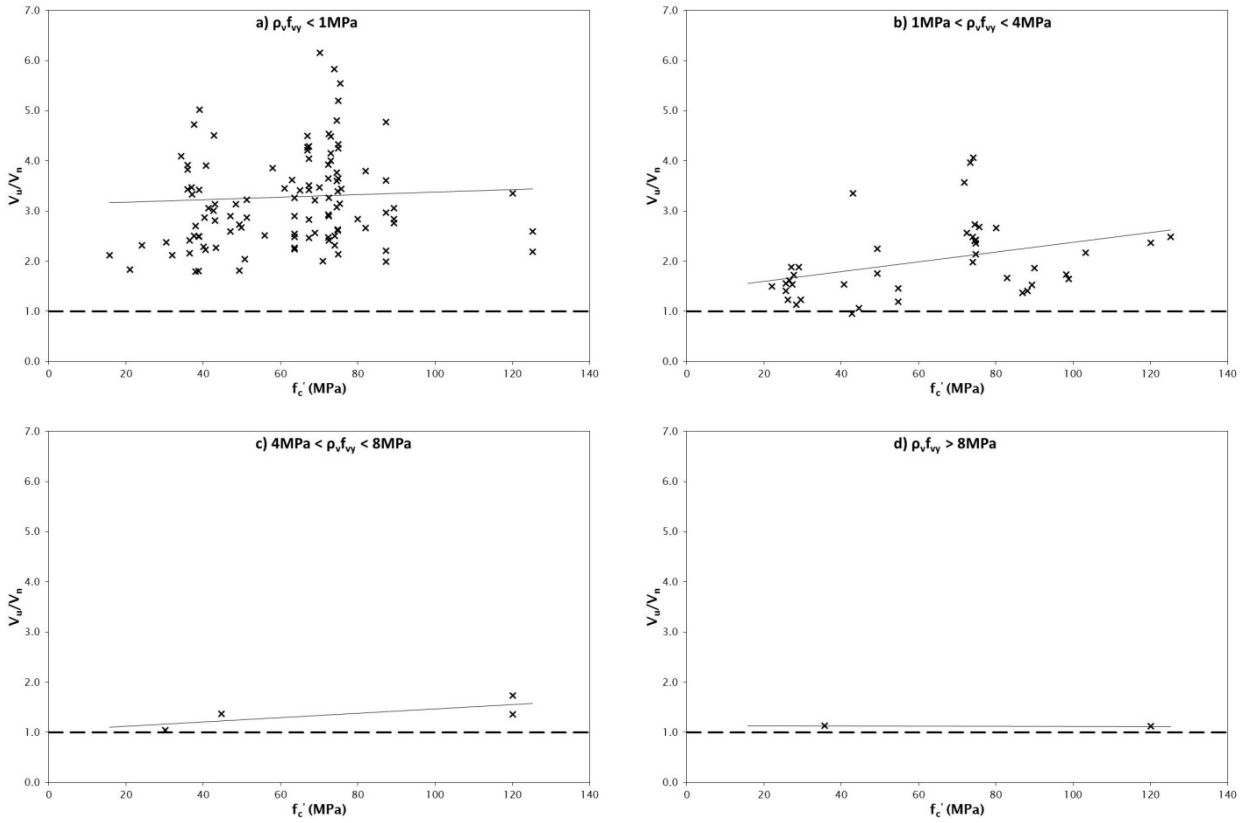

Figure 4.56 Influence of ultimate shear capacity on the accuracy of EC2 for beams in the RC database

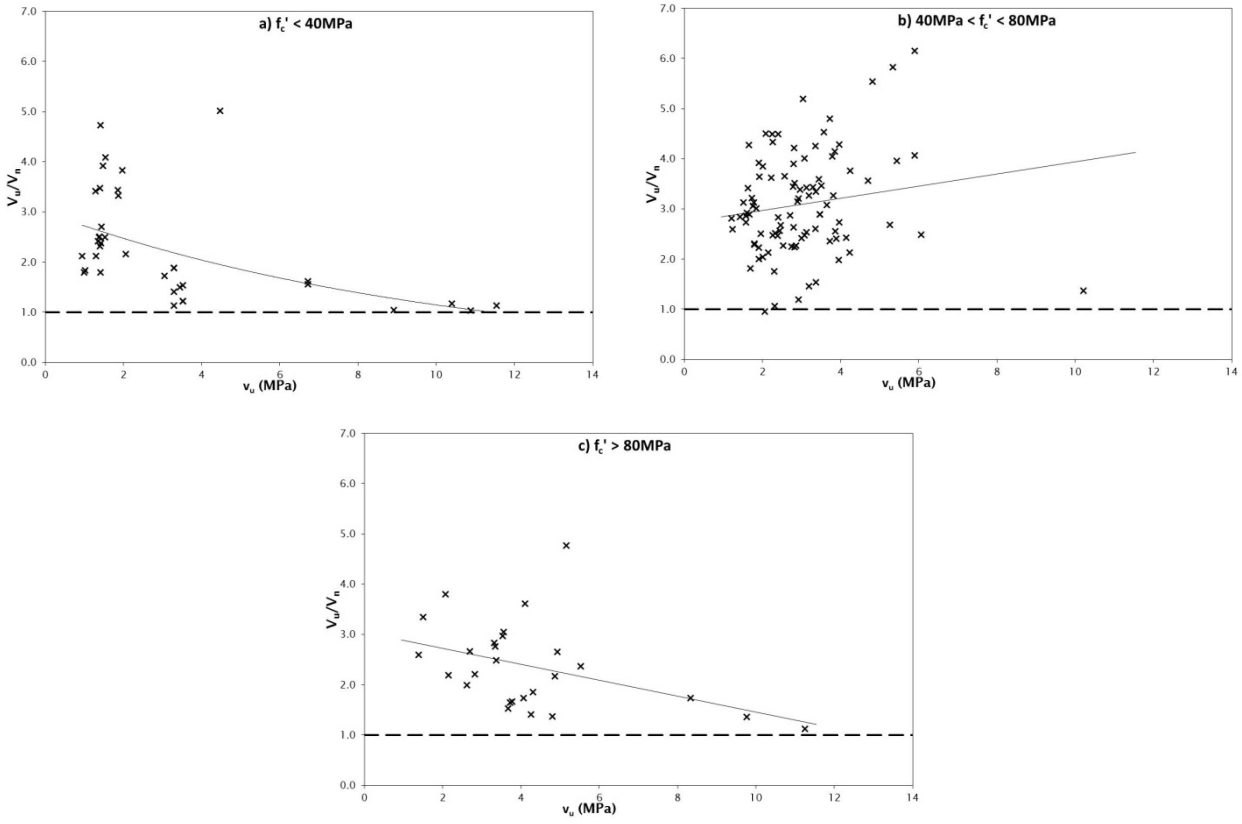

The accuracy of EC2 in predicting the ultimate shear capacity of RC beams was found to improve with increasing beam effective depth, as shown in figure 4.57. The design standard was also observed to be equally conservative for all values of a/d greater than 2.5, although the ratios of measured to predicted shear capacities closest to unity were observed for beams tested with a/d ratios of 2.5–3.0. This trend is shown in figure 4.58.

Figure 4.57 Influence of effective depth on the accuracy of EC2 for beams in the RC database

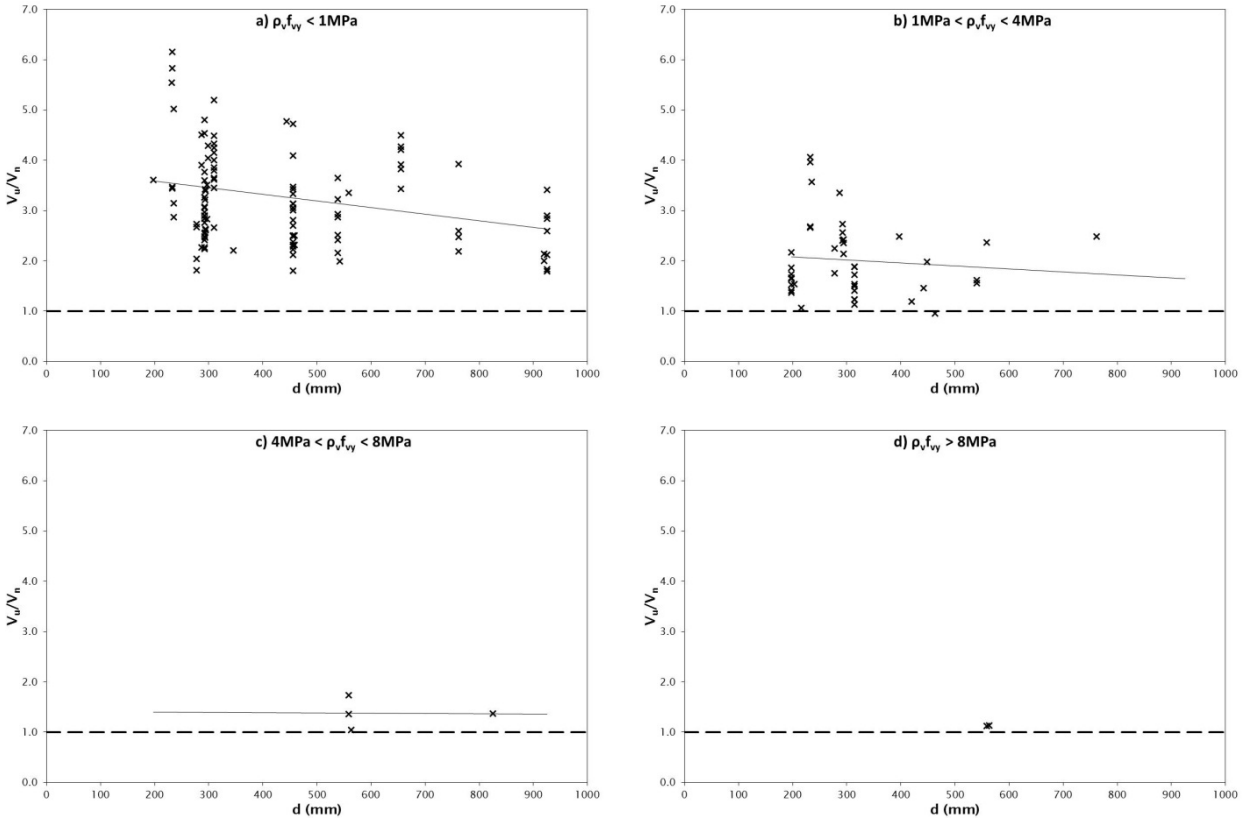

Figure 4.58 Influence of shear a/d on the accuracy of EC2 for beams in the RC database

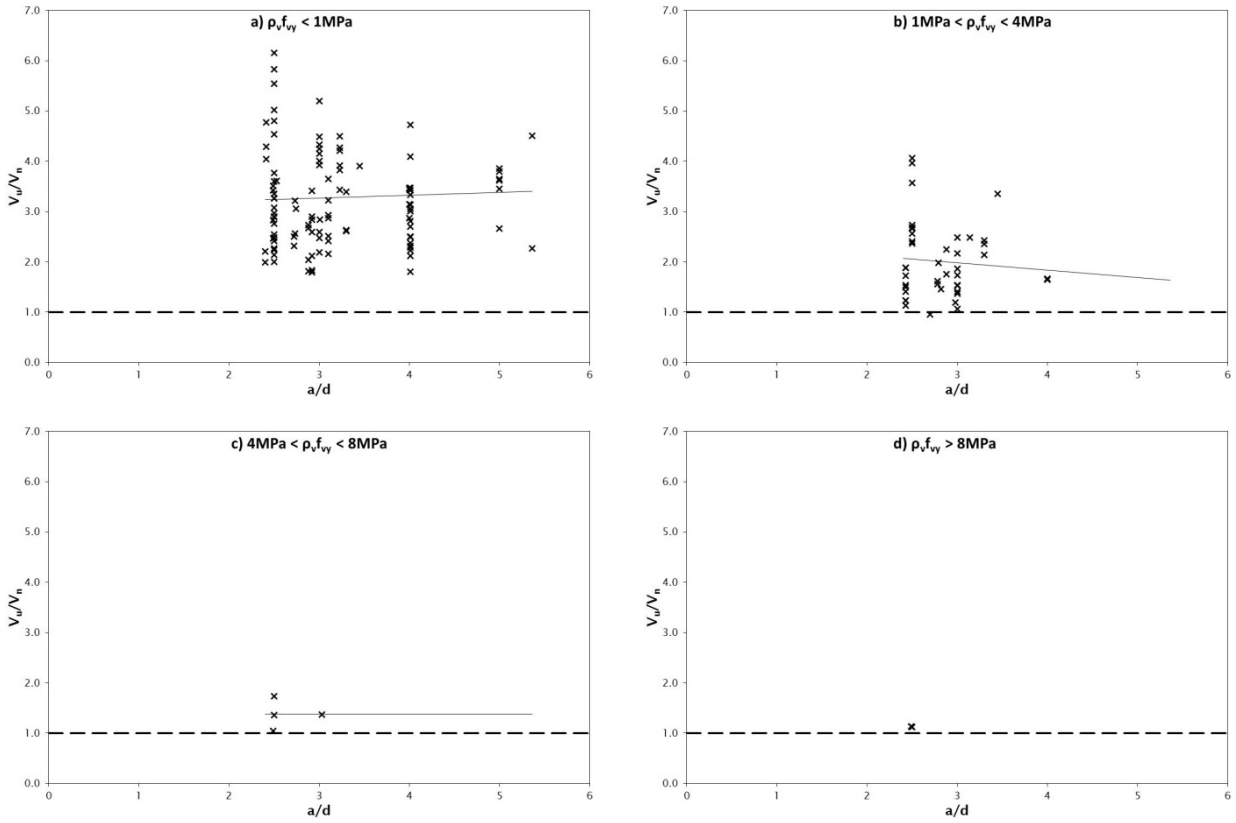

For beams with a low level of transverse reinforcement ($\rho_v f_{vy} \leq$ 1MPa), EC2 was found to provide increasingly conservative ultimate shear capacity predictions with increasing levels of longitudinal reinforcement. However, as shown in figure 4.59, this trend was not true for beams with $\rho_v f_{vy}$ > 1MPa, for which EC2 was observed to be relatively accurate regardless of the quantity of longitudinal reinforcement.

Figure 4.59 Influence of longitudinal reinforcement on the accuracy of EC2 for beams in the RC database

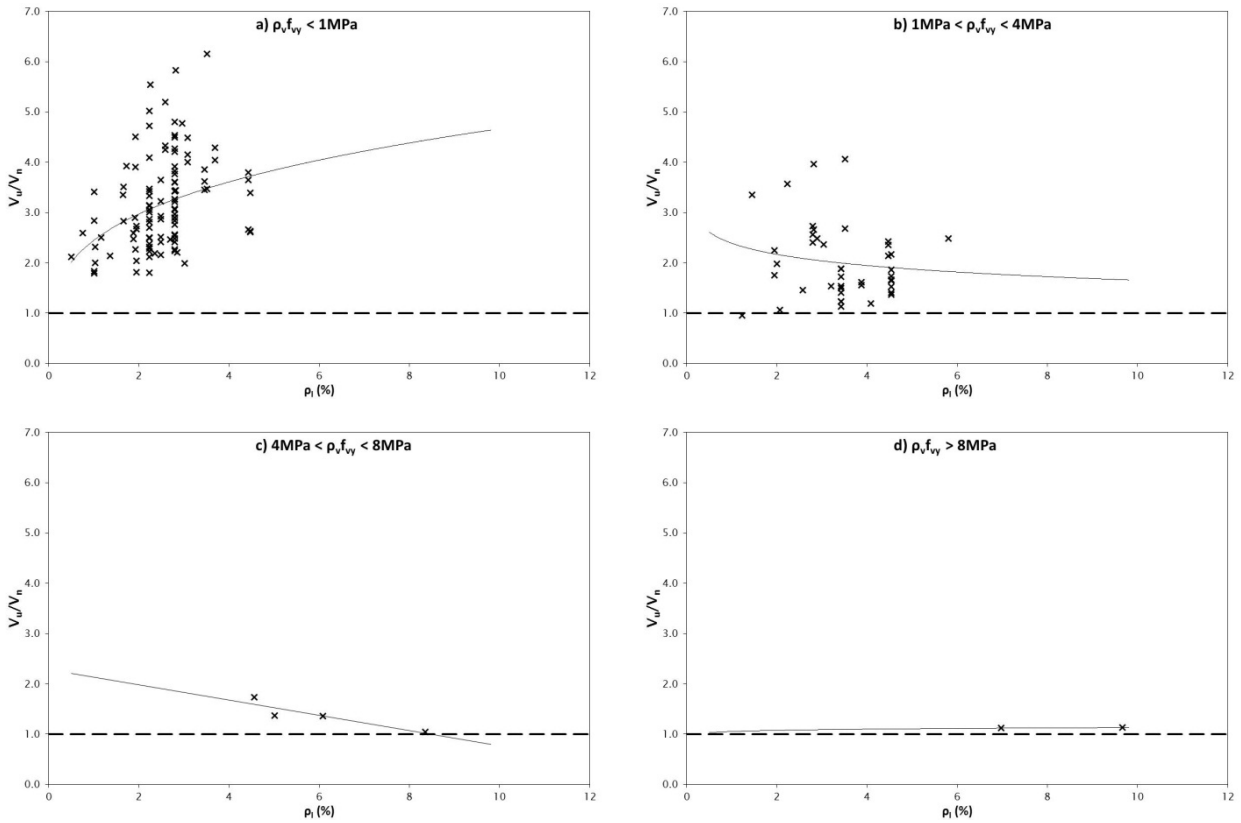

As seen in figure 4.60, EC2 was found to be conservative for beams with low levels of transverse reinforcement ($\rho_v f_{vy} \leq$ 1MPa), but reasonably accurate for beams with greater levels of transverse reinforcement (particularly those beams with $\rho_v f_{vy}$ > 2MPa. This trend was caused by the provisions of the design standard failing to account for the contribution of concrete to ultimate shear capacity. The concrete contribution is independent of the quantity of transverse reinforcement, and is therefore of greater relative significance for beams with low levels of transverse reinforcement.

Figure 4.60 Influence of transverse reinforcement on the accuracy of EC2 for beams in the RC database

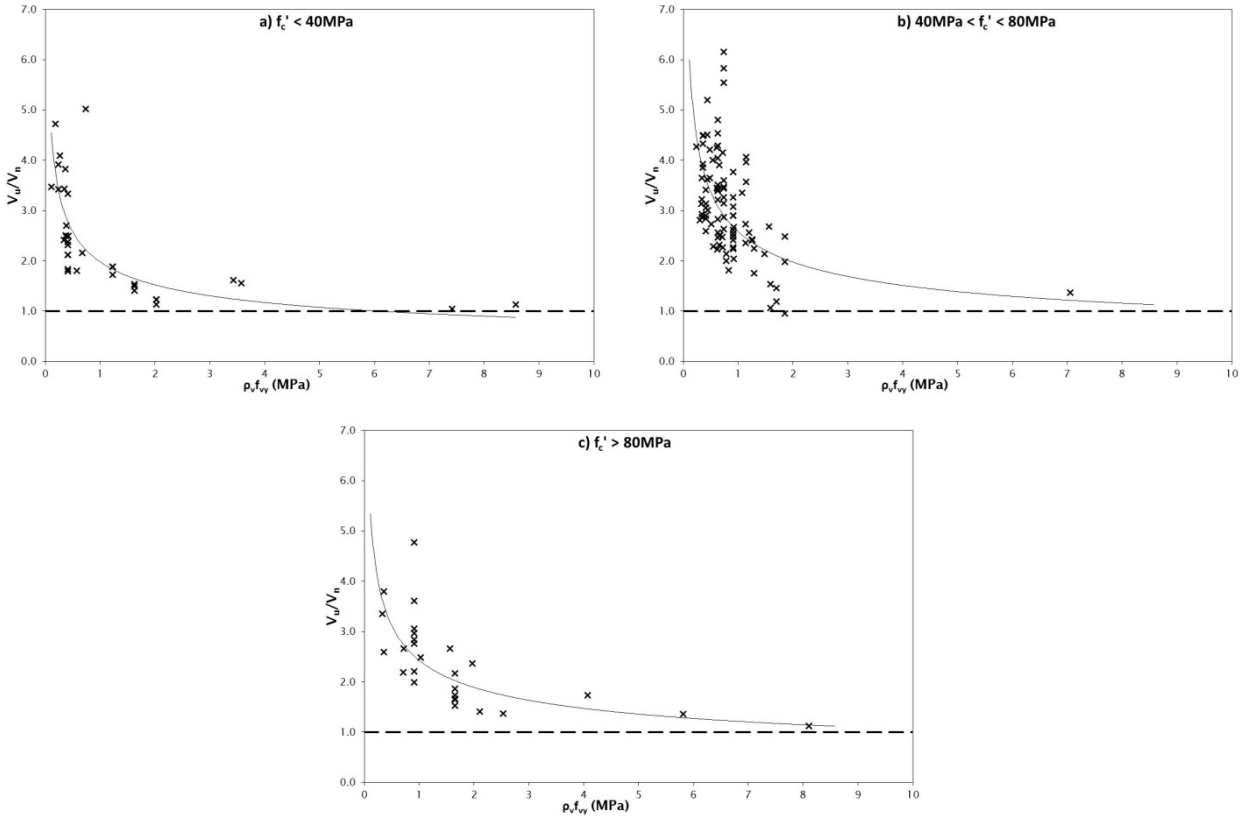

4.4.4.2 PC database

Figures 4.61–4.66 show the influence of concrete compressive strength, shear stress capacity, beam effective depth, shear a/d ratio, and levels of longitudinal and transverse reinforcement on the accuracy of EC2 to predict the ultimate shear capacity of PC beams. EC2 was found to be exceptionally conservative for predicting the ultimate shear capacity of PC beams, with this conservatism being considerably greater than for any of the other design standards evaluated in this chapter. The average ratio of measured to predicted shear capacity was 2.73, with corresponding standard deviation and coefficient of variation of 1.42 and 0.52, respectively. EC2 provided conservative shear capacity predictions for 159 (97%) of the 164 PC beams used for this evaluation.

The influence of concrete compressive strength and shear stress capacity on the accuracy of EC2 was similar to the influence observed for RC beams, with increasingly conservative capacities predicted for beams with increasing concrete compressive strengths, and increasingly accurate predictions for beams failing at higher shear stresses. The influence of beam effective depth was found to be insignificant for all beams except those containing moderate quantities of transverse reinforcement (2MPa < $\rho_v f_{vy}$ < 6MPa), for which EC2 provided increasingly conservative predictions of shear capacity for increasing effective beam depths.

Figure 4.61 Influence of concrete compressive strength on the accuracy of EC2 for beams in the PC database

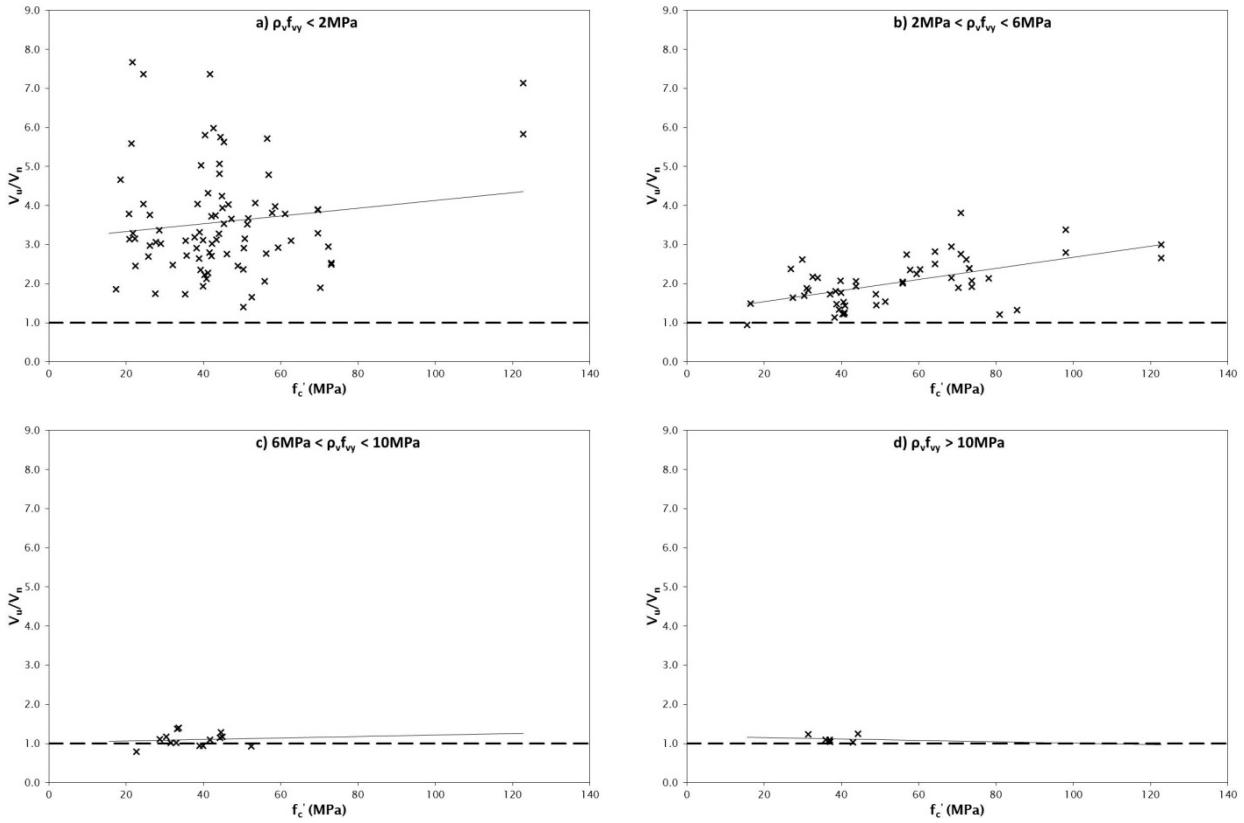

Figure 4.62 Influence of ultimate shear capacity on the accuracy of EC2 for beams in the PC database

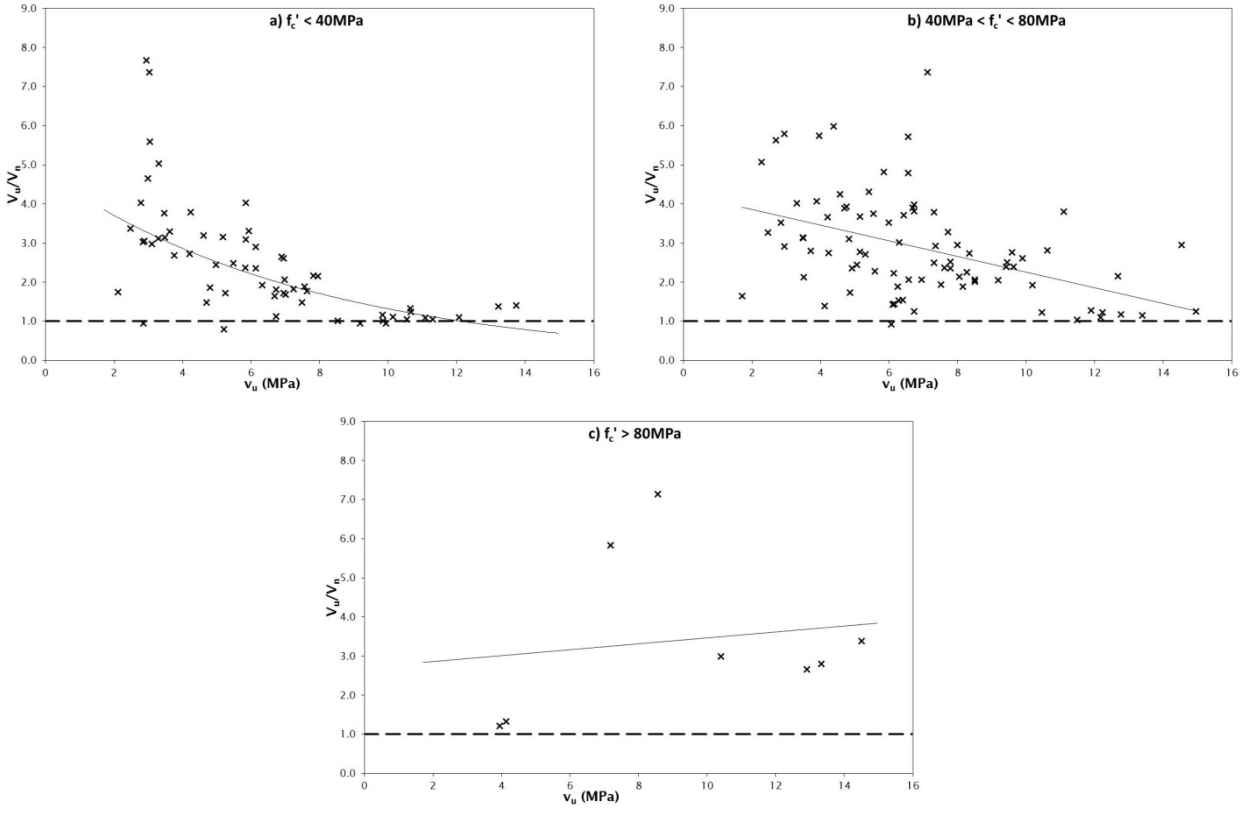

Figure 4.63 Influence of effective depth on the accuracy of EC2 for beams in the PC database

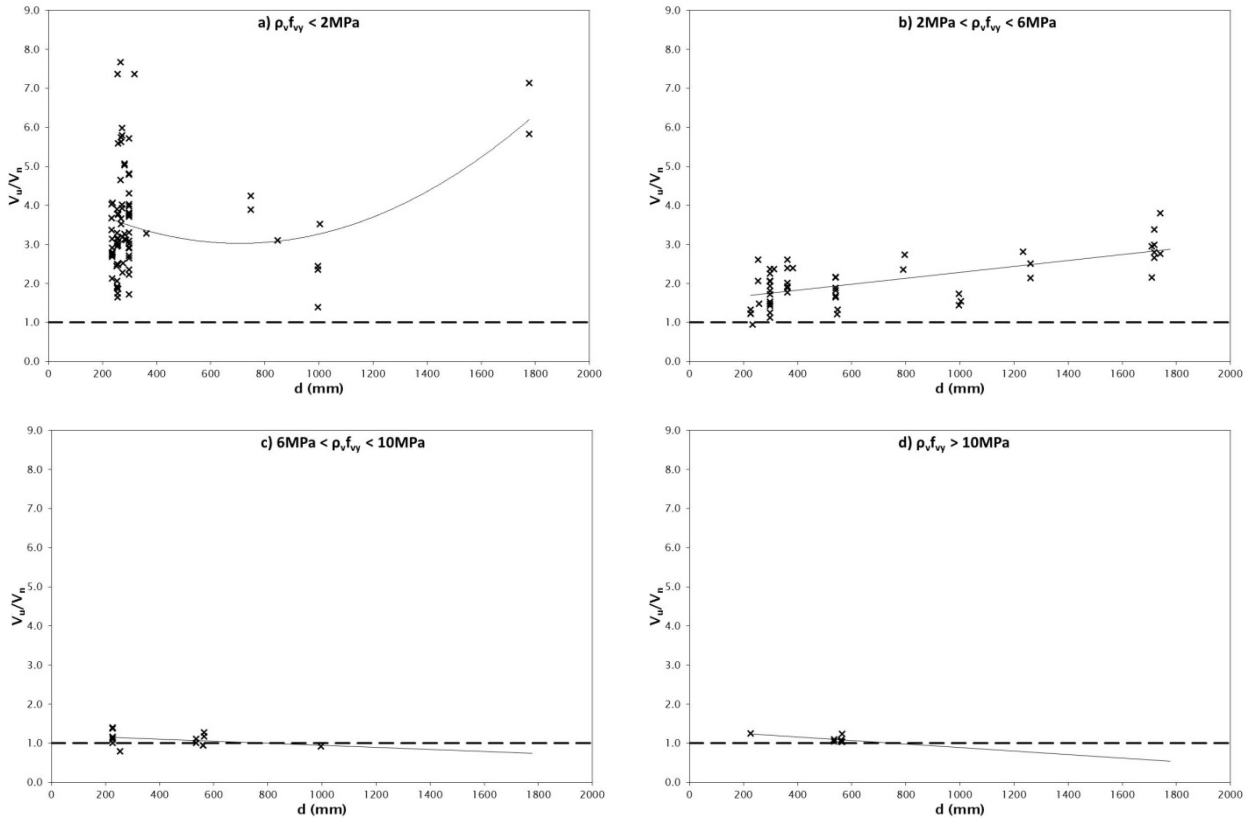

EC2 was observed to provide increasingly conservative ultimate shear capacity predictions with increasing shear a/d ratios for all levels of transverse reinforcement, while the influence of longitudinal and transverse reinforcement was similar to that observed for RC beams.

Figure 4.64 Influence of shear a/d ratio on the accuracy of EC2 for beams in the PC database

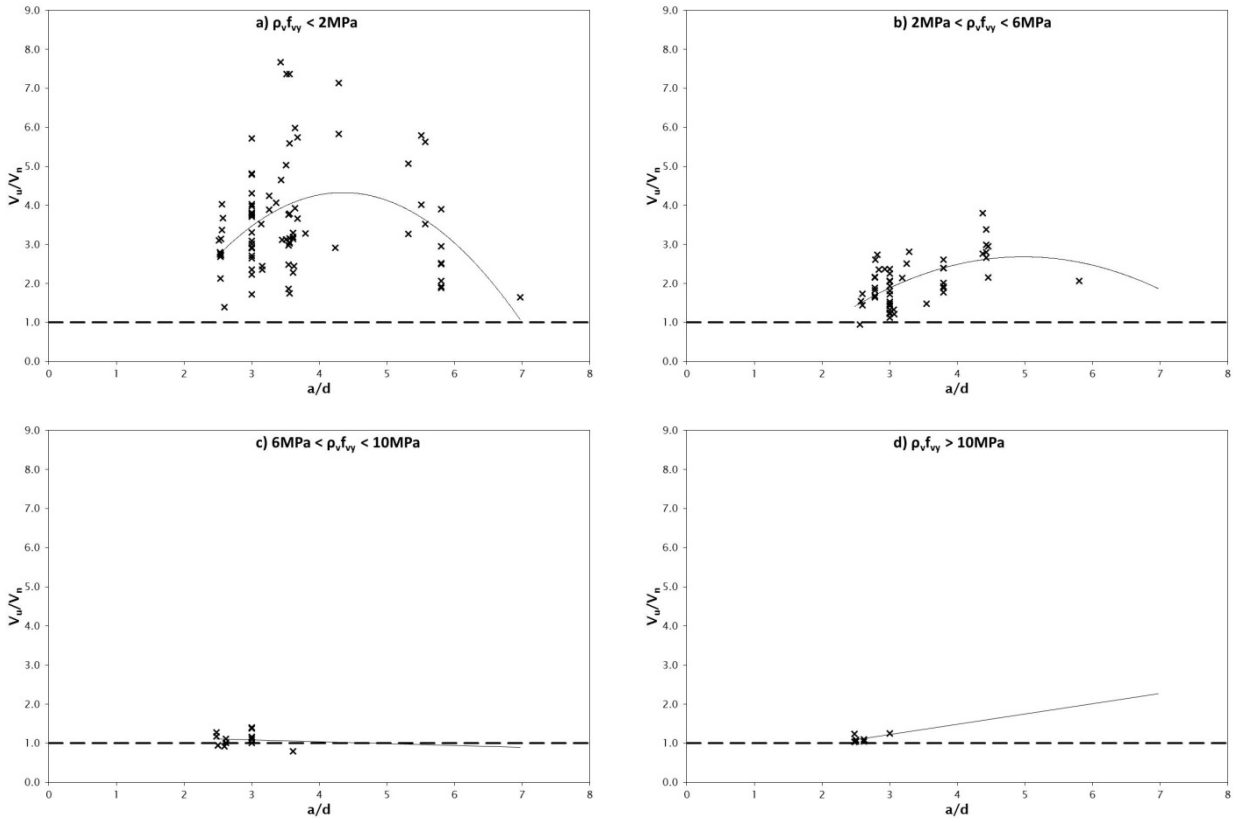

Figure 4.65 Influence of longitudinal reinforcement on the accuracy of EC2 for beams in the PC database

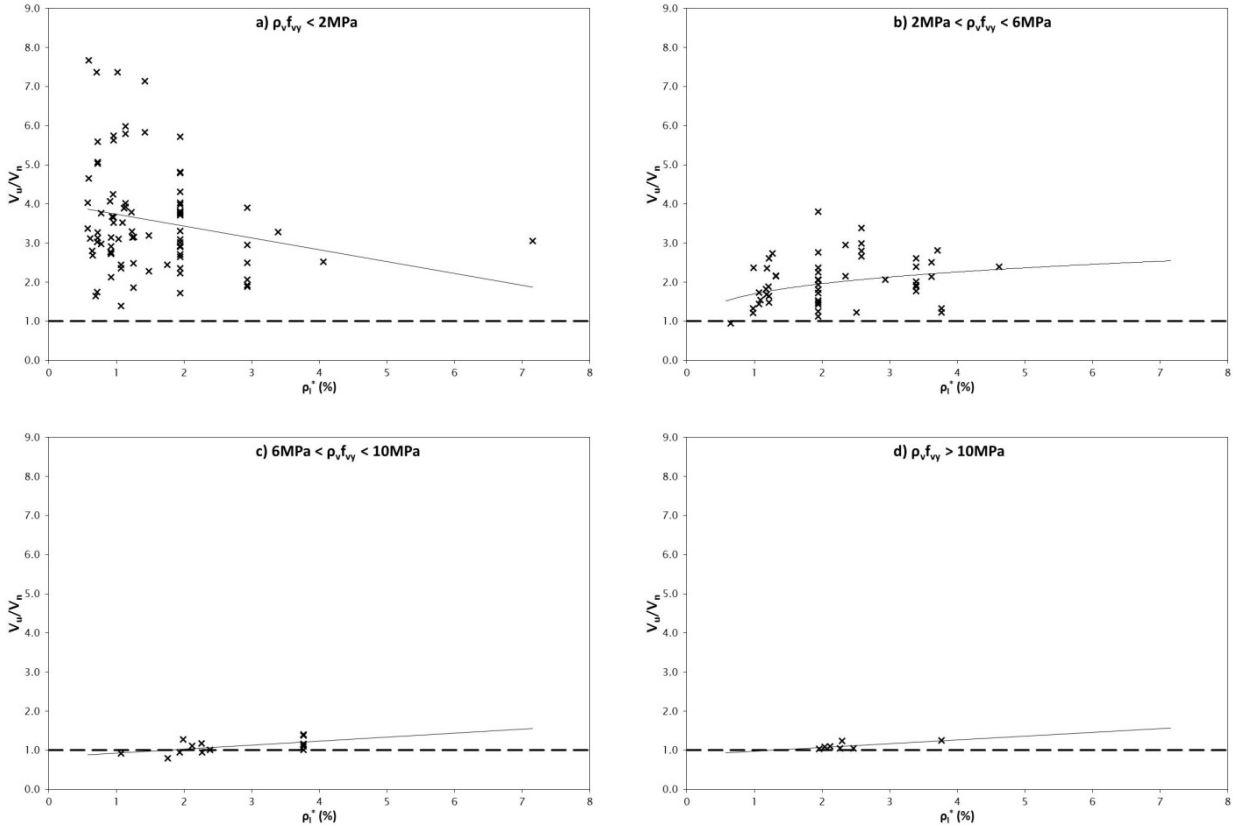

Figure 4.66 Influence of transverse reinforcement on the accuracy of EC2 for beams in the PC database

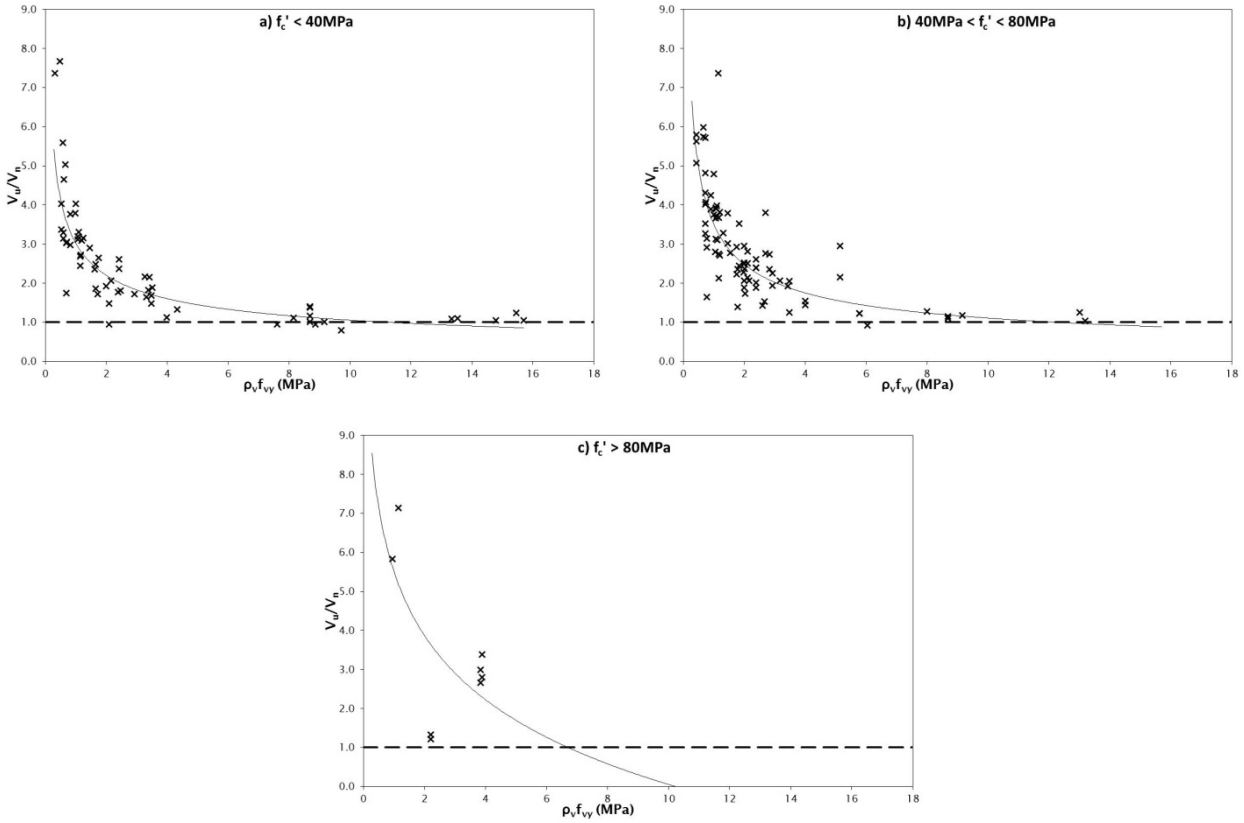

4.4.5 fib model code 2010

As the shear design provisions of the fib model code are based on the Modified Compression Field Theory, the same provisions can be used to estimate the ultimate shear capacity of RC beams and PC beams. The provisions were detailed earlier in section 3.5, and were used to estimate the ultimate shear capacity of beams in the RC and PC databases, as detailed below.

4.4.5.1 RC database

Figures 4.67–4.72 show the influence of concrete compressive strength, shear stress capacity, beam effective depth, shear a/d ratio, and levels of longitudinal and transverse reinforcement on the accuracy of the fib model code in predicting the shear capacity of RC beams. The fib model code was found to be fairly conservative for predicting the ultimate shear capacity of RC beams, with an average ratio of measured to predicted shear capacity of 1.82. The corresponding standard deviation and coefficient of variation were 1.25 and 0.68, respectively. The fib model code provided non-conservative shear capacity predictions for 19 of the 160 RC beams used for this evaluation.

As shown in figure 4.67, the shear capacities predicted by the shear design provisions of the fib model code were observed to slightly increase in conservatism with increasing concrete compressive strength, although instances of non-conservative predictions of shear capacity were also observed for beams with a very high concrete compressive strength ($f_c' \approx$ 120MPa). This trend was not influenced by the level of transverse reinforcement in the beams. The design standard predictions were also found to rapidly increase in conservatism with increasing shear stress capacities for shear stress capacities less than 6MPa, as shown in figure 4.68. For shear capacities greater than 6MPa, the shear design provisions of the fib model code were observed to consistently provide non-conservative shear capacity predictions for normal-

strength concrete ($f_c' \leq 40$MPa) and conservative shear capacity predictions for high-strength concrete ($f_c' \geq 40$MPa).

Figure 4.67 Influence of concrete compressive strength on the accuracy of the fib model code for beams in the RC database

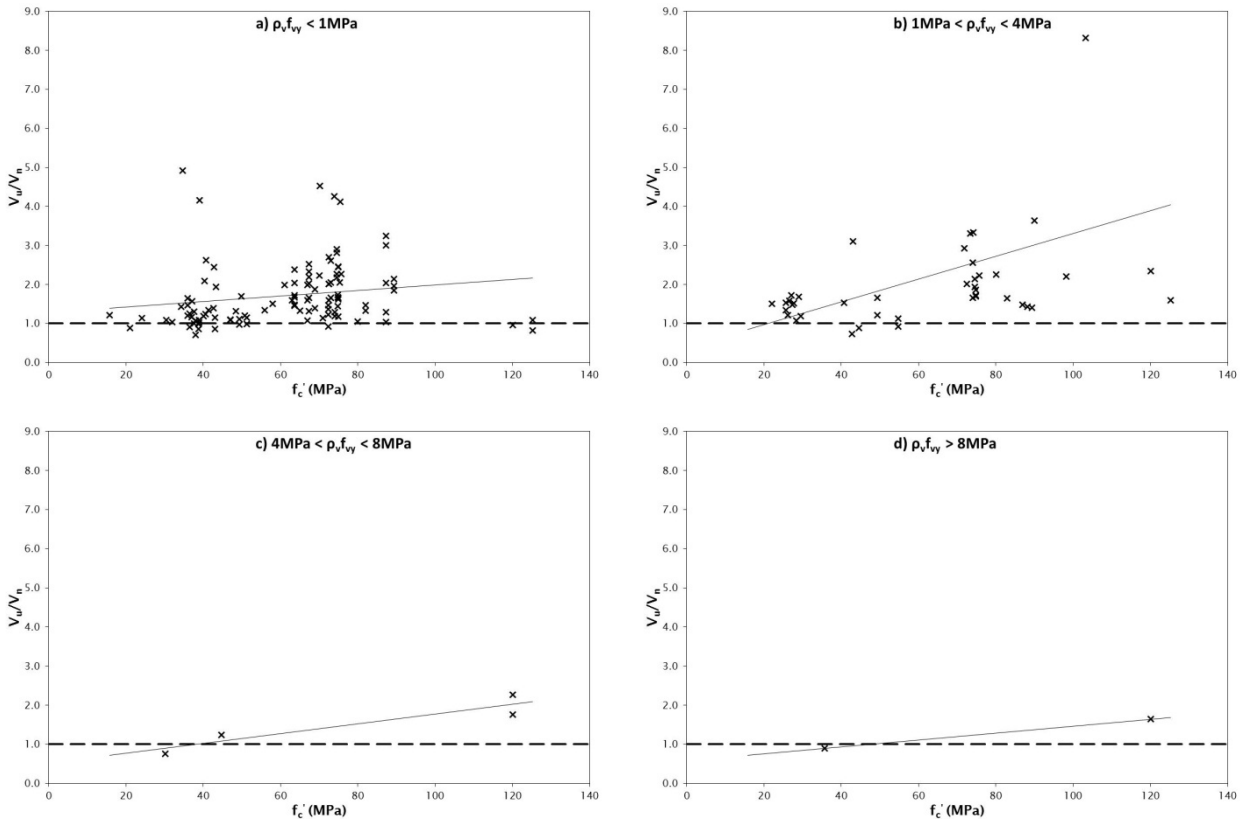

Figure 4.68 Influence of ultimate shear capacity on the accuracy of the fib model code for beams in the RC database

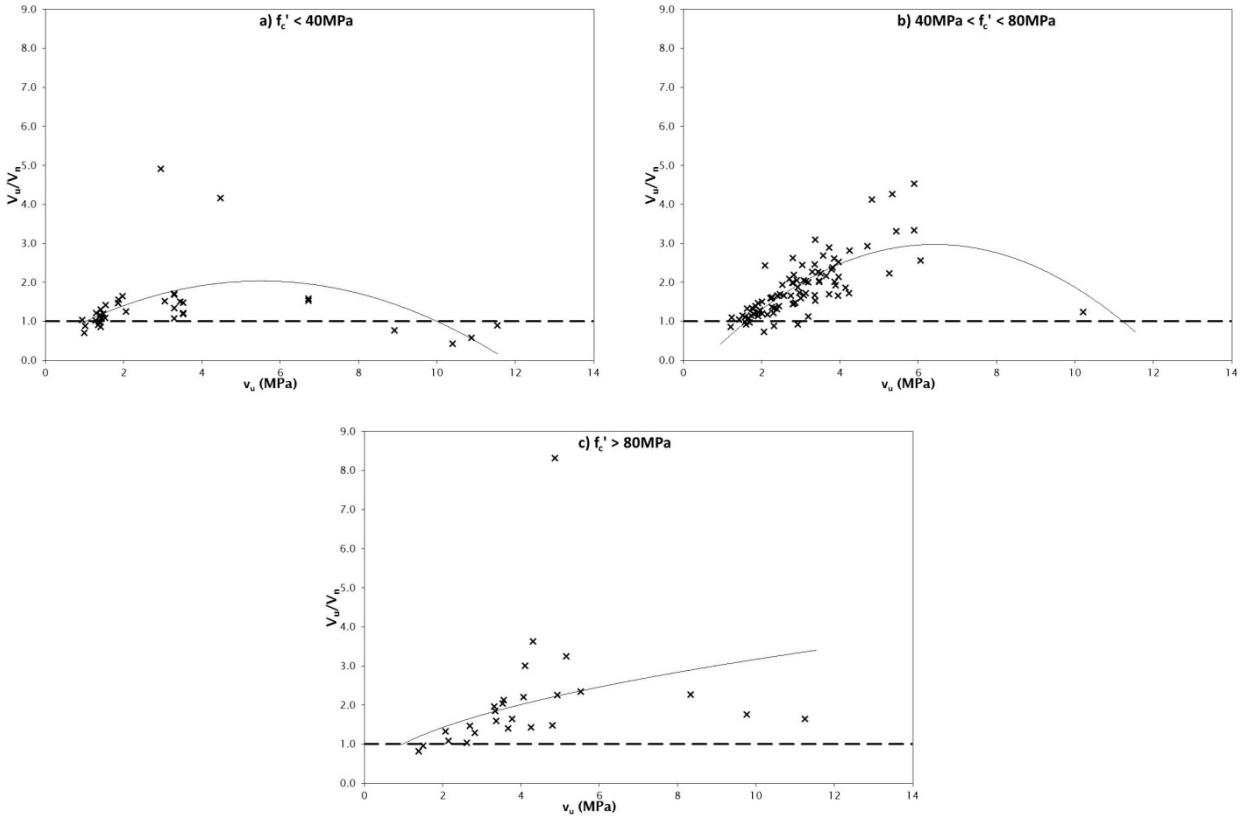

The accuracy of the fib model code in predicting the ultimate shear capacity of RC beams was found to improve with increasing beam effective depth, as shown in figure 4.69. The design standard was also observed to be equally conservative for all values of a/d ratio greater than 2.5, and was observed to provide non-conservative predictions of shear capacity mostly for beams tested with a/d ratios of 2.5–3.0. This trend is shown in figure 4.70.

Figure 4.69 Influence of effective depth on the accuracy of the fib model code for beams in the RC database

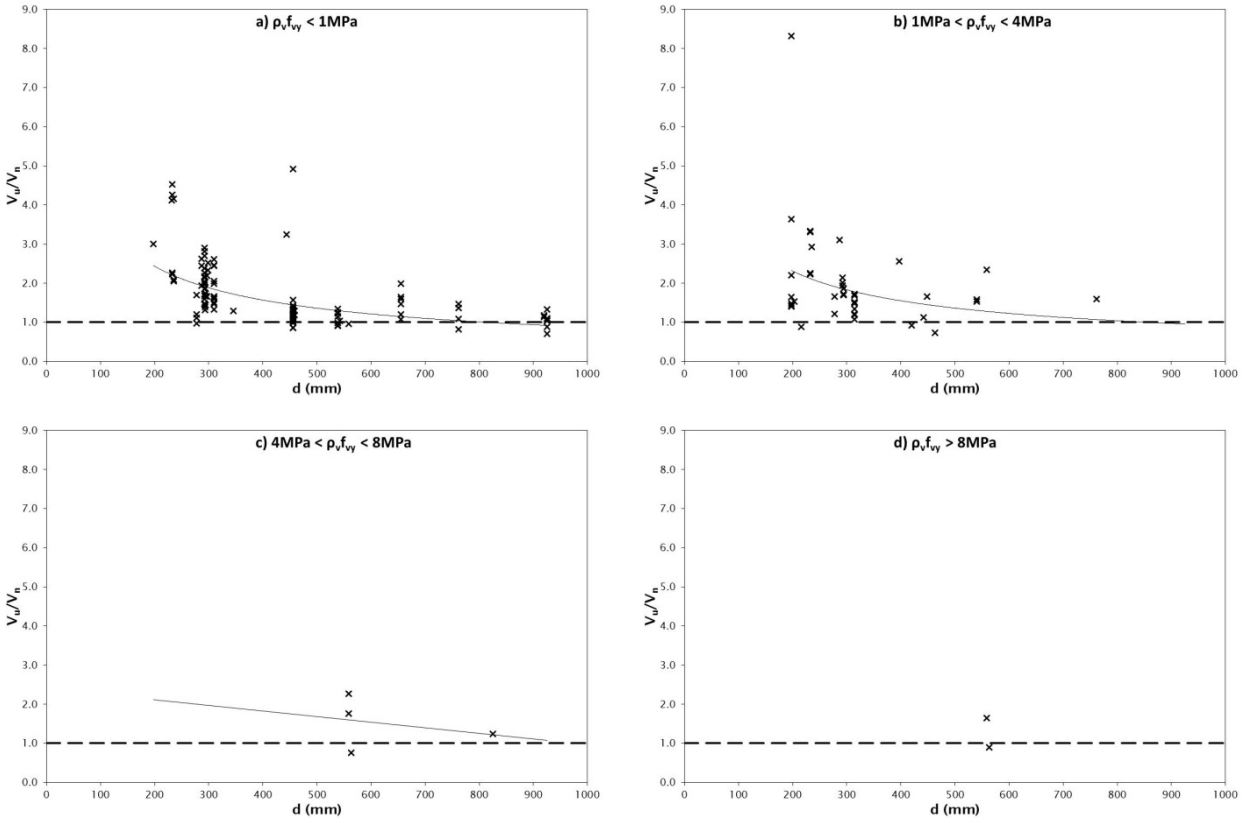

Figure 4.70 Influence of shear a/d ratio on the accuracy of the fib model code for beams in the RC database

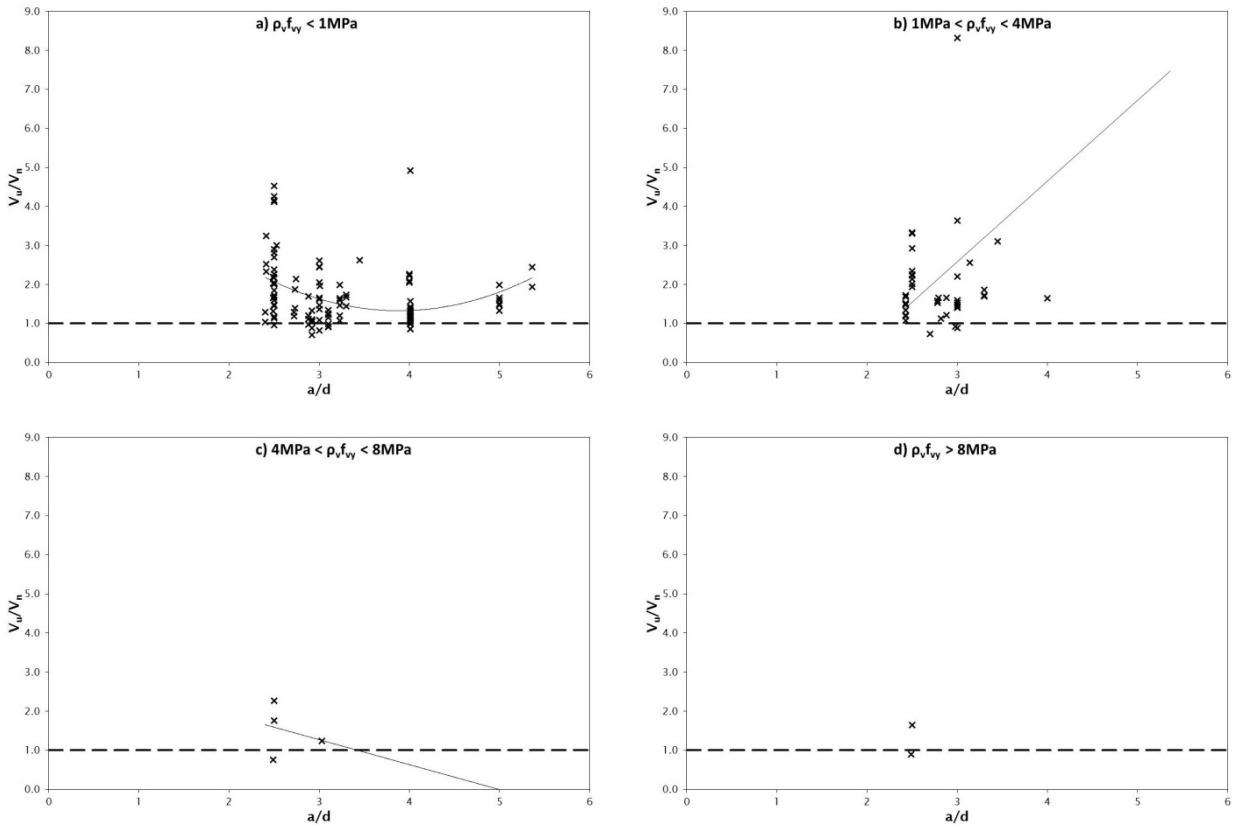

As shown in figure 4.71, when using the fib model code the predicted shear capacities of RC beams increased in conservatism with increasing ratios of longitudinal reinforcement for beams with a longitudinal reinforcement ratio of less than 6%. The large amount of scatter visible in figure 4.72 illustrates the absence of a relationship between accuracy of predicted ultimate shear capacity and level of transverse reinforcement, although the design standard was observed to provide consistently more conservative predictions for beams that had high-strength concrete (f_c' > 40MPa) than for beams that had normal-strength concrete (f_c' ≤ 40MPa).

Figure 4.71 Influence of longitudinal reinforcement on the accuracy of the fib model code for beams in the RC database

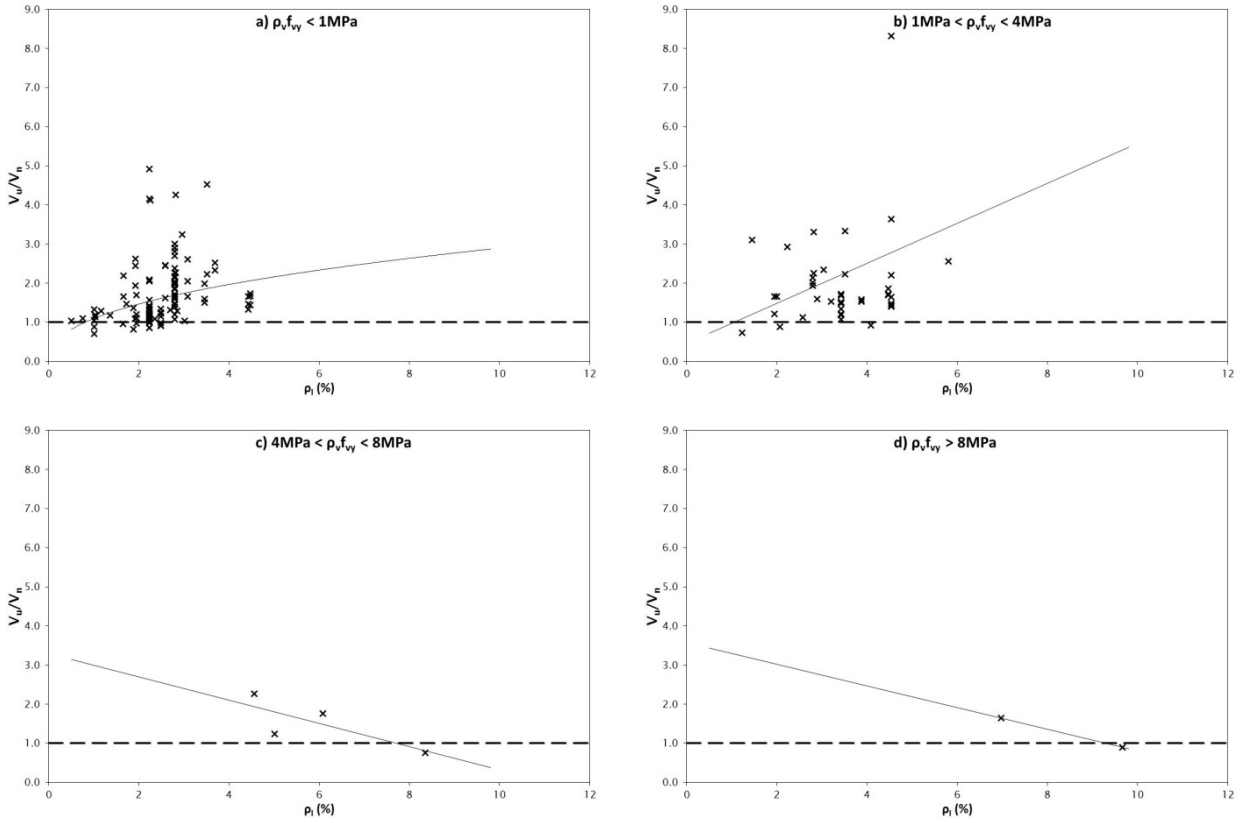

Figure 4.72 Influence of transverse reinforcement on the accuracy of the fib model code for beams in the RC database

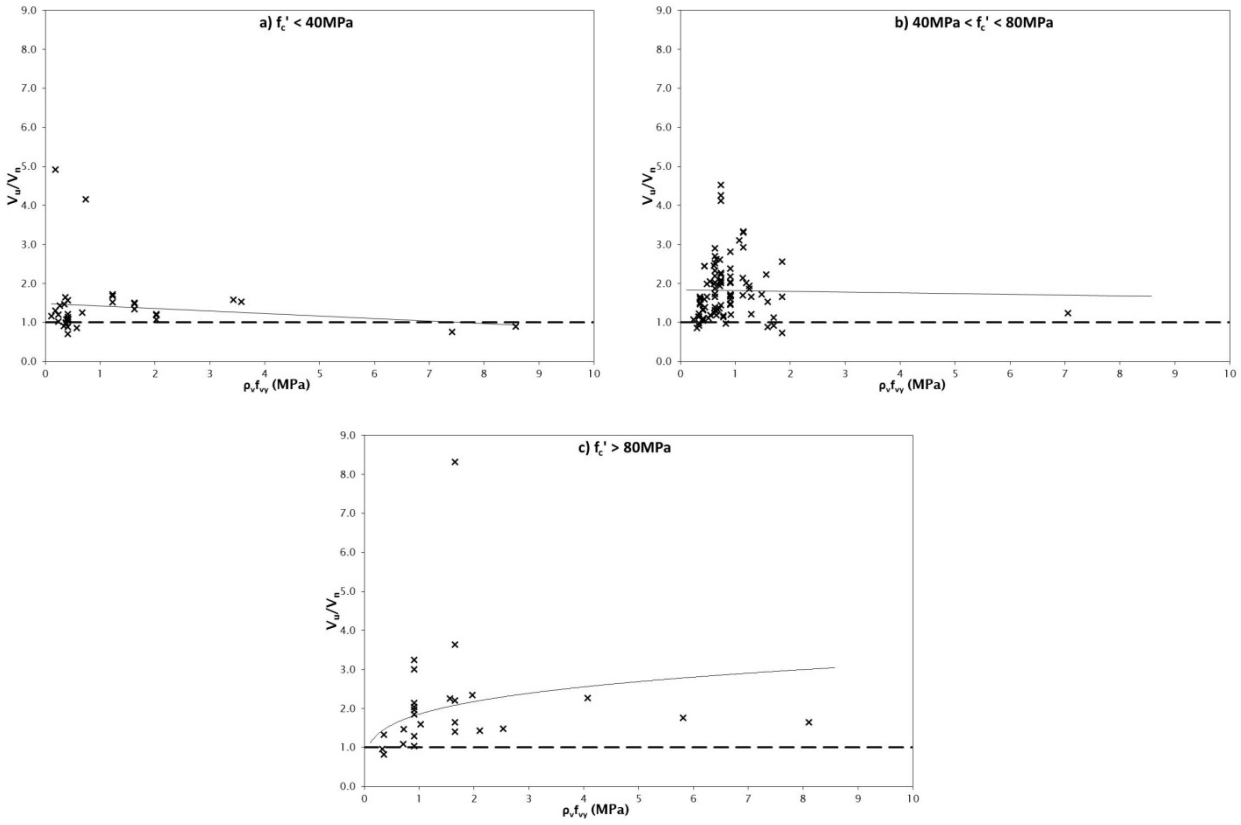

4.4.5.2 PC database

Figures 4.73–4.78 show the influence of concrete compressive strength, shear stress capacity, beam effective depth, shear a/d ratio, and levels of longitudinal and transverse reinforcement on the accuracy of the fib model code in predicting the shear capacity of PC beams. The fib model code was found to be excessively conservative for predicting the ultimate shear capacity of RC beams, with an average ratio of measured to predicted shear capacity of 3.92. The corresponding standard deviation and coefficient of variation were 2.82 and 0.72, respectively. The fib model code provided non-conservative shear capacity predictions for 7 of the 164 PC beams used for this evaluation.

As shown in figure 4.73, the shear design provisions of the fib model code were found to provide increasingly conservative, and therefore decreasingly accurate, predictions of shear capacity for PC beams that had increasing concrete compressive strengths. The shear capacity predictions were markedly more conservative for beams with low quantities of transverse reinforcement ($\rho_v f_{vy}$ < 2MPa), and the only observed non-conservative predictions were for beams that had approximately normal-strength concrete ($f_c' \approx$ 40MPa or lower) and with high (6MPa < $\rho_v f_{vy}$ < 10MPa) and very high ($\rho_v f_{vy}$ > 10MPa) quantities of transverse reinforcement. Figure 4.74 shows that the shear capacity predictions of the fib model code for PC beams increased in accuracy with increasing ultimate shear capacity.

Figure 4.73 Influence of concrete compressive strength on the accuracy of the fib model code for beams in the PC database

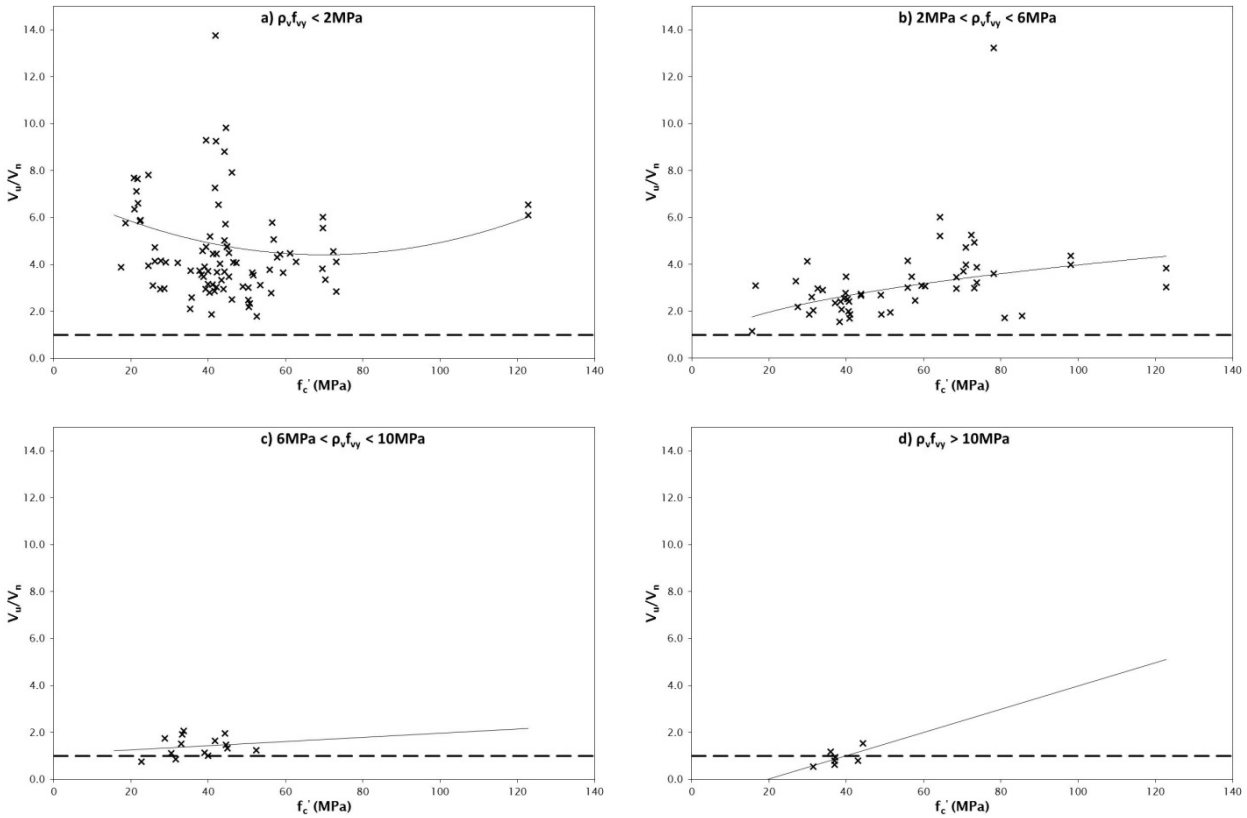

Figure 4.74 Influence of ultimate shear capacity on the accuracy of the fib model code for beams in the PC database

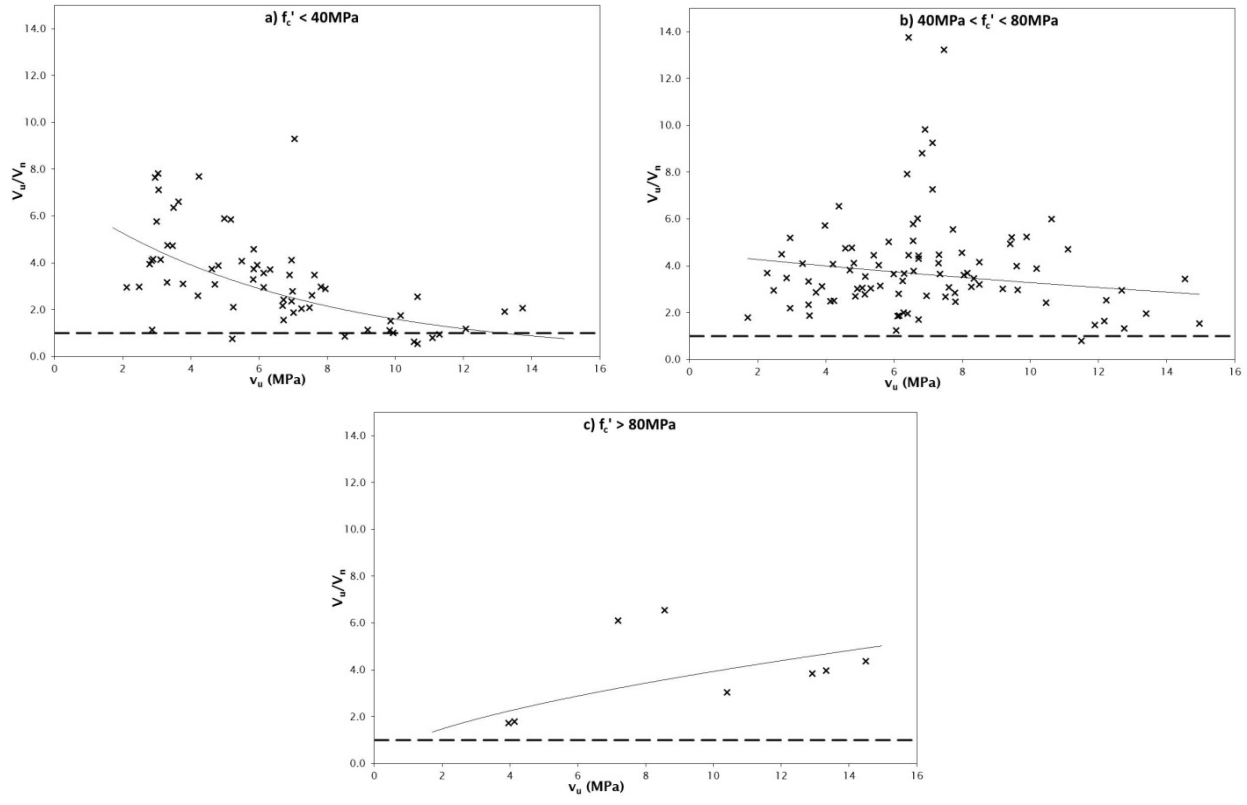

Figure 4.75 shows that the shear capacity predictions of the fib model code are most accurate for PC beams with an effective depth of 500–1000mm, and are significantly more conservative for beams with low quantities of transverse reinforcement ($\rho_v f_{vy}$ < 2MPa).

Figure 4.75 Influence of effective depth on the accuracy of the fib model code for beams in the PC database

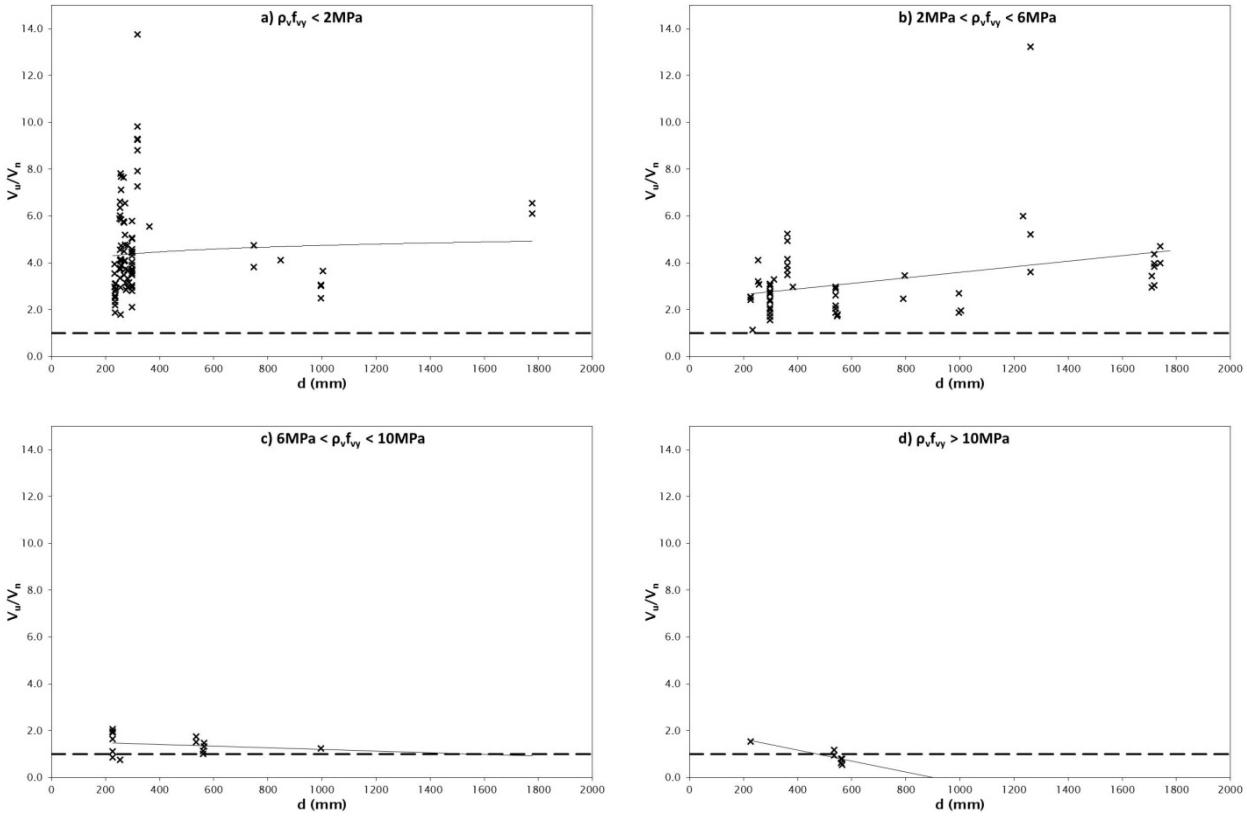

Figure 4.76 Influence of shear a/d ratio on the accuracy of the fib model code for beams in the PC database

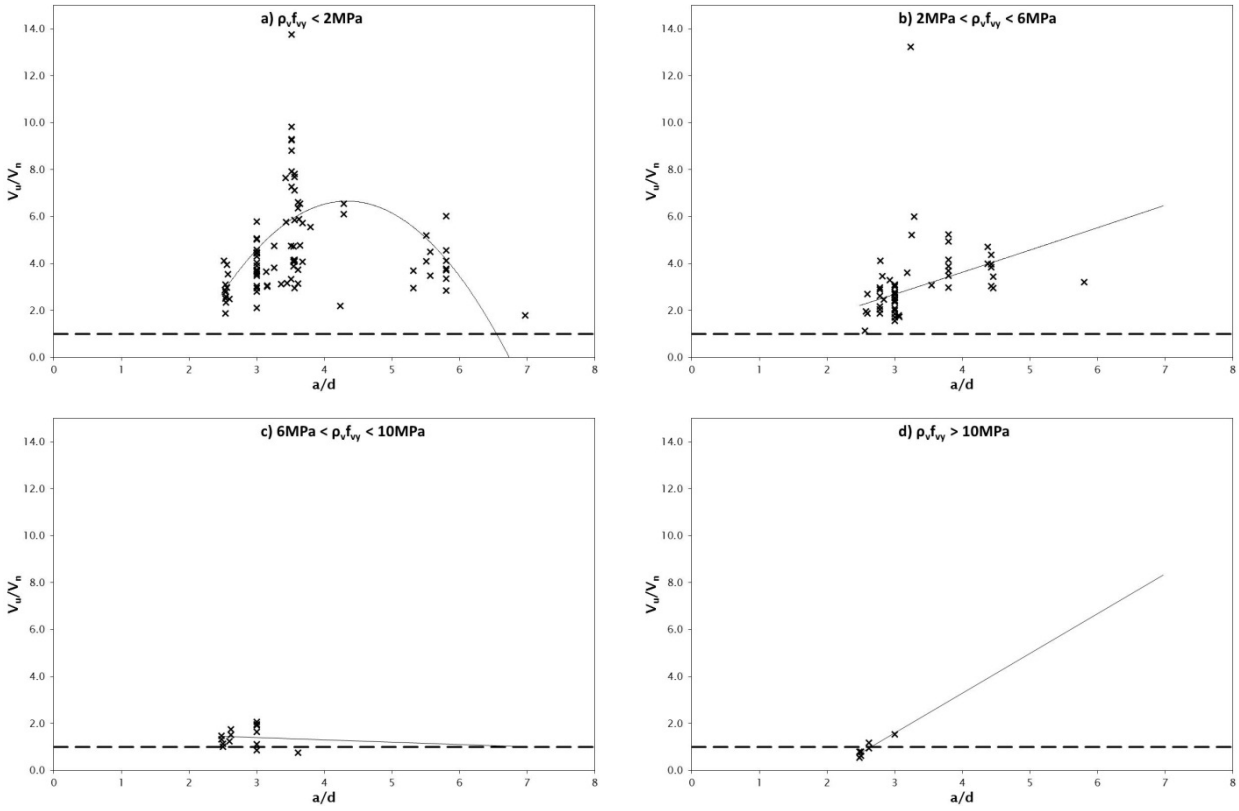

In figures 4.77 and 4.78, the shear design provisions of the fib model code were noted to provide shear capacity predictions increasing in accuracy for PC beams with increasing levels of longitudinal and transverse reinforcement.

Figure 4.77 Influence of longitudinal reinforcement on the accuracy of the fib model code for beams in the PC database

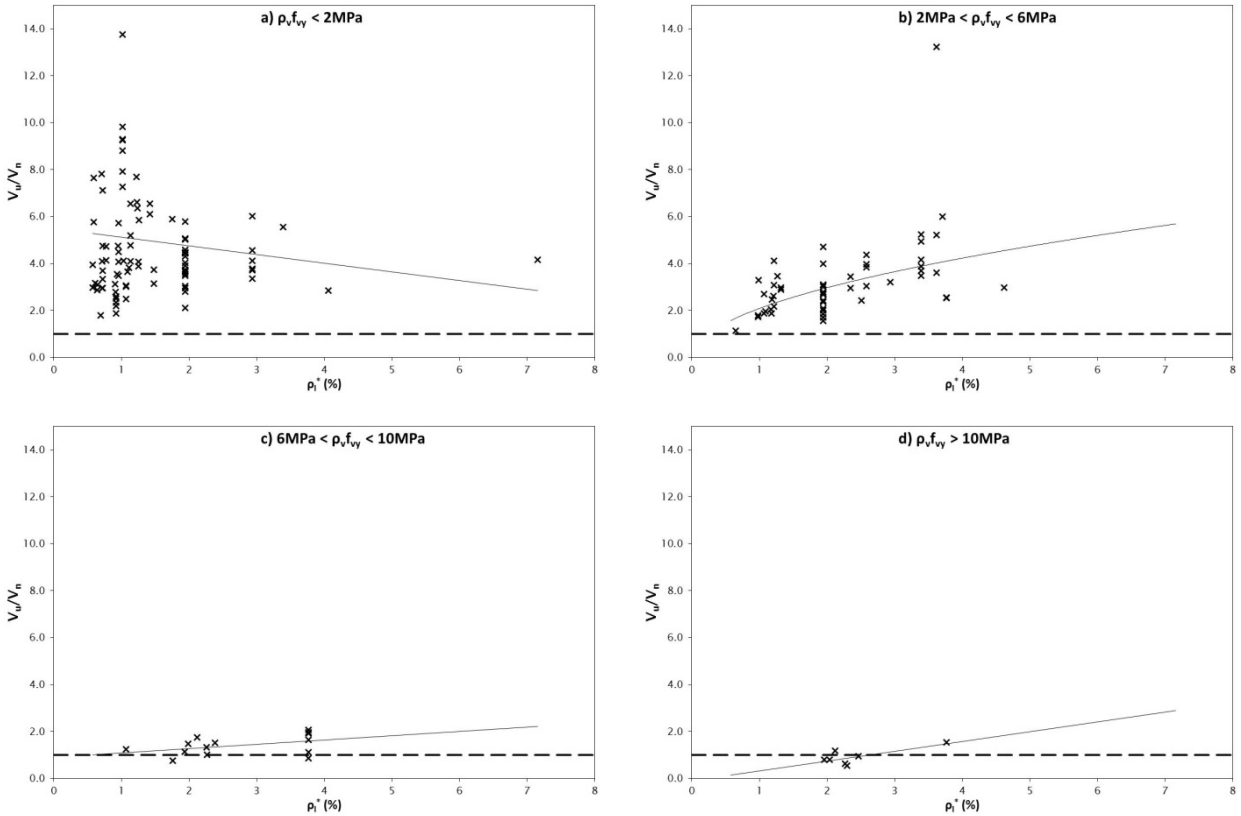

Figure 4.78 Influence of transverse reinforcement on the accuracy of the fib model code for beams in the PC database

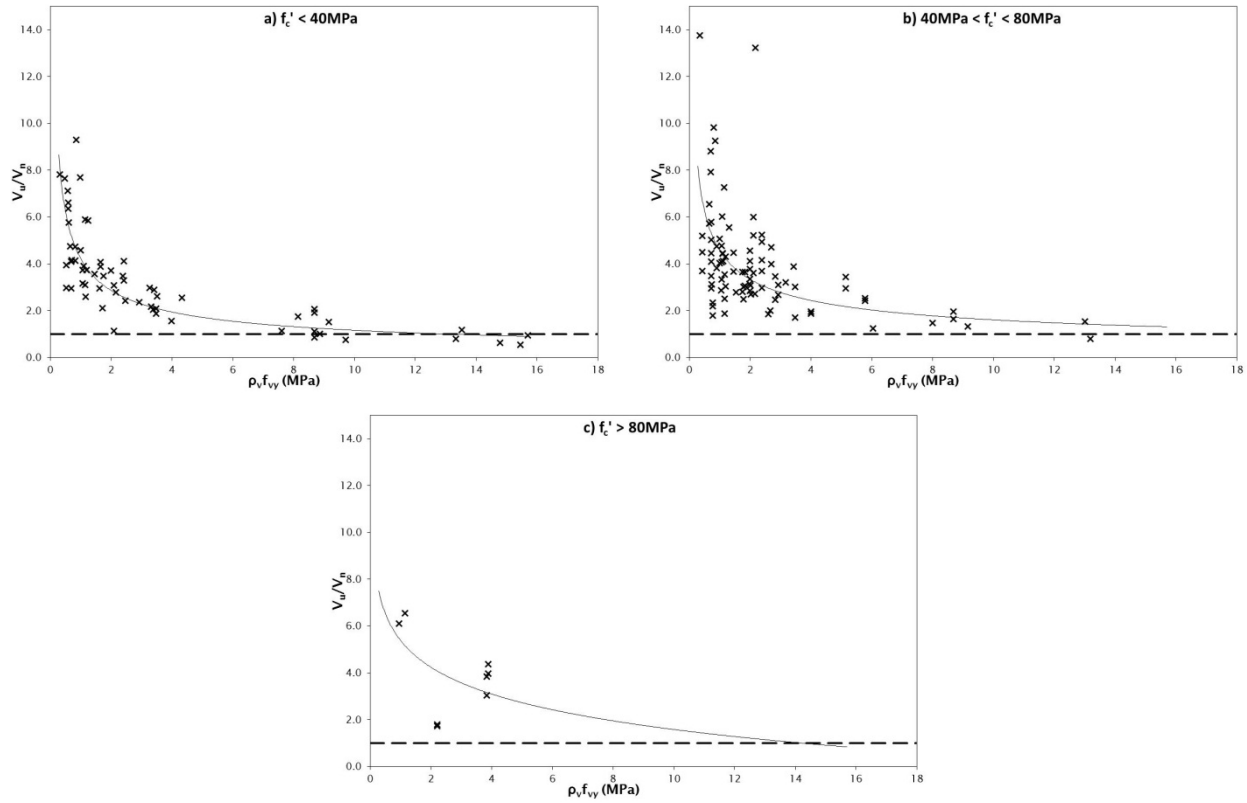

4.5 Conclusions

In this chapter the RC and PC shear test databases were introduced, which are two databases of the experimental results gathered from all accessible published concrete shear testing. The databases were used to identify knowledge gaps in previous experimental testing, as reported in section 4.2, while in sections 4.3 and 4.4 respectively, the databases were used to observe the influence of various design parameters on ultimate shear capacity and on the accuracy of shear capacity predictions from the six design standards detailed in chapter 3.

It was found in section 4.2 that there is an overrepresentation of beams constructed of low-to-normal strength concrete in previous experimental research, with only 26% of the RC database and 38% of the PC database consisting of beams with a concrete compressive strength greater than 40MPa. Similarly, only 5% of the RC database and 2% of the PC database comprised tests on beams with a concrete compressive strength greater than 80MPa. It was also found in section 4.2 that there is paucity within previous research of experimental shear testing on beams with an effective depth greater than 400mm (17% of the RC database and 10% of the PC database), and on beams with an ultimate shear capacity greater than 8MPa (2% of the RC database and 9% of the PC database).

In section 4.3, the RC and PC databases were individually analysed for the influence of six design parameters on measured ultimate shear capacity. For beams in the RC database, measured ultimate shear capacity was observed to increase with increasing concrete compressive strength, longitudinal reinforcement ratio, and transverse reinforcement ratio, while decreasing for increasing beam effective depths and shear a/d ratios. Measured ultimate shear capacities of beams in the PC database were observed to increase for increasing values of concrete compressive strength, beam effective depth, longitudinal reinforcement ratio, and transverse reinforcement ratio, while decreasing for increasing shear a/d ratios.

In section 4.4 the accuracy of the six design standards detailed in chapter 3 was evaluated and the influence of the six design parameters on the accuracy of each standard was identified. ACI 318 was found to be reasonably accurate for both RC and PC beams, with average ratios of measured to predicted shear capacity of 1.30 and 1.18 respectively. However, ACI 318 was observed to inadequately account for the influence of increasing effective depths of RC beams and increasing quantities of transverse reinforcement in PC beams, as the standard provided non-conservative predictions of shear capacity for large values of both parameters.

NZS 3101 was found to provide fairly accurate predictions of ultimate shear capacity for both RC and PC beams, with average ratios of measured to predicted shear capacity of 1.39 and 1.12 respectively. The shear design provisions in NZS 3101 were found to adequately account for the influence of the design parameters used to evaluate the ultimate shear capacity of RC beams, although there was increasing conservatism noted for both RC and PC beams with a shear capacity of 3–6MPa. The provisions in NZS 3101 were also observed to overestimate the ultimate shear capacity of PC beams with 40MPa concrete and high quantities of transverse reinforcement. Of particular note was the absence of any discernible influence of ultimate shear capacity on the accuracy of the design provisions for shear capacities greater than 8MPa, despite the omission of the 8MPa limit on allowable shear capacity during this evaluation. This absence of influence indicates that the design provisions of NZS 3101 adequately account for large ultimate shear capacities, without the need for an absolute limit of 8MPa.

The shear design provisions contained in CSA A23.3 and AASHTO LRFD were found to provide ultimate shear capacity predictions with an average measured to predicted capacity ratio of 1.23 for RC beams and 2.34 for PC beams. CSA A23.3 and AASHTO LRFD were found to provide ultimate shear capacity

predictions of notable conservatism for RC beams with a shear capacity of 3–6MPa, while providing somewhat non-conservative predictions for RC beams with an effective depth greater than 700mm. It was noted that the provisions in the standards provided accurate results for PC beams with moderate-to-high quantities of transverse reinforcement.

EC2 was found to be the most conservative of the design standards considered in this chapter, with average ratios of measured to predicted ultimate shear capacities of 2.84 for RC beams and 2.73 for PC beams. The design standard was found to be particularly conservative for RC and PC beams with low quantities of transverse reinforcement. This excessive conservatism was attributed to the design standard not accounting for the contribution of concrete to shear capacity in the often critical term of the provisions, which is a term based on the transverse reinforcement's contribution to shear capacity.

The shear design provisions of the fib model code were found to be reasonably accurate for RC beams, with an average ratio of measured to predicted ultimate shear capacity of 1.82, but markedly more conservative for PC beams, with an average ratio of 3.92. The fib model code was observed to provide particularly conservative predictions of shear capacity for RC and PC beams containing low quantities of transverse reinforcement.

EC2 was found to be the most conservative of the six design standards considered in this chapter for the prediction of the shear capacity of concrete beams, while CSA A23.3 and AASHTO LRFD were found to be the most accurate for predicting the shear capacity of RC beams, and NZS 3101 was the most accurate for predicting the shear capacity of PC beams. However, a third of the beams in the RC database exhibited ultimate shear capacities lower than those predicted by CSA A23.3 and AASHTO LRFD, and 40% of the beams in the PC database failed at ultimate shear capacities lower than those predicted by NZS 3101.

Therefore it can be concluded that the accuracy of NZS 3101 in predicting the ultimate shear capacity of PC beams comes at the cost of reasonable conservatism. Also, despite the omission of the 8MPa limit on allowable shear capacity during this evaluation, the absence of any discernible influence of ultimate shear capacity on the accuracy of the design provisions for ultimate shear capacities greater than 8MPa led us to conclude that removal of the limit would not unduly affect the integrity of the design provisions in NZS 3101.

5 Experimental investigation

This chapter describes the development of new testing facilities at Stresscrete, Papakura, the design of the test beams and testing procedure for the experimental investigation undertaken as part of the project, details of the instrumentation used when testing the beams, and the test results. The results of this investigation, and the results of the data analysis detailed in the subsequent chapter, were pivotal to informing the conclusions reached at the completion of this project.

5.1 Objectives and scope

The main objective of the experimental phase of the research undertaken to investigate the shear capacity of concrete bridge beam webs was to assess the validity of the maximum allowable shear stress limit of 8MPa imposed on all concrete beams as specified in clause 7.5.2 of NZS 3101:2006:

> *The nominal shear stress for shear added to the shear stress due to torsion, or the shear stress due to shear friction, shall be equal to or less than v_{max}, which is the smaller of $0.2f'_c$ or 8MPa.*

Specifically, clause 9.3.9.3.3 in NZS 3101:2006 for RC beams and clause 19.3.11.1 for PC beams both refer to the standard's clause 7.5.2 for determining the maximum allowable shear stress on a section.

The above objective was investigated through a series of experimental testing, which was also used to inform and calibrate the analytical investigation of all previous shear testing, as detailed in chapter 4. The experimental investigation consisted of testing 12 single-tee PC beams loaded to failure at applied shear stresses of 8MPa and higher.

5.2 Test rig

The first task in preparing for the experimental component of this research was the design and construction of a test rig. Several possibilities were considered for the location and design of the rig, including:

- the construction of a temporary rig in the Department of Civil and Environmental Engineering's Test Hall
- a temporary or permanent rig at another University of Auckland (UoA) location (most likely at the Tamaki Campus)
- a temporary rig at a leased location outside of the University
- a permanent rig at the premises of an industry partner.

The construction of a test rig at UoA premises (at the Test Hall or otherwise) was impracticable because of lack of space and limited crane capacity – this meant that severe constraints would be placed on both the size of the rig and the time frame available for testing. The option of constructing a test rig within leased premises was deemed possible but rather costly.

The best option was to construct the test rig in collaboration with an industry partner at the company's premises. While a number of companies were identified as strong possibilities for collaboration, 'Stresscrete Precast' was determined to be the most suitable industry partner – the department had had previous successful research collaborations with Stresscrete Precast.

Apart from the space issue, there were significant advantages to collaboration with an industry partner:

- An industry partner's facilities and materials (cranes, welding facilities, etc) would be superior to those at the UoA, resulting in cost savings in the construction process.
- Virtually all costs relating to transportation of test beams would be eliminated, as construction and testing of the beams would occur at the same premises.
- Collaboration between the UoA and a member of the precast concrete construction industry was, in itself, a much-desired outcome, as collaboration not only leads to the formation of strong relationships, but also allows for the concrete industry to help define the direction of current and future research at the UoA towards research topics that would ultimately be more useful for the industry.

Stresscrete Precast was chosen, for the following reasons:

- Stresscrete already possessed a test rig that they had used in the past (see figure 5.1).
- There was sufficient space at the Stresscrete yard to allow for storage of test beams and testing equipment, development of the test rig and a workspace for the UoA researchers to use.
- Current concrete researchers from UoA had developed a strong working relationship with Stresscrete through other recent research, and Stresscrete had shown a strong enthusiasm for continuing this relationship with the researchers and the Department of Civil and Environmental Engineering.

Figure 5.1 Condition of test rig at Stresscrete premises prior to project commencement

It was acknowledged at the start of the experimental testing programme that the existing test rig located at Stresscrete premises required significant development over time in order to meet the needs of the various projects that were expected to be undertaken using the rig. Several of the support beams needed either further reinforcement or replacement for strength purposes. Meanwhile, the rig was relocated to a

permanent position in the Stresscrete yard, close to both the materials laboratory and an office that was assigned to UoA researchers. The materials laboratory was used for testing the compressive strength of concrete cylinders on test days. The researcher office was used during the set-up of tests, for data acquisition and processing during and immediately after testing, and for storage of test equipment and instrumentation between tests.

During the experimental testing, the test rig had a form that consisted of two small steel I-beams, on which the ends of the test beams were seated, spanning 1.5m between two larger steel I-beams. The large I-beams were seated on large concrete blocks spaced 6m apart, leading to a 6m potential test span. The load frame consisted of two steel rectangular hollow sections (RHS), with one RHS beam positioned below the two large I-beams and one RHS beam positioned above the test beam, which were connected by two large, threaded steel rods. The bottom RHS was connected to the two large I-beams via a moving mechanism, incorporating wheels, seated on the inner bottom flanges of the I-beams. The top RHS had holes drilled to allow for mounting of the load jack and related equipment and instrumentation. To improve the stability of the load frame, four chains were wrapped around the top RHS and connected to the large I-beams. The final form of the test rig, in use, can be seen in figure 5.2.

Figure 5.2 Condition of test rig during experimental testing

5.3 Design of test beams and setup

A total of 12 beams were tested in the experimental investigation. A number of factors needed consideration during design of the test beams, particularly regarding the capacity of the testing facility. All components of the test rig, including the loading beam, the support beams, and the connections needed to have sufficient strength to withstand the load required for failure of the test beams. This restriction was critical when determining the maximum size of test beams.

Another significant factor considered during the design of the test beams was cost and ease of production. Due to the location of the test rig at the Papakura premises of Stresscrete, it was deemed practically and economically efficient for the test beams to be constructed at Stresscrete. This meant lower production costs, due to previous agreements with Stresscrete, and virtually no transportation costs. Therefore, the number of beams able to be constructed and tested within the allotted budget was maximised. However, this decision did restrict the type of unit cross section to be used.

Tee beams are one of the four recommended typical beam sections for New Zealand bridge designers (Beca and Opus 2008). The three other beam sections are I-beams, single hollow core sections, and double hollow core sections. The casting moulds available at Stresscrete Papakura for hollow core sections were for flooring units, rather than bridge sections, and did not allow for placement of significant transverse reinforcement. Therefore, construction and testing of hollow core units for the experimental investigation was deemed to not be a viable option, as it would not allow for application of high shear stresses ($v_n \geq 8$MPa). The option of construction and testing of I-beams was also considered, but due to the lack of regularly operational relevant casting moulds at the premises of Stresscrete Papakura, this option would have incurred high construction and transportation costs. Therefore, single-tee beams were selected as the optimal section for testing. The single-tee beams were poured in double-tee casting beds and cut into single-tee sections after the concrete had cured.

A total of 12 single-tee beams, 300mm deep, were designed, using the shear capacity design provisions in NZS 3101:2006, and with the basic geometry shown in figure 5.3. There were four beams each with target concrete strengths of 40, 60 and 80MPa, with two beams of each concrete strength designed to fail at an applied shear stress of 8MPa and the other two beams of each concrete strength designed to fail at an applied shear stress of 9–10MPa. These higher values of applied shear stress were the maximum possible within the limitations of the test rig available, and levels of design shear stress higher than 10MPa would have required applied loads that would risk damaging the test rig. The choice of applied shear stresses at failure of ~8MPa and ~10MPa was valuable in meeting the objective of the experimental investigation, as it allowed for examination of the behaviour of beams that were designed for a maximum shear stress within the 8MPa limit specified in NZS 3101:2006, as well as the behaviour of beams that were designed for a maximum shear stress that significantly exceeded the 8MPa limit (by approximately 25%). Table 5.1 shows the test unit matrix with the designated name for each unit. The design of two identical beams for each combination of concrete strength and applied shear stress allowed for some statistical corroboration of test results.

Figure 5.3 Geometry of single-tee test units (dimensions in mm)

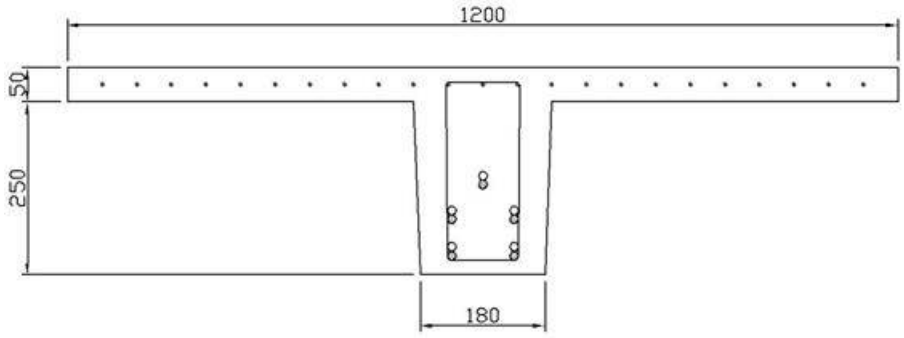

Table 5.1 Experimental test matrix for single-tee beams

Concrete strength	Applied shear stress at failure			
	8MPa		~10MPa	
40MPa	40-8A	40-8B	40-10A	40-10B
60MPa	60-8A	60-8B	60-10A	60-10B
80MPa	80-8A	80-8B	80-10A	80-10B

To achieve the relatively high applied shear stresses required for this testing, ample transverse reinforcement was provided in all test beams, as detailed in table 5.2. Also seen in table 5.2 are the longitudinal reinforcement details for each unit, with P representing the number of prestressed strands and U representing the number of unstressed strands. '12.7 Super' strands were used as both prestressed and unstressed longitudinal reinforcement in the test units, with an effective cross-sectional area of 100.1mm^2, a yield stress of 1560MPa and an ultimate failure stress of 1840MPa. The column of P_M^*/P_V^* values shows the ratios of the loads required for flexure failure to the loads required for shear failure.

Both flexural and shear capacities were calculated based on the specifications of NZS 3101:2006, in which clause 19.3.6 governs for flexure and clause 19.3.11 governs for shear. For beams with an applied shear stress in excess of 8MPa, the ratio refers to the load required for shear failure discounting the 8MPa limit. Sufficient longitudinal reinforcement had to be provided to ensure that beams failed in shear rather than flexure. This design criterion was somewhat complicated by the overly conservative nature of concrete shear design provisions compared with flexural design provisions. This conservatism can be explained by two factors: the theoretical premise that concrete flexure is better understood than concrete shear; and the brittle nature of concrete web-shear failure making this a failure mode that, from a design perspective, is best avoided.

Table 5.2 Reinforcement details for test beams

Unit ID	Transverse reinforcement	Applied shear stress (MPa)	Longitudinal reinforcement	$\frac{P_M^*}{P_V^*}$
40-8	D12 @ 80mm c/c	7.3	5P + 5U	1.36
40-10	D12 @ 50mm c/c	10.1	5P + 5U	1.22
60-8	D12 @ 80mm c/c	7.6	5P + 5U	1.38
60-10	D12 @ 50mm c/c	10.4	5P + 5U	1.18
80-8	D12 @ 80mm c/c	7.8	5P + 5U	1.39
80-10	D12 @ 50mm c/c	10.6	5P + 5U	1.15

The relative efficiency of a unit in shear and flexure is also dependent on the unit geometry (span) and loading geometry (applied load type and placement). The maximum unit span allowed by the test rig was 6m, but this span was deemed inefficient in terms of flexural capacity. As shown in figure 5.4, a span of 4.5m was chosen in order to impose lower bending moments during loading, while also providing a sufficiently high a/d ratio to avoid deep-beam effects. It was acknowledged during the design phase of the experimental investigation that the test span and point of load application may need to be adjusted over the course of the testing, to account for any unexpected effects or failure mechanisms.

The instrumentation employed in the test beams consisted of:

- a load cell with a capacity of 1000 kilonewton (kN)
- portal gauges for displacement measurements able to measure up to ±50mm
- internal concrete strain gauges (model PML-60-2L)
- concrete surface strain gauges (model PL-90-11-3L)
- reinforcement strain gauges attached to the stirrups prior to casting (model WFLA-6-11-3L).

The load cell and portal gauges used were obtained from the Civil Engineering Test Hall, while the strain gauges were purchased from Tokyo Sokki Kenkyujo Ltd.

Figure 5.4 Test setup (dimensions in mm)

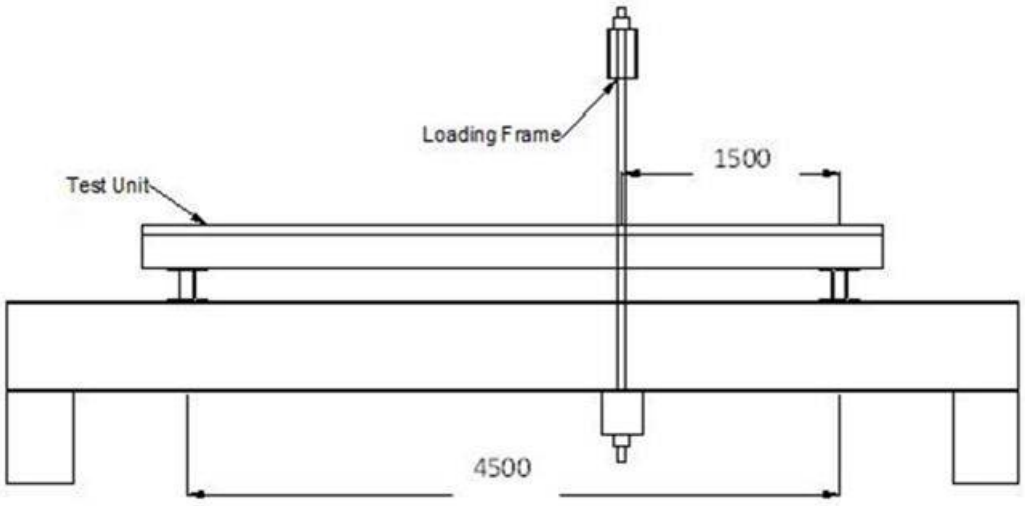

5.4 Construction of test beams

As with any concrete construction, the beams had to be set up in the moulds prior to concrete placement. Set-up included oiling the precast moulds with a release agent, bending and placing the stirrups at the designed spacings, running and prestressing the strands, tying the unstressed strands onto the prestressed strands, placing and tying the flange mesh, and placing and securing the instrumentation.

The internal concrete strain gauges were placed, one per test unit, inside the centre of the webs at a distance of approximately d/2 from the anticipated location of load application (~300mm from the support). The gauges were vertically aligned such that the centre of the gauges coincided with the centre of the web and were secured in place using strings attached to nearby reinforcement. The internal stirrup strain gauges were attached to three stirrups along the load span of each unit, using the provided epoxy-based adhesive. Figure 5.5 shows the three types of strain gauges used in various numbers in each unit.

Figure 5.5 Strain gauges installed during construction

(a) Internal concrete strain gauge (b) Internal stirrup strain gauge (c) External concrete strain gauge

On the day of concrete placement, a number of concrete cylinders were made (see figure 5.6) for each of the three concrete mixes: 7, 8 and 10 cylinders for the 40, 60 and 80MPa mixes respectively. The concrete was vibrated and screeded during pouring, and then covered to allow for accelerated curing in the heated moulds. The concrete cylinders were placed next to the heated moulds, under cover, to allow for curing conditions that were similar to those for the test units.

Figure 5.6 Making concrete cylinders

The beams were allowed to cure in the moulds until the concrete was deemed to have achieved sufficient strength to withstand the transfer process, a concrete compressive strength of 28MPa. The concrete cylinders were tested prior to de-moulding, to prove the compressive strength of the three concrete mixes, after which the strands were cut at the ends of the mould and the beams were pulled out and craned to a location near the test rig.

5.5 Testing

Testing was conducted at Stresscrete premises in Papakura, Auckland, over a two-week period in September 2011. The beams were tested in order of ascending concrete strengths.

The day of testing began with relocation of the unit from the storage area of the yard to the test rig, and aligning the unit correctly along the test rig such that the internal strain gauges in the unit were in the desired location relative to the supports and loading position. Locations were then marked out on the unit for the desired positions of the loading beam and displacement gauges. A layer of sand was placed on top of the unit where the loading beam was to be located, and was levelled to allow for an even load distribution across the width of the unit, resulting in the loading beam configuration shown in figure 5.7(a). Meanwhile, holes 7mm in diameter were drilled in the underside of the webs of each unit, to a depth of 15mm, at the desired displacement gauge locations, and threaded dongles were glued (using an Araldite™ epoxy adhesive) into the holes, onto which threaded rods could be attached for positioning the portal gauges. Figure 5.7(b) shows a portal gauge in place on test day. For later tests in which Linear Variable Differential Transformers (LVDTs), shown in figure 5.7(c), were preferred over portal gauges, this process of drilling and gluing was unnecessary.

Figure 5.7 Test-day instrumentation in place

(a) Load jack with load cell attached **(b) Portal gauge** **(c) LVDT**

A number of concrete cylinders of the appropriate concrete mix were tested in compression on each test day to ascertain the compressive strength of the concrete during testing. Detailed results of the cylinder testing are provided in appendix C. The average compressive strength of the cylinders tested on each test day are mentioned for the appropriate test unit in the next section.

As detailed in next section, both the overall test span and the location of the point of load application were varied throughout the test series in an attempt to ensure a shear-based failure mode for each test unit.

5.6 Test results

This section presents the details and observations from the test of each unit, along with the direct results of each test.

There are two consistent features of the load displacement response curves presented in this section that may need clarification. First, there is some 'noise' present in the data collected, which was due to the data acquisition system used and was deemed to be of an acceptably low level to be inconsequential. Also, there are a number of obvious points of unloading and reloading in each test, which were instituted to allow the researcher the opportunity for comprehensive photography of crack development, when deemed necessary. Video recording was also used in the majority of tests, as this allowed for a more exhaustive post-test examination of the unit's cracking behaviour than could be achieved with still photography. Due to the limitations of the hydraulic pump system used, it was not possible to hold the level of applied load constant, and this resulted in the small drops in load at those points. Comprehensive analysis of the results is presented in chapter 6.

It is important to note that as with the values in table 5.2, the design shear stress values mentioned in the following sections were calculated using a modified version of the 'General method' found in NZS 3101:2006, in which absolute limits on concrete strength and allowed shear stress are ignored.

5.6.1 Unit 40-8-A

Unit 40-8-A was the first unit to be tested, on 22 September 2011. The unit was designed with a concrete compressive strength of 40MPa to fail at an applied shear stress of 7.3MPa, which was achieved by placing the R12 stirrups at a spacing of 80mm. The measured concrete compressive strength on the day of testing, based on the concrete cylinders tested, was 36.3MPa. The unit was tested with a span of 4550mm and the load was applied at 1500mm from one support, with the internal concrete strain (ICS) gauge located 350mm from the same support. The stirrup strain (ISS) gauges were located at 330mm, 500mm,

and 1050mm from the support. The surface concrete strain (ECS) gauges were placed at the same locations as the ISS gauges on one side of the web and at the 330mm and 1050mm locations on the other side of the web. The displacement portal (PG) gauges were placed at 300mm, 1070mm and 1500mm from the support, on the underside of the web.

Table 5.3 summarises all relevant test-day information for all beams with a design concrete strength of 40MPa.

Table 5.3 Testing details of 40MPa beams

	40-8-A	40-8-B	40-10-A	40-10-B
f_c' (MPa)	36.3	36.3	37.4	37.4
Span (mm)	4550	3500	3500	3535
Load span (mm)	1500	1000	700	692
Location of ICS (mm)	350	350	350	300
Location of ISS1 (mm)	330	350	330	290
Location of ISS2 (mm)	500	520	500	540
Location of ISS3 (mm)	1050	1050	1000	1080
Location of ECS1 (mm)	330	360	330	300
Location of ECS2 (mm)	500	1070	1000	700
Location of ECS3 (mm)	1050	1250	1250	1080
Location of ECS4 (mm)	330	360	300	300
Location of ECS5 (mm)	1050	1250	700	1080
Location of PG1 (mm)	300	360	300	310
Location of PG2 (mm)	1070	1000	700	690
Location of PG3 (mm)	1500	N/A	N/A	1070

Unit 40-8-A was specifically selected as the first unit to be tested as it was one of the two lowest-strength beams, both in terms of concrete compressive strength and design shear stress capacity, and was therefore less crucial to the overall findings of the research.

This decision was important, as during the first test in a series, numerous issues can arise that may be remedied, whether relating to instrumentation and data acquisition or the overall set-up design. In this case, it was clear during the second half of the test, and particularly at failure, that shear was not dominating the response of the beam. This observation led to the unit failing in flexure and prompted a redesign of the loading configuration. In subsequent tests, the span was shortened by approximately one metre, and the load span (the shortest distance between the point of load application and a support) was varied to achieve shear failure. While the flexural mode of failure resulted in the failure load and maximum shear stress sustained being irrelevant to the capacity analysis, this test did provide useful data for analysis of the distribution of stresses and strains in various elements that form the shear resistance mechanisms of the unit during loading.

The load displacement response of unit 40-8-A is presented in figure 5.8, along with the applied load required to reach the calculated flexural capacity and shear capacity. The unit failed at an applied load of 277.5kN, at a displacement of 13.2mm, corresponding to a shear force and bending moment at failure of 188.0kN and 284.9 kilonewton-metre (kNm), respectively.

Figure 5.8 Load displacement response of unit 40-8-A

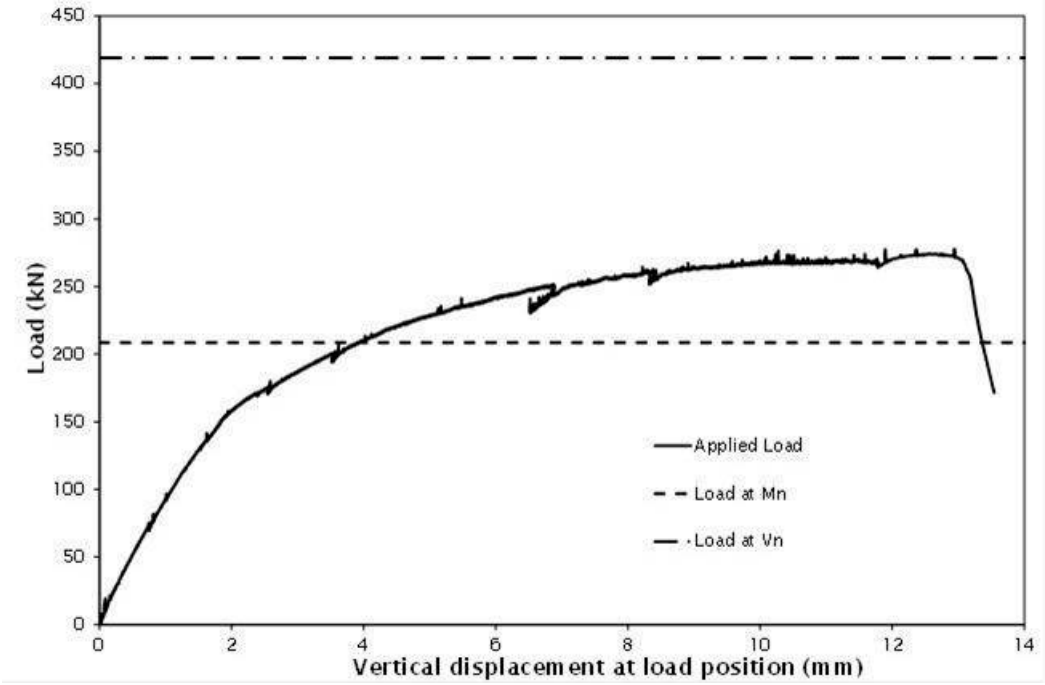

Figure 5.9(a) shows the cracks that developed during loading, and figure 5.9(b) shows the most prominent cracks at failure. It can be seen from these pictures that while there was definite evidence of shear cracking during loading, the dominating flexural cracks at failure confirm a flexural mode of failure. The major cracks observed in this test had angles of inclination ranging between 60˚ and 90˚.

Figure 5.9 Web cracking behaviour of unit 40-8-A

(a) Shear cracks developed in web during loading **(b) Crack pattern at failure**

There was significant damage to the flange observed during testing of unit 40-8-A, as can be seen in figure 5.10. Figure 5.10(a) illustrates the cracking witnessed in the flange, with most cracking being concentrated in close proximity to the location of the loading beam. Figure 5.10(b), which is a view of the bottom surface of the flange, illustrates the extent of the flange damage, with a combination of concrete spalling and buckling of the flange mesh in the longitudinal direction of the unit. Despite the severity of

damage, it was concluded that this extensive cracking and crushing due to flexure did not significantly affect the shear behaviour and shear capacity of the unit, as the damage occurred away from the shear-resisting portions of the unit and therefore had no measurable influence on the shear-resistance mechanisms.

Figure 5.10 Flange damage in unit 40-8-A

(a) Cracking **(b) Spalling**

5.6.2 Unit 40-8-B

Unit 40-8-B was the second unit to be tested, also on 22 September 2011. The unit design was identical to that of unit 40-8-A, and the same value of concrete compressive strength as unit 40-8-A was adopted for unit 40-8-B, since both units were tested on the same day. The unit was tested with a span of 3500mm and the load was applied at 1000mm from one support. This test configuration was changed from the first unit to counteract the flexural failure witnessed in the previous test. The test span was reduced by increasing the overhang at one end of the test unit. The locations of the various strain and displacement gauges were detailed earlier in table 5.3. Due to damage in one of the wires causing erratic readings from one of the displacement gauges, which was not detected until the data-processing phase, only readings from two displacement gauges from this test could be used.

The load displacement response of unit 40-8-B can be seen in figure 5.11. The load at failure was 383.2kN, and the corresponding vertical displacement directly under the load was 5.3mm, corresponding to a peak shear force of 275.7kN and a peak bending moment of 276.9kNm.

Figure 5.11 Load displacement response of unit 40-8-B

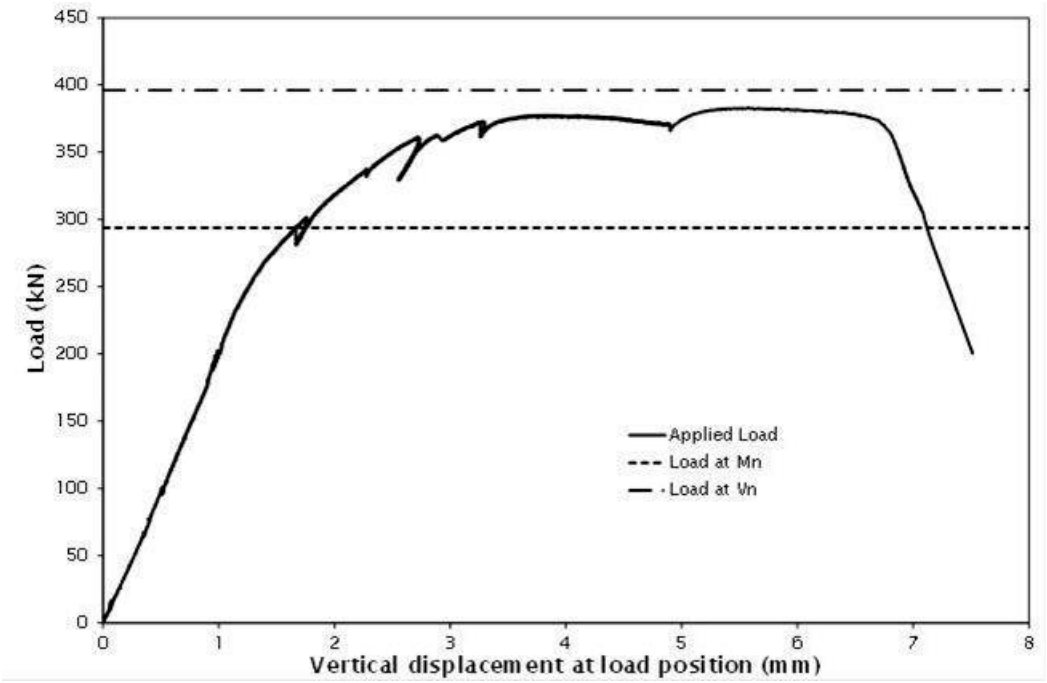

As mentioned in the previous section, the flexural failure of unit 40-8-A led to a rearrangement of the test configuration with both a shortened span (reducing the applied bending moment) and a shorter distance between load and support (increasing the applied shear relative to the applied load). The results of the modified loading configuration can be seen in figure 5.12 – significant shear cracking was observed during loading (figure 5.12(a)) and at failure (figures 5.12(b)–(d)), in the form of both web-shear and flexural-shear cracks. Figures 5.12(b) and (c) show the dominant crack at failure, as observed on both sides of the web. The measured crack angles, both during loading and at failure, ranged between 40˚ and 50˚ (approximately 42˚ for the major crack at failure). As with unit 40-8-A, there was cracking and concrete spalling in the flange, which had little effect on the shear behaviour of the unit. Meanwhile, there was substantial spalling in the web, and a greater prevalence of wide cracks was observed during this test than in the first test.

Figure 5.12 Web cracking behaviour of unit 40-8-B

(a) Cracking during loading

(b) Dominant crack at failure

(c) Dominant crack at failure, opposite side of web **(d) Web damage at failure**

5.6.3 Unit 40-10-A

Unit 40-10-A was the third unit to be tested, on 23 September 2011. The unit was designed with a concrete compressive strength of 40MPa to fail at an applied shear stress of 10.1MPa, which was achieved by placing the R12 stirrups at a spacing of 50mm. The measured concrete compressive strength on the day of testing, based on the concrete cylinders tested, was 37.4MPa. The unit was tested with a span of 3500mm and the load was applied at 700mm from one support, with the strain and displacement gauges located as outlined earlier in table 5.3. Due to damage to a cable used in connecting one of the displacement gauges to the data acquisition system, only two displacement-gauge readings from this test could be used.

Figure 5.13 shows that the unit failed at an applied load of 289.1kN (displacement of 3.7mm), which equated to an applied shear force and bending moment of 233.9kN and 164.4kNm, respectively. Relocation of the load application, to 700mm from the support, resulted in the stiffer initial response (evident in figure 5.13) than that observed in the previous two tests, and this increased stiffness was consistent with the relative decrease in applied moments.

Figure 5.13 Load displacement response of unit 40-10-A

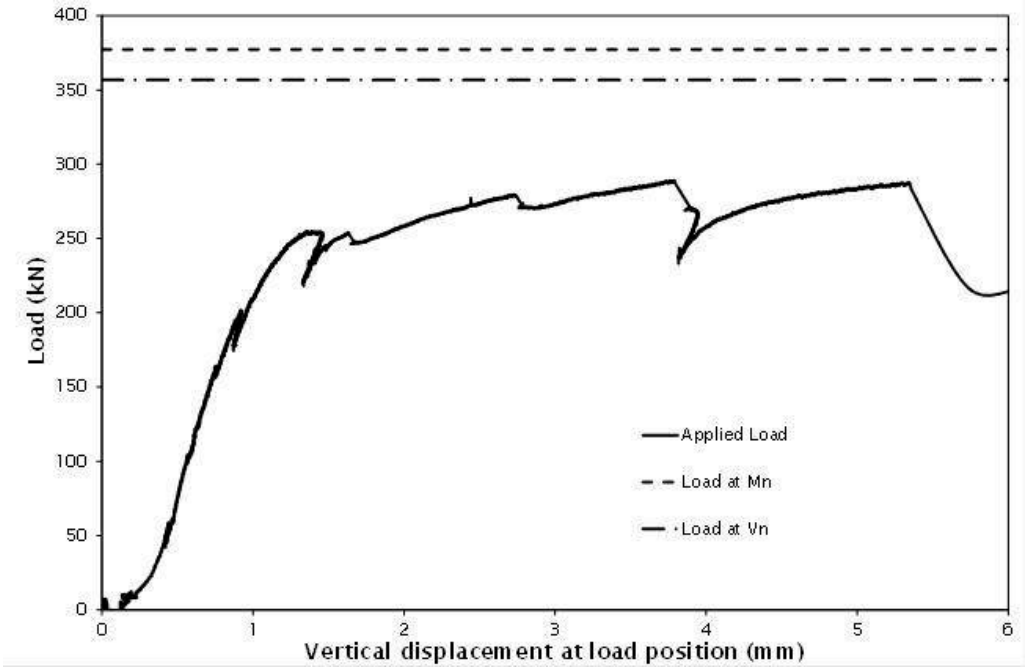

Despite the rearranged loading configuration, it is clear from examining the cracks developed during loading, as shown in figure 5.14, that the dominant failure mode of this unit was flexural. This flexural dominance is evident by the widest cracks at failure being those with the steepest angles of inclination (approximately 65°), which is an indicator of flexural stresses governing the response of the unit at failure. The calculated bending moment at failure was less than 80% of the predicted ultimate flexural capacity of the unit, and it is thought that this premature flexural failure was caused by substantial slip of the longitudinal strands. This hypothesis was supported by observations of considerable 'pull-in' of the strands at the end of the unit.

While unfortunate, the inability to achieve shear failure in this test was not a major setback because the test data was still useful for investigating the distribution and development of strain throughout the unit when subjected to progressive loading, and the most critical tests in the series, in terms of the shear capacity investigation, were those beams constructed of higher concrete strength ($f_c' > 40$MPa). While there was moderate cracking in the flange during this test, the level of damage at failure was much lower than that observed in the previous two tests.

Figure 5.14 Web cracking behaviour of unit 40-10-A

(a) Dominant crack during loading **(b) Dominant crack at failure**

5.6.4 Unit 40-10-B

Unit 40-10-B was the fourth unit to be tested, on 26 September 2011. The unit design was identical to that of unit 40-10-A, and the unit was tested with a span of 3535mm and with the load applied at 692mm from one support. Further testing details, such as the placement of various gauges, were outlined in table 5.3.

As with unit 40-10-A, the shorter load span adopted for the testing of unit 40-10-B resulted in a stiffer response in the elastic range. This increased stiffness can be seen in figure 5.15. Failure was achieved at an applied load of 347.2kN and a displacement of 2.8mm, corresponding to a shear force and bending moment at failure of 282.0kN and 195.8kNm, respectively.

Figure 5.15 Load displacement response of unit 40-10-B

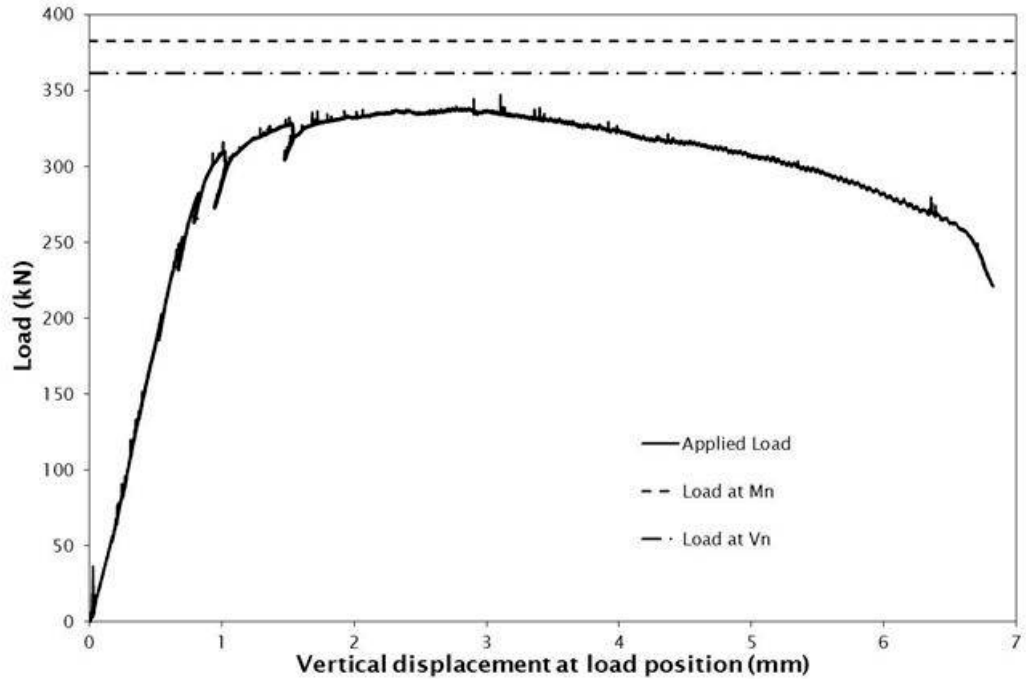

During loading of unit 40-10-B, a combination of flexure and shear cracks developed, with shear cracks forming at angles of 35–45˚. Significant flexural cracking developed during loading, as evident in figure 5.16(a), but the dominant cracks at failure were due to shear, as seen in figure 5.16(b), with angles of 35˚ and 40˚. As with unit 40-10-A, the level of damage in the flange at failure was significantly lower than that observed in the first two tests.

Figure 5.16 Web cracking behaviour of unit 40-10-B

(a) Dominant crack during loading **(b) Dominant crack at failure**

5.6.5 Unit 60-8-A

The first of the 60MPa beams was tested on 27 September 2011. Unit 60-8-A was designed with a concrete compressive strength of 60MPa and with R12 stirrups spaced at 80mm, to achieve a design shear stress at failure of 7.6MPa. The measured compressive concrete strength of the 60MPa mix on the day of testing was 56MPa, and the test was carried out with a span of 3500mm and a load span of 700mm. Locations of the instrumentation used in this test, and for all other beams with a design concrete strength of 60MPa, are outlined in table 5.4 below.

Table 5.4 Testing details of 60MPa beams

	60-8-A	60-8-B	60-10-A	60-10-B
f_c' (MPa)	56	56	56	56
Span (mm)	3500	3500	3560	3515
Load span (mm)	700	700	700	700
Location of ICS (mm)	340	380	350	380
Location of ISS1 (mm)	330	330	330	350
Location of ISS2 (mm)	530	520	540	520
Location of ISS3 (mm)	1010	1090	1070	1070
Location of ECS1 (mm)	350	380	330	350
Location of ECS2 (mm)	700	1150	700	700
Location of ECS3 (mm)	1010	1260	1060	1070
Location of ECS4 (mm)	350	380	330	350
Location of ECS5 (mm)	1010	700	700	700
Location of PG1 (mm)	350	350	340	330
Location of PG2 (mm)	700	670	690	670
Location of PG3 (mm)	1070	1050	1070	1060

As shown below in figure 5.17, unit 60-8-A failed at an applied load of 435.1kN (ignoring the spikes in load that were caused by noise in the data acquisition system), with a corresponding displacement of 20.9mm. The noticeable step-up in load at 13mm displacement was due to an unanticipated spike in hydraulic pressure in the pump, which resulted in an unexpected rise in loading rate. The applied load at failure equates to an applied shear force and bending moment, at the respective critical sections, of 350.8kN and 246.2kNm.

Figure 5.17 Load displacement response of unit 60-8-A

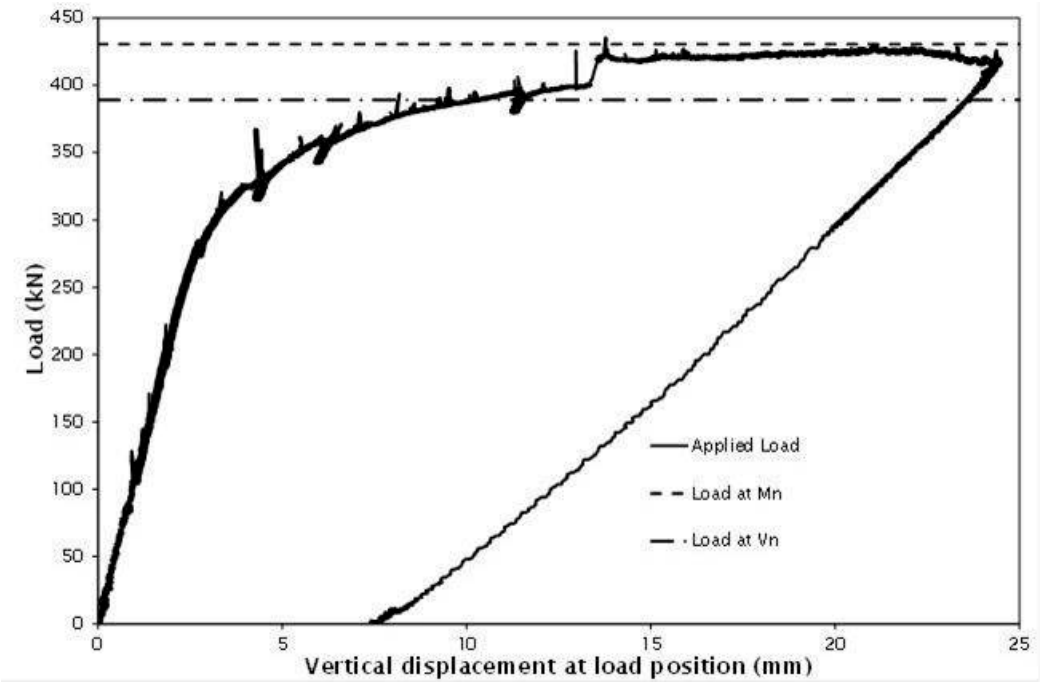

During loading of unit 60-8-A, a combination of flexural and shear cracking was observed, with the observed angles of crack inclination being almost vertical and ~40° respectively. An example of the shear cracks that developed during loading can be seen in figure 5.18(a). However, near failure the flexural cracks widened while the shear cracks became more distributed, resulting in the predominantly flexure-based failure crack seen in figure 5.18(b). This crack pattern at failure indicates that while the unit surpassed both its calculated shear and flexural capacities, the dominant failure mode was flexural. Only minor damage was observed in the flange during this test.

Figure 5.18 Web cracking behaviour of unit 60-8-A

(a) Dominant crack during loading **(b) Dominant crack at failure**

5.6.6 Unit 60-8-B

Testing of unit 60-8-B, which had an identical design to that of unit 60-8-A, took place on 27 September 2011. The test span and load span had dimensions of 3500mm and 700mm respectively, while the cylinder strength of the concrete on day of testing was 56MPa. The locations of the various instrumentation used was shown earlier in table 5.4. The load displacement plot is shown in figure 5.19, in which it can be seen that the unit failed at an applied load of 489.8kN and a displacement of 16.4mm. The measured failure load corresponded to a maximum applied shear force of 394.5kN and a peak bending moment of 276.8kNm.

Figure 5.19 Load displacement response of unit 60-8-B

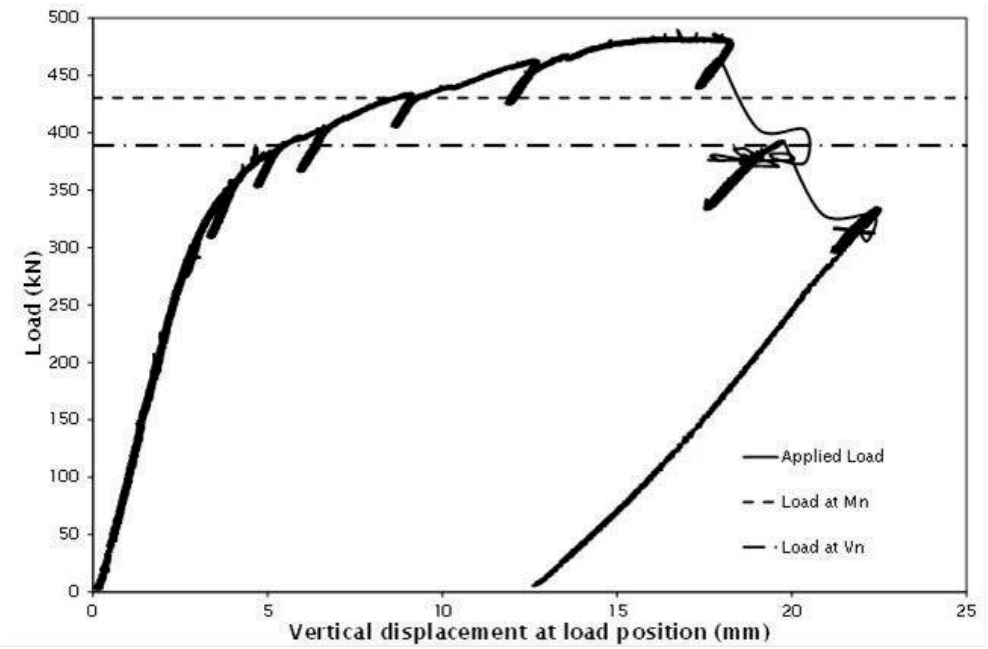

The majority of the cracking observed during testing of unit 60-8-B was shear cracking, forming at angles of 35–45° – figure 5.20(a) provides a good example of this crack behaviour. The same crack pattern was also true of the widest cracks at failure, as evident in figure 5.20(b). While there was noticeable cracking in the flange at failure, this flange damage was not deemed significant to the overall performance of the unit.

Figure 5.20 Web cracking behaviour of unit 60-8-B

(a) Dominant crack during loading **(b) Dominant crack at failure**

5.6.7 Unit 60-10-A

Unit 60-10-A, tested on 27 September 2011, was designed with a concrete strength of 60MPa and with R12 stirrups spaced at 50mm, to achieve a design shear stress of 10.4MPa. The unit was tested with a measured cylinder strength of 56MPa, with a span of 3560mm and a load span of 700mm. The remaining details, including exact locations of instrumentation used in this test, were shown earlier in table 5.4. The resulting load displacement response, as shown in figure 5.21, indicated a failure load of 485.7kN at a displacement of 13.8mm. For the loading configuration used in this test, this failure load resulted in a maximum shear force of 393.0kN and a peak bending moment of 275.7kNm at the respective critical sections.

Figure 5.21 Load displacement response of unit 60-10-A

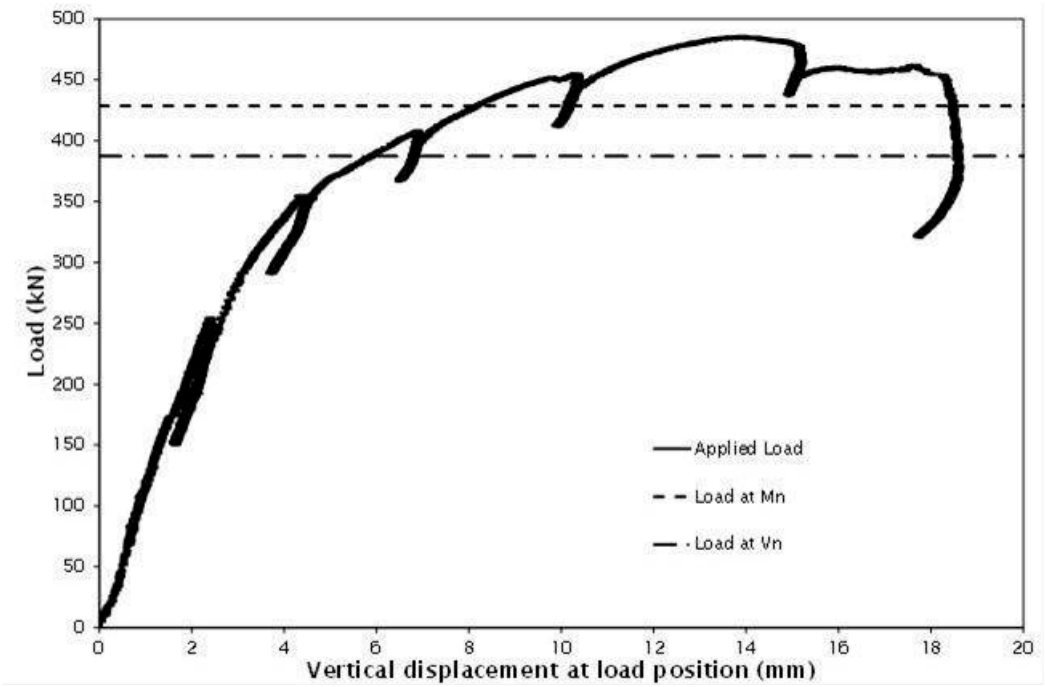

When testing unit 60-10-A, a major crack formed early, at an angle of 55°, with a distribution of other cracks developing at shallower angles radiating back towards the support, as shown in figure 5.22(a). The crack pattern at failure of the unit can be seen in figure 5.22(b). There was evidence of minor damage in the flange prior to testing, caused by various construction and transport loads. This damage was not significantly exacerbated during testing, confirming the inconsequential influence of the flange damage on the overall unit's performance.

Figure 5.22 Web cracking behaviour of unit 60-10-A

(a) Crack pattern during loading **(b) Dominant crack at failure**

5.6.8 Unit 60-10-B

Unit 60-10-B was tested on 28 September 2011, and had a measured cylinder strength of 56MPa. The design of the unit was identical to that of unit 60-10-A, and the test was carried out with a span of 3515mm and a load span of 700mm. Details of the locations of various instrumentation used in this test were outlined earlier in table 5.4, while figure 5.23 shows the load displacement response of the unit. The applied load at failure of 452kN, at a displacement of 12.6mm, corresponded to a 365.7kN shear force and a 253.7kNm bending moment, at the respective critical sections, for the load configuration adopted for this test.

Figure 5.23 Load displacement response of unit 60-10-B

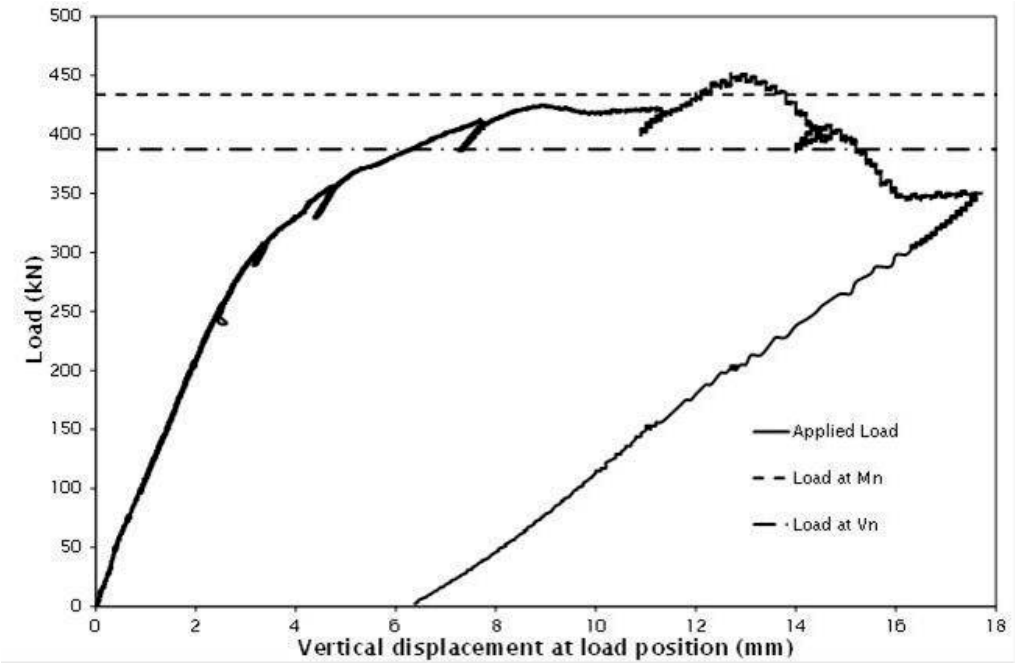

There was an

even distribution of shear and flexure cracking throughout unit 60-10-B during testing, with the flexure cracks widening at a faster rate than the shear cracks – this is shown in figure 5.24(a), when the unit was nearing failure. The critical crack at failure, which can be seen in figure 5.24 (b), was flexure-dominated. The average measured angle of inclination for the shear cracks was 33°, and some of the larger shear cracks extended up into the flange.

Figure 5.24 Web cracking behaviour of unit 60-10-B

(a) Crack pattern during loading **(b) Crack pattern at failure**

5.6.9 Unit 80-8-A

Unit 80-8-A was designed with a concrete strength of 80MPa and with R12 stirrups located at a spacing of 50mm, resulting in a design shear stress of 7.8MPa. The test was carried out on 29 September 2011, with a measured concrete strength of 70.3MPa, a span of 3550mm, and a load span of 800mm. Locations of the instrumentation employed throughout this test are recorded in table 5.5 below, along with similar details for all beams that had a design concrete strength of 80MPa. Damage to one of the cards in the data acquisition system resulted in an insufficient number of ports to accommodate all the gauges, and therefore the signals from only four concrete surface gauges were recorded during this test.

Table 5.5 Testing details for 80MPa beams

	80-8-A	80-8-B	80-10-A	80-10-B
f_c' (MPa)	70.3	70.3	70.3	70. 3
Span (mm)	3550	3550	3525	3525
Load span (mm)	800	800	800	700
Location of ICS (mm)	300	290	370	310
Location of ISS1 (mm)	320	300	300	300
Location of ISS2 (mm)	490	480	500	500
Location of ISS3 (mm)	1050	1050	1050	1050
Location of ECS1 (mm)	320	300	320	300
Location of ECS2 (mm)	470	480	1000	1050
Location of ECS3 (mm)	1050	1050	1240	1250
Location of ECS4[a] (mm)	320	650	320	700
Location of ECS5[a] (mm)	N/A	N/A	800	N/A
Location of PG1 (mm)	330	340	330	330
Location of PG2 (mm)	670	680	670	670
Location of PG3 (mm)	1060	N/A	1060	1060

a) Opposite side of the web from first 3 gauges.

Figure 5.25 shows the response of unit 80-8-A during testing, indicating that a failure load of 506kN was reached at a displacement of 15.0mm. The critical shear force experienced by the unit at this level of loading was 394.6kN, with the critical bending moment being 316.5kNm.

Figure 5.25 Load displacement response of unit 80-8-A

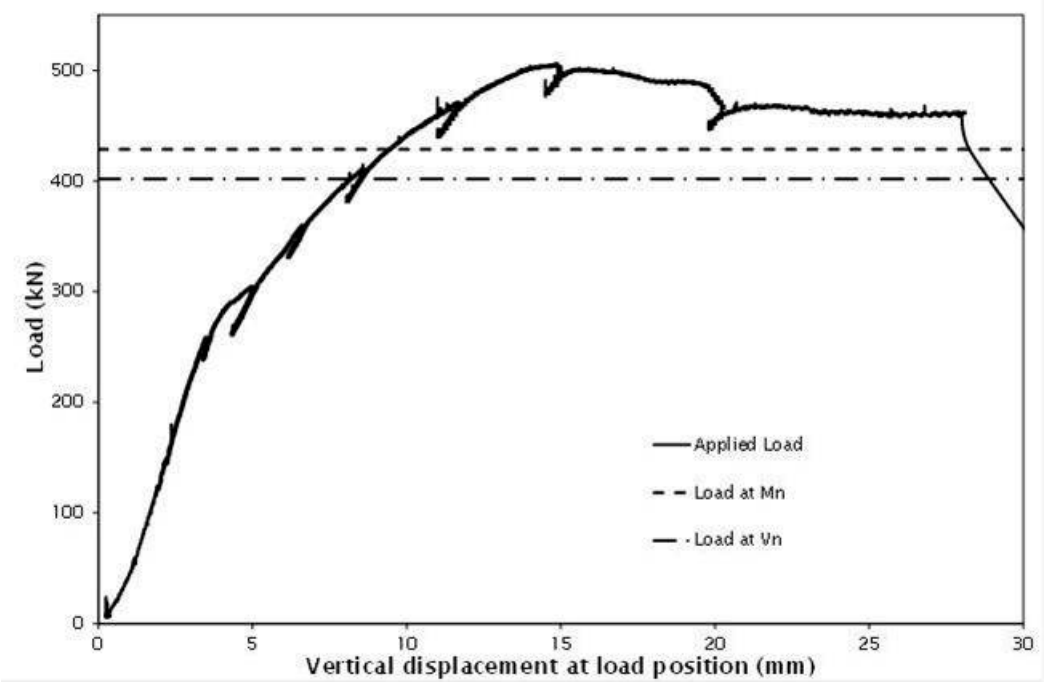

The majority of the prominent cracks that developed throughout the test were caused by shear stresses, with an average angle to the horizontal of 35˚ – figure 5.26(a) provides a good example of this shear cracking. The critical crack at failure, as seen in figure 5.26(b), exhibited similar cracking patterns, and significant spalling due to excessive damage was observed at the location of the failure crack. A number of relatively wide cracks formed in the region of the flange surrounding the loading beam.

Figure 5.26 Web cracking behaviour of unit 80-8-A

(a) Crack pattern during loading **(b) Crack pattern at failure**

5.6.10 Unit 80-8-B

The design of unit 80-8-B was identical to that of unit 80-8-A and was the last unit tested, also on 29 September 2011. The concrete strength was 70.3MPa, the test span was 3550mm, and the load span was 800mm. Exact instrumentation locations were outlined earlier in table 5.5. Due to damage to one of the cards in the data acquisition system, the signals from only four concrete surface strain gauges and two displacement gauges were recorded during this test.

The load displacement response for unit 80-8-B, as shown in figure 5.27, indicated that the unit failed at an applied load of 642.3kN and at a displacement of 21.3mm. The corresponding critical shear force and bending moment at this level of loading was 500.2kN and 401.0kNm, respectively.

Figure 5.27 Load displacement response of unit 80-8-B

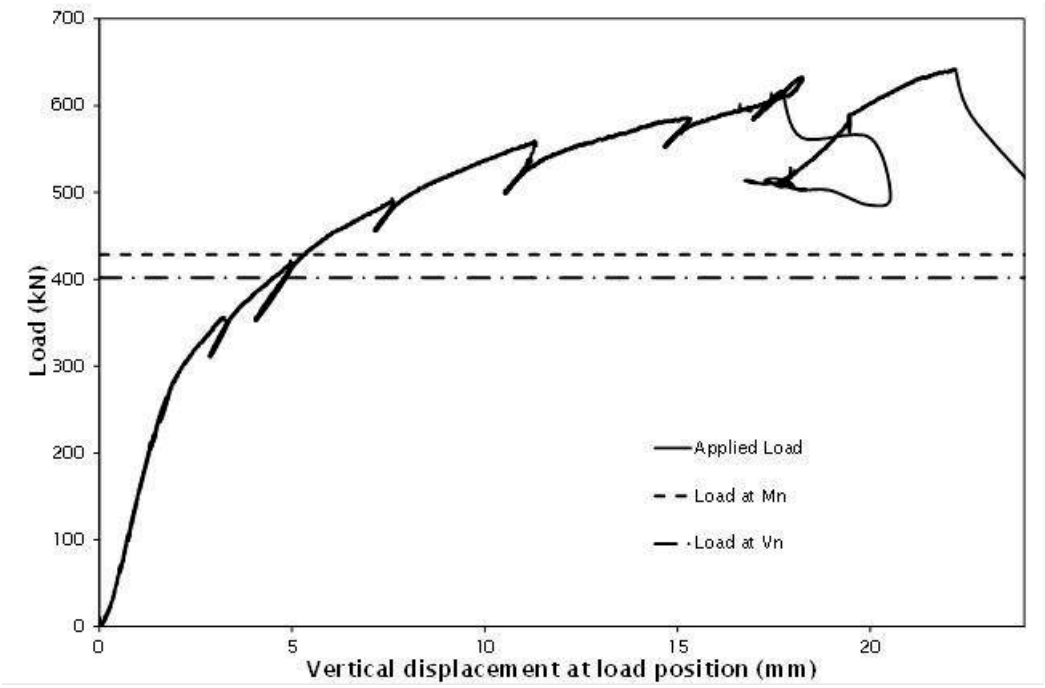

The cracking witnessed during testing of unit 80-8-B was evenly distributed and included a variety of inclination angles, as can be seen in figure 5.28(a). The critical crack at failure, shown in figure 5.28(b), was primarily caused by shear and was orientated at an angle of 40° to the horizontal. Wide cracks were also observed in the flange at the location directly beneath the point of load application, with some spalling on the bottom surface of the flange in other regions.

Figure 5.28 Web cracking behaviour of unit 80-8-B

(a) Crack pattern during loading **(b) Crack pattern at failure**

5.6.11 Unit 80-10-A

The design of unit 80-10-A consisted of an 80MPa concrete mix design, with R12 stirrups spaced at 50mm and a predicted critical shear stress at failure of 10.6MPa. This unit was tested on 28 September 2011, and had a concrete measured cylinder strength of 70.3MPa, a span of 3525mm and a load span of 800mm. Table 5.5 provided specific details of the instrumentation used for this test.

As can be gathered from figure 5.29, unit 80-10-A failed at an applied load of 522.2kN, which was reached at a displacement of 25.6mm. The critical shear force and bending moment were 406.3kN and 325.9kNm, respectively.

Figure 5.29 Load displacement response of unit 80-10-A

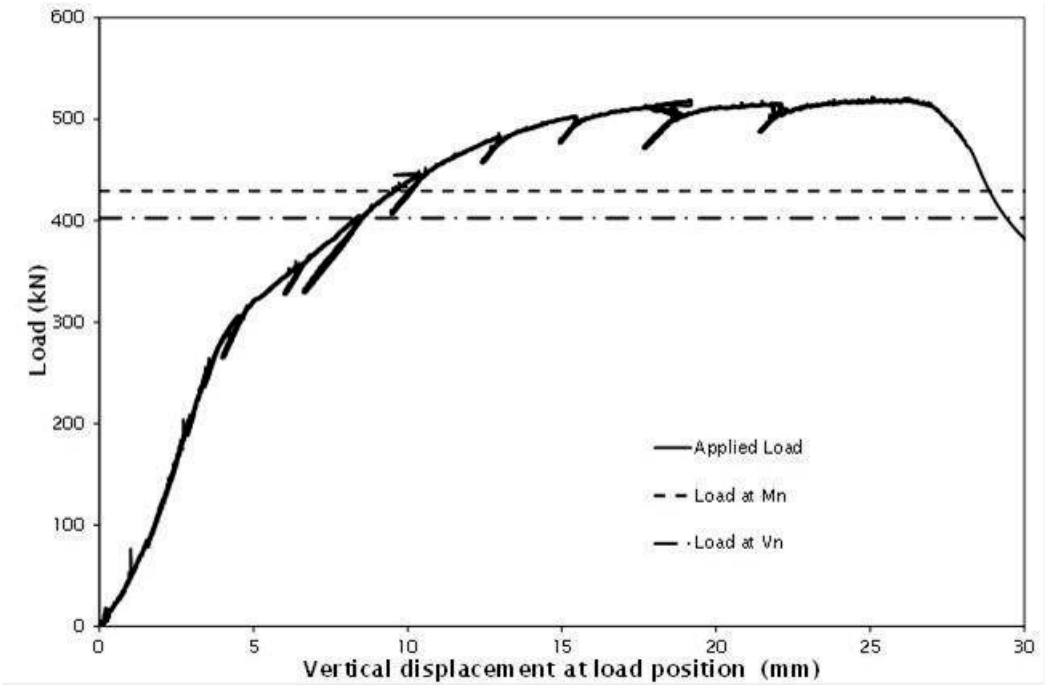

While a variety of shear and flexural cracks formed during testing of unit 80-10-A, as can be seen in figure 5.30(a), it was the former that dominated the unit's failure mechanism. The critical crack, shown in figure 5.30(b), was formed at an angle of 47° to the horizontal, and propagated up into the flange.

Figure 5.30 Web cracking behaviour of unit 80-10-A

(a) Crack pattern during loading **(b) Crack pattern during loading**

5.6.12 Unit 80-10-B

Unit 80-10-B was tested on 28 September 2011. Its design was identical to that of unit 80-10-A, and it had a measured concrete strength of 70.3MPa on the day of testing. The load configuration consisted of a 3525mm span with a 700mm load span. A total of eight gauges were used to monitor various parameters in the unit – details of these gauges were outlined earlier in table 5.5.

Through gradual loading, unit 80-10-B remained elastic until a load of approximately 280kN (4.1mm displacement) was applied, at which point cracking began to significantly 'soften' the response of the unit. This softening effect continued until failure, at an ultimate load of 440.0kN (16.0mm displacement), with a critical shear force and bending moment of 355.4kN and 249.5kNm respectively. This behaviour is shown in figure 5.31.

Figure 5.31 Load displacement response of unit 80-10-B

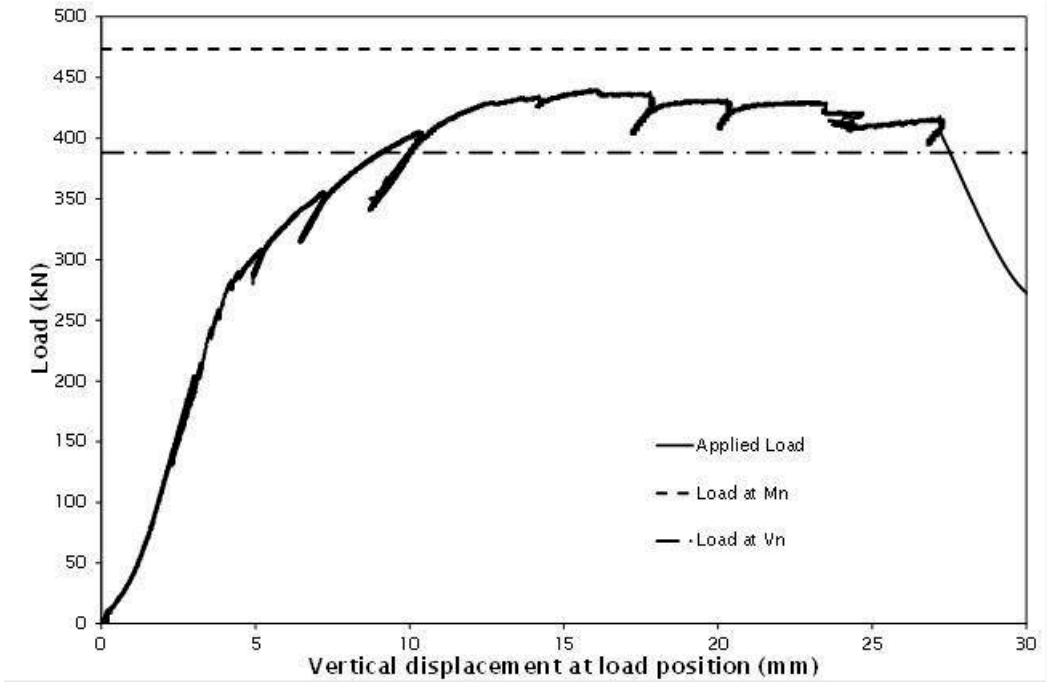

While a number of smaller cracks formed throughout testing of unit 80-10-B, two main cracks dominated the response of the unit, being the shear crack shown in figures 5.32(a) and (b) with an angle of 40°, and

the flexural crack shown in figures 5.32(c) with an angle of 78°. The influence of both of these cracks led to a combined mode of failure that could not be classified as either 'pure shear' (whether web-shear or flexure-shear), nor 'pure flexure', and is thought to have undermined the potential shear capacity of the unit. Both cracks also propagated up into the flange.

Figure 5.32 Web cracking behaviour of unit 80-10-B

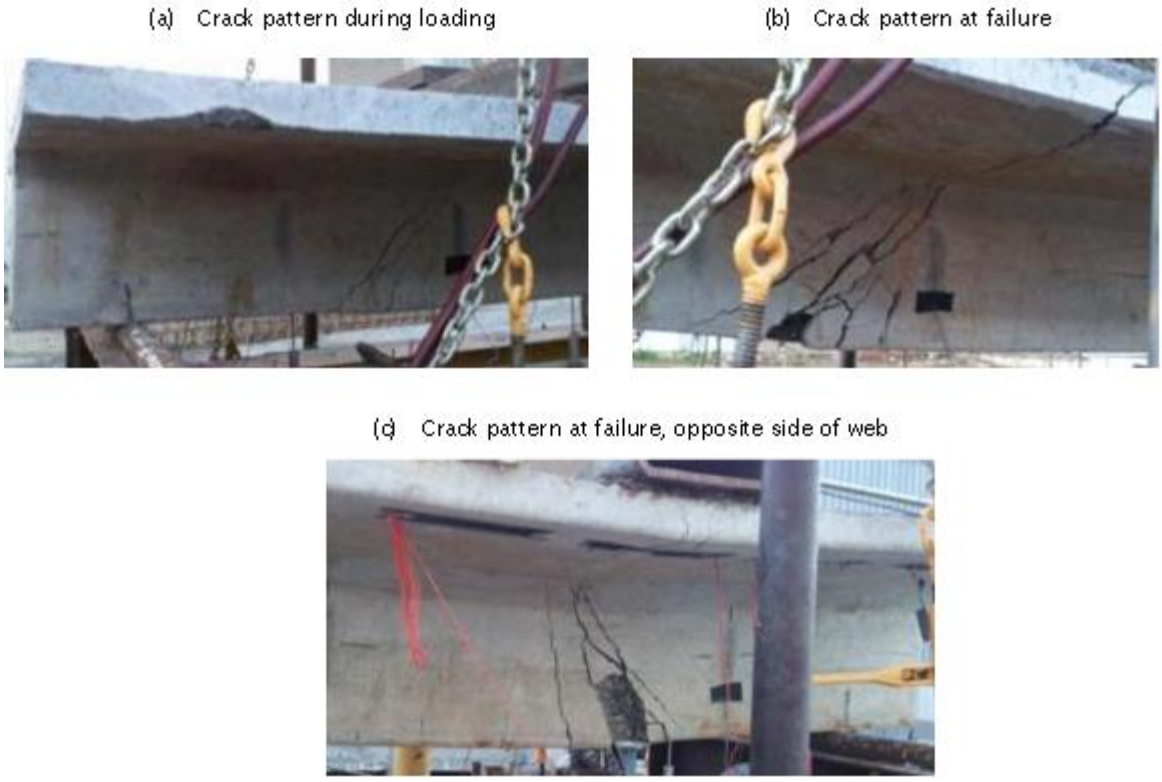

5.6.13 Summary

Table 5.6 presents a summary of the major results from the experimental testing.

Table 5.6 Summary of experimental test results

Unit	Applied load (kN)	Shear force (kN)	Vertical displacement (mm)	Bending moment (kNm)
40-8-A	277.5	188.0	13.2	284.9
40-8-B	383.2	275.7	5.3	276.9
40-10-A	289.1	233.9	3.7	164.4
40-10-B	347.2	282.0	2.8	195.8
60-8-A	435.1	350.8	13.0	246.2
60-8-B	489.8	394.5	16.4	276.8
60-10-A	485.7	393.0	13.8	275.7
60-10-B	452.0	365.7	12.6	253.7
80-8-A	506.0	394.6	15.0	316.5
80-8-B	642.3	500.2	21.3	401.0
80-10-A	522.2	406.3	25.6	325.9
80-10-B	440.0	355.4	16.0	249.5

5.7 Conclusions

This chapter presented the details of the experimental investigation, undertaken as part of this project, to assess the performance of high-strength concrete prestressed beams subjected to shear stresses equal to and exceeding NZS 3101-specified limits. The development of test facilities at the premises of an industry partner was identified as the preferred option, and details of the test facilities were presented in section 5.2. The process for the design and construction of the experimental test units, including details of the instrumentation utilised throughout the experimental investigation, was described in sections 5.3 and 5.4. The test-day protocol was presented in section 5.5.

Preliminary results and observations for each test unit were presented in section 5.6. Two of the four test units designed to have a concrete compressive strength of 40MPa failed in flexure at shear stresses lower than the predicted shear capacity, while another test unit with 40MPa concrete failed due to strand slip. The remainder of the test units all failed at shear stresses greater than the design shear capacities, with strong evidence of predominantly shear failure modes. A thorough analysis of the results of the experimental investigation detailed in this chapter is provided in chapter 6.

6 Analysis of investigation results

The data obtained from the experimental investigation detailed in chapter 5 was analysed using a number of methods. A comparative analysis of the response of the experimental test units is presented in section 6.1, and an analysis of the performance of the international design standards in predicting the shear capacity of the test units, as discussed in chapter 3, is detailed in section 6.2. Finally, section 6.3 presents a statistical analysis of five alternative limits on design shear capacity proposed for use in NZS 3101, and the limits that are deemed to be most suitable are recommended.

6.1 Capacity analysis

The individual applied-load vertical displacement response of each test unit was discussed earlier in section 5.6. This section presents the shear force at the critical shear section plotted against measured vertical displacement at the load position for groups of test units that had similar levels of expected performance.

Figure 6.1 shows the shear force at the critical shear section plotted versus vertical displacement for each unit that was designed with a target ultimate shear capacity of 8MPa. As discussed in section 5.6, units 40-8-A and 40-8-B both exhibited flexural modes of failure, and therefore they are not included in further analyses in this chapter. However, the data from these two tests has been included in figure 6.1, for completeness. Also included in the figure is a line to represent an applied shear stress of 8MPa. It can be seen in figure 6.1 that while units 40-8-A and 40-8-B did not reach an ultimate shear capacity of 8MPa, due to observed flexural failure, the remaining four units that had been designed to have approximate ultimate shear capacities of approximately 8MPa all achieved ultimate shear capacities substantially greater than 8MPa.

The design ultimate shear capacities, calculated using the design provisions of NZS 3101, were 221kN for unit 40-8-A, 235kN for unit 40-8-B, 254kN for the 60MPa test units, and 249kN for the 80MPa test units.

Unit 80-8-B failed at an ultimate shear capacity that was 73% greater than predicted by the shear design provisions of NZS 3101. Unit 80-8-A failed at an ultimate shear capacity that was 36% greater than predicted, despite being of identical design and being tested with the same loading configuration as unit 80-8-B. Units 60-8-A and 60-8-B were also of identical design and were tested having the same loading configuration as each other, and failed at ultimate shear capacities that were 21% and 36% greater, respectively, than predicted by NZS 3101. This substantial variation in measured shear capacities between test units that were, by all known parameters, identical, was characteristic of the highly variable nature of concrete shear behaviour.

Figure 6.1 Shear performance of test units with v_u = 8MPa

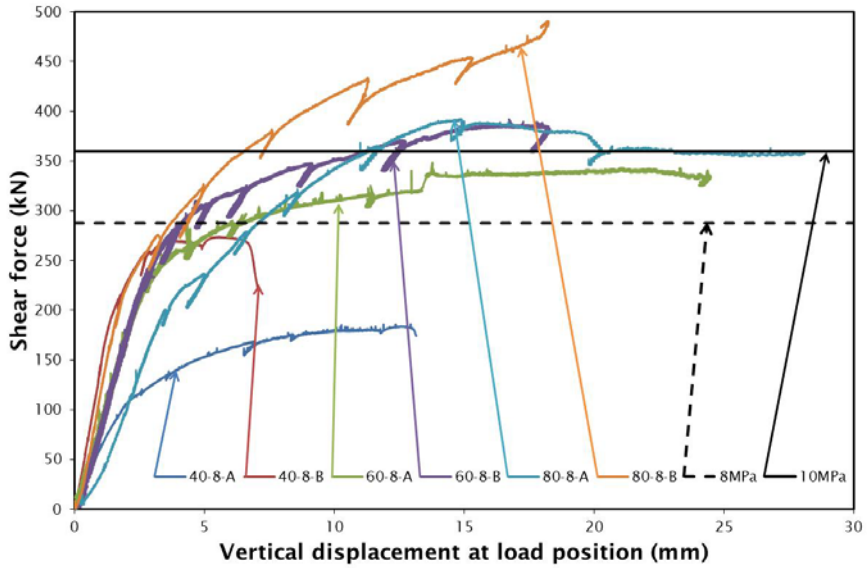

Figure 6.2 shows the applied shear force at the critical shear section plotted against vertical displacement at load position for all test units that had a design shear capacity of 10MPa when designed using the provisions of NZS 3101, without any imposed limits on maximum shear capacity. Also plotted in the figure are lines that represent 8MPa and 10MPa shear capacities. As noted in section 5.6.3, unit 40-10-A failed in flexure, and is therefore only included in figure 6.2 for completeness.

The design ultimate shear capacity, calculated using the design provisions of NZS 3101, including the 8MPa limit, was 269kN for unit 40-10-B and 288kN for the 60MPa and 80MPa units. The design ultimate shear capacities for the 40MPa, 60MPa and 80MPa test units, calculated using the provisions of NZS 3101 without the 8MPa limit, were 363kN, 365kN and 367kN, respectively.

Unit 40-10-B was the only test unit that was constructed of normal-strength concrete ($f_c' \leq$ 40MPa) and resulted in a shear failure mode. While this unit did not achieve the design shear capacity of 10MPa, when ignoring maximum NZS 3101 limits of 8MPa, it did exceed the shear capacity equivalent to $0.2f_c'$ (= 7.48MPa) by 5%. This observed performance indicates that the primary mode of failure was web crushing of the diagonal concrete struts, and provides some support to the validity of imposing a limit on the maximum design shear capacity to account for this failure mode. However, the ability of the test units that had a higher concrete compressive strength than unit 40-10-B to consistently achieve greater ultimate shear capacities indicated that this limit is proportional to the concrete compressive strength of the test unit, as represented by the limit of $0.2f_c'$. All four of these test units with high-strength concrete ($f_c' >$ 40MPa) failed at ultimate shear capacities within 12% of the predicted shear capacity of 10MPa, supporting the hypothesis that an absolute limit of 8MPa imposed on the maximum design shear capacity is excessively conservative and unduly restrictive to concrete shear design.

Figure 6.2 Shear performance of test units with $v_u \approx 10$MPa

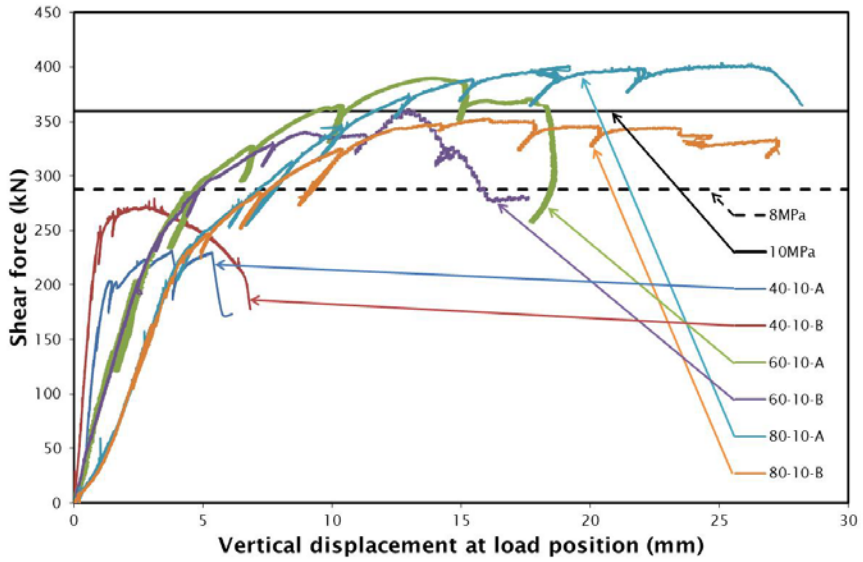

6.1.1 Summary of experimental investigation results

It is important to note that test units constructed with high-strength concrete (f_c' > 40MPa) consistently reached experimentally determined ultimate shear capacities greater than the 8MPa limit imposed on nominal shear capacity by the shear design provisions of NZS 3101. All high-strength concrete test units failed at ultimate shear capacities equal to or greater than the design shear capacities predicted by the provisions of NZS 3101, while ignoring the 8MPa absolute limit. The single normal-strength concrete test unit that failed in shear did not reach the design shear capacity of 10MPa, but rather, failed at an ultimate shear capacity approximately equal to $0.2f_c'$. These results challenge the necessity of placing an absolute limit on nominal design shear capacity, but support the validity of a limit that is proportional to concrete compressive strength.

6.2 Design code based analysis

The PC beam shear design provisions of the standards detailed in chapter 3 were used to predict the ultimate shear capacity of nine of the 12 experimental test units described in chapter 5. Three of the units designed with a target concrete compressive strength of 40MPa were omitted from this analysis, as they were observed to not fail in shear, as noted in section 5.6. The predictions of ultimate shear capacity presented in this chapter were arrived at using unit design parameters measured during testing.

It was necessary during calculation of the predicted ultimate shear capacity of the nine experimental units to estimate the prestress in the longitudinal strands after all losses, at the commencement of testing, and therefore to estimate the prestress losses for each layer of strands. The estimated prestress losses consisted of elastic shortening, creep, shrinkage and relaxation. Detailed calculation of the prestress losses, and the resulting predicted prestress in each layer of longitudinal reinforcement at the commencement of testing, are provided in appendix B. It was estimated that after all losses, a prestress of 865.4MPa was present in the bottom layer of longitudinal reinforcement, a prestress of 953.4MPa was present in the middle layer of longitudinal reinforcement, and a prestress of 1051.1MPa was present in the top layer of longitudinal reinforcement.

For the purposes of the analysis presented in this section, the effective level of transverse reinforcement in each test unit was calculated as the product of the transverse reinforcement ratio, ρ_v, and the yield strength of the transverse reinforcement, f_{vy}. $\rho_v f_{vy}$ was found to be 5.14MPa for test units that had a transverse reinforcement spacing of 80mm, and was found to be 8.23MPa for test units that were constructed with a transverse reinforcement spacing of 50mm. These two sets of test units were designated as '$\rho_v f_{vy}$ = 5MPa' and '$\rho_v f_{vy}$ = 8MPa' units, respectively, in the plots presented in the following sections.

6.2.1 ACI 318

The predicted ultimate shear capacities of the nine test units used in this analysis were calculated using the shear design provisions of ACI 318. These design provisions were detailed in section 3.1 and impose a limit on the contribution of transverse reinforcement to the design shear capacity, found in equation 3.4. The accuracy of the shear design provisions in this standard was assessed for predicting shear capacities both with and without the imposed limit on transverse reinforcement contribution.

Figure 6.3 shows the ratios of measured to predicted shear capacity, with the imposed limit on maximum transverse reinforcement contribution plotted against measured concrete compressive strength for the two levels of transverse reinforcement of the nine experimental units observed to fail in shear. It was noted that all of the units exhibited ultimate shear capacities greater than those predicted by ACI 318. The shear capacities predicted by the design standard increased in conservatism with increasing values of concrete compressive strength for units with a lower quantity of transverse reinforcement ($\rho_v f_{vy}$ = 5MPa), but were of consistent accuracy for units having high quantities of transverse reinforcement ($\rho_v f_{vy}$ = 8MPa).

Figure 6.3 Influence of concrete compressive strength and transverse reinforcement on the accuracy of ACI 318, with imposed limit, for nine experimental units reported in chapter 5

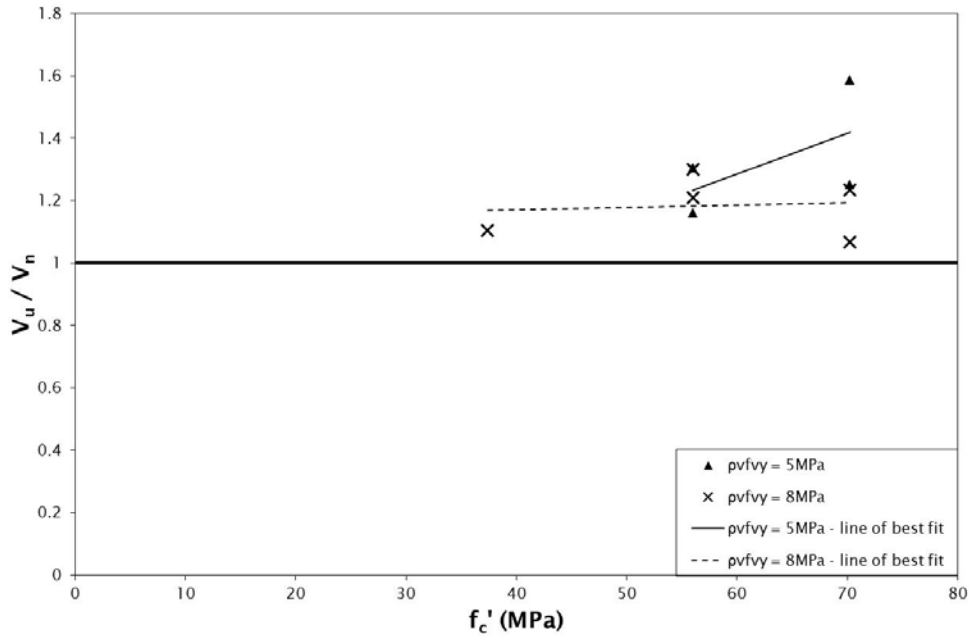

Figure 6.4 presents the measured to predicted shear capacity ratios for the test units using the ACI 318 provisions, but without enforcing the limit on the contribution of transverse reinforcement. The shear design provisions were observed to provide conservative shear capacity predictions for the test units with a lower quantity of transverse reinforcement ($\rho_v f_{vy}$ = 5MPa), with increasing conservatism for units with

higher concrete compressive strengths. However, without the limit on transverse reinforcement contribution, the shear capacities predicted using the provisions in ACI 318 were consistently non-conservative for test units with a high quantity of transverse reinforcement ($\rho_v f_{v_y}$ = 8MPa). By comparison with the trend observed when using the provisions of ACI 318 with the limit on transverse reinforcement contribution enforced, it was clear that this limit was specified due to a well-founded acknowledgement of the deficiencies of the provisions to accurately predict the shear capacity of beams containing a large quantity of transverse reinforcement. It was concluded that these deficiencies were caused by the assumption of a 45° shear cracking angle inherent in the shear design provisions of ACI 318, and the inability of the provisions to account for cracking angles that differ from 45°, which would significantly influence the quantity of transverse reinforcement that provides shear resistance at an inclined crack. The influence of this assumption is greater for beams with increasing quantities of transverse reinforcement, as the shear capacity of such beams is increasingly dependent on the contribution of transverse reinforcement to the nominal shear capacity.

Figure 6.4 Influence of concrete compressive strength and transverse reinforcement on the accuracy of ACI 318, without imposed limit, for nine experimental units reported in chapter 5

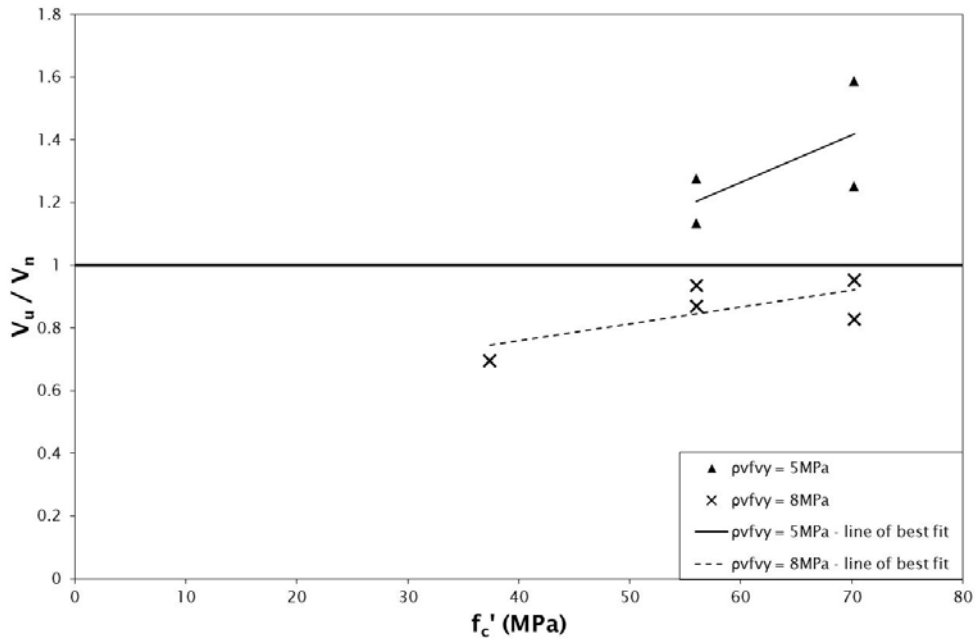

6.2.2 NZS 3101

The shear design provisions specified in NZS 3101 (detailed in section 3.2 of this report) include a limit of 8MPa imposed on the allowable design shear capacity of concrete beams. The predicted shear capacity of the nine test units reported in chapter 5 was predicted using the shear design provisions in NZS 3101, with and without enforcing the 8MPa limit. For both cases, the limit of $0.2f_c'$ was imposed on the allowable design shear capacity. The ratios of measured shear capacity of the nine test units to the shear capacity predicted using the shear design provisions of NZS 3101, with and without the 8MPa limit, are plotted against concrete compressive strength in figures 6.5 and 6.6, respectively.

As can be seen in figure 6.5, the shear provisions of NZS 3101 provided conservative shear capacity predictions for all of the nine test units when the limit of 8MPa was imposed on the allowable design shear capacity. This conservatism was observed to slightly increase, on average, with increasing concrete compressive strength and for units that had a lower quantity of transverse reinforcement.

The effect of ignoring the 8MPa limit on allowable design shear capacity when predicting the shear capacity of the nine test units is shown in figure 6.6. It was observed that the provisions of NZS 3101, with this 8MPa limit omitted, provided increasingly conservative predictions of shear capacity for units with a large quantity of transverse reinforcement ($\rho_v f_{vy}$ = 5MPa) and increasingly non-conservative predictions for units with a high quantity of transverse reinforcement ($\rho_v f_{vy}$ = 8MPa) with increasing concrete compressive strength. The accuracy of the predicted shear capacities was also observed to decrease with increasing concrete compressive strength, for units with a large or very large quantity of transverse reinforcement.

Figure 6.5 Influence of concrete compressive strength and transverse reinforcement on the accuracy of NZS 3101, with absolute limit of 8MPa, for nine experimental units reported in chapter 5

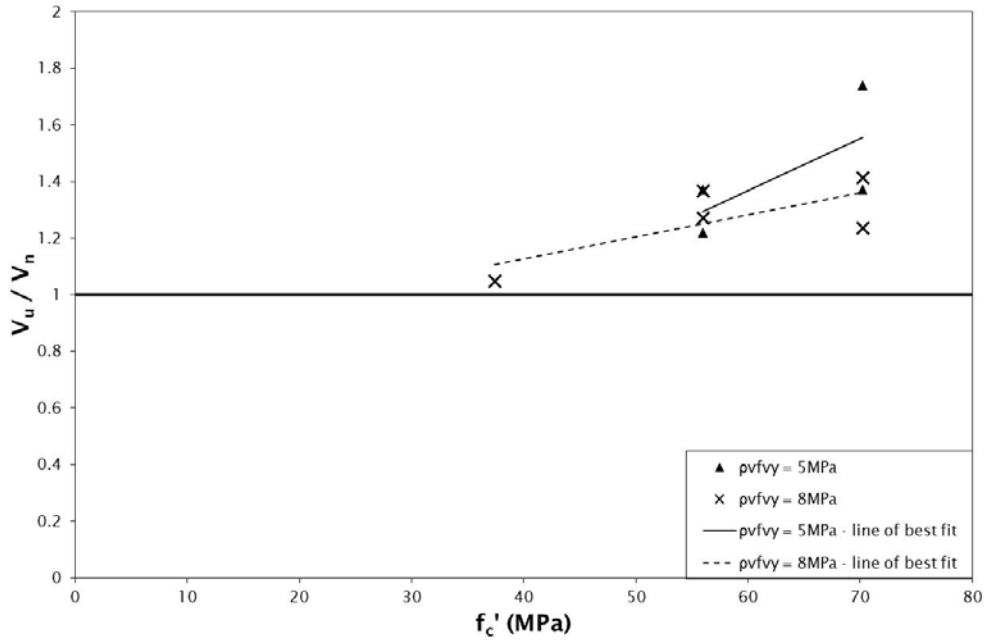

Figure 6.6 Influence of concrete compressive strength and transverse reinforcement on the accuracy of NZS 3101, without imposed limit, for nine experimental units reported in chapter 5

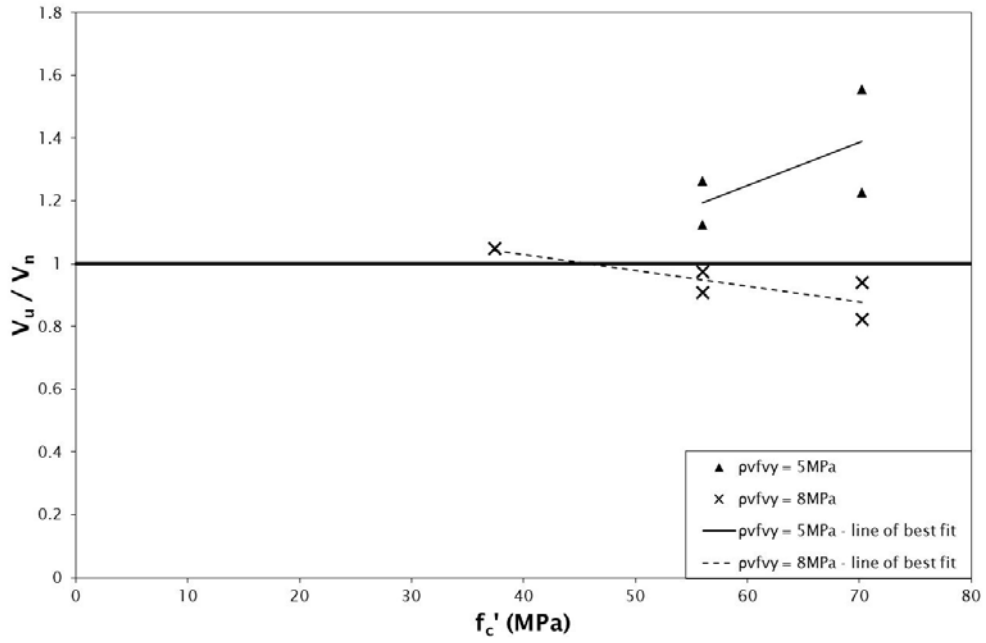

Two main conclusions were drawn from the analyses presented in this section, and from comparison of the analyses:

- The shear design provisions of NZS 3101 were deemed to inadequately account for the influence of concrete compressive strength on ultimate shear capacity, as evident by the increased inaccuracy of the predicted shear capacities as applied to increasing concrete compressive strengths.
- There was some validation of the necessity for the 8MPa limit imposed on allowable design shear capacity in the shear design provisions of NZS 3101, as evident by the non-conservative shear capacities predicted for units with a large quantity of transverse reinforcement ($\rho_v f_{vy}$ = 8MPa) when the 8MPa limit was not accounted for.

However, the 8MPa limit, combined with the observed inaccuracy of the provisions to account for the influence of concrete compressive strength, resulted in exceedingly conservative design shear capacities being calculated through the provisions of NZS 3101. It was observed that this conservatism is reduced if the absolute limit is increased to 10MPa, as shown in figure 6.7 – the implications of this for possible alternative limits in NZS 3101 are discussed in section 6.3.

Figure 6.7 Influence of concrete compressive strength and transverse reinforcement on the accuracy of NZS 3101, with absolute limit of 10MPa, for nine experimental units reported in chapter 5

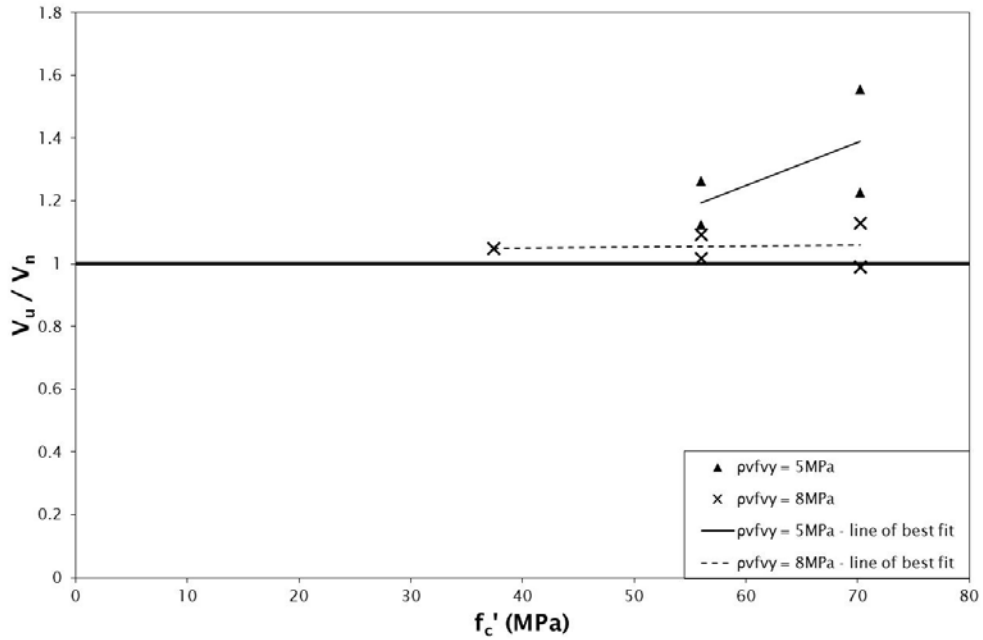

It was notable that for all three cases of limits presented for NZS 3101 in this section, the design standard provided significantly more conservative predictions of shear capacity for units with a lower quantity of transverse reinforcement ($\rho_v f_{vy}$ = 5MPa) than the units with a greater quantity of transverse reinforcement ($\rho_v f_{vy}$ = 8MPa). This trend indicated an inconsistency in the accuracy of shear capacity predictions with varying levels of transverse reinforcement, and therefore an inadequacy in accounting for the contribution of varying levels of transverse reinforcements.

6.2.3 CSA A23.3 and AASHTO LRFD

The accuracy of the shear design provisions in CSA A23.3 and AASHTO LRFD in predicting the ultimate shear capacity of the nine test units that failed in shear, as detailed in chapter 5, is shown in figure 6.8. The provisions were observed to be considerably non-conservative for the unit that had a concrete

compressive strength of 40MPa and a large quantity of transverse reinforcement ($\rho_v f_{vy}$ = 8MPa), but increasingly conservative for increasing concrete compressive strengths. This conservatism was noted to be more pronounced for units with a large quantity of transverse reinforcement ($\rho_v f_{vy}$ = 5MPa) than for units with a very large quantity of transverse reinforcement ($\rho_v f_{vy}$ = 8MPa) – one of the units that had a measured concrete compressive strength of 70.3MPa and a large quantity of transverse reinforcement was observed to fail at a shear capacity 3.88 times greater than that predicted by the provisions of CSA A23.3 and AASHTO LRFD.

Figure 6.8 Influence of concrete compressive strength and transverse reinforcement on the accuracy of CSA A23.3 and AASHTO LRFD for nine experimental units reported in chapter 5

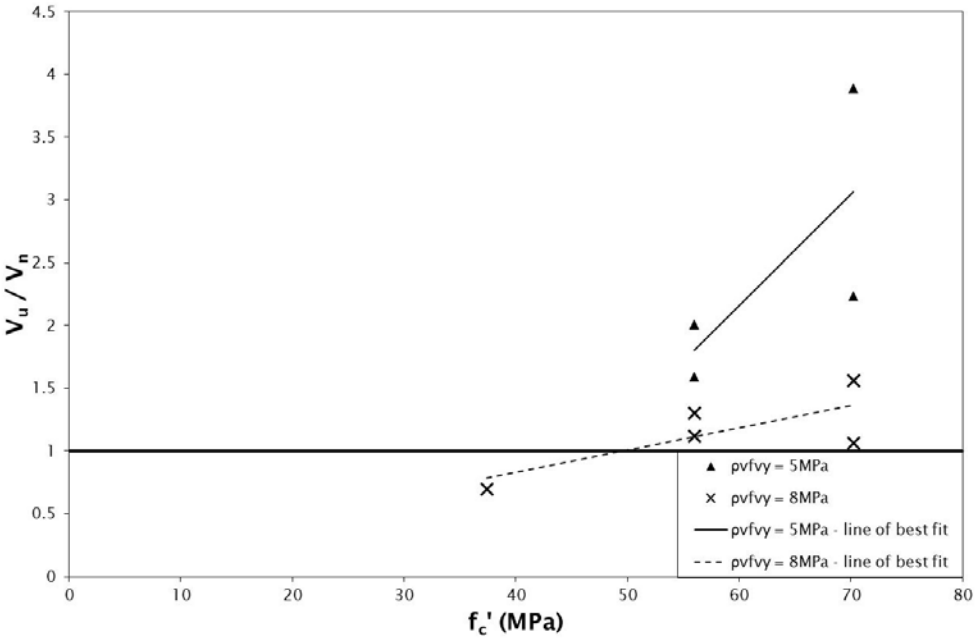

6.2.4 Eurocode 2 (EC2)

Figure 6.9 presents the influence of concrete compressive strength and quantity of transverse reinforcement on the accuracy of the shear design provisions of Eurocode 2 (EC2) in predicting the ultimate shear capacity of the nine test units. The performance of EC2 was observed to be similar to the performance of CSA A23.3 and AASHTO LRFD, as detailed in the previous section. Test units constructed of high-strength concrete (f_c' > 40MPa) failed at ultimate shear stresses considerably greater than predicted through the shear design provisions of EC2, and this trend was considerably more prominent for units constructed with a large quantity of transverse reinforcement ($\rho_v f_{vy}$ = 5MPa) than for units with a very large quantity of transverse reinforcement ($\rho_v f_{vy}$ = 8MPa). This conservatism was noted to increase with increasing concrete compressive strengths. The shear design provisions of EC2 provided a non-conservative prediction of ultimate shear capacity for the single unit constructed of normal-strength concrete (f_c' = 37.4MPa), which was observed to fail in shear as reported in chapter 5.

Figure 6.9 Influence of concrete compressive strength and transverse reinforcement on the accuracy of EC2 for nine experimental units reported in chapter 5

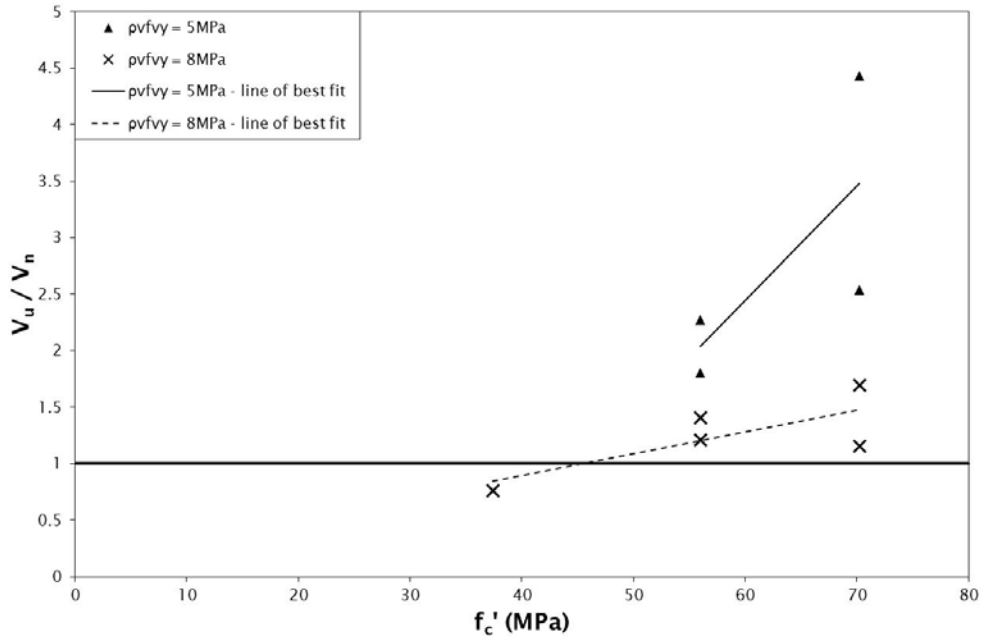

6.2.5 fib model code 2010

The accuracy of the shear design provisions of the fib model code in predicting the ultimate shear capacity of the nine test units that failed in shear, as detailed in chapter 5, is shown in figure 6.10. The provisions were observed to underestimate the shear capacity of all nine units, and particularly so for units constructed with high-strength concrete (f_c' > 40MPa). This conservatism was noted to be more pronounced for units with a large quantity of transverse reinforcement ($\rho_v f_{vy}$ = 5MPa) than for units with a very large quantity of transverse reinforcement ($\rho_v f_{vy}$ = 8MPa).

Figure 6.10 Influence of concrete compressive strength and transverse reinforcement on the accuracy of the fib model code for nine experimental units reported in chapter 5

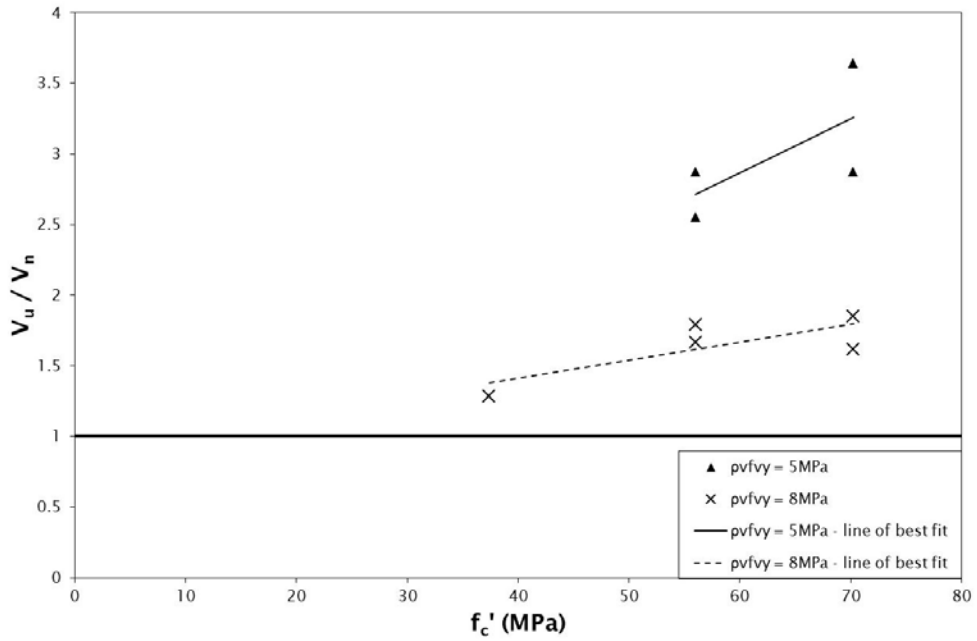

6.2.6 Comparison of limits in design standards

The performance of the nine test units that were observed to fail in shear, as reported in chapter 5, is plotted in figure 6.10, along with the maximum design shear capacity that is allowed in the six design standards discussed in chapter 3. It is important to note that the plotted shear capacities for the test units were experimentally obtained and do not represent maximum achievable capacities, but rather are shear capacities of test units designed to fail at shear capacities of approximately 8MPa and 10MPa. It can be seen from figure 6.10 that all nine of the test units were able to achieve ultimate shear capacities greater than allowed for by the limits imposed in NZS 3101. In particular, test units that had concrete compressive strengths of approximately 56MPa and 70MPa were all observed to considerably exceed the maximum shear capacity allowed by the limits within NZS 3101. The same observation was also true for the shear design provisions of ACI 318, and is a clear indicator that beams constructed with an appropriate quantity of transverse reinforcement and with sufficient concrete compressive strength are able to achieve shear capacities substantially greater than allowed for by the shear design provisions of both NZS 3101 and ACI 318.

However, while the ultimate shear capacity of the test unit with a concrete compressive strength of 37.4MPa exceeded the shear capacity allowed by the limits present in NZS 3101, the test unit did not achieve the design shear capacity of 10MPa. Therefore, it was concluded that while the NZS 3101's 8MPa limit on design shear capacity is excessively conservative, as evident by the performance of the high-strength concrete test units, the performance of the normal-strength concrete test unit supported the validity of the $0.2f_c'$ limit also imposed in NZS 3101. None of the test units were designed to fail at ultimate shear capacities greater than the limits of CSA A23.3, AASHTO LRFD or EC2 – assessment of the validity of limits found within the shear design provisions of other design standards was outside the scope of this project.

Figure 6.11 Performance of nine test units reported in chapter 5, compared with the shear stress limits of five international design standards

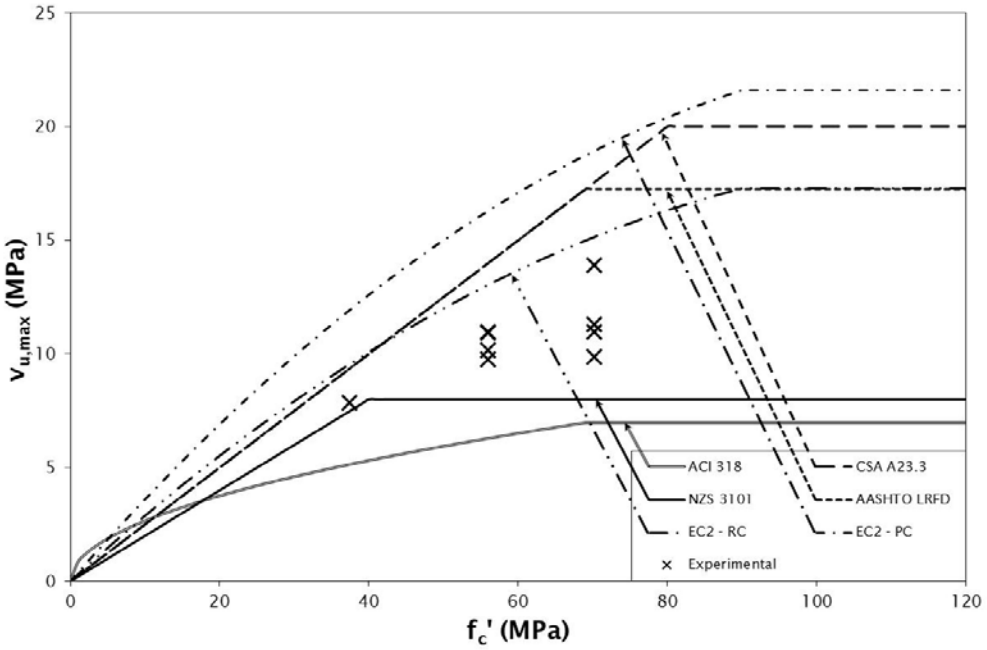

6.3 Alternative limits for NZS 3101

In section 6.2.2, the 8MPa limit on allowable design shear capacity in NZS 3101 was concluded to be excessively conservative in predicting the ultimate shear capacity of the nine test units detailed in chapter 5. It was also observed in section 6.2.2 that the accuracy of NZS 3101 was improved by increasing the absolute limit on allowable design shear capacity to 10MPa, without resulting in non-conservative shear capacity predictions. To further investigate possible alternative limits, the influence of a number of proposed limits on the accuracy of the design provisions was assessed using both the RC and PC shear test databases detailed in chapter 4 and the results of the experimental investigation detailed in chapter 5.

As the shear design provisions of NZS 3101 impose two limits ($0.2f_c'$ and 8MPa) on the design shear capacity of any concrete beam, alternative sets of limits were arrived at by variation of these two limits. The main alternative considered for the first limit was to increase the proportion of concrete compressive strength to $0.25f_c'$, to match the limit imposed in CSA A23.3 and AASHTO LRFD. A total of five sets of limits, including the existing limits in NZS 3101 and four alternative sets of limits, were assessed:

- minimum of $0.2f_c'$ and 8MPa (existing limits)
- minimum of $0.2f_c'$ and 10MPa
- $0.2f_c'$, with no absolute limit
- minimum of $0.25f_c'$ and 8MPa
- minimum of $0.25f_c'$ and 10MPa.

The alternative limits were assessed by evaluation of two primary parameters. The average ratio of measured to predicted shear capacity was used to assess the overall accuracy of the shear design provisions with the proposed limits, and the number of beams observed to fail at a lower than predicted shear capacity was used to identify the quantities of transverse reinforcement for which the proposed limit could be deemed non-conservative. These two parameters were evaluated for four ranges of transverse reinforcement quantity, using the RC and PC shear test databases and the results from the experimental investigation reported in chapter 5.

Three of the five sets of limits assessed in this section were discussed earlier in section 6.2.2, and the performance of those three limits with regards to the results of the experimental investigation was assessed. It was observed in section 6.2.2 that the shear design provisions of NZS 3101, with existing limits, provided considerably conservative ultimate shear capacities for test units with high-strength concrete (f_c' > 40MPa). Removal of the absolute limit on the design shear capacity of 8MPa resulted in non-conservative predictions of the shear capacities of test units that were constructed with high-strength concrete and had a very large quantity of transverse reinforcement ($\rho_v f_{vy} \geq$ 8MPa) – however, an increase of the absolute limit to 10MPa substantially improved the accuracy of the predicted shear capacities of those units without adversely affecting the accuracy of the predicted shear capacities for the remaining units. These findings are summarised in table 6.1 below.

For the proposed limits of $0.2f_c'$ and 10MPa, one the five test units that contained a very large quantity of transverse reinforcement ($\rho_v f_{vy} \geq$ 8MPa) failed at a measured shear capacity lower than predicted by the modified design provisions. However, the ratio of measured to predicted shear capacity for this unit was 0.99, and the predicted shear capacity was deemed to not be unduly non-conservative. An increase of the limit to $0.25f_c'$ with an absolute limit of 8MPa was observed to not provide a significant improvement in accuracy. Increasing the absolute limit to 10MPa in this case was found to provide non-conservative shear

capacity predictions for two of the five test units that had a very large quantity of transverse reinforcement ($\rho_v f_{vy} \geq$ 8MPa), with one such unit observed to fail at an ultimate shear capacity that was 16% lower than predicted.

Table 6.1 Assessment of proposed NZS 3101 shear capacity limits for nine experimental test units

		5MPa < $\rho_v f_{vy}$ < 8MPa	$\rho_v f_{vy} \geq$ 8MPa
0.2f_c' & 8MPa	$\left(\frac{V_u}{V_n}\right)ave$	1.425	1.266
	$n\left(\frac{V_u}{V_n}<1\right)$	0	0
0.2f_c' & 10MPa	$\left(\frac{V_u}{V_n}\right)ave$	1.293	1.055
	$n\left(\frac{V_u}{V_n}<1\right)$	0	1
0.2f_c'	$\left(\frac{V_u}{V_n}\right)ave$	1.293	0.921
	$n\left(\frac{V_u}{V_n}<1\right)$	0	4
0.25f_c' & 8MPa	$\left(\frac{V_u}{V_n}\right)ave$	1.425	1.253
	$n\left(\frac{V_u}{V_n}<1\right)$	0	1
0.25f_c' & 10MPa	$\left(\frac{V_u}{V_n}\right)ave$	1.293	1.013
	$n\left(\frac{V_u}{V_n}<1\right)$	0	2

Table 6.2 shows that for beams in the RC database, increasing the absolute limit to 10MPa improved the accuracy of the shear capacity predictions for units with a large (5MPa < $\rho_v f_{vy}$ < 8MPa) and very large ($\rho_v f_{vy} \geq$ 8MPa) quantity of transverse reinforcement. This improvement in accuracy was also observed for limits of 0.25f_c', and was particularly pronounced for the combined limits of 0.25f_c' and 10MPa. These improvements in accuracy were achieved without compromising the conservatism inherent in the design provisions. It was noted that omission of an absolute limit did not yield an improvement in accuracy over the combined limits of 0.2f_c' and 10MPa, and therefore results from the analysis of beams in the RC database could not be used to support removal of an absolute limit on ultimate shear capacity.

Table 6.2 Assessment of proposed shear capacity limits for beams in the RC database

		$\rho_v f_{vy}$ < 2MPa (# of units: 145)	2MPa < $\rho_v f_{vy}$ < 5MPa (# of units: 8)	5MPa < $\rho_v f_{vy}$ < 8MPa (# of units: 3)	$\rho_v f_{vy}$ ≥ 8MPa (# of units: 4)
0.2f_c' & 8MPa	$\left(\frac{V_u}{V_n}\right)ave$	1.411	1.324	1.379	1.511
	$n\left(\frac{V_u}{V_n}<1\right)$	19	0	0	0
0.2f_c' & 10MPa	$\left(\frac{V_u}{V_n}\right)ave$	1.411	1.324	1.370	1.408
	$n\left(\frac{V_u}{V_n}<1\right)$	19	0	0	0
0.2f_c'	$\left(\frac{V_u}{V_n}\right)ave$	1.411	1.324	1.370	1.408
	$n\left(\frac{V_u}{V_n}<1\right)$	19	0	0	0
0.25f_c' & 8MPa	$\left(\frac{V_u}{V_n}\right)ave$	1.411	1.324	1.281	1.424
	$n\left(\frac{V_u}{V_n}<1\right)$	19	0	0	0
0.25f_c' & 10MPa	$\left(\frac{V_u}{V_n}\right)ave$	1.411	1.324	1.271	1.247
	$n\left(\frac{V_u}{V_n}<1\right)$	19	0	0	0

The accuracy of the shear design provisions in NZS 3101 with the five sets of limits assessed in this section for beams in the PC database is presented in table 6.3. The shear design provisions of NZS 3101, with the existing limits on design shear capacity, were found to provide excessively conservative predictions of shear capacity for beams with large (5MPa < $\rho_v f_{vy}$ < 8MPa) and very large ($\rho_v f_{vy}$ ≥ 8MPa) quantities of transverse reinforcement. An increase of the absolute limit to 10MPa resulted in improved accuracy for all beams except those containing the lowest quantity of transverse reinforcement ($\rho_v f_{vy}$ < 2MPa). Increasing the primary limit from 0.2f_c' to 0.25f_c' resulted in improved accuracy for all ranges of transverse reinforcement quantity, and increasing the absolute limit to 10MPa resulted in further improvements in accuracy of shear capacity prediction. All of the four proposed alternative sets of limits assessed in this section resulted in a greater number of non-conservative predictions of shear capacity, although not significantly so. As with the analysis of beams in the RC database, it was noted that omission of an absolute limit did not yield an improvement in accuracy over the combined limits of 0.2f_c' and 10MPa, and therefore results from the analysis of beams in the PC database could not be used to support removal of an absolute limit on ultimate shear capacity.

Table 6.3 Assessment of proposed shear capacity limits for beams in the PC database

		$\rho_v f_{vy}$ < 2MPa (# of units: 90)	2MPa < $\rho_v f_{vy}$ < 5MPa (# of units: 49)	5MPa < $\rho_v f_{vy}$ < 8MPa (# of units: 7)	$\rho_v f_{vy}$ ≥ 8MPa (# of units: 18)
0.2f_c' & 8MPa	$\left(\frac{V_u}{V_n}\right)ave$	1.206	1.144	1.380	1.587
	$n\left(\frac{V_u}{V_n}<1\right)$	27	17	1	0
0.2f_c' & 10MPa	$\left(\frac{V_u}{V_n}\right)ave$	1.206	1.118	1.253	1.549
	$n\left(\frac{V_u}{V_n}<1\right)$	27	21	1	0
0.2f_c'	$\left(\frac{V_u}{V_n}\right)ave$	1.206	1.118	1.253	1.549
	$n\left(\frac{V_u}{V_n}<1\right)$	27	21	1	0
0.25f_c' & 8MPa	$\left(\frac{V_u}{V_n}\right)ave$	1.203	1.129	1.376	1.424
	$n\left(\frac{V_u}{V_n}<1\right)$	27	18	1	1
0.25f_c' & 10MPa	$\left(\frac{V_u}{V_n}\right)ave$	1.203	1.092	1.123	1.269
	$n\left(\frac{V_u}{V_n}<1\right)$	27	22	2	2

The effect on the accuracy of the shear design provisions of NZS 3101 of increasing the absolute limit on design shear capacity from 8MPa to 10MPa was illustrated earlier in figure 6.11 for the nine experimental test units, and in figure 6.12 (following) for the mean values when combining the RC database, the PC database, and the test units. It is clear from these figures that an increase of the limit to 10MPa significantly improves the accuracy of the shear design provisions in NZS 3101 for beams constructed of high-strength concrete and containing large quantities of transverse reinforcement. This improvement would result in more efficient and economical designs for concrete bridge beams being possible.

Figure 6.12 Performance of NZS 3101 shear design provisions with existing and proposed absolute limits for nine experimental test units reported in chapter 5

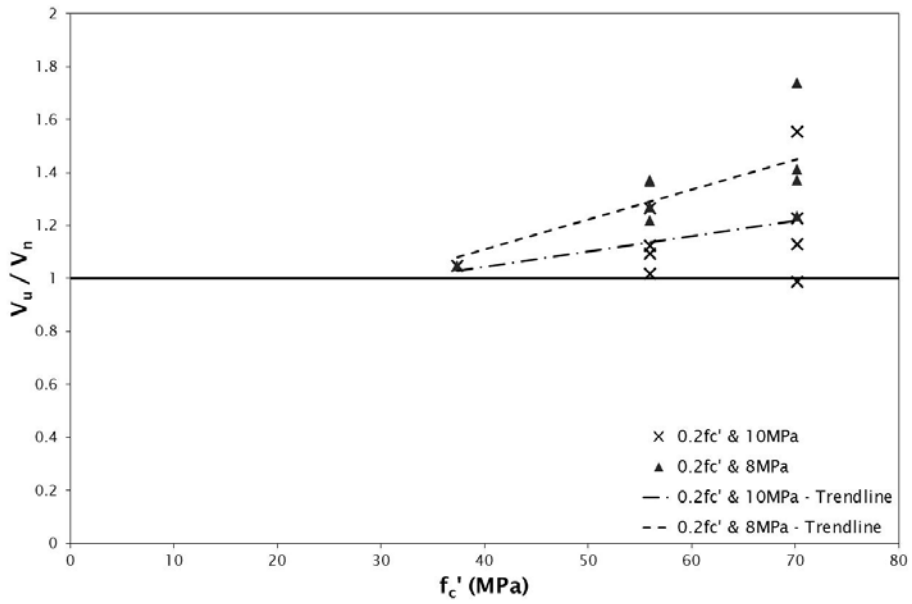

Figure 6.13 Performance of NZS 3101 shear design provisions with existing and proposed absolute limits for all previous relevant experimental testing

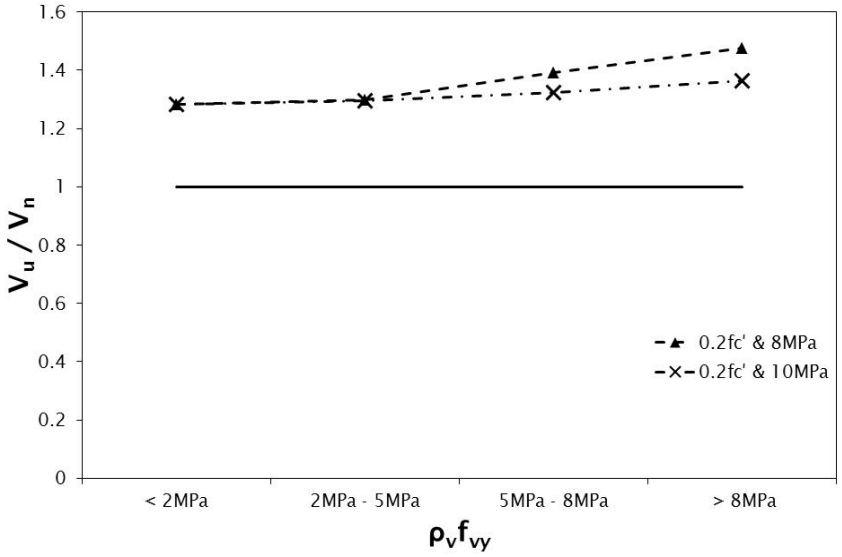

6.4 Conclusions

This chapter presented a number of analyses that were conducted using the results of the experimental investigation presented in the previous chapter. A comparative analysis of the performance of the nine experimental test units known to fail in shear supported the need for a limit on the nominal design shear capacity, but the performance of the high-strength concrete test units indicated that an absolute limit of 8MPa is overly conservative.

An analysis of the nine test units using the shear design provisions of the six international design standards discussed in chapter 3, with and without absolute limits, was detailed earlier in section 6.2. It was observed that using ACI 318 and NZS 3101 with their existing limits provided conservative predictions of shear capacity for the test units, while omission of the absolute limits in these two standards resulted in non-conservative predictions of shear capacity. The shear design provisions of CSA A23.3, AASHTO LRFD, EC2 and the fib model code all provided overly conservative predictions of shear capacity for the high-strength concrete test units, and this conservatism was more pronounced for units constructed with large quantities of transverse reinforcement ($\rho_v f_{vy}$ = 5MPa).

Finally, a statistical analysis of the effect of four alternatives to the existing limits imposed on shear capacity in NZS 3101 was conducted using the results of the experimental investigation, the beams in the RC database, and the beams in the PC database. It was concluded that the existing limits on design shear capacity in the provisions of NZS 3101 could be modified to 'the minimum of $0.2f_c'$ and 10MPa' to improve the accuracy of the design provisions for beams that had large quantities of transverse reinforcement, without compromising the conservatism inherent in any design standard for safety. This conclusion was guided by the non-conservative predictions of ultimate shear capacity allowed by the other proposed alternative limits for the experimental test units. The proposed increase of the absolute limit on design shear capacity to 10MPa would both improve the accuracy of the shear design provisions of NZS 3101 and allow for more efficient design of concrete bridge beams than allowed by the 8MPa limit currently imposed by the design standard. In particular, the revised 10MPa limit on shear capacity would result in the threshold concrete compressive strength for which an elevated shear capacity could be

accounted for to increase from f_c' = 40MPa to f_c' = 50MPa. The proposed change to limits on design shear capacity would only affect beams containing large quantities of transverse reinforcement, as beams with low or moderate quantities of transverse reinforcement cannot exceed the existing maximum design shear capacity.

7 Conclusions and recommendations

The primary objective of the research presented in this report was to assess the validity of limits imposed by the shear design provisions of NZS 3101 on concrete beams, with a particular focus on the influence of these limits on the design of high-strength concrete beams. A critique of the purpose of these limits in relation to concrete shear behaviour, and a critique of the manner in which other international design standards achieve this purpose, were also central objectives for this project.

By examination of the various mechanisms that influence the behaviour of concrete beams when subjected to shear loading, and of the interaction between those mechanisms, it was clear that the phenomenon of concrete shear behaviour continues to be difficult to understand. A number of parameters were identified as influential to the response of a concrete beam when subjected to shear loading, including concrete compressive strength, beam depth, shear a/d ratio, and quantities of transverse reinforcement and longitudinal reinforcement. The various behavioural models developed to predict the response of concrete beams when subjected to shear loading accounted for these parameters through markedly different methods, further emphasising the deficiency in understanding of this phenomenon. Due to this acknowledged deficiency in existing models, all current design standards were found to rely, to various extents, on experimentally determined empirical relations. Reliance on empirical data is only adequate for the range of values of each parameter over which the empirical relationships were developed, and it is for this reason that a number of limits, including the 8MPa limit on allowable shear capacity found in NZS 3101, are imposed on concrete shear design provisions.

This report also examined the shear design provisions of six international design standards that utilised four considerably different approaches to the design of a concrete beam for shear loading. Two of the provisions present unified approaches for RC and PC beam shear design, while the other two provisions provide separate specifications for RC and PC beams. The six design standards differ not only in the approaches they employ for shear design, but also in the limits imposed by each standard on the allowable shear capacities. ACI 318 and EC2 both eschew specifying a direct limit on nominal design shear capacity, although EC2 does impose limits on concrete compressive strength, inclination angle of compression struts, and effective area of transverse reinforcement, which indirectly limit the predicted ultimate shear capacity. Meanwhile, CSA A23.3, AASHTO LRFD and NZS 3101 all limit the maximum allowable shear capacity to a proportion of the concrete compressive strength, which is 0.25 for the first two standards and 0.2 for NZS 3101. However, NZS 3101 also specifies an absolute limit of 8MPa for the maximum allowable shear capacity for all concrete beams. The maximum design shear capacities allowed in NZS 3101 are significantly lower than those allowed in CSA A23.3, AASHTO LRFD and EC2, and markedly lower for high-strength concrete beams. This trend was also found to hold true for two other design standards that were briefly investigated: CHBDC and AS 5100.5.

Two databases of experimental results were compiled to assess the approaches employed for concrete shear design in the six design standards, with one database focused on RC beams and the other focused on PC beams. The databases demonstrated the strong over-representation in previous experimental research of normal-strength concrete beams with low quantities of transverse reinforcement.

The RC and PC databases were individually analysed for the influence of five design parameters on measured ultimate shear capacity. The measured ultimate shear capacity of beams in the RC database was observed to increase with increasing values of concrete compressive strength, longitudinal reinforcement ratio, and transverse reinforcement ratio, while decreasing for increasing values of beam effective depth and shear a/d ratio. For beams in the PC database, the measured ultimate shear capacity of a beam was observed to increase for increasing values of concrete compressive strength, beam effective depth,

longitudinal reinforcement ratio and transverse reinforcement ratio, while decreasing for increasing ratios of shear a/d.

The accuracy of the six design standards assessed in this report was evaluated and the influence of six design parameters on the accuracy of each standard was identified using the RC and PC databases. EC2 was found to be the most conservative of the six design standards for the prediction of the shear capacity of concrete beams; CSA A23.3 and AASHTO LRFD were found to be the most accurate for predicting the shear capacity of RC beams; and NZS 3101 was found to be the most accurate for predicting the shear capacity of PC beams. However, a third of the beams in the RC database exhibited ultimate shear capacities lower than predicted by CSA A23.3 and AASHTO LRFD, and 40% of the beams in the PC database failed at ultimate shear capacities lower than predicted by NZS 3101. Therefore it was concluded that the ability of NZS 3101 to accurately predict the ultimate shear capacity of PC beams comes at the cost of reasonable conservatism. An absence of any discernible influence of ultimate shear capacity on the accuracy of the design provisions for ultimate shear capacities greater than 8MPa was also observed, despite the omission of the 8MPa limit on allowable shear capacity during this evaluation. This observation led to the conclusion that the removal of the 8MPa absolute limit on the allowable shear capacity of concrete beams would not unduly affect the integrity of the design provisions in NZS 3101.

To further assess the validity of the 8MPa absolute limit imposed in NZS 3101 on design shear capacity, a series of 12 single-tee PC units were designed to fail at shear capacities at or greater than 8MPa. The test units were designed with a variety of concrete compressive strengths and varying quantities of transverse reinforcement, to remedy a paucity of previous experimental research on high-strength concrete beams that had a high ultimate shear capacity. A comparative analysis of the performance of the nine experimental test units known to fail in shear supported the need for a limit on the nominal design shear capacity, but the performance of the high-strength concrete test units indicated that an absolute limit of 8MPa is overly conservative. The shear design provisions of NZS 3101, with its existing limits, provided conservative predictions of shear capacity for the test units, while omission of the absolute limits resulted in non-conservative predictions of shear capacity. A similar trend was observed in an analysis of ACI 318, while the shear design provisions of CSA A23.3, AASHTO LRFD and EC2 all provided overly conservative predictions of shear capacity for the high-strength concrete test units. NZS 3101 provided significantly more conservative predictions of shear capacity for units that had a lower amount of transverse reinforcement ($\rho_v f_{vy}$ = 5MPa) than the units that had greater quantities of transverse reinforcement ($\rho_v f_{vy}$ = 8MPa). This trend indicated an inconsistency in the accuracy of shear capacity predictions with varying levels of transverse reinforcement, and therefore an inadequacy of accounting for the contribution of varying levels of transverse reinforcements.

Four alternatives to the existing limits imposed in NZS 3101 on shear capacity were proposed and analysed, using the results of the experimental investigation, the beams in the RC database, and the beams in the PC database. It was concluded that the existing absolute limit on design shear capacity in the provisions of NZS 3101 could be increased to 10MPa to improve the accuracy of the design provisions for beams that had a large quantities of transverse reinforcement, without compromising the conservatism inherent in any design standard for safety. This conclusion was guided by the non-conservative predictions of ultimate shear capacity allowed by the other proposed alternative limits for the experimental test units. The proposed increase of the absolute limit on design shear capacity to 10MPa would both improve the accuracy of the shear design provisions of NZS 3101 and allow for more efficient design of concrete bridge beams than permitted by the 8MPa limit currently imposed by the design standard. In particular, the revised 10MPa limit on shear capacity would result in the threshold concrete compressive strength for which an elevated shear capacity could be accounted for to increase from f_c' = 40MPa to f_c' = 50MPa.

7.1 Recommendations

- The main recommendation resulting from the work presented in this report is that the limits imposed in NZS 3101 on the shear capacity of concrete beams should be modified to 'the minimum of $0.2f_c'$ and 10MPa', allowing for more efficient design of high-strength concrete beams containing large quantities of transverse reinforcement. Only beams with large quantities of transverse reinforcement would be affected by this recommendation, as beams containing less transverse reinforcement are not currently constrained by the existing limits on design shear capacity.
- If the proposed absolute limit of 10MPa is to be raised further, an extensive series of experimental testing will be required, focusing on the performance of concrete beams that have a concrete compressive strength greater than 50MPa and a predicted shear capacity significantly greater than 10MPa.
- An investigation into the NZS 3101 method of accounting for the contribution of varying levels of transverse reinforcement to shear capacity is also recommended, as the design standard was observed to significantly vary in conservatism with varying quantities of transverse reinforcement.

8 References

American Association of State Highway and Transportation Officials (AASHTO) (2012) *AASHTO LRFD bridge design specifications*. Washington, DC: American Association of State Highway and Transportation Officials.

American Concrete Institute (ACI) (2011) Building code requirements for structural concrete. *ACI 318-11*. Farmington Hills, MI: American Concrete Institute.

American Society of Civil Engineers (ASCE-ACI) (1998) Recent approaches to shear design of structural concrete: by ASCE-ACI committee 445 on shear and torsion. *Journal of Structural Engineering 124*: 1375–1417.

Baumann, T (1972) Zur frage der netzbewehrung von flachentragwerken. *Der Bauingenieur 46*: 367–377.

Bazant, ZP and P Gambarova (1980) Rough cracks in reinforced concrete. *ASCE Journal Structural Division 106*: 819–842.

Bazant, ZP and MT Kazemi (1991) Size effect on diagonal shear failure of beams without stirrups. *ACI Structural Journal 88*: 268–276.

Bazant, ZP and JK Kim (1984) Size effect in shear failure of longitudinally reinforced beams. *Journal of the American Concrete Institute 81*: 456–468.

BECA and OPUS (2008) Standard precast concrete bridge beams. *NZ Transport Agency research report 364*. 57pp.

CEN (European Committee for Standardization) (2005) Design of concrete structures – Concrete bridges – Design and detailing rules. *Eurocode 2 (EC2).* Brussels: European Committee for Standardization.

Collins, MP, D Mitchell, P Adebar and FJ Vecchio (1996) A general shear design method. *ACI Structural Journal 93*: 36–45.

CSA (Canadian Standards Association) (2004) Design of concrete structures. *A23.3-04.* Mississauga: Canadian Standards Association.

Day, RL (1994) Strength measurement of concrete using different cylinder sizes: a statistical analysis. *Cement, Concrete, and Aggregates 16*: 21–30.

Elias, IS and JF Robert (2009) Influence of flexural reinforcement on shear strength of prestressed concrete beams. *ACI Structural Journal 106*: 60–68.

Elzanaty, AH, AH Nilson and FO Slate (1986) Shear capacity of prestressed concrete beams using high-strength concrete. *Journal of the American Concrete Institute 83*: 359–368.

Fib (International Federation for Structural Concrete) (2010) *fib Bulletin 66: model code.* Lausanne, Switzerland: federation internationale du beton (fib).

Gray, A, P Gaby, G Brown, D Kirkcaldie, R Cato and P Sweetman (2003) New standard precast concrete bridge beams: stage 1 – identification of New Standard beam shapes. *Transfund New Zealand research report 252.* 70pp.

Hsu, TTC (1988) Softened truss model theory for shear and torsion. *ACI Structural Journal 85*: 624–635.

Hsu, TTC (1994) Unified theory of reinforced concrete – a summary. *Structural Engineering and Mechanics 2*: 1–16.

Jelić, I, MN Pavlović and MD Kotsovos (1999) Study of dowel action in reinforced concrete beams. *Magazine of Concrete Research 51*: 131–141.

Kim, KS (2004) *Shear behavior of reinforced concrete beams and prestressed concrete beams.* Ph.D. thesis, University of Illinois at Urbana-Champaign.

Kupfer, H (1964) Erweiterung der morschschen fachwerkanalogie mit hilfe des prinzips vom minimum formanderungarbeit (Extension to the truss-analogy of morsch using the principle of minimum potential energy). *CEB Bulletin d'Information.* Paris: federation internationale du beton (fib).

Lyngberg, BS (1976) Ultimate shear resistance of partially prestressed reinforced concrete i-beams. *Journal of the American Concrete Institute 73*: 214–222.

Mehta, PK and PJM Monteiro (2006) *Concrete: microstructure, properties, and materials*. New York: McGraw-Hill.

Mörsch, E (1902) *Der eisenbetonbau, seine anwendung und theorie.* Neustadt a. d. Haardt, Germany: Wayss and Freytag, AG, Im Selbstverlag der Firma.

Pang, XB and TTC Hsu (1995) Behavior of reinforced concrete membrane elements in shear. *ACI Structural Journal 92*: 665–679.

Ritter, W (1899) *Die bauweise hennebique.* Zurich: Schweizerishe Bauzeitung.

Smith, KN and AS Vantsiotis (1982) Shear strength of deep beams. *Journal of the American Concrete Institute 79*: 201–213.

So, KO and BL Karihaloo (1993) Shear capacity of longitudinally reinforced beams – a fracture mechanics approach. *ACI Materials Journal 90*: 591–600.

Standards New Zealand (SNZ) (2006) Concrete structures standard: part 1 – the design of concrete structures. *NZS 3101:2006*. Wellington: Standards New Zealand.

Sun, S (2007) *Shear behavior and capacity of large scale pretressed high strength concrete bulb-tee girders.* PhD, Civil Engineering, University of Illinois at Urbana-Champaign.

Tan, KH, FK Kong, S Teng and L Guan (1995) High-strength concrete deep beams with effective span and shear span variations. *ACI Materials Journal 92*: 395–405.

Transit New Zealand (TNZ) (2003) *Transit New Zealand bridge manual.* Wellington: Transit New Zealand.

Vecchio, F and MP Collins (1981) Stress-strain characteristics of reinforced concrete in pure shear. Pp211–225 in *Reports of the working commissions. RILEM* (Eds). Delft: International Association for Bridge and Structural Engineering (IABSE).

Vecchio, F and MP Collins (1986) Modified compression-field theory for reinforced concrete elements subjected to shear. *Journal of the American Concrete Institute 83*: 219–231.

Vecchio, F and MP Collins (1993) Compression response of cracked reinforced concrete. *ASCE Journal of Structural Engineering 119*: 3590–3610.

Wagner, H (1929) Flat sheet metal girder with very thin metal web. *Zeitschrift fur Flugtechnik Motorlurftschiffahrt 20*: 200–207, 227–233, 256–262, 279–284.

Walraven, JC (1981) Fundamental analysis of aggregate interlock. *Journal of Structural Division ASCE 108*: 2245–2270.

Yang, KH and SF Ashour (2008) Code modelling of reinforced-concrete deep beams. *Magazine of Concrete Research 60*: 441–454.

Appendix A Shear test databases

The notation used in the RC database and PC database, presented in tables A.2 and A.3 respectively, are shown in table A.1.

Table A.1 Notation used in RC and PC databases

Classification	Symbol	Content
Section geometry	Shape R/T/I	Cross-sectional shape (R=rectangular, T=tee-shaped, I=i-shaped)
	h	Overall beam depth
	b_w	Beam web width
	d	Beam effective depth
	b_{top}	Width of top flange
	b_{bot}	Width of bottom flange
	t_{top}	Thickness of top flange
	t_{bot}	Thickness of bottom flange
Loading geometry	L	Span length
	a/d	Shear span-to-depth ratio
	Loading configuration	Support & loading conditions (SS=simply supported, SE=continuous beam, FF=fixed ends, PL=point load, UDL=uniformly distributed load
Concrete properties	f_c'	Concrete compressive strength
	a_g	Maximum aggregate size
Prestressed reinforcement	A_{ps}	Area of prestressed longitudinal reinforcement
	f_{py}	Tensile yield strength of prestressed reinforcement
	f_{pu}	Tensile ultimate strength of prestressed reinforcement
	ρ_{pl}	Prestressed reinforcement ratio, $A_{ps}/b_w d$
	f_{se}	Prestress in prestressed reinforcement at time of testing, after all losses
Longitudinal reinforcement	A_s	Area of nonprestressed longitudinal reinforcement
	f_y	Tensile yield strength of nonprestressed longitudinal reinforcement
	ρ_l	Longitudinal reinforcement ratio, $A_s/b_w d$
Transverse reinforcement	A_v	Area of transverse reinforcement
	f_{vy}	Tensile yield strength of transverse reinforcement
	s	Centre-to-centre spacing of transverse reinforcement
	ρ_v	Transverse reinforcement ratio, $A_v/b_w s$
Capacity	V_u	Measured shear capacity
	V_n - ACI	Predicted shear capacity using the design provisions of ACI 318
	V_n - NZS	Predicted shear capacity using the design provisions of NZS 3101
	V_n - CSA	Predicted shear capacity using the design provisions of CSA A23.3 and AASHTO LRFD
	V_n – EC2	Predicted shear capacity using the design provisions of EC2
	V_n - fib	Predicted shear capacity using the design provisions of the fib model code

Table A-2: Reinforced Concrete Beam Database

Reference Information				Section Geometry							Loading Geometry			Concrete Properties		Longitudinal Reinforcement			Transverse Reinforcement				Capacity					
#	Author and Notes	Year	Beam Name	Shape R/T/I	h (mm)	b_w (mm)	d (mm)	b_{top} (mm)	b_{bot} (mm)	t_{top} (mm)	t_{bot} (mm)	L (mm)	a/d	Loading Geometry	f_c' (MPa)	a_g (mm)	A_s (mm^2)	f_y (MPa)	ρ_l (%)	A_v (mm^2)	f_{vy} (MPa)	s (mm)	ρ_v (%)	V_u (kN)	V_n - ACI (kN)	Vn - NZS (kN)	Vn - CSA (kN)	Vn - EC2 (kN)	V_n - fib (kN)
1	Adebar	1996	ST4	R	309.88	359.92	277.88	0	0	0	0	1600.2	2.88	FF-END	49.29	19.05	1567.74	535.72	1.95	103.23	459.88	314.96	0.11	158.18	153.80	180.31	171.76	57.96	141.44
2	Collins	1996	ST5	R	309.88	359.92	277.88	0	0	0	0	1600.2	2.88	FF-END	49.29	19.05	1567.74	535.72	1.95	103.23	459.88	193.04	0.18	168.99	180.25	206.76	202.32	92.96	173.98
3		1996	ST6	R	309.88	359.92	277.88	0	0	0	0	1600.2	2.88	FF-END	49.29	19.05	1567.74	535.72	1.95	103.23	459.88	124.46	0.28	230.11	217.90	244.42	220.61	131.04	188.99
4		1996	ST7	R	309.88	359.92	277.88	0	0	0	0	1600.2	2.88	FF-END	49.29	19.05	1567.74	535.72	1.95	103.23	459.88	124.46	0.28	275.12	217.90	244.42	201.33	122.29	166.28
5		1996	ST18	R	309.88	359.92	277.88	0	0	0	0	1600.2	2.88	FF-END	49.79	19.05	1567.74	535.72	1.95	103.23	459.88	172.72	0.20	246.30	188.79	215.50	178.00	92.10	145.57
6		1996	ST19	R	309.88	359.92	277.88	0	0	0	0	1600.2	2.88	FF-END	50.79	19.05	1567.74	535.72	1.95	103.23	459.88	172.72	0.20	201.42	189.80	215.80	198.09	98.73	167.96
7	Ahmed	1994	LNW-3	R	254.00	127.00	215.90	0	0	0	0	1295.4	3	SS-1PL	44.61	12.7	567.74	420.58	2.07	64.52	324.05	101.60	0.49	63.30	73.83	77.04	86.79	59.38	71.49
8	Xie	1994	LHW-3	R	254.00	127.00	198.12	0	0	0	0	1193.8	3	SS-1PL	89.29	12.7	1135.48	420.58	4.54	64.52	324.05	99.06	0.51	92.43	82.31	73.50	103.21	60.39	65.94
9	Yu	1994	LNW-3	R	254.00	127.00	198.12	0	0	0	0	1193.8	3	SS-1PL	88.18	12.7	1135.48	420.58	4.54	64.52	324.05	76.20	0.65	107.02	94.64	86.04	115.09	75.93	74.92
10		1994	LNW-3	R	254.00	127.00	198.12	0	0	0	0	1193.8	3	SS-1PL	86.94	12.7	1135.48	420.58	4.54	64.52	324.05	63.50	0.78	120.68	105.27	96.92	124.52	88.35	81.36
11		1994	LHW-3	R	254.00	127.00	198.12	0	0	0	0	1574.8	4	SS-1PL	82.94	12.7	1135.48	420.58	4.54	64.52	324.05	99.06	0.51	94.79	79.44	73.50	92.64	56.91	57.74
12	Angelakos	2001	DBO530M	R	1000.00	299.97	925.07	0	0	0	0	5410.2	2.92	SS-1PL	31.99	9.906	1400.00	550.20	0.50	70.97	508.14	299.72	0.08	263.02	343.67	271.40	291.00	124.10	253.93
13	Bentz	2001	DB120M	R	1000.00	299.97	925.07	0	0	0	0	5410.2	2.92	SS-1PL	20.99	9.906	2799.99	550.20	1.01	141.94	508.14	599.44	0.08	282.02	309.40	296.11	358.73	153.70	316.83
14	Collins	2001	DBO530M	R	1000.00	299.97	925.07	0	0	0	0	5410.2	2.92	SS-1PL	37.99	9.906	2799.99	550.20	1.01	70.97	508.14	299.72	0.08	276.99	372.10	359.91	433.17	154.40	390.90
15		2001	DBO530M	R	1000.00	299.97	925.07	0	0	0	0	5410.2	2.92	SS-1PL	64.98	9.906	2799.99	550.20	1.01	70.97	508.14	299.72	0.08	451.98	447.32	396.51	397.58	132.30	339.59
16		2001	DBO530M	R	1000.00	299.97	925.07	0	0	0	0	5410.2	2.92	SS-1PL	79.98	9.906	2799.99	550.20	1.01	70.97	508.14	299.72	0.08	395.00	482.28	396.51	461.99	139.04	377.30
17	Ceruti, Marti	1987	CM2_B	TI	899.92	150.11	824.99	450.09	899.92	150.11	187.45	7493	3.03	SE-UDL	44.69		6199.99	435.06	5.01	200.00	550.89	104.14	1.28	1264.99	1026.20	1013.57	1004.43	923.33	1023.47
18	Clark	1951	D2-6	R	381.00	152.40	314.20	0	0	0	0	3048	2.43	SS-2PL	29.51		1632.25	320.61	3.42	141.94	330.95	152.40	0.61	168.41	145.56	141.06	182.03	137.32	141.88
19		1951	D2-7	R	381.00	152.40	314.20	0	0	0	0	3048	2.43	SS-2PL	28.41		1632.25	320.61	3.42	141.94	330.95	152.40	0.61	157.29	144.85	140.23	185.00	139.42	146.01
20		1951	D2-8	R	381.00	152.40	314.20	0	0	0	0	3048	2.43	SS-2PL	26.13		1632.25	320.61	3.42	141.94	330.95	152.40	0.61	168.41	143.36	138.45	179.39	137.32	138.81
21		1951	D4-1	R	381.00	152.40	314.20	0	0	0	0	3048	2.43	SS-2PL	27.37		1632.25	320.61	3.42	141.94	330.95	190.50	0.49	168.41	124.82	120.06	152.92	109.86	114.13
22		1951	D4-2	R	381.00	152.40	314.20	0	0	0	0	3048	2.43	SS-2PL	25.65		1632.25	320.61	3.42	141.94	330.95	190.50	0.49	157.29	123.67	118.70	154.85	111.54	116.80
23		1951	D4-3	R	381.00	152.40	314.20	0	0	0	0	3048	2.43	SS-2PL	22.06		1632.25	320.61	3.42	141.94	330.95	190.50	0.49	165.07	121.16	115.71	149.46	110.36	109.99
24		1951	D5-1	R	381.00	152.40	314.20	0	0	0	0	3048	2.43	SS-2PL	27.72		1632.25	320.61	3.42	141.94	330.95	254.00	0.37	146.17	105.67	100.96	131.80	84.94	96.08
25		1951	D5-2	R	381.00	152.40	314.20	0	0	0	0	3048	2.43	SS-2PL	29.03		1632.25	320.61	3.42	141.94	330.95	254.00	0.37	157.29	106.51	101.96	129.73	83.65	93.41
26		1951	D5-3	R	381.00	152.40	314.20	0	0	0	0	3048	2.43	SS-2PL	27.10		1632.25	320.61	3.42	141.94	330.95	254.00	0.37	157.29	105.27	100.48	128.17	83.65	91.63
27	Collins	1999	SE100A-M-69	R	1000.00	294.89	919.99	0	0	0	0	4597.4	2.5	SE-2PL	70.98	9.906	2799.99	482.63	1.03	200.00	521.93	439.42	0.15	516.31	564.24	500.64	525.08	257.76	454.07
28	Kuchma	1999	SE100B-M-69	R	1000.00	294.89	919.99	0	0	0	0	4597.4	2.5	SE-2PL	74.98	9.906	3703.22	482.63	1.36	200.00	521.93	439.42	0.15	583.21	579.45	544.67	579.70	273.32	497.34
29		1999	SE50A-M-69	R	500.13	168.91	458.98	0	0	0	0	2489.2	2.72	SE-2PL	73.98	9.906	800.00	482.63	1.03	51.61	592.95	276.86	0.11	138.52	151.03	131.35	137.98	59.88	115.91
30		1999	SE50B-M-69	R	500.13	168.91	458.98	0	0	0	0	2489.2	2.72	SE-2PL	73.98	9.906	903.22	482.63	1.16	51.61	592.95	276.86	0.11	151.82	151.66	137.40	140.33	60.59	117.40
31		1999	BM100	R	1000.00	299.97	925.07	0	0	0	0	5410.2	2.92	SS-1PL	46.99	9.906	2103.22	550.20	0.76	141.94	508.14	599.44	0.08	342.02	395.42	347.36	356.33	131.92	310.47
32		1999	BM100D	R	1000.00	299.97	925.07	0	0	0	0	5410.2	2.92	SS-1PL	46.99	9.906	5303.22	550.20	1.91	141.94	508.14	599.44	0.08	461.01	414.16	434.67	493.20	159.17	424.97
33	Johnson	1989	1	R	609.60	304.80	538.73	0	0	0	0	4267.2	3.1	SS-2PL	36.40		4096.77	524.69	2.49	58.06	479.19	137.16	0.14	338.06	273.43	277.71	331.21	156.54	270.08
34	Ramirez	1989	2	R	609.60	304.80	538.73	0	0	0	0	4267.2	3.1	SS-2PL	36.40		4096.77	524.69	2.49	64.52	479.19	279.40	0.07	222.41	223.76	228.04	308.16	92.16	245.88
35		1989	3	R	609.60	304.80	538.73	0	0	0	0	4267.2	3.1	SS-2PL	72.33		4096.77	524.69	2.49	64.52	479.19	279.40	0.07	262.45	281.72	257.00	371.15	89.73	284.93
36		1989	4	R	609.60	304.80	538.73	0	0	0	0	4267.2	3.1	SS-2PL	72.33		4096.77	524.69	2.49	64.52	479.19	279.40	0.07	315.82	281.72	257.00	342.25	86.63	256.87
37		1989	5	R	609.60	304.80	538.73	0	0	0	0	4267.2	3.1	SS-2PL	55.85		4096.77	524.69	2.49	58.06	479.19	137.16	0.14	382.55	307.20	306.67	353.61	152.09	285.62
38		1989	7	R	609.60	304.80	538.73	0	0	0	0	4267.2	3.1	SS-2PL	51.30		4096.77	524.69	2.49	64.52	479.19	279.40	0.07	284.69	250.23	257.00	315.86	88.42	246.57
39		1989	8	R	609.60	304.80	538.73	0	0	0	0	4267.2	3.1	SS-2PL	51.30		4096.77	524.69	2.49	64.52	479.19	279.40	0.07	258.00	250.23	257.00	329.01	90.00	260.43
40	Kong	1998	S1-1	R	350.01	249.94	292.10	0	0	0	0	1955.8	2.5	SS-2PL	63.58		2045.16	451.61	2.80	38.71	568.82	99.06	0.16	228.28	162.11	152.69	184.37	89.90	132.60
41	Rangan	1998	S1-2	R	350.01	249.94	292.10	0	0	0	0	1955.8	2.5	SS-2PL	63.58		2045.16	451.61	2.80	38.71	568.82	99.06	0.16	208.31	162.11	152.69	191.55	91.91	140.20
42		1998	S1-3	R	350.01	249.94	292.10	0	0	0	0	1955.8	2.5	SS-2PL	63.58		2045.16	451.61	2.80	38.71	568.82	99.06	0.16	206.09	162.11	152.69	192.39	92.14	141.09
43		1998	S1-4	R	350.01	249.94	292.10	0	0	0	0	1955.8	2.5	SS-2PL	63.58		2045.16	451.61	2.80	38.71	568.82	99.06	0.16	277.88	162.11	152.69	168.82	85.16	116.41
44		1998	S1-5	R	350.01	249.94	292.10	0	0	0	0	1955.8	2.5	SS-2PL	63.58		2045.16	451.61	2.80	38.71	568.82	99.06	0.16	253.28	162.11	152.69	176.16	87.47	124.02
45		1998	S1-6	R	350.01	249.94	292.10	0	0	0	0	1955.8	2.5	SS-2PL	63.58		2045.16	451.61	2.80	38.71	568.82	99.06	0.16	224.10	162.11	152.69	185.82	90.32	134.13
46		1998	S2-1	R	350.01	249.94	292.10	0	0	0	0	1955.8	2.5	SS-2PL	72.48		2045.16	451.61	2.80	38.71	568.82	149.86	0.11	260.31	145.73	130.68	150.48	57.38	96.61
47		1998	S2-2	R	350.01	249.94	292.10	0	0	0	0	1955.8	2.5	SS-2PL	72.48		2045.16	451.61	2.80	38.71	568.82	124.46	0.13	232.51	154.49	139.44	170.99	71.22	115.80
48		1998	S2-3	R	350.01	249.94	292.10	0	0	0	0	1955.8	2.5	SS-2PL	72.48		2045.16	451.61	2.80	38.71	568.82	99.06	0.16	253.28	167.74	152.69	182.17	87.47	125.92
49		1998	S2-4	R	350.01	249.94	292.10	0	0	0	0	1955.8	2.5	SS-2PL	72.48		2045.16	451.61	2.80	38.71	568.82	99.06	0.16	219.39	167.74	152.69	194.04	90.79	137.81
50		1998	S2-5	R	350.01	249.94	292.10	0	0	0	0	1955.8	2.5	SS-2PL	72.48		2045.16	451.61	2.80	38.71	568.82	76.20	0.21	282.11	187.22	172.16	198.67	110.20	140.05
51		1998	S3-1	R	350.01	249.94	296.93	0	0	0	0	1981.2	2.49	SS-2PL	67.38		1232.26	450.23	1.66	25.81	631.56	99.06	0.10	209.20	144.36	138.06	135.17	59.54	95.18
52	Kong	1998	S3-2	R	350.01	249.94	296.93	0	0	0	0	1981.2	2.49	SS-2PL	67.38		1232.26	450.23	1.66	25.81	631.56	99.06	0.10	178.02	144.36	138.06	147.22	62.93	106.97
53	Rangan	1998	S3-3	R	350.01	249.94	293.12	0	0	0	0	1955.8	2.49	SS-2PL	67.38		2045.16	451.61	2.79	25.81	631.56	99.06	0.10	228.59	148.21	136.29	164.47	66.80	112.89
54		1998	S3-4	R	350.01	249.94	293.12	0	0	0	0	1955.8	2.49	SS-2PL	67.38		2045.16	451.61	2.70	25.81	631.56	99.06	0.10	174.90	147.75	136.29	184.41	70.90	132.80
55		1998	S3-5	R	350.01	249.94	298.96	0	0	0	0	1930.4	2.41	SS-2PL	67.38		2761.28	441.95	3.69	25.81	631.56	99.06	0.10	296.61	156.42	139.01	172.55	69.19	117.77
56		1998	S3-6	R	350.01	249.94	298.96	0	0	0	0	1930.4	2.41	SS-2PL	67.38		2761.28	441.95	3.69	25.81	631.56	99.06	0.10	282.91	156.42	139.01	176.15	69.95	121.48
57		1998	S4-1	R	599.95	249.94	542.04	0	0	0	0	3098.8	2.4	SS-2PL	87.28		4090.31	451.61	3.02	38.71	568.82	99.06	0.16	353.99	330.51	283.33	418.31	177.62	342.42
58		1998	S4-2	R	500.13	249.94	443.99	0	0	0	0	2641.6	2.41	SS-2PL	87.28		3283.86	432.99	2.96	38.71	568.82	99.06	0.16	572.80	270.16	232.08	248.47	120.11	176.56
59		1998	S4-3	R	400.05	249.94	345.95	0	0	0	0	2159	2.4	SS-2PL	87.28		2464.51	450.23	2.85	38.71	568.82	99.06	0.16	243.41	209.90	180.83	253.34	110.32	189.41
60		1998	S4-4	R	350.01	249.94	292.10	0	0	0	0	1955.8	2.5	SS-2PL	87.28		2045.16	451.61	2.80	38.71	568.82	99.06	0.16	258.09	176.38	152.69	189.72	87.01	126.63
61		1998	S4-6	R	249.94	249.94	198.12	0	0	0	0	1498.6	2.53	SS-2PL	87.28		1380.64	441.95	2.79	38.71	568.82	99.06	0.16	202.88	119.49	103.56	119.04	56.21	67.61
62		1998	S5-1	R	350.01	249.94	292.10	0	0	0	0	2260.6	3.01	SS-2PL	89.38		2045.16	451.61	2.80	38.71	568.82	99.06	0.16	241.72	175.17	152.69	184.65	85.25	122.74

Table A-2: Reinforced Concrete Beam Database, cont.

Reference Information				Section Geometry								Loading Geometry			Concrete Properties		Longitudinal Reinforcement			Transverse Reinforcement				Capacity					
#	Author and Notes	Year	Beam Name	Shape R/T/I	h (mm)	b_w (mm)	d (mm)	b_{top} (mm)	b_{bot} (mm)	t_{top} (mm)	t_{bot} (mm)	L (mm)	a/d	Loading Geometry	f_c' (MPa)	a_g (mm)	A_s (mm^2)	f_y (MPa)	ρ_l (%)	A_v (mm^2)	f_{vy} (MPa)	s (mm)	ρ_v (%)	V_u (kN)	V_n - ACI (kN)	Vn - NZS (kN)	Vn - CSA (kN)	Vn - EC2 (kN)	V_n - fib (kN)
63		1998	S5-2	R	350.01	249.94	292.10	0	0	0	0	2108.2	2.74	SS-2PL	89.38		2045.16	451.61	2.80	38.71	568.82	99.06	0.16	259.91	176.32	152.69	184.40	85.17	121.70
64		1998	S5-3	R	350.01	249.94	292.10	0	0	0	0	1955.8	2.5	SS-2PL	89.38		2045.16	451.61	2.80	38.71	568.82	99.06	0.16	243.81	177.54	152.69	196.03	88.38	131.58
65		1998	S6-3	R	350.01	249.94	293.12	0	0	0	0	1981.2	2.73	SS-4PL	68.89		2045.16	451.61	2.79	25.81	631.56	99.06	0.10	178.42	147.92	136.29	179.21	69.66	127.69
66		1998	S6-4	R	350.01	249.94	293.12	0	0	0	0	1981.2	2.73	SS-4PL	68.89		2045.16	451.61	2.79	25.81	631.56	99.06	0.10	214.40	147.92	136.29	165.37	66.76	114.09
67		1998	S7-1	R	350.01	249.94	293.88	0	0	0	0	1930.4	3.3	SS-1PL	74.78		3283.86	432.99	4.47	38.71	568.82	149.86	0.11	217.21	150.97	131.47	187.01	64.07	125.02
68		1998	S7-2	R	350.01	249.94	293.88	0	0	0	0	1930.4	3.3	SS-1PL	74.78		3283.86	432.99	4.47	38.71	568.82	124.46	0.13	205.42	159.79	140.28	204.42	77.94	142.54
69		1998	S7-3	R	350.01	249.94	293.88	0	0	0	0	1930.4	3.3	SS-1PL	74.78		3283.86	432.99	4.47	38.71	568.82	99.06	0.16	246.52	173.12	153.62	209.45	94.52	147.40
70		1998	S7-4	R	350.01	249.94	293.88	0	0	0	0	1930.4	3.3	SS-1PL	74.78		3283.86	432.99	4.47	38.71	568.82	78.74	0.20	273.61	189.97	170.47	224.61	116.20	161.63
71		1998	S7-5	R	350.01	249.94	293.88	0	0	0	0	1930.4	3.3	SS-1PL	74.78		3283.86	432.99	4.47	38.71	568.82	71.12	0.22	304.39	198.78	179.28	227.19	125.34	163.06
72		1998	S7-6	R	350.01	249.94	293.88	0	0	0	0	1930.4	3.3	SS-1PL	74.78		3283.86	432.99	4.47	38.71	568.82	60.96	0.26	310.62	213.94	194.44	246.08	145.47	180.67
73		1998	S8-1	R	350.01	249.94	292.10	0	0	0	0	1955.8	2.5	SS-2PL	74.58		2045.16	451.61	2.80	38.71	568.82	149.86	0.11	272.10	147.00	130.68	148.48	56.65	93.94
74		1998	S8-2	R	350.01	249.94	292.10	0	0	0	0	1955.8	2.5	SS-2PL	74.58		2045.16	451.61	2.80	38.71	568.82	124.46	0.13	251.01	155.76	139.44	166.38	69.79	110.44
75		1998	S8-3	R	350.01	249.94	292.10	0	0	0	0	1955.8	2.5	SS-2PL	74.58		2045.16	451.61	2.80	38.71	568.82	99.06	0.16	309.60	169.01	152.69	166.73	82.29	109.86
76		1998	S8-4	R	350.01	249.94	292.10	0	0	0	0	1955.8	2.5	SS-2PL	74.58		2045.16	451.61	2.80	38.71	568.82	99.06	0.16	265.78	169.01	152.69	179.50	86.29	122.32
77		1998	S8-5	R	350.01	249.94	292.10	0	0	0	0	1955.8	2.5	SS-2PL	74.58		2045.16	451.61	2.80	38.71	568.82	78.74	0.20	289.22	185.77	169.44	194.13	105.83	134.90
78		1998	S8-6	R	350.01	249.94	292.10	0	0	0	0	1955.8	2.5	SS-2PL	74.58		2045.16	451.61	2.80	38.71	568.82	71.12	0.22	283.89	194.52	178.19	207.22	117.85	146.91
79	Krefeld	1966	Ss2-26-1	R	508.00	254.00	455.68	0	0	0	0	3657.6	4.01	SS-1PL	40.13		2580.64	386.11	2.23	64.52	341.29	152.40	0.16	206.84	181.61	190.48	207.56	90.52	173.02
80	Thurston	1966	Ss2-29a-1	R	508.00	254.00	455.68	0	0	0	0	3657.6	4.01	SS-1PL	38.82		2580.64	386.11	2.23	64.52	341.29	228.60	0.11	159.69	157.94	166.48	197.42	64.04	162.50
81		1966	Ss2-29b-1	R	508.00	254.00	455.68	0	0	0	0	3657.6	4.01	SS-1PL	37.65		2580.64	386.11	2.23	64.52	341.29	228.60	0.11	160.14	156.37	164.61	195.16	64.00	160.44
82		1966	Ss2-213.5-1	R	508.00	254.00	455.68	0	0	0	0	3657.6	4.01	SS-1PL	38.89		2580.64	386.11	2.23	64.52	341.29	342.90	0.07	148.13	143.40	151.96	182.23	43.33	145.06
83		1966	Ss2-29a-2	R	508.00	254.00	455.68	0	0	0	0	3657.6	4.01	SS-1PL	37.16		2580.64	386.11	2.23	64.52	372.32	228.60	0.11	216.63	159.71	167.83	174.55	65.04	138.53
84		1966	Ss2-29b-2	R	508.00	254.00	455.68	0	0	0	0	3657.6	4.01	SS-1PL	41.37		2580.64	386.11	2.23	64.52	372.32	228.60	0.11	202.39	165.26	174.43	186.59	66.20	150.30
85		1966	Ss2-29c-2	R	508.00	254.00	455.68	0	0	0	0	3657.6	4.01	SS-1PL	24.13		2580.64	386.11	2.23	64.52	372.32	228.60	0.11	161.47	140.14	144.54	174.24	69.70	141.04
86		1966	Ss2-29d-2	R	508.00	254.00	455.68	0	0	0	0	3657.6	4.01	SS-1PL	30.41		2580.64	386.11	2.23	64.52	372.32	228.60	0.11	165.03	150.09	156.38	185.35	69.39	152.43
87		1966	Ss2-29e-2	R	508.00	254.00	455.68	0	0	0	0	3657.6	4.01	SS-1PL	48.47		2580.64	386.11	2.23	64.52	372.32	228.60	0.11	206.40	174.03	184.87	194.67	65.87	157.18
88		1966	Ss2-29g-2	R	508.00	254.00	455.68	0	0	0	0	3657.6	4.01	SS-1PL	15.72		2580.64	386.11	2.23	64.52	372.32	228.60	0.11	149.91	124.47	125.89	158.51	70.74	123.74
89		1966	Ss2-213.5a-2	R	508.00	254.00	455.68	0	0	0	0	3657.6	4.01	SS-1PL	36.96		2580.64	386.11	2.23	64.52	372.32	342.90	0.03	161.47	143.47	151.53	175.84	46.47	139.23
90		1966	Ss2-218a-2	R	508.00	254.00	455.68	0	0	0	0	3657.6	4.01	SS-1PL	37.58		2580.64	386.11	2.23	64.52	372.32	457.20	0.05	164.14	136.33	144.55	164.03	34.73	125.97
91		1966	Ss2-29-3	R	508.00	254.00	455.68	0	0	0	0	3657.6	4.01	SS-1PL	34.27		2580.64	386.11	2.23	64.52	237.18	228.60	0.11	177.93	138.33	145.68	161.56	43.49	124.94
92		1966	Ss2-318-1	R	508.00	254.00	455.68	0	0	0	0	3657.6	4.01	SS-1PL	40.54		2580.64	386.11	2.23	141.94	517.11	457.20	0.12	220.19	189.46	198.43	212.17	98.93	177.46
93		1966	Ss2-321-1	R	508.00	254.00	455.68	0	0	0	0	3657.6	4.01	SS-1PL	38.75		2580.64	386.11	2.23	141.94	517.11	533.40	0.11	163.69	176.66	185.18	222.51	91.02	190.46
94		1966	Ss2-318-2	R	508.00	254.00	455.68	0	0	0	0	3657.6	4.01	SS-1PL	38.89		2580.64	386.11	2.23	141.94	351.63	457.20	0.12	177.04	163.88	172.44	197.13	71.00	162.37
95		1966	Ss2-321-2	R	508.00	254.00	455.68	0	0	0	0	3657.6	4.01	SS-1PL	37.99		2580.64	386.11	2.23	141.94	351.63	533.40	0.11	166.81	155.58	163.91	190.51	61.65	155.27
96		1966	Ss2-313.5-3	R	508.00	254.00	455.68	0	0	0	0	3657.6	4.01	SS-1PL	42.68		2580.64	386.11	2.23	141.94	275.79	342.90	0.16	213.51	171.07	180.56	189.34	70.93	152.91
97		1966	Ss2-318-3	R	508.00	254.00	455.68	0	0	0	0	3657.6	4.01	SS-1PL	43.02		2580.64	386.11	2.23	141.94	275.79	457.20	0.12	174.82	158.50	168.07	189.46	55.84	152.54
98		1966	Ss2-321-3	R	508.00	254.00	455.68	0	0	0	0	3657.6	4.01	SS-1PL	43.02		2580.64	386.11	2.23	141.94	275.79	533.40	0.11	140.56	152.93	162.50	200.08	50.00	163.09
99		1966	Ss2-218b-2	R	508.00	254.00	455.68	0	0	0	0	3657.6	4.01	SS-1PL	34.61		2580.64	386.11	2.23	64.52	372.32	457.20	0.05	341.18	132.25	139.70	106.12	27.94	69.38
100	Lyngberg	1976	5A-0	TI	599.95	119.89	540.00	700.02	379.98	95.00	124.97	5003.8	2.78	SS-2PL	25.70		2516.12	639.83	3.88	103.23	673.62	157.48	0.53	434.99	300.81	294.23	317.85	279.80	284.19
101		1976	5B-0	TI	599.95	119.89	540.00	700.02	379.98	95.00	124.97	5003.8	2.78	SS-2PL	26.59		2516.12	639.83	3.88	103.23	646.73	157.48	0.53	434.99	292.10	285.67	307.34	268.63	273.99
102	Moayer, Regar	1974	P5	T	320.04	149.86	287.02	599.44	0	81.28	0	1981.2	3.45	SS-1PL	43.02		625.81	641.21	1.45	64.52	255.11	101.60	0.42	145.01	89.90	94.46	66.48	43.29	46.80
103	Moayer	1974	P20	T	320.04	149.86	287.02	599.44	0	81.28	0	1981.2	3.45	SS-1PL	40.68		806.45	641.21	1.92	45.16	310.26	152.40	0.21	120.10	69.68	73.03	62.28	30.79	45.71
104	Regan	1974	P21	T	320.04	149.86	287.02	599.44	0	81.28	0	2997.2	5.36	SS-1PL	42.82		806.45	641.21	1.92	45.16	310.26	228.60	0.14	89.85	60.44	65.44	50.74	19.95	36.83
105		1974	P22	T	320.04	149.86	287.02	599.44	0	81.28	0	2997.2	5.36	SS-1PL	43.30		806.45	641.21	1.92	64.52	255.11	101.60	0.28	108.98	89.57	94.61	74.89	48.08	56.36
106	Ozcebe	1999	ACI56	R	359.92	150.11	309.88	0	0	0	0	3505.2	5	SS-2PL	57.98	14.99	1606.45	450.23	3.46	25.81	255.11	119.38	0.14	93.59	73.21	77.93	85.61	24.30	62.03
107	Ersoy	1999	TH56	R	359.92	150.11	309.88	0	0	0	0	3505.2	5	SS-2PL	62.98	14.99	1606.45	450.23	3.46	25.81	255.11	99.06	0.17	103.51	78.85	81.43	88.87	28.59	64.94
108	Tankut	1999	TS56	R	359.92	150.11	309.88	0	0	0	0	3505.2	5	SS-2PL	60.98	14.99	1606.45	450.23	3.46	25.81	255.11	71.12	0.24	129.22	86.10	89.52	89.17	37.46	65.11
109		1999	ACI59	R	359.92	150.11	309.88					3505.2	5	SS-2PL	81.98	14.99	2058.06	424.72	4.43	25.81	255.11	119.38	0.14	96.48	84.32	77.93	107.40	25.41	72.73
110		1999	TH59	R	359.92	150.11	309.88					3505.2	5	SS-2PL	74.98	14.99	2058.06	424.72	4.43	25.81	255.11	88.90	0.19	119.30	87.56	83.79	102.59	32.67	71.79
111		1999	TS59	R	359.92	150.11	309.88					3505.2	5	SS-2PL	81.98	14.99	2058.06	424.72	4.43	25.81	255.11	60.96	0.28	125.40	100.70	94.30	118.15	47.09	85.13
112		1999	ACI36	R	359.92	150.11	309.88					2260.6	3	SS-2PL	74.98	14.99	1206.45	450.23	2.59	25.81	255.11	119.38	0.14	105.29	81.52	77.93	94.08	24.31	64.93
113		1999	TH36	R	359.92	150.11	309.88					2260.6	3	SS-2PL	74.98	14.99	1206.45	450.23	2.59	25.81	255.11	99.06	0.17	141.01	85.02	81.43	85.67	27.15	57.70
114		1999	TS36	R	359.92	150.11	309.88					2260.6	3	SS-2PL	74.98	14.99	1206.45	450.23	2.59	25.81	255.11	71.12	0.24	155.91	93.11	89.52	91.49	36.65	63.36
115		1999	ACI39	R	359.92	150.11	309.88					2260.6	3	SS-2PL	72.98	14.99	1432.26	424.72	3.08	25.81	255.11	119.38	0.14	111.78	82.05	77.93	98.13	24.90	67.49
116		1999	TH39	R	359.92	150.11	309.88					2260.6	3	SS-2PL	72.98	14.99	1432.26	424.72	3.08	25.81	255.11	78.74	0.21	142.92	90.87	86.75	99.34	35.68	69.52
117		1999	TS39	R	359.92	150.11	309.88					2260.6	3	SS-2PL	72.98	14.99	1432.26	424.72	3.08	25.81	255.11	60.96	0.28	179.22	98.42	94.30	98.46	43.21	68.62
118	Rangan	1991	I-1	I	614.93	73.91	563.12	400.1	400.1	112.5	112.5	3759.2	2.49	SS-2PL	36.49		3477.41	455.05	8.35	103.23	484.70	50.80	2.72	453.10	614.47	379.74	774.31	437.85	790.63
119		1991	I-2	I	614.93	73.91	563.12	400.1	400.1	112.5	112.5	3759.2	2.49	SS-2PL	30.19		3477.41	455.05	8.35	58.06	484.70	50.80	1.53	370.98	368.57	314.17	475.30	356.53	485.48
120		1991	I-3	I	614.93	62.99	563.12	400.1	400.1	112.5	112.5	3759.2	2.49	SS-2PL	31.19		3477.41	455.05	9.81	103.23	484.70	50.80	3.19	369.11	606.88	276.61	811.21	313.78	864.84
121		1991	I-4	I	614.93	64.01	563.12	400.1	400.1	112.5	112.5	3759.2	2.49	SS-2PL	35.69		3477.41	455.05	9.66	58.06	484.70	50.80	1.77	416.00	366.71	321.64	458.18	368.33	462.50
122	Roller	1990	No. 1	R	635.00	355.60	558.80					2794	2.5	SS-1PL	120.11	12.70	3277.41	472.29	1.65	58.06	406.79	215.90	0.08	297.32	394.72	311.38	486.40	88.76	309.42
123	Russell	1990	No. 2	R	679.45	355.60	558.80					2794	2.5	SS-1PL	120.11	12.70	6038.70	430.92	3.04	258.06	448.16	165.10	0.44	1097.42	743.97	641.69	721.66	464.34	467.82
124		1990	No. 3	R	717.55	355.60	558.80					2794	2.5	SS-1PL	120.11	12.70	9058.05	430.92	4.56	400.00	457.81	127.00	0.89	1655.01	1178.98	1055.99	1210.12	953.78	730.34

Table A-2: Reinforced Concrete Beam Database, cont.

Reference Information				Section Geometry								Loading Geometry			Concrete Properties		Longitudinal Reinforcement			Transverse Reinforcement				Capacity					
#	Author and Notes	Year	Beam Name	Shape R/T/I	h (mm)	b_w (mm)	d (mm)	b_{top} (mm)	b_{bot} (mm)	t_{top} (mm)	t_{bot} (mm)	L (mm)	a/d	Loading Geometry	f_c' (MPa)	a_g (mm)	A_s (mm^2)	f_y (MPa)	ρ_l (%)	A_v (mm^2)	f_{vy} (MPa)	s (mm)	ρ_v (%)	V_u (kN)	V_n - ACI (kN)	Vn - NZS (kN)	Vn - CSA (kN)	Vn - EC2 (kN)	V_n - fib (kN)
125		1990	No. 4	R	717.55	355.60	558.80					2794	2.5	SS-1PL	120.11	12.70	12077.40	430.92	6.08	400.00	457.81	88.90	1.27	1940.00	1545.01	1401.31	1709.91	1429.66	1101.22
126		1990	No. 5	R	742.95	355.60	558.80					2794	2.5	SS-1PL	120.11	12.70	13858.04	472.29	6.97	400.00	457.81	63.50	1.77	2234.56	2017.57	1861.74	2278.35	1998.83	1360.06
127		1990	No. 6	R	869.95	457.20	762.00					4572	3	SS-1PL	72.39	12.70	6038.70	464.02	1.73	141.94	445.40	381.00	0.08	665.36	584.34	565.18	616.52	169.55	453.79
128		1990	No. 7	R	869.95	457.20	762.00					4572	3	SS-1PL	72.40	12.70	6554.83	483.32	1.88	141.94	445.40	198.12	0.16	787.87	704.06	681.89	740.90	317.86	574.61
129		1990	No. 8	R	869.95	457.20	762.00					4572	3	SS-1PL	125.28	12.70	6554.83	483.32	1.88	141.94	445.40	381.00	0.08	482.81	720.92	565.18	927.38	186.35	590.76
130		1990	No. 9	R	869.95	457.20	762.00					4572	3	SS-1PL	125.28	12.70	8193.53	483.32	2.35	141.94	445.40	198.12	0.16	749.44	846.99	681.89	999.68	342.11	685.31
131		1990	No. 10	R	869.95	457.20	762.00					4572	3	SS-1PL	125.28	12.70	10064.50	464.02	2.89	141.94	445.40	134.62	0.23	1172.20	972.43	796.58	1040.04	472.24	733.79
132	Sarsam	1992	AL2-N	R	270.00	180.09	234.95					2286	4	SS-2PL	40.39	11.94	941.93	495.04	2.23	25.81	819.79	149.86	0.09	114.72	75.63	80.44	72.77	40.01	54.80
133	Al-Musawi	1992	AL2-H	R	270.00	180.09	234.95					2286	4	SS-2PL	75.28	11.94	941.93	495.04	2.23	25.81	819.79	149.86	0.09	122.59	89.66	85.77	81.67	38.99	59.58
134		1992	AS2-N	R	270.00	180.09	234.95					1574.8	2.5	SS-2PL	38.99	11.94	941.93	495.04	2.23	25.81	819.79	149.86	0.09	189.32	77.38	79.62	66.79	37.74	45.52
135		1992	AS2-H	R	270.00	180.09	231.90					1549.4	2.5	SS-2PL	75.48	11.94	941.93	495.04	2.26	25.81	819.79	149.86	0.09	201.02	91.04	84.66	74.45	36.27	48.79
136		1992	AS3-H	R	270.00	180.09	234.95					1574.8	2.5	SS-2PL	71.78	11.94	941.93	495.04	2.23	25.81	819.79	99.06	0.14	199.10	107.86	102.78	93.82	55.83	67.98
137		1992	BL2-H	R	270.00	180.09	232.92					2260.6	4	SS-2PL	75.68	11.94	1180.64	542.62	2.82	25.81	819.79	149.86	0.09	138.30	90.08	85.03	85.91	40.25	61.08
138		1992	BS2-H	R	270.00	180.09	232.92					1574.8	2.5	SS-2PL	73.88	11.94	1180.64	542.62	2.82	25.81	819.79	149.86	0.09	223.52	92.50	85.03	79.75	38.37	52.47
139		1992	BS3-H	R	270.00	180.09	232.92					1574.8	2.5	SS-2PL	73.38	11.94	1180.64	542.62	2.82	25.81	819.79	99.06	0.14	228.10	109.18	101.89	98.21	57.56	68.89
140		1992	BS4-H	R	270.00	180.09	232.92					1574.8	2.5	SS-2PL	80.08	11.94	1180.64	542.62	2.82	25.81	819.79	76.20	0.19	206.89	126.40	116.81	123.30	77.80	91.51
141		1992	CL2-H	R	270.00	180.09	232.92					2260.6	4	SS-2PL	70.09	11.94	1470.96	542.62	3.51	25.81	819.79	149.86	0.09	147.19	89.36	85.03	91.29	42.46	65.89
142		1992	CS2-H	R	270.00	180.09	232.92					1574.8	2.5	SS-2PL	70.18	11.94	1470.96	542.62	3.51	25.81	819.79	149.86	0.09	247.19	93.18	85.03	84.03	40.18	54.56
143		1992	CS3-H	R	270.00	180.09	232.92					1574.8	2.5	SS-2PL	74.18	11.94	1470.96	542.62	3.51	25.81	819.79	99.06	0.14	247.19	111.45	101.89	105.87	60.79	74.12
144		1992	CS4-H	R	270.00	180.09	232.92					1574.8	2.5	SS-2PL	75.68	11.94	1470.96	542.62	3.51	25.81	819.79	76.20	0.19	220.72	126.89	116.81	131.36	82.20	98.77
145	Tan, et al.	1995	G-2.70-5.38	R	500.13	109.98	463.04					2489.2	2.7	SS-2PL	42.79		625.81	555.03	1.23	154.84	384.73	299.72	0.48	105.02	143.60	146.68	150.23	110.20	142.43
146	Tan	1997	1-2.00/2.50	R	500.13	109.98	448.31					3505.2	2.79	SS-2PL	74.08		987.09	537.79	2.00	154.84	384.73	299.72	0.48	195.01	155.79	148.37	143.18	98.60	117.28
147	Teng	1997	2-2.58/0.25	R	500.13	109.98	442.47					3505.2	2.82	SS-2PL	54.69		1258.06	498.49	2.58	154.84	353.01	299.72	0.48	155.02	139.74	139.19	158.22	106.16	137.20
148	Kong	1997	3-4.08/2.50	R	500.13	109.98	420.12					3505.2	2.98	SS-2PL	54.79		1883.87	498.49	4.08	154.84	353.01	299.72	0.48	135.00	136.32	132.16	179.73	113.63	147.01
149	Lu	1997	4-5.80/2.50	R	500.13	109.98	397.51					3505.2	3.14	SS-2PL	74.08		2535.48	537.79	5.80	154.84	384.73	299.72	0.48	264.98	146.61	131.56	163.89	106.49	103.40
150	Yoon	1996	N1-N	R	750.06	374.90	655.07					4292.6	3.23	SS-1PL	35.99	20.07	6877.41	399.90	2.80	103.23	430.23	325.12	0.08	457.01	336.45	384.15	419.97	133.07	310.36
151	Cook	1996	N2-S	R	750.06	374.90	655.07					4292.6	3.23	SS-1PL	35.99	20.07	6877.41	399.90	2.80	141.94	300.00	464.82	0.08	363.02	306.98	354.67	413.49	92.73	301.97
152	Mitchell	1996	N2-N	R	750.06	374.90	655.07					4292.6	3.23	SS-1PL	35.99	20.07	6877.41	399.90	2.80	141.94	300.00	325.12	0.12	482.99	332.76	380.46	405.02	126.25	294.34
153		1996	M1-N	R	750.06	374.90	655.07					4292.6	3.23	SS-1PL	66.98	9.91	6877.41	399.90	2.80	103.23	300.00	325.12	0.08	405.01	386.03	357.61	510.45	94.77	376.48
154	Yoon	1996	M2-S	R	750.06	374.90	655.07					4292.6	3.23	SS-1PL	66.98	9.91	6877.41	399.90	2.80	141.94	300.00	325.12	0.12	552.02	409.43	381.01	476.47	122.79	346.91
155	Cook, Mitchell	1996	M2-N	R	750.06	374.90	655.07					4292.6	3.23	SS-1PL	66.98	9.91	6877.41	399.90	2.80	141.94	300.00	231.14	0.16	688.99	444.31	415.89	474.11	163.59	346.88
156	Xie	1994	NNW-3	R	254.00	127.00	203.20					1219.2	3	SS-1PL	40.75	19.05	825.80	420.58	3.20	64.52	324.05	101.60	0.49	87.05	70.07	74.29	82.29	56.76	57.04
157	Ahmad	1994	NHW-3	R	279.40	127.00	198.12					1193.8	3	SS-1PL	98.25	19.05	1135.48	420.58	4.54	64.52	324.05	99.06	0.51	102.44	83.97	76.89	101.41	59.02	46.52
158	Yu	1994	NHW-3a	R	304.80	127.00	198.12					1193.8	3	SS-1PL	89.98	19.05	1135.48	420.58	4.54	64.52	324.05	99.06	0.51	108.23	82.44	76.89	97.54	58.25	29.80
159	Hino	1994	NHW-3b	R	330.20	127.00	198.12					1193.8	3	SS-1PL	103.21	19.05	1135.48	420.58	4.54	64.52	324.05	99.06	0.51	122.55	84.86	76.89	95.44	56.39	14.74
160	Chung	1994	NHW4	R	355.60	127.00	203.20					1574.8	4	SS-1PL	98.87	19.05	1135.48	420.58	4.54	64.52	324.05	99.06	0.51	93.72	82.45	76.89	96.37	57.08	7.60

Table A-3: Prestressed Concrete Beam Database

Reference Information				Section Geometry							Loading Geometry			Concrete Properties		Prestressed Reinforcement					Nonprestressed Reinforcement			Transverse Reinforcement				Capacity					
#	Author	Year	Beam Name	Shape R/T/I	h (mm)	d (mm)	b_w (mm)	b_{top} (mm)	b_{bot} (mm)	t_{top} (mm)	t_{bot} (mm)	L (mm)	a/d	Loading Configuration	f_c' (MPa)	a_g (mm)	A_{ps} (mm^2)	f_{py} (MPa)	f_{pu} (MPa)	ρ_{pl} (%)	f_{se} (MPa)	A_s (mm^2)	f_y (MPa)	ρ_l (%)	A_v (mm^2)	f_{vy} (MPa)	s (mm)	ρ_v (%)	V_u (kN)	V_n - ACI (kN)	Vn - NZS (kN)	Vn - CSA (kN)	Vn - EC2 (kN)	V_n - fib (kN)
1	Bennett	1971	3A2	I	254.00	225.55	25.40	152.40	152.40	57.15	57.15	2743.20	3.00	SS-2PL	41.71		232.26	1516.85	1620.27	4.05	878.39	64.52	265.45	1.10	32.26	265.45	38.10	3.27	69.75	78.15	45.83	59.74	63.69	42.66
2	Balasooriya	1971	3C2	I	254.00	225.55	25.40	152.40	152.40	57.15	57.15	2743.20	3.00	SS-2PL	33.23		232.26	1516.85	1620.27	4.05	759.80	64.52	265.45	1.10	32.26	265.45	38.10	3.27	75.71	74.73	38.08	47.60	54.98	39.46
3		1971	3C3	I	254.00	225.55	25.40	152.40	152.40	57.15	57.15	2743.20	3.00	SS-2PL	33.65		232.26	1516.85	1620.27	4.05	881.15	64.52	265.45	1.10	32.26	265.45	38.10	3.27	78.73	77.10	38.55	48.19	56.26	37.92
4		1971	3C4	I	254.00	225.55	25.40	152.40	152.40	57.15	57.15	2743.20	3.00	SS-2PL	30.47		232.26	1516.85	1620.27	4.05	658.45	64.52	265.45	1.10	32.26	265.45	38.10	3.27	56.36	72.40	34.92	43.65	48.34	50.82
5		1971	3C5	I	254.00	225.55	25.40	152.40	152.40	57.15	57.15	2743.20	3.00	SS-2PL	31.58		232.26	1516.85	1620.27	4.05	563.99	64.52	265.45	1.10	32.26	265.45	38.10	3.27	48.84	70.77	36.18	45.23	48.17	56.16
6		1971	3D1	I	254.00	225.55	25.40	152.40	152.40	57.15	57.15	2743.20	3.00	SS-2PL	44.26		232.26	1516.85	1620.27	4.05	750.15	64.52	265.45	1.10	32.26	265.45	25.40	4.90	85.72	101.37	45.83	63.40	68.63	55.72
7		1971	3D2	I	254.00	225.55	25.40	152.40	152.40	57.15	57.15	2743.20	3.00	SS-2PL	44.26		232.26	1516.85	1620.27	4.05	774.97	64.52	265.45	1.10	32.26	265.45	38.10	3.27	76.73	76.50	45.83	63.40	66.68	38.94
8		1971	3D3	I	254.00	225.55	25.40	152.40	152.40	57.15	57.15	2743.20	3.00	SS-2PL	40.33		232.26	1516.85	1620.27	4.05	718.43	64.52	265.45	1.10	32.26	265.45	58.42	2.18	70.06	57.29	45.83	57.77	57.28	27.71
9		1971	3D4	I	254.00	225.55	25.40	152.40	152.40	57.15	57.15	2743.20	3.00	SS-2PL	39.37		232.26	1516.85	1620.27	4.05	744.63	64.52	265.45	1.10	32.26	265.45	76.20	1.63	61.03	49.95	45.11	52.21	45.73	23.90
10		1971	3E3	I	254.00	225.55	38.10	152.40	152.40	57.15	57.15	2743.20	3.00	SS-2PL	40.75		232.26	1516.85	1620.27	2.70	757.04	64.52	265.45	0.74	32.26	265.45	38.10	2.18	89.85	86.53	68.75	77.71	73.32	37.15
11	Bennett	1974	NL-6-240	I	329.95	298.45	51.05	151.89	151.89	56.90	56.90	3606.80	3.00	SS-2PL	41.22		232.26	1633.37	1719.55	1.52	1415.49	316.13	410.24	2.06	32.26	279.93	238.76	0.26	82.38	92.72	93.70	31.94	19.09	18.47
12	Debaiky	1974	NM-6-240	I	329.95	298.45	51.05	151.89	151.89	56.90	56.90	3606.80	3.00	SS-2PL	38.49		232.26	1633.37	1719.55	1.52	1485.82	316.13	410.24	2.06	25.81	417.82	238.76	0.24	89.01	96.60	97.54	33.37	22.05	19.45
13		1974	NH-6-240	I	329.95	298.45	51.05	151.89	151.89	56.90	56.90	3606.80	3.00	SS-2PL	35.44		232.26	1633.37	1719.55	1.52	1486.51	316.13	410.24	2.06	25.81	544.69	238.76	0.22	89.01	99.60	100.51	40.06	28.74	23.81
14		1974	NL-6-160	I	329.95	298.45	51.05	151.89	151.89	56.90	56.90	3606.80	3.00	SS-2PL	39.09		232.26	1633.37	1719.55	1.52	1487.89	316.13	410.24	2.06	32.26	279.93	160.02	0.39	90.52	100.25	101.20	38.36	27.34	23.18
15		1974	NM-6-160	I	329.95	298.45	51.05	151.89	151.89	56.90	56.90	3606.80	3.00	SS-2PL	38.24		232.26	1633.37	1719.55	1.52	1488.58	316.13	410.24	2.06	25.81	417.82	160.02	0.35	93.50	103.24	104.18	42.64	32.17	26.16
16		1974	NH-6-160	I	329.95	298.45	51.05	151.89	151.89	56.90	56.90	3606.80	3.00	SS-2PL	38.84		232.26	1633.37	1719.55	1.52	1489.96	316.13	410.24	2.06	25.81	544.69	160.02	0.32	105.02	109.61	110.56	48.42	39.63	30.13
17		1974	NL-6-80	I	329.95	298.45	51.05	151.89	151.89	56.90	56.90	3606.80	3.00	SS-2PL	39.77		232.26	1633.37	1719.55	1.52	1490.65	316.13	410.24	2.06	32.26	279.93	78.74	0.77	106.40	117.98	118.94	60.02	51.40	38.26
18		1974	NM-6-80	I	329.95	298.45	51.05	151.89	151.89	56.90	56.90	3606.80	3.00	SS-2PL	37.14		232.26	1633.37	1719.55	1.52	1491.34	316.13	410.24	2.06	25.81	417.82	78.74	0.70	106.00	123.71	113.17	70.16	61.49	44.98
19		1974	NH-6-80	I	329.95	298.45	51.05	151.89	151.89	56.90	56.90	3606.80	3.00	SS-2PL	38.75		232.26	1633.37	1719.55	1.52	1492.71	316.13	410.24	2.06	25.81	544.69	78.74	0.64	114.01	136.74	118.08	84.95	77.14	54.71
20		1974	NM-8-240	I	329.95	298.45	51.05	151.89	151.89	56.90	56.90	3606.80	3.00	SS-2PL	35.27		232.26	1633.37	1719.55	1.52	1493.40	316.13	410.24	2.06	51.61	419.89	238.76	0.41	79.98	109.32	107.47	59.89	46.38	37.86
21		1974	NM-8-160	I	329.95	298.45	51.05	151.89	151.89	56.90	56.90	3606.80	3.00	SS-2PL	40.96		232.26	1633.37	1719.55	1.52	1494.78	316.13	410.24	2.06	51.61	419.89	160.02	0.62	93.01	124.74	121.90	75.37	64.81	49.92
22		1974	NL-10.240	I	329.95	298.45	51.05	151.89	151.89	56.90	56.90	3606.80	3.00	SS-2PL	39.34		232.26	1633.37	1719.55	1.52	1495.47	316.13	410.24	2.06	70.97	279.93	238.76	0.58	93.50	108.61	109.57	50.19	39.72	31.71
23		1974	NM-10-240	I	329.95	298.45	51.05	151.89	151.89	56.90	56.90	3606.80	3.00	SS-2PL	40.62		232.26	1633.37	1719.55	1.52	1496.85	316.13	410.24	2.06	77.42	410.24	238.76	0.65	95.81	123.98	121.90	72.86	62.78	47.96
24		1974	NL-10-160	I	329.95	298.45	51.05	151.89	151.89	56.90	56.90	3606.80	3.00	SS-2PL	38.49		232.26	1633.37	1719.55	1.52	1497.54	316.13	410.24	2.06	70.97	279.93	160.02	0.88	102.49	120.61	117.31	65.82	56.70	42.35
25		1974	NM-10-160	I	329.95	298.45	51.05	151.89	151.89	56.90	56.90	3606.80	3.00	SS-2PL	38.24		232.26	1633.37	1719.55	1.52	1498.92	316.13	410.24	2.06	77.42	410.24	160.02	0.97	102.49	142.75	116.53	99.77	90.66	66.09
26		1974	PL-6-240	I	329.95	298.48	51.05	151.89	151.89	56.90	56.90	3606.80	3.00	SS-2PL	44.19		232.26	1633.37	1719.55	1.52	1499.61	316.13	410.24	2.06	32.26	279.93	238.76	0.26	89.01	96.89	97.90	29.78	18.46	17.68
27		1974	PM-6-240	I	329.95	298.45	51.05	151.89	151.89	56.90	56.90	3606.80	3.00	SS-2PL	43.09		232.26	1633.37	1719.55	1.52	1500.30	316.13	410.24	2.06	25.81	417.82	238.76	0.24	84.52	98.73	99.73	34.86	22.55	21.01
28		1974	PH-6-240	I	329.95	298.45	51.05	151.89	151.89	56.90	56.90	3606.80	3.00	SS-2PL	42.06		232.26	1633.37	1719.55	1.52	1501.68	316.13	410.24	2.06	25.81	544.69	238.76	0.22	81.00	102.53	103.51	43.15	29.93	26.70
29		1974	PL-6-160	I	329.95	298.45	51.05	151.89	151.89	56.90	56.90	3606.80	3.00	SS-2PL	42.06		232.26	1633.37	1719.55	1.52	1502.37	316.13	410.24	2.06	32.26	279.93	160.02	0.39	97.99	101.82	102.81	36.09	26.35	22.04
30		1974	PM-6-160	I	329.95	298.45	51.05	151.89	151.89	56.90	56.93	3606.80	3.00	SS-2PL	42.24		232.26	1633.37	1719.55	1.52	1503.75	316.13	410.24	2.06	25.81	417.82	160.02	0.35	95.99	105.20	106.19	41.83	31.77	26.13
31		1974	PH-6-160	I	329.95	298.45	51.05	151.89	151.89	56.90	56.90	3606.80	3.00	SS-2PL	40.36		232.26	1633.37	1719.55	1.52	1504.44	316.13	410.24	2.06	25.81	544.69	160.02	0.32	93.50	110.69	111.66	52.41	41.93	33.43
32		1974	PL-6-80	I	329.95	298.45	51.05	151.89	151.89	56.90	56.90	3606.80	3.00	SS-2PL	43.76		232.26	1633.37	1719.55	1.52	1505.81	316.13	410.24	2.06	32.26	279.93	78.74	0.77	106.00	119.91	120.92	60.17	51.50	38.89
33		1974	PM-6-80	I	329.95	298.45	51.05	151.89	151.89	56.90	56.90	3606.80	3.00	SS-2PL	43.76		232.26	1633.37	1719.55	1.52	1506.50	316.13	410.24	2.06	25.81	417.82	78.74	0.70	114.50	126.58	121.90	66.80	59.04	42.87
34		1974	PH-6-80	I	329.95	298.45	51.05	151.89	151.89	56.90	56.90	3606.80	3.00	SS-2PL	40.79		232.26	1633.37	1719.55	1.52	1507.88	316.13	410.24	2.06	25.81	544.69	78.74	0.64	102.49	138.03	121.90	90.65	81.54	60.05
35		1974	CL-6-240	I	329.95	298.45	51.05	151.89	151.89	56.90	56.90	3606.80	3.00	SS-2PL	56.51		232.26	1633.37	1719.55	1.52	1508.57	316.13	410.24	2.06	32.26	279.93	238.76	0.26	100.00	101.06	102.20	26.94	17.49	17.30
36		1974	CM-6-240	I	329.95	298.45	51.05	151.89	151.89	56.90	56.90	3606.80	3.00	SS-2PL	56.94		232.26	1633.37	1719.55	1.52	1509.95	316.13	410.24	2.06	25.81	417.82	238.76	0.24	100.00	103.43	104.58	30.33	20.88	19.74
37		1974	CH-6-240	I	329.95	298.45	51.05	151.89	151.89	56.90	56.90	3606.80	3.00	SS-2PL	57.78		232.26	1633.37	1719.55	1.52	1510.64	316.13	410.24	2.06	25.81	544.69	238.76	0.22	102.49	107.79	108.95	36.00	26.89	23.76
38		1974	CL-6-160	I	329.95	298.45	51.05	151.89	151.89	56.90	56.90	3606.80	3.00	SS-2PL	58.63		232.26	1633.37	1719.55	1.52	1511.33	316.13	410.24	2.06	32.26	279.93	160.02	0.39	102.49	107.34	108.50	34.89	25.77	23.07
39		1974	CM-6-160	I	329.95	298.45	51.05	151.89	151.89	56.90	56.90	3606.80	3.00	SS-2PL	61.18		232.26	1633.37	1719.55	1.52	1512.71	316.13	410.24	2.06	25.81	417.82	160.02	0.35	111.52	111.38	112.58	37.53	29.47	24.85
40		1974	CH-6-160	I	329.95	298.45	51.05	151.89	151.89	56.90	56.90	3606.80	3.00	SS-2PL	59.32		232.26	1633.37	1719.55	1.52	1513.40	316.13	410.24	2.06	25.81	544.69	160.02	0.32	112.01	116.98	118.16	46.33	38.32	30.69
41		1974	CL-6-80	I	329.95	298.45	51.05	151.89	151.89	56.90	56.90	3606.80	3.00	SS-2PL	60.34		232.26	1633.37	1719.55	1.52	1514.78	316.13	410.24	2.06	32.26	279.93	78.74	0.72	116.01	125.34	121.90	56.71	49.09	37.62
42		1974	CM-6-80	I	329.95	298.45	51.05	151.89	151.89	56.90	56.90	3606.80	3.00	SS-2PL	59.49		232.26	1633.37	1719.55	1.52	1515.47	316.13	410.24	2.06	25.81	417.82	78.74	0.70	126.02	131.76	121.90	62.71	55.91	40.73
43		1974	CH-6-80	I	329.95	298.45	51.05	151.89	151.89	56.90	56.90	3606.80	3.00	SS-2PL	55.92		232.26	1633.37	1719.55	1.52	1516.85	316.13	410.24	2.06	25.81	544.69	78.74	0.64	139.99	143.19	121.90	74.23	68.32	46.47
44	Cederwall	1974	824-1B	R	262.89	236.98	132.08					2997.20	2.53	SS-2PL	41.65		225.81	882.53	911.49	0.72	303.37	225.81	637.08	0.72	58.06	495.04	200.66	0.21	116.19	66.25	82.31	52.49	41.46	40.43
45	Hedman	1974	824-2B	R	261.87	235.97	131.06					2997.20	2.54	SS-2PL	25.72		225.81	882.53	911.49	0.73	550.89	225.81	637.08	0.73	58.06	519.86	200.66	0.22	116.41	75.04	87.53	54.08	43.24	37.44
46	Losberg	1974	824-1C	R	260.10	233.93	132.08					2997.20	2.56	SS-2PL	15.69		225.81	882.53	911.49	0.73	368.87	225.81	637.08	0.73	58.06	488.15	99.06	0.43	88.25	94.86	96.93	108.01	93.52	77.07
47		1974	803-2S	R	260.10	233.93	130.05					2997.20	2.56	SS-2PL	28.63		225.81	882.53	911.49	0.74	455.74	116.13	882.53	0.37	58.06	235.11	200.66	0.22	75.53	51.46	62.01	36.93	22.40	25.38
48		1974	803-15	R	260.10	233.93	130.05					2997.20	2.56	SS-2PL	24.55		225.81	882.53	911.49	0.74	407.48	116.13	882.53	0.37	58.06	235.11	200.66	0.22	84.92	48.17	57.93	33.63	21.05	21.46
49		1974	842-6	R	261.87	235.97	131.06					2997.20	2.54	SS-2PL	46.12		225.81	882.53	911.49	0.73	529.52	451.61	637.08	1.46	58.06	529.52	200.66	0.22	130.91	79.52	96.24	60.19	47.55	52.15
50		1974	842-7B	R	260.10	234.95	131.06					2997.20	2.55	SS-2PL	35.69		225.81	882.53	911.49	0.73	555.03	451.61	637.08	1.47	58.06	529.52	200.66	0.22	129.44	77.96	92.66	60.20	47.52	49.79
51		1974	842-8	R	261.87	235.97	132.08					2997.20	2.54	SS-2PL	56.23		225.81	882.53	911.49	0.73	594.33	451.61	637.08	1.45	58.06	529.52	149.86	0.29	160.36	96.91	113.24	68.35	57.81	57.70
52		1974	842-10	R	261.11	234.95	131.06					2997.20	2.55	SS-2PL	50.75		225.81	882.53	911.49	0.73	520.55	451.61	637.08	1.47	58.06	353.01	200.66	0.22	107.38	67.73	84.92	49.18	34.12	46.00
53		1974	842-11	R	260.10	235.97	131.06					2997.20	4.24	SS-2PL	50.51		225.81	882.53	911.49	0.73	520.55	451.61	637.08	1.46	58.06	353.01	200.66	0.22	91.19	54.88	75.54	43.56	31.27	41.55
54		1974	842-13	R	259.08	238.00	132.08					2997.20	3.36	SS-2PL	53.49		225.81	882.53	911.49	0.72	472.98	451.61	637.08	1.44	58.06	353.01	200.66	0.21	122.10	58.71	78.25	41.28	29.99	39.17
55		1974	842-14	R	261.87	235.97	131.06					2997.20	2.54	SS-2PL	40.87		225.81	882.53	911.49	0.73	182.02	451.61	637.08	1.46	58.06	529.52	200.66	0.22	108.85	63.83	78.15	66.17	51.19	58.32
56		1974	842-16	R	259.08	232.92	131.06					2997.20	2.58	SS-2PL	51.61		225.81	882.53	911.49	0.74	312.33	451.61	637.08	1.48	58.06	529.52	200.66	0.22	157.38	69.61	86.57	53.18	42.78	44.37
57	Cumming	1998	IA	I	1397.00	1260.09	152.40	762.00	660.40	184.15	234.95	12141.20	3.24	SS-1PL	78.12	16.00	6767.73	1758.16	1861.58	3.52	848.06				258.06	517.11	4064.00	0.42	1433.22	1277.46	1294.43	291.91	74.65	108.28
58	Shield	1998	IB	I	1397.00	1260.09	152.40	762.00	660.40	184.15	234.95	12115.80	3.19	SS-1PL	78.12	16.00	6767.73	1758.16	1861.58	3.52	848.06				258.06	501.25	406.40	0.42	1545.76	1637.16	1536.31	940.83	723.57	428.28
59	French	1998	IIC	I	1397.00	1260.09	152.40	762.00	660.40	184.15	234.95	12217.40	3.25	SS-1PL	64.22	19.05	6767.73	1758.16	1861.58	3.52	848.06				258.06	501.25	406.40	0.42	1814.87	1591.25	1536.31	940.83	723.57	348.45
60		1998	IID	I	1397.00	1233.42	152.40	762.00	660.40	184.15	234.95	12065.00	3.29	SS-1PL	64.22	19.05	6767.73	1758.16	1861.58	3.60	848.06				258.06	501.25	406.40	0.42	1996.81	1557.57	1503.79	920.92	708.25	332.24
61	Durrani	1987	3	T	508.00	317.50	76.20	609.60	76.20	76.20		3352.80	3.52	SS-2PL	46.11		296.77	1817.46	1913.30	0.96	958.37				19.35	503.32	152.40	0.14	154.35	93.95	95.60	24.83	19.12	19.46
62		1987	4	T	508.00	317.50	76.20	609.60	76.20	76.20		3352.80	3.52	SS-2PL	44.13		296.77	1817.46	1913.30	0.96	1061.79				19.35	503.32	152.40	0.14	165.25	95.73	97.33	22.32	17.27	18.76
63		1987	5	T	508.00	317.50	76.20	609.60	76.20	76.20		3352.80	3.52	SS-2PL	44.63		296.77	1817.46	1913.30	0.96	1054.90				19.35	444.02	152.40	0.18	167.03	93.41	95.03	20.00	15.02	16.99
64		1987	6	T	508.00	317.50	76.20	609.60	76.20	76.20		3352.80	3.52	SS-2PL	41.85		296.77	1817.46	1913.30	0.96	1034.21				19.35	503.32	304.80	0.07	155.69	83.61	85.17	15.06	9.44	11.32
65		1987	8	T	508.00	317.50	76.20	609.60	76.20	76.20		3352.80	3.52	SS-2PL	39.44		296.77	1817.46	1913.30	0.96	1054.90				25.81	388.86	152.40	0.22	170.37	93.60	95.12	22.52	17.54	18.32
66		1987	9	T	508.00	317.50	76.20	609.60	76.20	76.20		3352.80	3.52	SS-2PL	41.79		296.77	1817.46	1913.30	0.96	1048.00				25.81	518.49	152.40	0.22	172.37	101.68	103.24	28.37	23.39	23.74
67		1987	10	T	508.00	317.50	76.20	609.60	76.20	76.20		3352.80	3.52	SS-2PL	42.04		296.77	1817.46	1913.30	0.96	1048.00				25.81	388.86	152.40	0.22	172.37	94.84	96.41	22.52	17.54	18.63
68		1987	12	T	508.00	317.50	76.20	609.60	76.20	76.20		3352.80	3.52	SS-2PL	41.54		296.77	1817.46	1913.30	0.96	1082.48				6.45	346.81	152.40	0.08	159.02	79.26	80.82	9.61	4.20	7.09
69		1987	13	T	508.00	317.50	76.20	609.60	76.20	76.20		3352.80	3.52	SS-2PL	41.30		296.77	1817.46	1913.30	0.96	1048.00				6.45	346.81	152.40	0.08	144.57	78.20	79.75	11.28	4.81	7.63
70	Gregor	1995	CW 10	I	457.20	362.71	50.80	203.20	203.20	101.60	101.60	3810.00	3.80	SS-2PL	73.08	12.70	561.29	1758.16	1861.58	3.01	784.62	212.90	434.37	1.16	70.97	434.37	254.00	0.55	173.48	134.62	136.20	86.41	72.43	35.10
71	`	1995	CW11	I	457.20	362.71	50.80	203.20	203.20	101.60	101.60	3810.00	3.80	SS-2PL	55.85	12.70	561.29	1758.16	1861.58	3.01	766.01	212.90	434.37	1.16	70.97	434.37	254.00	0.55	156.58	127.81	129.18	96.94	77.95	37.72
72		1995	CW12	I	457.20	362.71	50.80	203.20	203.20	101.60	101.60	3810.00	3.80	SS-2PL	39.99	12.70	561.29	1758.16	1861.58	3.01	768.77	212.90	434.37	1.16	70.97	434.37	254.00	0.55	140.56	121.82	122.99	100.26	79.41	40.31
73		1995	CW13	I	457.20	362.71	50.80	203.20	203.20	101.60	101.60	3810.00	3.80	SS-2PL	72.39	12.70	561.29	1758.16	1861.58	3.01	1079.03	212.90	434.37	1.16	70.97	434.37	254.00	0.55	182.38	151.26	147.41	82.04	69.75	34.76
74		1995	CW 14	I	457.20	362.71	50.80	203.20	203.20	101.60	101.60	3810.00	3.80	SS-2PL	73.77	12.70	561.29	1758.16	1861.58	3.01	1090.06	212.90	434.37	1.16	70.97	434.37	177.80	0.79	187.71	171.19	147.41	108.90	97.45	48.27
75		1995	CW15	I	457.20	362.71	50.80	203.20	203.20	101.60	101.60	3810.00	3.80	SS-2PL	70.33	12.70	561.29	1758.16	1861.58	3.01	772.90	212.90	434.37	1.16	70.97	434.37	254.00	0.55	150.35	133.08	134.63	100.26	79.41	40.61
76		1995	CW 16	I	457.20	381.76	50.80	203.20	203.20	101.60	101.60	3810.00	3.80	SS-2PL	73.08	12.70	561.29	1758.16	1861.58	3.01	1083.17	1161.29	434.37	5.99	70.97	434.37	254.00	0.55	186.83	159.68	155.15	94.23	78.09	62.70

Table A-3: Prestressed Concrete Beam Database, cont.

Reference Information				Section Geometry								Loading Geometry			Concrete Properties		Prestressed Reinforcement					Nonprestressed Reinforcement			Transverse Reinforcement				Capacity					
#	Author	Year	Beam Name	Shape R/T/I	h (mm)	d (mm)	b_w (mm)	b_{top} (mm)	b_{bot} (mm)	t_{top} (mm)	t_{bot} (mm)	L (mm)	a/d	Loading Configuration	f_c' (MPa)	a_g (mm)	A_{ps} (mm^2)	f_{py} (MPa)	f_{pu} (MPa)	ρ_{pl} (%)	f_{se} (MPa)	A_s (mm^2)	f_y (MPa)	ρ_l (%)	A_v (mm^2)	f_{vy} (MPa)	s (mm)	ρ_v (%)	V_u (kN)	V_n - ACI (kN)	Vn - NZS (kN)	Vn - CSA (kN)	Vn - EC2 (kN)	V_n - fib (kN)
77		1995	CW17	I	457.20	362.71	50.80	203.20	203.20	101.60	101.60	3810.00	3.80	SS-2PL	69.64	12.70	561.29	1758.16	1861.58	3.01	1085.92	212.90	434.37	1.16	38.71	434.37	254.00	0.30	142.34	130.77	132.31	64.16	43.32	25.62
78		1995	CI10	TI	355.60	254.00	76.20	508.00	152.40	50.80	127.00	3810.00	5.80	SS-2PL	73.08	12.70	561.29	1758.16	1861.58	2.58	785.31	212.90	434.37	1.10	70.97	434.37	203.20	0.46	141.45	121.76	126.38	67.03	56.68	34.44
79		1995	CI11	TI	355.60	254.00	76.20	508.00	152.40	50.80	127.00	3810.00	5.80	SS-2PL	55.85	12.70	561.29	1758.16	1861.58	2.58	768.77	212.90	434.37	1.10	70.97	434.37	203.20	0.46	127.22	117.94	124.60	74.91	61.61	33.75
80		1995	CI12	TI	355.60	254.00	76.20	508.00	152.40	50.80	127.00	3810.00	5.80	SS-2PL	39.99	12.70	561.29	1758.16	1861.58	2.58	772.21	212.90	434.37	1.10	70.97	434.37	203.20	0.46	122.33	115.56	118.12	78.18	63.45	32.89
81		1995	C113	TI	355.60	254.00	76.20	508.00	152.40	50.80	127.00	3810.00	5.80	SS-2PL	72.39	12.70	561.29	1758.16	1861.58	2.58	1075.58	212.90	434.37	1.10	70.97	434.37	203.20	0.46	154.80	145.13	147.64	61.10	52.53	33.95
82		1995	C114	TI	355.60	254.00	76.20	508.00	152.40	50.80	127.00	3810.00	5.80	SS-2PL	73.77	12.70	561.29	1758.16	1861.58	2.58	1094.89	212.90	434.37	1.10	70.97	434.37	127.00	0.73	164.58	169.99	154.84	87.19	79.58	51.15
83		1995	C115	TI	355.60	254.00	76.20	508.00	152.40	50.80	127.00	3810.00	5.80	SS-2PL	70.33	12.70	561.29	1758.16	1861.58	2.58	773.59	212.90	434.37	1.10	70.97	434.37	203.20	0.46	120.99	120.43	125.44	79.15	63.97	36.14
84		1995	C116	TI	355.60	275.08	76.20	508.00	152.40	50.80	127.00	3810.00	5.80	SS-2PL	73.08	12.70	561.29	1758.16	1861.58	2.58	1086.61	1161.29	434.37	5.54	70.97	434.37	203.20	0.46	163.25	142.39	149.23	77.64	64.64	57.10
85		1995	C117	TI	355.60	254.00	76.20	508.00	152.40	50.80	127.00	3810.00	5.80	SS-2PL	69.64	12.70	561.29	1758.16	1861.58	2.58	1084.55	212.90	434.37	1.10	38.71	434.37	203.20	0.25	129.44	127.96	129.68	45.89	33.17	21.47
86		1995	CM5_A	TI	899.92	790.96	150.11	450.09	899.92	150.11	187.45	2260.60	2.84	SE-1PL	57.78		393.55	1762.99	1855.38	0.37	1484.44	3903.22	417.82	3.29	103.23	615.70	144.78	0.46	925.99	654.86	604.27	430.57	393.84	375.72
87		1995	CM6_A	TI	899.92	796.80	150.11	450.09	899.92	150.11	187.45	2260.60	2.82	SE-1PL	56.89		787.10	1762.99	1855.38	0.73	1484.44	2503.22	417.82	2.09	103.23	615.70	144.78	0.46	998.00	742.15	722.15	396.62	364.24	287.58
88	Jacob, Russell	1999	JJ3_North	TI	610.11	546.35	75.95	584.20	254.00	63.50	120.65	5791.20	3.07	SS-2PL	80.98		393.55	1766.44	1859.52	0.95	1487.89				25.81	690.17	99.06	0.32	164.01	279.34	267.32	154.62	135.69	95.18
89		1999	JJ4_North	TI	610.11	548.39	75.95	584.20	254.00	63.50	120.65	5791.20	3.06	SS-2PL	85.48		393.55	1766.44	1859.52	0.95	1487.89				25.81	690.17	99.06	0.32	172.01	283.36	267.69	146.53	129.54	95.52
90	Kaufman, et al.	1988	II-1	I	914.40	846.58	152.40	304.80	457.20	190.50	241.30	6096.00	2.52	SS-2PL	62.67		1290.32	1768.51	1861.58	1.00	1236.92				258.06	338.53	508.00	0.33	622.75	670.82	651.67	259.70	200.94	151.20
91	Kim	2004	1E	TI	1854.20	1739.90	152.40	1066.80	660.40	114.30	209.55	15240.00	4.38	SS-UDL	70.88	20.32	4516.12	1758.16	1861.58	1.89	1107.99				258.06	482.63	304.80	0.56	2544.38	1661.08	1786.93	651.12	921.71	638.14
92		2004	1W	TI	1854.20	1739.90	152.40	1066.80	660.40	114.30	209.55	15240.00	4.38	SS-UDL	70.88	20.32	4516.12	1758.16	1861.58	1.89	1107.99				258.06	482.63	304.80	0.56	2944.63	1661.08	1786.93	651.12	773.38	624.29
93		2004	2E	TI	1854.20	1709.93	152.40	1066.80	660.40	114.30	209.55	15240.00	4.46	SS-UDL	68.53	20.32	5354.83	1758.16	1861.58	2.28	1079.72				400.00	546.75	279.40	0.94	3304.76	2390.80	2084.74	1176.70	1536.43	1115.15
94		2004	2W	TI	1854.20	1709.93	152.40	1066.80	660.40	114.30	209.55	15240.00	4.46	SS-UDL	68.53	20.32	5354.83	1758.16	1861.58	2.28	1079.72				400.00	546.75	279.40	0.94	3789.17	2390.80	2084.74	1176.70	1284.83	1098.00
95		2004	3E	TI	1854.20	1718.82	152.40	1066.80	660.40	114.30	209.55	15240.00	4.43	SS-UDL	98.11	12.70	5935.47	1758.16	1861.58	2.51	1054.90				258.06	467.46	203.20	0.83	3491.68	2189.95	2095.58	910.12	1246.27	877.82
96		2004	3W	TI	1854.20	1718.82	152.40	1066.80	660.40	114.30	209.55	15240.00	4.43	SS-UDL	98.11	12.70	5935.47	1758.16	1861.58	2.51	1054.90				258.06	467.46	203.20	0.83	3798.96	2189.95	2095.58	910.12	1124.41	869.26
97		2004	5E	TI	1854.20	1778.00	152.40	1066.80	660.40	114.30	209.55	15240.00	4.29	SS-UDL	122.73	10.16	3354.83	1758.16	1861.58	1.38	1188.66				141.94	635.70	508.00	0.18	2318.32	1204.81	1190.46	320.72	324.71	353.41
98		2004	5W	TI	1854.20	1778.00	152.40	1066.80	660.40	114.30	209.55	15240.00	4.29	SS-UDL	122.73	10.16	3354.83	1758.16	1861.58	1.38	1188.66				141.94	527.45	508.00	0.18	1947.43	1151.03	1136.68	275.60	333.90	318.64
99		2004	6E	TI	1854.20	1718.82	152.40	1066.80	660.40	114.30	209.55	15240.00	4.43	SS-UDL	122.73	10.16	5935.47	1758.16	1861.58	2.51	1124.53				400.00	446.09	304.80	0.86	3383.98	2268.25	2095.58	898.21	1274.62	882.38
100		2004	6W	TI	1854.20	1718.82	152.40	1066.80	660.40	114.30	209.55	15240.00	4.43	SS-UDL	122.73	10.16	3677.41	1758.16	1861.58	2.51	1187.28				400.00	446.09	304.80	0.86	2723.47	1944.58	1934.15	898.21	909.69	898.23
101	Lyngberg	1976	2A-3	I	599.95	540.00	119.89	700.02	379.98	95.00	124.97	5003.80	2.78	SS-2PL	32.59		677.42	1750.58	1842.28	1.05	930.10	612.90	441.95	0.95	103.23	615.70	157.48	0.53	505.99	401.82	405.52	251.18	232.96	170.33
102		1976	2B-3	I	599.95	540.00	119.89	700.02	379.98	95.00	125.00	5003.80	2.78	SS-2PL	33.89		677.42	1750.58	1842.28	1.05	9273.45	612.90	441.26	0.95	103.23	642.59	157.48	0.53	515.02	1101.47	438.87	257.01	239.23	177.86
103		1976	3A-2	I	599.95	540.00	119.89	700.02	379.98	95.00	124.97	5003.80	2.78	SS-2PL	31.10		451.61	1750.58	1842.28	0.70	931.48	1232.26	445.40	1.90	103.23	662.59	157.48	0.53	488.99	390.44	394.05	278.22	259.04	187.02
104		1976	3B-2	I	599.95	540.00	119.89	700.02	379.98	95.00	124.97	5003.80	2.78	SS-2PL	27.50		451.61	1750.58	1842.28	0.70	931.48	1232.26	446.09	1.90	103.23	624.67	157.48	0.53	432.99	370.77	356.02	285.79	263.91	198.56
105		1976	4A-1	I	599.95	540.00	119.89	700.02	379.98	95.00	124.97	5003.80	2.78	SS-2PL	31.50		225.81	1750.58	1842.28	0.35	959.75	1870.96	481.25	2.89	103.23	639.14	157.48	0.53	469.02	344.44	347.51	276.98	256.91	229.41
106		1976	4B-1	I	599.95	540.00	119.89	700.02	379.98	95.00	124.97	5003.80	2.78	SS-2PL	30.39		225.81	1750.58	1842.28	0.35	924.59	1870.96	485.39	2.89	103.23	657.76	157.48	0.53	453.99	347.82	350.83	289.49	268.85	241.99
107	MacGregor	1960	BV.14.30	I	304.80	256.54	74.93	151.13	151.13	73.66	73.66	2743.20	3.56	SS-2PL	27.72	9.65	154.84	15099.52	1765.06	0.81	848.06				25.81	253.73	127.00	0.28	55.60	50.37	51.98	26.86	18.18	13.38
108		1960	BV.14.32A	I	304.80	257.30	72.39	149.86	149.86	73.66	73.66	2743.20	3.55	SS-2PL	26.20	9.65	154.84	1572.00	1758.16	0.84	772.21				25.81	253.73	114.30	0.32	57.83	49.10	50.70	27.06	19.42	13.94
109		1960	BV.14.32B	I	304.80	257.30	72.39	149.86	149.86	73.66	73.66	2743.20	3.55	SS-2PL	26.20	9.65	154.84	1572.00	1758.16	0.84	772.21				25.81	253.73	114.30	0.32	64.54	49.10	50.70	23.19	17.16	13.64
110		1960	BW.14.34	I	304.80	256.54	73.66	149.86	149.86	73.66	73.66	2743.20	3.56	SS-2PL	24.55	9.65	154.84	1503.06	1778.85	0.81	845.30				25.81	234.42	266.70	0.13	57.38	42.10	43.65	15.80	7.78	7.35
111		1960	BW.14.38	I	304.80	256.79	74.93	152.40	152.40	73.66	73.66	2743.20	3.56	SS-2PL	21.44	9.65	154.84	1530.64	1840.90	0.81	827.37				6.45	299.92	63.50	0.19	58.72	43.01	44.39	18.70	10.49	8.26
112		1960	BW.14.58	I	304.80	253.24	73.91	152.40	152.40	73.66	73.66	2743.20	3.61	SS-2PL	21.82	9.65	238.71	1668.53	1930.53	1.26	754.29				19.35	296.47	127.00	0.20	68.06	56.84	61.55	41.82	20.64	10.29
113		1960	BW.14.60	I	304.80	253.49	73.41	153.42	153.42	73.66	73.66	2743.20	3.61	SS-2PL	20.86	9.65	238.71	1668.53	1930.53	1.27	757.04				19.35	296.47	127.00	0.20	64.94	56.77	61.34	41.71	20.66	10.22
114		1960	BW.18.15	I	304.80	255.02	76.20	153.92	153.92	73.66	73.66	2743.20	6.97	SS-2PL	52.57	9.65	154.84	1503.06	1778.85	0.79	728.09				96.77	548.13	889.00	0.14	33.18	38.17	44.08	28.16	20.12	18.42
115		1960	CW.13.28	I	304.80	254.76	44.45	152.40	152.40	79.50	79.50	2743.20	2.79	SS-2PL	29.85	9.65	154.84	1509.95	1765.06	1.38	817.03				25.81	253.73	63.50	0.95	78.73	58.21	58.83	33.67	30.11	19.08
116		1960	CW.14.17	I	304.80	266.45	44.70	152.40	152.40	79.50	79.50	2743.20	3.43	SS-2PL	21.65	9.65	77.42	1530.64	1840.90	0.66	868.05				6.45	299.92	127.00	0.16	35.10	25.86	23.91	8.22	4.57	4.59
117		1960	CW.14.22	I	304.80	257.56	43.43	151.13	151.13	79.50	79.50	2743.20	3.55	SS-2PL	32.13	9.65	154.84	1530.64	1840.90	1.40	838.40				19.35	246.14	63.50	0.67	61.39	52.06	52.69	29.03	24.72	15.06
118		1960	CW.14.23	I	304.80	266.19	44.45	152.40	152.40	79.50	79.50	2743.20	3.44	SS-2PL	18.55	9.65	77.42	1530.64	1840.90	0.66	867.36				12.90	253.73	127.00	0.24	35.45	27.99	26.19	11.14	7.61	6.16
119		1960	CW.14.37	I	304.80	256.79	43.18	151.13	151.13	79.50	79.50	2743.20	3.56	SS-2PL	22.34	9.65	154.84	1530.64	1840.90	1.41	832.89				12.90	253.73	63.50	0.49	57.38	42.58	43.11	23.22	18.21	9.82
120		1960	CW.14.39	I	304.80	257.05	44.45	152.40	152.40	79.50	79.50	2743.20	3.56	SS-2PL	20.75	9.65	154.84	1530.64	1840.90	1.37	825.99				6.45	299.92	63.50	0.33	48.49	37.20	37.72	21.31	12.81	6.31
121		1960	CW.14.47	I	304.80	257.56	43.18	152.40	152.40	79.50	79.50	2743.20	3.55	SS-2PL	17.48	9.65	154.84	1530.64	1840.90	1.40	819.10				38.71	246.14	127.00	0.67	53.38	46.67	38.88	34.90	28.76	13.71
122		1960	CW.14.50	I	304.80	257.81	44.45	152.40	152.40	79.50	79.50	2743.20	3.55	SS-2PL	16.55	9.65	154.84	1530.64	1840.90	1.36	837.71				51.61	234.42	127.00	0.89	53.82	52.60	37.93	42.42	36.24	17.43
123		1960	CW.14.51	I	304.80	251.97	45.72	153.16	153.16	79.50	79.50	2743.20	3.63	SS-2PL	22.48	9.65	232.26	1503.06	1778.85	1.99	799.10				25.81	253.73	127.00	0.45	57.38	49.51	50.05	36.47	23.44	9.74
124		1960	CW.14.54	I	304.80	252.98	45.21	152.40	152.40	79.50	79.50	2743.20	3.61	SS-2PL	22.75	9.65	232.26	1503.06	1765.06	2.00	740.50				219.35	253.73	127.00	3.83	59.61	145.83	52.05	65.06	74.94	78.41
125		1960	FW.14.06	TI	355.60	312.42	44.45	152.40	152.40	79.50	79.50	2743.20	2.93	SS-2PL	26.96	9.65	154.84	1509.95	1765.06	1.12	812.20				25.81	253.73	63.50	0.95	80.96	69.02	69.74	38.00	34.14	24.58
126	Ramierz	1958	M10	I	307.34	256.54	74.93	151.13	151.13	73.66	73.66	2743.20	3.56	SS-2PL	27.58	9.65	154.84	1509.95	1765.06	0.81	779.11				25.81	248.21	127.00	0.28	40.79	48.30	49.81	45.09	23.34	13.80
127		1958	M11	I	307.34	256.54	74.93	151.13	151.13	73.66	73.66	2743.20	3.56	SS-2PL	28.96	9.65	154.84	1509.95	1765.06	0.81	889.42				25.81	248.21	127.00	0.28	54.76	51.97	53.52	27.08	18.07	13.40
128		1958	PC6S	TI	813.05	748.28	151.89	305.05	405.89	139.95	190.50	4876.80	3.26	SS-1PL	44.79	9.40	864.51	1766.44	1859.52	0.76	1131.43	774.19	415.06	0.68	141.94	502.63	508.00	0.18	520.00	354.43	394.04	159.24	122.44	109.63
129		1958	PC10S	TI	813.05	748.28	151.89	305.05	405.89	139.95	190.50	4876.80	3.26	SS-1PL	69.58	9.40	864.51	1766.44	1859.52	0.76	1125.91	1529.03	415.06	1.35	141.94	502.63	508.00	0.18	534.01	375.75	400.58	183.33	137.42	139.99
130	Moayer	1974	P4	T	320.04	287.02	149.86	599.44		81.28		1981.20	3.45	SS-1PL	39.99		109.68	1820.91	1916.74	0.25	281.31	400.00	641.21	0.93	64.52	255.11	101.60	0.42	141.90	84.58	95.94	56.15	45.49	44.79
131	Regan	1974	P8	T	320.04	271.78	149.86	599.44		81.28		1981.20	3.64	SS-1PL	42.68		296.77	1788.50	1882.27	0.73	1109.37	400.00	641.21	0.98	45.16	310.26	152.40	0.21	178.37	112.23	132.85	43.57	29.82	27.22
132		1974	P9	T	320.04	271.78	149.86	599.44		81.28		2997.20	5.51	SS-1PL	40.40		296.77	1788.50	1882.27	0.73	1109.37	400.00	641.21	0.98	45.16	310.26	228.60	0.14	120.10	78.24	102.04	35.55	20.71	23.10
133		1974	P13	T	320.04	281.94	149.86	599.44		81.28		1981.20	3.51	SS-1PL	39.37		148.39	1788.50	1882.27	0.35	1139.01	400.00	641.21	0.95	45.16	310.26	152.40	0.21	140.12	82.18	103.08	39.87	27.87	29.49
134		1974	P14	T	320.04	281.94	149.86	599.44		81.28		2997.20	5.32	SS-1PL	44.13		148.39	1788.50	1882.27	0.35	1139.01	400.00	641.21	0.95	45.16	310.26	228.60	0.14	96.53	60.11	86.15	31.51	19.04	26.08
135		1974	P18	T	320.04	269.24	149.86	599.44		81.28		1981.20	3.68	SS-1PL	44.47		296.77	1788.50	1882.27	0.74	1109.37	200.00	641.21	0.50	45.16	310.26	152.40	0.21	160.14	112.27	131.45	40.18	27.86	27.95
136		1974	P19	T	320.04	269.24	149.86	599.44		81.28		2997.20	5.57	SS-1PL	45.37		296.77	1788.50	1882.27	0.74	1109.37	200.00	641.21	0.50	45.16	310.26	228.60	0.14	108.98	79.10	102.43	32.58	19.36	24.26
137		1974	P24	T	320.04	281.94	149.86	599.44		81.28		1981.20	3.51	SS-1PL	43.44		148.39	1788.50	1882.27	0.35	1139.01	400.00	641.21	0.95	64.52	255.11	101.60	0.42	147.68	103.14	125.10	58.60	47.27	44.30
138		1974	P25	T	320.04	281.94	149.86	599.44		81.28		2997.20	5.32	SS-1PL	43.99		148.39	1788.50	1882.27	0.35	1139.01	400.00	641.21	0.95	64.52	255.11	152.40	0.28	104.09	73.24	99.24	43.29	31.80	35.20
139	Moayer	1974	P26	T	320.04	269.24	149.86	599.44		81.28		1981.20	3.68	SS-1PL	47.30		296.77	1788.50	1882.27	0.74	1109.37	200.00	641.21	0.50	64.52	255.11	101.60	0.42	169.92	131.91	151.69	57.65	46.38	41.59
140	Regan	1974	P27	T	320.04	269.24	149.86	599.44		81.28		2997.20	5.57	SS-1PL	45.37		296.77	1788.50	1882.27	0.74	1109.37	200.00	641.21	0.50	64.52	255.11	152.40	0.28	114.76	91.67	115.00	44.74	32.54	32.99
141		1974	P28	T	320.04	271.78	149.86	599.44		81.28		1981.20	3.64	SS-1PL	44.88		296.77	1788.50	1882.27	0.73	1109.37	400.00	641.21	0.98	64.52	255.11	101.60	0.42	193.94	131.90	153.04	61.60	49.27	40.67
142		1974	P29	T	320.04	271.78	149.86	599.44		81.28		2997.20	5.51	SS-1PL	46.54		296.77	1788.50	1882.27	0.73	1109.37	400.00	641.21	0.98	64.52	255.11	152.40	0.28	134.78	92.42	117.96	46.24	33.51	32.87
143		1974	P49	T	320.04	274.32	149.86	599.44		81.28		1981.20	3.61	SS-1PL	37.78		296.77	1788.50	1882.27	0.72	1109.37	800.00	641.21	1.94	64.52	255.11	101.60	0.42	189.94	130.27	149.96	77.05	59.55	50.88
144		1974	P50	T	320.04	274.32	149.86	599.44		81.28		1981.20	3.61	SS-1PL	41.16		296.77	1788.50	1882.27	0.72	1109.37	800.00	641.21	1.94	109.68	282.69	101.60	0.70	229.97	170.56	191.11	115.06	100.91	73.18
145	Rangan	1991	II-1	I	614.93	564.13	64.01	400.05	400.05	112.52	112.52	3759.20	2.48	SS-2PL	44.99		277.42	1739.55	1831.25	0.77	1159.70	2000.00	455.05	5.54	58.06	484.70	50.80	1.89	460.88	413.08	288.87	405.00	391.63	347.51
146		1991	II-2	I	614.93	564.13	62.99	400.05	400.05	112.52	112.52	3759.20	2.48	SS-2PL	31.50		277.42	1739.55	1831.25	0.78	1159.70	2000.00	455.05	5.63	103.23	484.70	50.80	3.19	378.81	643.39	223.84	279.80	305.32	698.34
147		1991	II-3	I	614.93	564.13	72.90	400.05	400.05	112.52	112.52	3759.20	2.48	SS-2PL	44.59		277.42	1739.55	1831.25	0.68	1159.70	2000.00	455.05	4.86	58.06	484.70	50.80	1.65	489.22	425.68	328.99	395.63	381.18	333.38
148		1991	II-4	I	614.93	564.13	73.91	400.05	400.05	112.52	112.52	3759.20	2.48	SS-2PL	42.99		277.42	1739.55	1831.25	0.67	1159.70	2000.00	455.05	4.79	103.23	484.70	50.80	2.72	479.38	668.77	333.58	448.13	463.28	601.25
149		1991	III-1	I	614.93	560.58	66.04	400.05	400.08	112.52	112.52	3759.20	2.50	SS-2PL	39.99		400.00	1739.55	1831.25	1.08	1159.70	1619.35	455.05	4.38	58.06	484.70	50.80	1.83	368.00	422.96	296.09	370.11	389.11	367.88
150		1991	III-2	I	614.93	560.58	66.04	400.05	400.08	112.52	112.52	3759.20	2.50	SS-2PL	36.99		400.00	1739.55	1831.25	1.08	1159.70	1619.35	455.05	4.38	103.23	484.70	50.80	3.05	390.51	661.91	273.88	342.35	370.60	629.63
151		1991	III-3	I	614.93	560.58	76.96	400.05	400.08	112.52	112.52	3759.20	2.50	SS-2PL	38.99		400.00	1739.55	1831.25	0.92	1159.70	1619.35	455.05	3.75	58.06	484.70	50.80	1.57	396.51	438.71	336.43	420.54	418.43	351.65
152		1991	III-4	I	614.93	560.58	72.90	400.05	400.08	112.52	112.52	3759.20	2.50	SS-2PL	36.99		400.00	1739.55	1831.25	0.97	1159.70	1619.35	455.05	3.96	103.23	484.70	50.80	2.75	453.01	672.21	302.32	377.90	415.65	567.52
153		1991	IV-1	I	614.93	535.43	61.98	400.05	400.05	112.52	112.52	3759.20	2.62	SS-2PL	37.09		716.13	1739.55	1831.25	2.16	1159.70	329.03	455.05	0.99	103.23	484.70	50.80	3.24	374.99	658.37	246.18	307.73	359.16	396.01
154		1991	IV-2	I	614.93	535.43	64.01	400.05	400.05	112.52	112.52	3759.20	2.62	SS-2PL	32.99		716.13	1739.55	1831.25	2.09	1159.70	329.03	455.05	0.96	58.06	484.70	50.80	1.89	337.80	427.98	226.14	282.67	333.25	222.75
155		1991	IV-3	I	614.93	535.43	71.88	400.05	400.05	112.52	112.52	3759.20	2.62	SS-2PL	35.99		716.13	1739.55	1831.25	1.86	1159.70	329.03	455.05	0.86	103.23	484.70	50.80	2.79	464.79	675.54	277.04	346.30	422.62	396.01
156		1991	IV-4	I	614.93	535.43	71.88	400.05	400.05	112.52	112.52	3759.20	2.62	SS-2PL	28.70		716.13	1739.55	1831.25	1.86	1159.70	329.03	455.05	0.86	58.06	484.70	50.80	1.68	390.60	437.65	220.89	276.11	352.11	222.75
157	Shahawy	1996	A1-00-M_N	TI	1117.60	996.95	152.40	304.80	457.20	190.50	228.60	12192.00	2.60	SS-1PL	50.33		1580.64	1758.16	1861.58	1.04	1061.79				258.06	482.63	457.20	0.37	627.20	783.23	785.74	565.48	448.55	252.84
158	Batchelor	1996	A1-00-M_S	TI	1117.60	996.95	152.40	304.80	457.20	190.50	228.60	9601.20	3.16	SS-1PL	50.33		1580.64	1758.16	1861.58	1.04	1061.79				258.06	482.63	457.20	0.37	747.30	702.11	722.79	365.98	316.71	248.21
159		1996	A1-00-R/2_N	TI	1117.60	996.95	152.40	304.80	457.20	190.50	228.60	12192.00	2.60	SS-1PL	48.95		1580.64	1758.16	1861.58	1.04	1061.79				258.06	482.63	406.40	0.42	738.40	815.02	818.02	497.39	426.36	273.20
160		1996	A1-00-R/2_S	TI	1117.60	996.95	152.40	304.80	457.20	190.50	228.60	9601.20	3.16	SS-1PL	48.95		1580.64	1758.16	1861.58	1.04	1061.79				258.06	482.63	444.50	0.38	769.54	707.96	728.88	360.57	314.21	252.12
161		1996	A1-00-R_N	TI	1117.60	996.95	152.40	304.80	457.20	190.50	228.60	12192.00	2.60	SS-1PL	49.04		1580.64	1758.16	1861.58	1.04	1061.79				258.06	482.63	203.20	0.83	934.13	1120.70	1123.70	687.59	645.58	497.58
162		1996	A1-00-3R/2_N	TI	1117.60	996.95	152.40	304.80	457.20	190.50	228.60	12192.00	2.60	SS-1PL	52.41		1580.64	1758.16	1861.58	1.04	1061.79				258.06	482.63	134.62	1.25	920.78	1437.21	1215.48	1035.97	992.76	737.11
163		1996	B0-00-R_N	TI	1117.60	1003.30	152.40	304.80	457.20	190.50	228.60	12192.00	2.58	SS-1PL	51.37		1619.35	1758.16	1861.58	1.06	1060.41				258.06	482.63	203.20	0.83	978.61	1137.42	1140.58	676.50	635.57	501.56
164		1996	B0-00-R_S	TI	1117.60	1003.30	152.40	304.80	457.20	190.50	228.60	9601.20	3.14	SS-1PL	51.37		1619.35	1758.16	1861.58	1.06	1060.41				258.06	482.63	444.50	0.38	916.33	720.18	741.83	295.71	260.40	250.42

Appendix B Calculation of prestress losses

Prestress losses for the 12 experimental test units were calculated according to accepted New Zealand practice. As described in chapter 5 of this report, the test units contained three layers of prestressed longitudinal reinforcement centred at 45mm, 90mm and 140mm from the bottom of the web. Four sources of prestress loss were considered for the pretensioned test units.

B.1 Elastic shortening losses

Stress in concrete due to prestressing at top fibre:

$$f_{ct} = -\frac{P}{A_g} + \frac{Pey_t}{I_g}$$

$$= 9.23\text{MPa}$$

Stress in concrete due to prestressing at bottom fibre:

$$f_{cb} = -\frac{P}{A_g} - \frac{Pey_b}{I_g}$$

$$= -19.34\text{MPa}$$

Stress in concrete due to prestressing at level of prestressed reinforcement:

$$f_c = (f_{ct} - f_{cb})\frac{y_{pb}}{h} + f_{cb}$$

$$f_{c,1} = -15.06\text{MPa}$$

$$f_{c,2} = -10.77\text{MPa}$$

$$f_{c,3} = -6.01\text{MPa}$$

Prestress in prestressed reinforcement after elastic shortening:

$$f_p = f_{ps} - f_c\frac{E_{ps}}{E_c}$$

$$f_{pi,1} = 1175.22\text{MPa}$$

$$f_{pi,2} = 1206.33\text{MPa}$$

$$f_{pi,3} = 1240.90\text{MPa}$$

B.2 Creep losses

A creep coefficient, φ_{cc}, of 1.90 was used for Auckland conditions with an age at loading of 56 days.

Creep strain at level of prestressed reinforcement:

$$\Delta\varepsilon_{cr} = \frac{\varphi_{cc} f_c}{E_c}$$

$$\Delta\varepsilon_{cr,1} = -1.0381\times10^{-3}$$

$$\Delta\varepsilon_{cr,2} = -0.7426\times10^{-3}$$

$$\Delta\varepsilon_{cr,3} = -0.4142\times10^{-3}$$

B.3 Shrinkage losses

The ultimate drying shrinkage strain, $\Delta\varepsilon_{sh,u}$, was assumed to be 700microstrain.

Shrinkage strain at time of loading:

$$\Delta\varepsilon_{sh,t} = \frac{t}{t+35}\Delta\varepsilon_{sh,u}$$

$$= -0.4\times10^{-3}$$

B.4 Relaxation losses

Initial prestrains in the prestressed reinforcement

$$\varepsilon_{pi,1} = -5.8761\times10^{-3}$$

$$\varepsilon_{pi,2} = -6.0317\times10^{-3}$$

$$\varepsilon_{pi,3} = -6.2045\times10^{-3}$$

Relaxation strains, with an assumed basic relaxation loss of 2.5% for low relaxation strand:

$$\Delta\varepsilon_{rel} = -\varepsilon_{pi}\left[0.025\left(1-\frac{\Delta\varepsilon_{cr}+\Delta\varepsilon_{sh}}{\varepsilon_{pi}}\right)\right]$$

$$\Delta\varepsilon_{rel,1} = -0.1110\times10^{-3}$$

$$\Delta\varepsilon_{rel,2} = -0.1222\times10^{-3}$$

$$\Delta\varepsilon_{rel,3} = -0.1348\times10^{-3}$$

B.5 Prestress after all losses

Prestress in strands at each layer at time of testing, after all losses are accounted for:

$$f_p = E_{ps}\left[\varepsilon_{pi} + (\Delta\varepsilon_{cr} + \Delta\varepsilon_{sh} + \Delta\varepsilon_{rel})\right]$$

$$f_{p,1} = 865.4\text{MPa}$$

$$f_{p,2} = 953.4\text{MPa}$$

$$f_{p,3} = 1051.1\text{MPa}$$

Appendix C Concrete cylinder tests

40MPa Concrete Cylinders													
Label	Date	Diameter 1 (mm)	Diameter 2 (mm)	Length 1 (mm)	Length 2 (mm)	Average Volume (mm^3)	Weight (in air)	Weight (in water)	Unit Weight (kN/m^3)	Gauge Reading	f_c' (MPa)	Daily Average Unit Weight (kN/m^3)	Daily Average f_c' (MPa)
40-1	21/9/2011	102	101.5	201	202	1638452.2	3.956	2.329	23.6860	5.85	35.5	23.6860	35.5
40-2	22/9/2011	100	100	200	200	1570796.3	3.776	2.216	23.5820	6.4	38.9		
40-3	22/9/2011	102	102	202	203	1654684.7	3.919	2.284	23.2343	5.5	33.2	23.3703	36.3
40-4	22/9/2011	100	100	200	200	1570796.3	3.73	2.168	23.2947	6.05	36.7		
40-5	26/9/2011	102	101.5	202	202	1642517.8	3.905	2.276	23.3228	6.05	36.7		
40-6	26/9/2011	100	100	200	201	1574723.3	3.777	2.21	23.5294	6.05	36.7	23.3686	37.4
40-7	26/9/2011	101	101.5	202.5	202	1628427.7	3.86	2.239	23.2535	6.4	38.9		

60MPa Concrete Cylinders													
Label	Date	Diameter 1 (mm)	Diameter 2 (mm)	Length 1 (mm)	Length 2 (mm)	Average Volume (mm^3)	Weight (in air)	Weight (in water)	Unit Weight (kN/m^3)	Gauge Reading	f_c' (MPa)	Daily Average Unit Weight (kN/m^3)	Daily Average f_c' (MPa)
60-1	21/9/2011	100	100.5	200	200	1578660.1	3.822	2.254	23.7504	6.8	41.4	23.7504	41.4
60-2	26/9/2011	99	100	200	200	1555127.6	3.803	2.344	23.9899	8.6	52.7	23.9899	52.7
60-3	27/9/2011	101.5	102	202	201	1638452.2	3.971	2.344	23.7758	*	*		
60-4	27/9/2011	101	102	203	204	1646593.4	3.998	2.359	23.8191	9.2	56.5	23.8502	56
60-5	27/9/2011	101	101.5	201	201	1618363.2	3.952	2.33	23.9558	9.05	55.5		
60-6	28/9/2011	100.5	100.5	200.5	200.5	1590509.9	3.915	2.321	24.1471	9.2	56.5		
60-7	28/9/2011	101.5	101.5	202	202	1634456.4	3.952	2.324	23.7199	*	*	23.8467	56
60-8	28/9/2011	100	100	201	202	1582577.3	3.819	2.255	23.6730	9.05	55.5		

80MPa Concrete Cylinders													
Label	Date	Diameter 1 (mm)	Diameter 2 (mm)	Length 1 (mm)	Length 2 (mm)	Average Volume (mm^3)	Weight (in air)	Weight (in water)	Unit Weight (kN/m^3)	Gauge Reading	f_c' (MPa)	Daily Average Unit Weight (kN/m^3)	Daily Average f_c' (MPa)
80-1	26/9/2011	99.5	100	200	200	1562952.2	3.85	2.29	24.1648	11	67.8	24.1648	67.8
80-2	28/9/2011	100	100	199	198	1559015.4	3.794	2.247	23.8735	11.3	69.7		
80-3	28/9/2011	99.5	100	199	200	1559044.8	3.841	2.294	24.1688	11.5	71		
80-4	28/9/2011	100	100	200	200	1570796.3	*	*	*	11.4	70.4	24.0715	70.3
80-5	28/9/2011	100	100	198.5	200	1564905.8	3.856	2.304	24.1723	11.35	70.1		
80-6	29/9/2011	100	99.5	199	199	1555137.4	3.805	2.264	24.0024	11.4	70.4		
80-7	29/9/2011	100	100	198.5	200	1564905.8	3.888	2.329	24.3729	11	67.8		
80-8	29/9/2011	101	102	203	204	1646593.4	4.063	2.42	24.2064	11.5	71	24.2668	70.3
80-9	29/9/2011	99.5	99.5	199.5	199	1549295.9	3.867	2.315	24.4855	11.65	71.9		